UNIVERSITÉ CATHOLIQUE DE LOUVAIN
Louvain Drug Research Institute
Advanced Drug Delivery and Biomaterials

UNIVERSITÉ D'ANGERS
INSERM UMR-S 1066 – CNRS 6021
Micro & Nanomedicines Translationnelles

Lauroyl-gemcitabine lipid nanocapsule hydrogel for the local treatment of glioblastoma

Chiara Bastiancich

Director: Prof. Véronique Préat
Co-directors: Dr. Fabienne Danhier, Prof. Frédéric Lagarce
Supervisor: Dr. Guillaume Bastiat

Education and Culture
Erasmus Mundus

2018

NanoFar
European Doctorate in nanomedicine and pharmaceutical innovation

ACKNOWLEDGEMENTS

The PhD is a long journey, in which you often feel lonely but you are constantly surrounded by people that give you the strength to continue. I want to deeply thank all these people, because the last 3½ years have been very stressful but also filled with smiles, suggestions and supporting words.

Firstly, I want to thank my supervisors Prof. Véronique Préat, Prof. Frédéric Lagarce, Dr. Fabienne Danhier and Dr. Guillaume Bastiat. They opened me the doors of two excellent laboratories and gave me the opportunity to develop an extremely interesting, challenging and multitasking project. I received from them unconditional trust and freedom in each phase of the realization of this work and almost unlimited funding support (thanks to the European Commission for the NanoFar Erasmus Mundus Joint Doctorate; Fondation contre le cancer; Fondation ARC pour la Recherche sur le Cancer; Ligue contre le Cancer). My choices and ideas have always been respected and discussed as an equal collaborator, and never as an inexpert researcher, and this helped me gaining experience and self-respect. You helped me, each one in a different way, in defining who I want to become as a researcher and academic professional giving me feedbacks and advise for my future career. I will always be grateful for your teachings and suggestions, and I hope to continue our collaborations in the future. Fabienne, being your first PhD student has been a great pleasure and a big responsibility, and I have done my best to make you proud!

I also want to thank the members of my committee Prof. Olivier Feron, Prof. Pierre Sonveaux and Prof. Bernard Gallez for their time and feedback at each stage of my PhD. Your suggestions pushed me to see this work from different perspectives, and to implement my knowledge and research plan. Also, I want to acknowledge Prof. Ruman Rahman and Prof. Geraldine Piel for accepting to be part of my jury, for their comments on my work and the stimulating discussion.

I want to thank my former supervisor, Prof. Cavalli for supporting since the beginning my choice of doing an Erasmus Mundus Doctorate. Thanks for being so confident on my future as a researcher, and so proud of me for what I have accomplished during this PhD.

This work would have not been the same without two amazing researchers that I had the pleasure to meet along the way, Dr. John Bianco and Dr. Laurent Lemaire. Working with you

has been a great honor, you passed me your knowledge with enthusiasm and helped me without any reserve. Your theoretical and practical advice had a huge impact on the accomplishments of this project. With good team mates, collaboration is the key for success in science!

I want to thank Dr. Marion Pitorre for her kindness and support from the beginning of my PhD. You were a great teacher during my first approach to Angers, and a nice and always-smiling colleague during my stay at MINT.

I want to thank Dr. Nicolas Joudiou for the time and patience that he dedicated to this work. Our endless MRI marathons have been a big part of this PhD! The acknowledgment is expanded to Dr. Pierre Danhier for its suggestions and to Stefania Acciardo for our nice talks in front of the MRI.

Both at ADDB and MINT I have felt part of a team made of wonderful people, always ready to help and smile at me when needed and able to cheer me up when I was feeling upset. In this sense Bernard, Kevin and Murielle must be the firsts to be mentioned. Thank you for your time, patience and help, for your energy and support. I want to thank Anne not only for including me in the BEWARE project and for the fruitful scientific discussions, but also for our lunch/dinner talks and for her inner enthusiasm which must be taken as an example. Thanks to Pauline (and Fabi and Ana) for our alternative dancing lab meetings! And thanks to almost Dr. Marie-Julie for sharing this PhD adventure with me from the beginning to the end, always with a smile. I also want to thank you and Loic for your help with the rheometer. Thank to Kiran and Tian for helping me when I arrived in the lab, and Neha for our long talks, for your help and for understanding me. Thank to Marline, Urszula, Célia and Silvia, for trusting me as their “supervisor”: teaching is my passion and following you has been a great experience. Thanks to all the others ADDB members who shared with me the last few years, for our discussions but our laughs too.

In Angers, Edith, Marion and Florence were always available for me and I really thank them for that.

I want to thank the NanoFar crew, as they made me feel part of a whole from day one. We are a unique mix of nationalities, cultures and languages and this is our biggest strength. We feel equally comfortable at discussing our different backgrounds and beliefs as well as

science topics, without fear to be judged. I am sure that with many of you we will stay friends for a long time and we will collaborate in a fruitful manner. Especially, I want to thank Reatul for our long scientific and life-related talks. Valentina for her intrinsic strength and sweetness. Hélène for her kindness. Natalija, Janske, Mathie and Bathabile (but Jamal and Baptiste too) because they are so full of life and joyful that I never felt lonely or sad with them around.

From the Angers experience, I must thank my “belline” Giulia and Maria. Showing/teaching you the research lab life was a great pleasure for me. In exchange, you were the sweetest and funniest of friends and you brought me back to the Erasmus life.

And finally, thanks to the most important part of me, my family. The “real” one but also my “Belgian” family. Therefore, thank you Alessandra, Dario and Ana – the name order was hazardously extracted – for EVERYTHING. I have no words to explain what you meant to me in the last few years, and how important how relationship is. I can’t count the laughs, the cries, the meals, the trips/concerts, the beers, the coffees and the Nutellas that we shared. I have shared with you every scientific or dailylife doubt that passed through my mind, every joy or pain, every idea. Thanks for the brainstormings and the constructive critics. I never felt alone with you by my side and I really hope that someday we will have our nanomedicine lab at Fiji, all together. Thank to Alex and my beloved little Lucas for being part of this amazing family of ours and for your smiles and presence in my life.

Thanks to the Bastiancich-Castagnoli-Bello-Bejà tribù for being my rocks. Thanks to mum and dad, to Neri and Kiki, to zia Totta. Thanks to Maia for coming to the world when we most needed her, and being the sunshine of our lives. To Mary and Mateo. Thanks for simply being there for me, all the time: for supporting me but also for filling me with doubts, so that I have to think and think and rethink to make sure that I am on the right path.

Lastly, thank to my “ragazzino” and wonderful husband Mattew. Your love and patience are the backbone of this PhD thesis. Thank you for making my future your priority, even if that meant giving up on some of your dreams. Thanks for sharing this goal and experience with me, for bearing me and for supporting me unconditionally. You have always believed in me more than myself. And thanks to little Snoopy, which is making our life crazy and normal in these last few months.

To my nonna Giuliana and all the other cancer patients,
in the hope that this work can contribute to finding a cure that makes you sing of joy

FOREWORD

Glioblastoma (GBM) is the most common and aggressive brain tumor in adults. Its rapid proliferation, ability to invade healthy brain tissue and resistance to chemotherapeutic treatments make this cancer an unsolved and challenging pharmaceutical and medical issue. Despite great advances in GBM knowledge – in terms of diagnosis, cancer biology and drug discovery – no effective treatment against GBM is currently available and GBM recurrences inevitably lead to patient's dead.

This work aims at evaluating if the innovative hydrogel based on lauroyl-gemcitabine lipid nanocapsule ($GemC_{12}$-LNC) could be used for the local management of GBM to avoid local recurrences. This formulation, uniquely formed of a nanocarrier and a potent cytotoxic drug, is simple to prepare, injectable *in situ* and combines the properties of nanomedicines and hydrogels.

Chapter I – Introduction gives an historical background on GBM and its challenges. To contextualize this work, the contribution of local delivery strategies, nanomedicines and gemcitabine for the treatment of GBM are extensively described.

Chapter II – Aim of the thesis exposes the objectives and potential impact of this work, which includes the evaluation of the feasibility, efficacy and tolerability of our hydrogel for the local treatment of GBM.

Chapter III – Lauroyl-gemcitabine loaded lipid nanocapsule hydrogel for the treatment of GBM: proof of concept reports the proof of concept of the use of $GemC_{12}$-LNC hydrogel for the treatment of GBM.

Chapter IV – Development of a surgical glioblastoma resection procedure in mice describes the development of a surgical resection technique in mice to have a preclinical model suitable to test the local efficacy of our hydrogel.

Chapter V – Lauroyl-gemcitabine loaded lipid nanocapsule hydrogel for the treatment of GBM: long-term efficacy and tolerability evaluates the long-term tolerability and efficacy of $GemC_{12}$-LNC hydrogel in mice for the treatment of GBM.

Chapter VI – Evaluation of Lauroyl-gemcitabine lipid nanocapsule hydrogel efficacy in glioblastoma rat models is focused on the adaptation of the surgical resection technique in rats and evaluation of the $GemC_{12}$-LNC hydrogel efficacy in this animal model.

Chapter VII – Discussion, conclusions and perspectives will explain how the present work can fit in the state of the art of GBM management. The future perspetives of this work as well as the experiments planned to answer some open questions will be described.

LIST OF ABBREVIATIONS

BBB	Blood-Brain Barrier
BCNU	Carmustine
CED	Convection Enhanced Delivery
CNS	Central Nervous System
CSCs	Cancer Stem Cells
CSF	Cerebrospinal Fluid
DiD	1,1'-Dioctadecyl-3,3,3',3'-Tetramethylindodicarbocyanine Perchlorate
DiI	1,1'-Dioctadecyl-3,3,3',3'-Tetramethylindocarbocyanine Perchlorate
EGFR	Epidermal Growth Factor Receptor
EMA	European Medicines Agency
FDA	US Food And Drug Administration
FRET	Fluorescence Resonance Energy Transfer
GBM	Glioblastoma
Gem	Gemcitabine
$GemC_{12}$	Lauroyl-gemcitabine
H&E	Haematoxylin And Eosin
HPLC	High Performance Liquid Chromatography
IC50	Half Maximal Inhibitory Concentration
LNC	Lipid Nanocapsules
MGMT	O6-Methylguanine-DNA-Methyltransferase
MRI	Magnetic Resonance Imaging
MTT	Thiazolyl Blue Tetrazolium Bromide
NFL	Neurofilament Light Subunit-Tubulin-Binding Site 40-63 Peptide
NP	Nanoparticles
PBS	Phosphate Buffered Saline
PEG	Polyethylene Glycol
PTX	Paclitaxel
RT	Radiotherapy
ST	Standard deviation
TMZ	Temozolomide
WHO	World Health Organisation

TABLE OF CONTENTS

CHAPTER I.

INTRODUCTION

Adapted from:

1. **Bastiancich C***, Bianco J*, Jankovski A, des Rieux A, Préat V, Danhier F. On glioblastoma and the search for a cure: where do we stand? *Cellular and Molecular Life Sciences* 74 (13): 2451-2466 (2017).
2. **Bastiancich C**, Danhier P, Préat V, Danhier F. Anticancer drug-loaded hydrogels as drug delivery systems for the local treatment of glioblastoma. *J Controlled Release* 243: 29-42 (2016).
3. **Bastiancich C**, Bastiat G, Lagarce F. Gemcitabine & glioblastoma: challenges and future perspectives. *Drug Discovery Today* 23:416-423 (2018)

TABLE OF CONTENTS

1. ON GLIOBLASTOMA AND THE SEARCH FOR A CURE: WHERE DO WE STAND?

Although brain tumours have been documented and recorded since the 19th century, 2016 marked 90 years since Percival Bailey and Harvey Cushing coined the term “glioblastoma multiforme”. Since that time, although extensive developments in diagnosis and treatment have been made, relatively little improvement on prognosis has been achieved. The resilience of GBM thus makes treating this tumour one of the biggest challenges currently faced by neuro-oncology. Aggressive and robust development, coupled with difficulties of complete resection, drug delivery and therapeutic resistance to treatment are some of the main issues that this nemesis presents today. Current treatments are far from satisfactory with poor prognosis, and focus on palliative management rather than curative intervention. However, therapeutic research leading to developments in novel treatment stratagems show promise in combating this disease. Here we present a chapter on GBM, looking at the present-day management of GBM and exploring future perspectives in treatment options that could lead to new treatments on the road to a cure.

1.1. CURRENT TREATMENT STRATEGIES FOR GLIOBLASTOMA

Brain tumors only count 2% of the adult population affected by cancer. However, they are considered among the worst diseases as they have a direct impact on patient’s life from a physical, psychological and neurological point of view [1]. Among brain tumors, glioblastoma (GBM), a grade IV astrocytoma, is the most common and aggressive in adults and also the most feared by patients, physicians and oncologists [2, 3]. Preventive measures, such as life style changes, early diagnosis and treatment unfortunately do not impede the development of the disease and do not improve its outcome, precluding the utility of screening for this tumor [1].

Based on the clinical history of the tumor, GBM can be divided into primary GBM (90%) or secondary GBM (10%): in the first case the tumor arises from astrocytes or supportive brain tissue in an acute *de novo* manner without previous lower grade pathology or symptoms, while the secondary GBM derives from the progressive evolution and transformation of

lower grade astrocytomas and normally affects younger patients [4]. The two subtypes of GBM present different genetic profiles and can be identified by specific cell markers but are morphologically and clinically indistinguishable. Moreover, both have the same poor prognosis (median survival below 15 months) and remain incurable [5]. Signs and symptoms from GBM usually result from infiltration or compression of normal brain by tumor, edema, hemorrhage or increased intracranial pressure and include headaches, seizures, focal neurologic deficits and changes in mental status [6]. Despite the low number of patients affected by this disease (the US and EU incidence is 3 in 10,000 persons) [7], in the last 90 years numerous scientists have focused their attention to find new efficacious treatment strategies to improve the quality of life of patients affected by GBM and their clinical outcome [8].

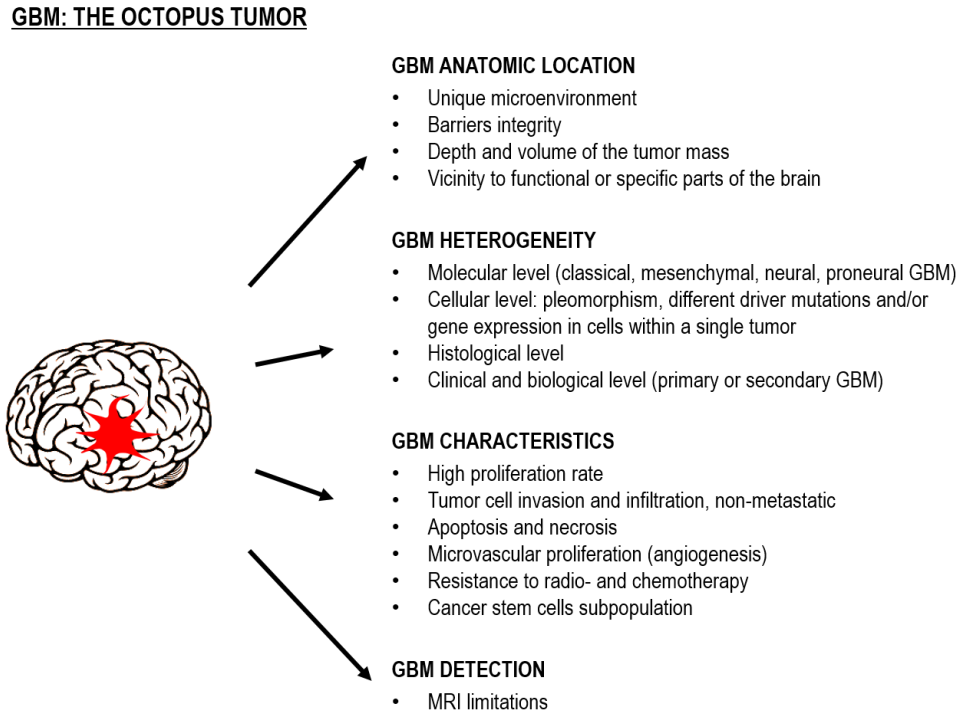

Figure 1. Obstacles for effective treatment of GBM that contribute to its fatal outcome.

Several obstacles limit the assessment of tumor response and the delivery of cytotoxic agents leading to a lack of effectiveness of GBM treatments (Figure 1): *(i)* the anatomical location of the tumor in the brain often impedes a complete surgical resection without damaging the neurological tissue and affects the cognitive functions of the patient. Moreover, the central nervous system (CNS) barriers (blood cerebrospinal fluid barrier;

arachnoid barrier; blood-brain barrier, BBB; blood-tumor barrier) represent a challenge to the delivery of cytotoxic drugs at therapeutic concentrations at the tumor site. *(ii)* GBM is highly heterogeneous at all levels, from the tissue level to the molecular and genetic point of view to the cell type [2, 9]. This heterogeneity, represented also within the same tumor, leads to high variability in tumor histopathology making the classification of these tumors very difficult and resulting in low predictability of tumor response to treatments [10]; *(iii)* the hallmark characteristics of GBM are uncontrolled cellular proliferation, propensity for necrosis and angiogenesis, resistance to apoptosis, high genomic instability, chemoresistance and fatal outcome [5]. GBM cells are able to extend their tendrils into the normal surrounding parenchyma infiltrating diffusely beyond the primary lesion in the early stages of tumor development (GBM is also known as "octopus tumor") [11]. Many individual genes implicated in GBM cells migration and invasion have been identified and their presence has been correlated with poor patient survival [12]. It has also been shown that GBM invasion is not random and occurs along white matter tracts, basement membranes of blood vessels, along the subependyma, adjacent to neurons and, sometimes, it reaches the contralateral hemisphere [5, 12, 13]. Moreover, the presence of a subpopulation of cancer stem cells able to act as "disease reservoirs" and self-renew themselves increases the ability of forming GBM recurrences [12, 14]; *(iv)* A key role in the diagnosis and GBM progression evaluation is played by the Magnetic Resonance Imaging (MRI). Indeed, due to its high soft tissue contrast, MRI is the preferred method for the noninvasive detection of brain tumors. On standard gadolinium-enhanced T_1-weighted images, GBM appears as heterogenous hyperintense signals at the tumor rim with the presence of a necrotic core [15]. Initial imaging exams aim to determine the location of the lesion for treatment/biopsy/resection planning, to evaluate mass effect on the brain, and characterizing tumor location, vascularity, mass effect, peritumoral edema, and proximity to areas of potential functional significance [16, 17]. Advanced MRI imaging techniques provide additional information on the tumor such as cellularity, invasiveness, mitotic activity, angiogenesis, and necrosis [18]. MRI is also important for characterizing early recurrences but this task is often difficult as recurrences have similar radiologic features than treatment-associated changes [15, 19]. However, conventional MRI of GBM suffers from important limitations. First, standard sequences hardly distinguish neoplastic from non-neoplastic tissues [20]. High-grade primary brain tumors, intracranial metastases, abscess, or inflammation induce BBB disturbances and

appear as contrast-enhancing lesions on Gd-enhanced T_1-weighted images. Secondly, conventional MRI poorly differentiates low-grade from high-grade gliomas meaning that biopsies and histological studies are required to establish a definitive diagnosis [17, 20]. Finally, GBM cells extents are not always detectable by modern neuroimaging meaning that MRI often fails to delineate the tumor margins [20, 21]. Indeed, Yamahara *et* al. showed that invasive tumor cells can be found from 6 to 14 mm beyond the enhancing area in high-grade GBM [11].

First line – surgical resection and postoperative radiotherapy

The complexity in management of GBM patients depends on many factors. These including tumor size and location, patients' age and Karnosky Performance Scale index, tumour histology, and molecular markers status such as O^6-methylguanine-DNA-methyltransferase (MGMT) promoter methylation, which has shown to induce greater sensitivity of tumours to chemotherapy. Despite the efforts of the scientific community, the standard of care therapy for GBM, which is based on surgery followed by irradiation, is yet to achieve satisfactory results [22]. Due to its aggressive nature and rapid development, the clinical endpoint in most patients with recurrent GBM is to stabilise the disease and improve the quality of life of the patient in the last months, rather than to significantly extend survival.

Standard of care therapy for GBM is represented by surgical resection of the accessible tumor (without causing neurological damage) followed by chemoradiation. This consists in radiotherapy and concomitant chemotherapy with Temozolomide (TMZ), carmustine (BCNU) or other cytotoxic agents (Figure 2) [23]. Some clinical factors have been associated to better prognosis such as younger age, lack of motor and language deficit, mutations in biological markers (e.g. MGMT promotor methylation, isocitrate dehydrogenase-1 mutations), increased extent of resection and minimal residual tumor volume, tumor location near neurogenic niches and not adjacent to the lateral ventricles [24-27].

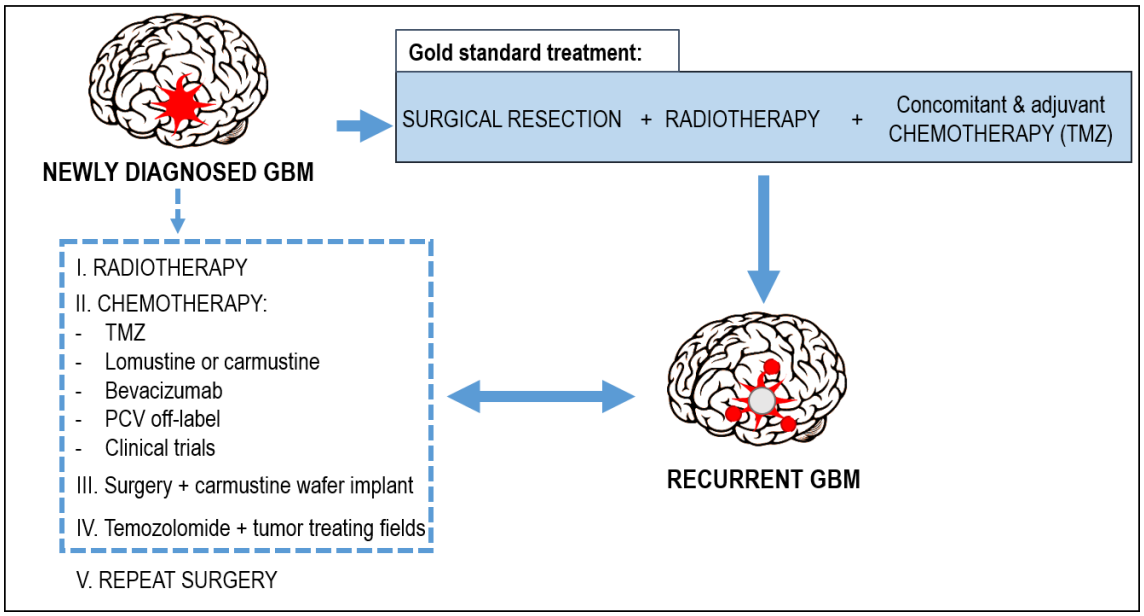

Figure 2. Schematic representation of GBM treatment strategies. TMZ: temozolomide; PCV: procarbazine, lomustine, vincristine.

Overall survival following surgical resection of the tumour is 3 to 6 months, including radiotherapy into the treatment paradigm increases this value to 12.1 months (2-year survival at 10.9%). A slight increase in survival to 14.6 months (2-year survival at 27.2%) can be achieved through the addition of concomitant and adjuvant TMZ chemotherapy [28]. These statistics point to the fact that, even if we now have major knowledge of GBM genomics, biology and microenvironment compared to the past, this malignant tumour is still incurable today, only 8% of GBM treated patients reaches the long-term survival status of 2.5 years and very few survive over this period [29].

At present, surgical removal is and has remained the mainstay in the treatment of GBM tumours, providing that unacceptable neurological deficits can be avoided [22]. However, the early and distant dissemination of malignant cells renders GBM a surgically incurable neoplasm. Indeed, 35% of newly diagnosed GBM patients cannot be considered for surgery while the remaining ones can receive a complete or partial resection, depending on the extension and the location of the tumor [30, 31]. Dr. Walter Dandy took the first critical steps in GBM management in the late 1920s through the surgical removal of the whole hemisphere in 5 patients diagnosed with glioma, two of which were comatose. In all of the cases hemiplegia was a common occurrence. In two of the cases, the tumour subsequently recurred, giving a glimpse as to just how invasive gliomas, and GBM, can be [28, 32]. Thanks

to important technical and imaging advances over the last century, the surgical resection of GBM is regarded as a generally safe procedure based on a number of combinatorial factors. Techniques of MRI, such as diffusion tensor imaging, and functional or perfusion MRI allow for improved pre-surgical planning, allowing a precise evaluation of the extent of resection to be performed, be it tissue biopsy, sub-total, or gross-total resection [33-36]. Several techniques can be used to obtain a safe maximal tumor reduction, such as awake craniotomy, neuronavigation and image-guided surgery, intraoperative MRI, laser interstitial thermal therapy or fluorescence-guided surgery [17]. The selection of the safest and appropriate method depends on tumor location, characteristics and size, and the clinical and neurological conditions of the patient before the surgery [17]. Studies have shown that significantly longer survival times are observed in patients who undertake aggressive resection surgery (<98% of tumor volume resected) and also if recurrences often develop, surgery has a critical role in the management of patients [30, 37]. Actually, it relieves symptoms resulting from mass effect, reduces the number of cells requiring treatment and often removes the hypoxic core of the tumor that is relatively resistant to radiation and inaccessible to chemotherapy [6]. Moreover, it allows an accurate diagnosis and provides adequate tissue for histological and molecular tumor characterization [6].

Following surgical resection, postoperative radiotherapy (RT) is the main course of action, even if begins weeks after surgical removal of the tumour as it can impact the wound healing process [38]. This treatment modality has been recognised as standard therapy since the 1970s [39]. Traditionally, whole brain radiation was performed. However, since it was established that the majority of recurrences ensued in the proximity of the resection cavity borders, in became common practice to irradiate smaller brain regions, thus reducing eventual side effects. In addition, experience and development introduced innovative technologies such as focal RT, intensity-modulated RT, 3D-conformal RT, which allowed for a more accurate and safe RT for the patient, as well as stereotactic radiosurgery, although this is more rarely indicated for GBM treatment. In present day management, the “standard” RT regimen for patients with GBM includes fractionated focal irradiation in daily fractions of 2 Gy, five times a week for 6 weeks (30 treatment days in total), for a total irradiation charge of 60 Gy. Attempts have been made to improve the therapeutic efficacy of RT, such as higher doses, altered fraction schemes, and the use of radiation sensitizers, however these

attempts have so far proved futile [22]. However, procedures with shorter and hypo-fractionated irradiation are proposed to elderly patients [40-42].

Chemotherapy and beyond

Chemotherapy, a term coined by Paul Ehrlich in the early 1900s, also has a long past, like GBM [43]. With this concept, the immunosuppressive effects of chemicals were observed by chance nearly a century ago [44, 45], and ultimately led to the first use of an intravenous chemotherapeutic agent to treat cancer in the 1940s [46]. The predicament of GBM is such that, since the advent of chemotherapy, nearly every new class of drug that has reached the market has been tested in GBM patients [47]. By 1996, more than 60 different anti-cancer drugs were registered in the USA for the treatment of cancer [48], and over the last 40 years, several chemotherapeutic drugs have received approval for the treatment of GBM by the U.S. Food and Drug Administration (FDA).

A big challenge for the effective delivery of chemotherapeutics into GBM is the BBB. The BBB of healthy patients is constituted by a continuous layer of specialized endothelial cells linked together by tight junctions and supported by adhesions and interactions with basement membranes, brain pericytes, astrocytes, and neurons. In GBM patients, the BBB is often leaky and partially – and heterogeneously – disrupted at the tumor site [49]. The BBB breakdown is evidenced by gadolinium enhancement on T_1-weighted MRI as this contrast medium is not able to cross the intact BBB but can diffuse in the compromised barrier of grade IV astrocytomas [50]. Systemically administered molecules (e.g. drugs, antibodies, nanoparticles) might be able to extravasate the BBB and reach the main bulk of GBM thanks to its compromised permeability. However, it is described that they are unable to reach single infiltrating tumoral cells, localized in brain areas where the BBB is not or less altered (Figure 3) [49, 50]. For this reason traversing the BBB remains a major obstacle for the delivery of chemotherapeutic agents, limiting the number of drugs currently available for GBM treatment. Radiation, which is part of the GBM treatment regimen, has been shown to disrupt the BBB, and thus could facilitate more successful delivery of therapeutic agents to cross into the brain parenchyma [51].

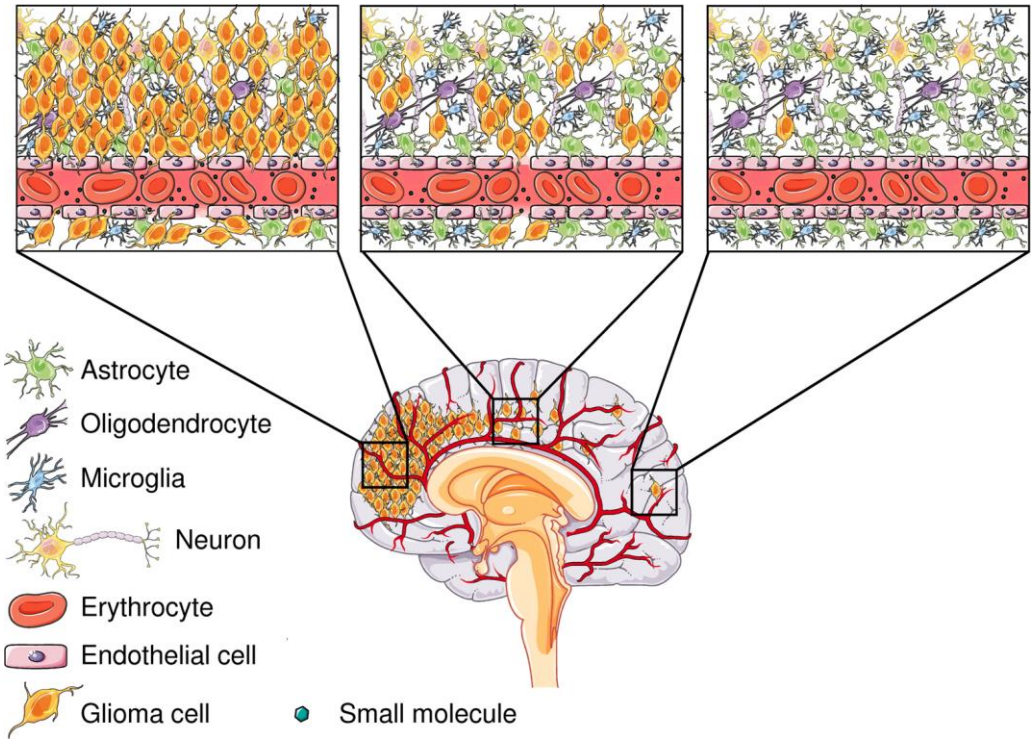

Figure 3. Schematic representation of the heterogeneity of the BBB and BBTB integrity in GBM patients. BBB breakdown is evident in the tumor region (left panel), allowing for molecules extravasation. In other regions of the brain, where infiltrating GBM cells are located, the BBB is less disrupted or normal maintaining, at least partially, its functional barrier role (middle and right) and limiting the diffusion of chemotherapeutic drugs. Adapted from [50].

Delivery route can also have an impact on drug concentrations in brain tumours, as can the tumour type. Although chemotherapeutic drugs are normally administered intravenously rather than orally, the route of administration is also determined by the chemical properties of the agent at hand [52]. In the mid-1970s, some alkylating nitrosoureas compounds received approval as a single agent, or in combination with other chemotherapeutic drugs, for the treatment of primary or metastatic brain tumours. Oral lomustine, or intravenous BCNU began to be administered after surgery and/or RT [53].

Between 1995 and 2003, in addition to the classical treatment regimen, Gliadel® wafers (composed of the biodegradable copolymer prolifeprospan 20) were developed for use within the resection cavity following surgery. This scaffold allows for the local delivery of BCNU following surgical resection over a one week period. The local delivery of chemotherapeutic drugs could take advantage of the protective role of the BBB allowing high brain drug concentration with limited systemic side effects and enhanced distribution towards infiltrating tumor cells. This treatment modality was first used in patients with

recurrent GBM, and then in patients with newly diagnosed primary GBM as adjunct to RT, and has become part of the first-line treatment options available for GBM [54-57]. In the same period where Gliadel® emerged as an alternative strategy for GBM, promising results were observed with the use of TMZ, which received accelerated approval in 1999 for GBM patients refractory to nitrosoureas and procarbazine. TMZ is available as both oral and intravenous formulations that have practically equivalent bioavailability and offering comparable benefits, resulting in the intravenous formulation to be rarely used in clinical practice [47]. Treatment through oral delivery would also mean less interference in the daily lives of the patients, with negligible impact on family and/or social activities [58]. Indeed, patients with terminal cancers do show a clear preference for oral chemotherapy, although they are not willing to sacrifice efficacy for their preference [59]. Since 2005, TMZ is recognised as the first-line treatment following surgery and concomitant RT for newly diagnosed GBM patients [53]. Despite the good tolerability and oral bioavailability of TMZ, only one third of GBM patients are responsive to treatment with alkylating agents, while some patients present innate or acquired chemoresistance. Regardless of treatment schemes used, all GBM patients develop recurrences within two years from the initial diagnosis [60-61]. In 2011, a fourth cancer treatment modality – tumour treating fields (TTFs) – was approved by the FDA initially for the treatment of recurrent GBM [62]. TTFs are low-intensity alternating electric fields that selectively target proliferating cells by disrupting mitosis [63]. Following a phase III clinical trial, the FDA extended their approval to include TTF treatment for newly diagnosed GBM patients in 2015 [64]. The NovoTTF-100A device (Optune®) is the first TTF device approved and is currently used as a concomitant therapy to TMZ following surgical resection and RT, both for newly diagnosed and recurrent supratentorial GBM [62, 65].

Towards something new – clinical trials

After this "gold standard" therapy, most patients develop GBM recurrence within two years of their original diagnosis [66]. Since there is no standardised regimen for treating recurrent GBM, clinicians need to determine the best treatment options that the clinical status of the patient presents [23]. This could include a second surgery (especially if the recurrent tumor exerts an acute mass effect), repeated RT (especially for small tumors [23]) or second-line chemotherapy (Figure 2). This last approach could include single therapies of drugs (such as

BCNU and lomustine), as well as combinatorial therapies using drugs “off label”, such as the combination of procarbastine, lomustine and vincristine. These chemotherapy regimens may achieve similar tumor control rates compared to TMZ [23, 67]. However, alkylating agents are subject by the same chemoresistance pathways as TMZ as their mechanism of action is similar, therefore their effectiveness is often limited [68]. Their chemoresistance is mediated by different mechanisms including DNA repair pathways, deregulation of apoptosis regulating genes or tumor cells overexpression of proteins such Galectin-1 or Epidermal Growth Factor Receptor (EGFR) [69, 70].

In 2009 the FDA approved the anti-angiogenic humanized monoclonal antibody bevacizumab for the first-line treatment of recurrent GBM patients. Its use, alone or in combination with irinotecan [71, 72], has shown the improvement of the progression-free survival and maintainment of the quality of life and performance status in these patients. However, its impact on the overall survival time is controversial [73-75]. The use of Bevacizumab is not currently approved for recurrent GBM in Europe, as the European Medicines Agency (EMA) still holds concerns about the activity of this antibody in recurrent GBM [76]. Nevertheless, the effects of Bevacizumab in GBM continued to be studied, and two phase III clinical trials testing the combination of Bevacizumab with standard care practices in newly diagnosed GBM patients have recently concluded [77]. One of the trials was conducted in the USA (Trial ID: NCT00884741) [78], while the other in Europe (AVAglio Trial ID: NCT00943826) [79], but both obtained similar results. While Bevacizumab use failed to increase overall survival of patients with GBM, progression free survival was slightly prolonged. Both trials also observed benefits of treatment with Bevacizumab on baseline quality of life, as well as in performance status. However, the rate of adverse effects was higher with treatment compared to placebo, and progression assessment was complicated due to pseudo progression in a relevant number of patients [78, 80, 81]. Although the FDA revoked approval of Bevacizumab for the treatment of breast cancer in December 2010 [82], it is still approved for the treatment of other cancers, including GBM. The balance between efficacy and toxicity may warrant its continued use in the treatment of GBM on one hand, but concerns that Bevacizumab does not have an impact on health-related quality of life during the progression-free period, and considering that its use in GBM settings is not cost-effective, its future use may become limited [77, 83].

Table 1: The total number of trials for GBM registered with clinicaltrials.gov as of 11.12.2017.

Glioblastoma		Open studies currently recruiting[a]	
Total	1201	Total	262
Known status	1131[a]	Phase 0	9
Closed studies	768	Phase 1	115
Interventional	1114	Phase 2	119
Observational	85	Phase 3/4	14
Studies with results	155	Open studies not yet recruiting[a]	
Closed, not recruiting	700[a]	Total	37
Open studies	431[a]		
Funded by	National Institute of Health (NIH)		94 open (371 total)
	Industry		175 open (469 total)
	Individuals; University; Organisations		173 open (392 total)
Studies during last 5 years (11.12.2016-11.12.2017): 435[a]			
Studies during 2016 (01.01.2017-11.12.2017): 89 (86 open, 59 recruiting)			

[a]Excluding unknown status

The intrinsic characteristics of GBM, such as high invasiveness, heterogeneity, rapid proliferation, and aggressive infiltration, lead to the fact that the optimal chemotherapy for GBM is still under investigation [84]. Increasing doses, of TMZ for example, is also not an option. A recent study showed that increasing the cumulative dose per cycle of treatment does not improve the efficacy of TMZ [85]. Numerous studies that examine ways to combat tumour growth and improve the overall survival of GBM patients are constantly being undertaken. For patients who do not respond to the current standards of care available, other options would be presented, and a prognostic decision must be made by the clinician, where an intensified approach or a palliative setting would be proposed. While taking into account safety and ethical concerns, and with the dismal prognosis of GBM that has recurred, participation in clinical trials should be encouraged, as their aim is to improve outcome. Therefore, salvage regimens or adjuvant therapies using drugs which are in a clinical trial stage can be proposed as an option [86, 87]. At present, the number of experimental therapies investigated in treating GBM is so high that it is impossible to list them all here. Table 1 summarised the total number of trials registered on the clinicaltrials.gov server [88] with the initial search parameter of “glioblastoma”. These were further categorised into known status, closed, interventional, observational, with results, closed, or open studies. Table 2 shows a selection of ongoing clinical trials that are no longer recruiting, in different phases and completion timelines. Although far from exhaustive, it outlines different strategies currently under investigation, which could be regarded as probable starting points/candidates for the future management of GBM.

Table 2: A sample of trials registered with clinicaltrials.gov which are currently ongoing, without further recruiting and at different stages of completion, showing the diversity of therapeutic strategies currently being assessed.

START DATE	ESTIMATED END DATE	THERAPEUTIC STRATEGY	TREATMENT ARMS	GBM INDICATION	PHASE	TRIAL ID	SPONSOR
12/2006	11/2016	Immunotherapy	• DCVax®-L	ND	3	NCT00045968	Northwest Biotherapeutics
11/2007	11/2017	Surgical resection	• Vorinostat • Isotretinoin • Temozolomide	R	1/2	NCT00555399	MD Anderson Cancer Center
08/2008	01/2015	Nanotechnology	• Nanoliposomal CPT-11	R	1	NCT00734682	University of California
04/2009	12/2016	Protease inhibitor	• Nelfinavir	ND	1	NCT01020292	Abramson Cancer Center of the University of Pennsylvania
09/2009	12/2016	Radiation, Chemotherapy	• Boron neutron capture therapy • X-ray radiation treatment • TMZ	ND	2	NCT00974987	Translational Research Informatics Center
12/2009	12/2017	Intraarterial cerebral infusion	• Cetuximab	R, Refractory	1	NCT01238237	Northwell Health
07/2011	07/2017	Hypofractionated radiotherapy	• Bevacizumab • Stereotactic radiotherapy	R	1	NCT01392209	Memorial Sloan Kettering Cancer Center
11/2011	11/2016	Immunotherapy	• Rindopepimut with GM-CSF • Temozolomide • KLH	ND, Resected, EGFRvIII mutation	3	NCT01480479	Celldex Therapeutics
01/2013	12/2016	EGFR inhibitor	• Erlotinib • Cytoreductive surgery	R, EGFRvIII mutation	0	NCT01257594	Andrew Lassman
03/2013	04/2019	Photodynamic therapy	• Photofrin (porfimer sodium)	R, Refractory	1	NCT01682746	Harry T Whelan, MD
05/2013	05/2018	Radiotherapy	• IMPT • IMRT	ND	2	NCT01854554	MD Anderson Cancer Center
10/2013	12/2016	Chemotherapy	• Cabazitaxel	ND	2	NCT01866449	University of Ulm
01/2014	11/2017	Immunotherapy	• ICT-121 DC vaccine	R	1	NCT02049489	ImmunoCellular Therapeutics
05/2014	09/2017	Radiation sensitizer	• NVX-108	ND	1	NCT02189109	NuvOx Pharma
10/2014	07/2018	Personalised vaccine	• APVAC1 vaccine + Poly-ICLC & GM-CSF • APVAC2 vaccine + Poly-ICLC & GM-CSF	ND	1	NCT02149225	immatics Biotechnologies GmbH
10/2016	12/2019	Nanotechnology	• EGFR(V)-EDV-Dox	R	1	NCT02766699	Engeneic Pty Limited

Legend: **ND:** Newly diagnosed; **R:** recurrent; **TMZ:** temozolomide; **EGFR:** epidermal growth factor receptor; **KLH:** keyhole limpet hemocyanin; **DC:** dendritic cells; **DCVax®-L:** dendritic cells pulsed with tumour lysate antigen; **GM-CSF:** Granulocyte macrophage colony-stimulating factor; **IMRT:** Intensity Modulated Radiotherapy; **IMPT:** Intensity Modulated Proton Radiotherapy; **CPT11:** irinotecan; **EGFR(V)-EDV-Dox:** doxorubicin-loaded EGFR-targeting nanocells.

It must be noted that when it comes to treating GBM, apart from the standard treatments of resection, radiotherapy, and chemotherapy, ancillary therapeutic agents are also essential. Anticonvulsant drugs, corticosteroids, and anticoagulant drugs play an important role in treating patients with brain tumours, as they control seizures, increased intracranial pressure, deep vein thrombosis and embolism, which may occur in up to 30% of patients with primary brain tumours [22].

Despite the efforts of the scientific community to increase the long-term benefits of GBM therapy, at the moment this tumor remains incurable. In many cases the clinical end point for GBM is to stabilize the disease, to slightly extend the life of the patients and to improve their quality of life in the latest phases of the disease [89]. The improvement of the treatment to reach an actual cure and a long-term survival is limited by several obstacles.

The location of the tumor in the brain does not always allow a complete resection of all tumor cells, firstly because of their invasiveness and secondly because broadening the resection area could lead to neurological deficit (motor, sensory, cognitive) and loss of functional brain tissue. On the other side, increasing the perimeter or intensity of the radiation could lead to harmful and unacceptable side effects. For what concerns the chemotherapy, the presence of the BBB, the intrinsic and acquired chemoresistance of GBM cells and the formation of recurrences close to the resection borders limit the achievement of effective treatments. Also, it is evident that a single therapy may not be enough, so combinations of treatments must be explored. Combinatorial therapy is not a novel concept, being proposed by Ehrlich in 1913. He also believed in the concept of an ideal therapy – a "magic bullet" – proposing that chemotherapeutic agents could be fashioned to specifically kill a targeted cell, in effect the equivalent of targeted drug delivery [43, 90]. Unfortunately, even though targeted delivery can be obtained today, there is no magic involved. The bullet hits, but does not make a "kill shot". New, specific and more effective drugs and/or multi-drug synergistic approaches that allow to target different tumorigenic pathways need to be discovered to reach the goal of eradicating GBM. Also, more efficient drug delivery strategies able to achieve the drug release at optimal concentrations over a sustained period of time and able to suppress tumor growth need to be used against GBM.

Currently we know where we stand when it comes to treating GBM. We also know the road travelled to reach this point. This voyage has been summarised in figure 4. What we must

ask now is, what does the future hold? What are the new directions being taken to overcome this disease of the brain? How many remaining options do we have? To have a glimpse of an answer, we must delve into the future.

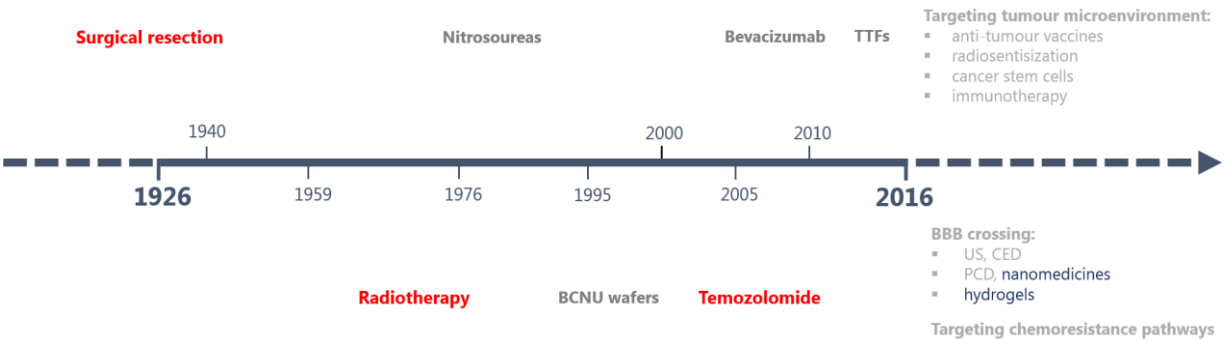

Figure 4: Graphical summary of the last 90 years outlining the major time points from the classification of GBM by Bailey and Cushing to treatments available today, with on outlook of what treatment modalities the future may hold. Legend: TMZ: Temozolomide; BCNU: Carmustine; WHO: World Health Organization; TTFs: Tumour Treating Fields; BBB: Blood Brain Barrier; CED: Convection Enhanced Delivery; PCD: Peptide-carrier Mediated Delivery; US: Ultrasound Mediated Delivery.

1.2. FUTURE TREATMENT STRATEGIES FOR GLIOBLASTOMA

GBM remain the most common brain tumour in adults today. In all its history, GBM has had a dismal prognosis ranging from 9 – 12 months. As described in the first WHO edition on tumour classification, a grade IV tumour is malignant, with a 6 – 15 month survival following surgery [91], and GBM is right on the mark. Today, patients undergoing maximum safe resection and adjuvant chemotherapy treatment can expect a 14 month overall median survival [92]. Elderly patients have an overall survival that rarely exceeds 8.5 months [93]. In essence, prognosis for GBM has not changed significantly in 90 years, despite the years of research and technical developments that are currently available. However, there is hope on the horizon as new and differing research is continued to be undertaken to tackle the enigma that is GBM. The most promising of these, which could ultimately lead to more specialised and targeted therapeutic strategies, are outlined below.

Heterogeneity without borders

The complexity of GBM has led to new direction in drug therapy being taken. Indeed, a unique set of challenges are present in relation to GBM treatment. The first major obstacle consists of the specific and heterogeneous tumour microenvironment. One hallmark of GBM

is a diffuse and infiltrative nature, which more often than not leads to incomplete surgical resection on a cellular level, even though it can be complete in term of contrast enhancement on an MRI. This in turn leads to the need for additional therapies. For drugs to be effective, and to accumulate in the tumour, they must be able to effectively cross the BBB. At present, this obstacle is not readily overcome, thus the chemotherapeutic possibilities in clinical use are drastically reduced. Even when treatments get past this barrier, new obstacles appear in the form of therapeutic resistance, with some cell populations present within the tumour showing substantial radio- and/or chemo-resistance [42]. Thus, the first hurdle that needs to be overcome is the microenvironment of GBM.

GBM can express an extraordinary repertoire of immunosuppressive adaptations, and so has historically been considered as an anti-immunogenic malignancy. To this end, anti-tumour vaccines have caught the eye as an immunotherapeutic approach to combat GBM. Vaccines are particularly attractive because they would be able to induce potent anti-tumour immunity, with long lasting immunological memory, while also sparing normal tissues [94]. A variety of anti-tumour vaccine strategies are currently being studied, including peptide vaccines, heat shock protein vaccines, dendritic cell vaccines, whole tumour vaccines, and human umbilical vein endothelial cell vaccines, as well as personalised vaccines [42, 95-97].

GBM is a vastly vascularised tumour characterised by extensive angiogenesis [98]. Despite the mitigating success of Bevacizumab in recurrent GBM by prolonging progression-free survival, a variety of other anti-angiogenic agents are currently being investigated as “radiosensitizers” for the treatment of GBM. These include small molecule inhibitors such as vandetanib and sorafenib to block vascular endothelial growth factor signalling, as well as protein kinase C inhibitors such as enzastaurin, and cilengitide, an inhibitor of integrin [99]. The rationale for targeting the angiogenesis pathway, particularly through vascular endothelial growth factor inhibition, for radiosensitization is multifactorial. Firstly, anti-angiogenic drugs may improve tumour oxygenation through vascular normalisation. The cytotoxic effects of radiation, which are dependent of the presence of reactive oxygen species, can be amplified by supplying the tumour with increased oxygen [100]. Additionally, radiation-induced secretion of vascular endothelial growth factor in GBM may contribute to radioresistance of GBM by reducing the damaging effects of radiotherapy on endothelial cells [42, 95, 101]. Even though some of these anti-angiogenic compounds failed as

radiosensitizers in robust preclinical and early-phase studies, this strategy is still being extensively investigated, as the reasons for the failures remain unclear, although possible explanations are being considered. These include inadequate dosage and timing with respect to radiation, as well as inaccuracy of the preclinical models used for predicting a response in human GBM [42].

Another strategy is to target DNA repair facilitated by poly ADP ribose polymerase (PARP) through the use of PARP inhibitors (PARPis). These molecules block the base excision repair pathway which leads to an increase in single strand breaks present within cells of the tumour, rendering it unstable [102, 103]. PARPis gained notoriety through two landmark papers presented in the journal Nature, which demonstrated a synthetic lethal interaction between PARPis and homologous recombinant-deficient breast cancer cells [104, 105]. More recent studies indicate synergistic interactions between PARPis and TMZ, as well as with radiotherapy. More importantly, this strategy could sensitise both MGMT methylated and unmethylated GBM. Numerous studies have also established PARPis as radiosensitizers [106, 107]. Radiosensitization based on the inhibition of key DNA damage response proteins is not a novel strategy, emerging initially in the 1980s and 90s. Indeed, many of the most clinically relevant inhibitors against key DNA damage response and repair proteins were developed within the last 25 years. However, as our understanding of GBM and the genetic surrounding this tumour type have evolved, interest in this approach has re-emerged, and is certainly warranted [42].

The cancer stem cell

As the GBM microenvironment is heterogeneous in nature, and our understanding of cancers show that they arise from mutations in a single or a few founder cells, the presence of cancer stem cells (CSCs) within tumours can be expected. CSCs were first identified and isolated in the late 1990s [108], and not long after, in 2004, Galli and colleagues reported for the first time the presence of CSCs in human GBM [109]. Self-renewing and tumorigenic CSCs contribute to tumour initiation and have been shown to be resistant to standard chemo- and radiotherapy, underscoring their role in disease progression and recurrence.

To effectively eliminate CSCs, it is critical to target their essential functions and their interactions with the microenvironment. Treatment with TMZ may be able to kill CSCs that

contain a higher expression of the DNA repair protein O^6-alkylguanine DNA alkyltransferase, however TMZ cannot prevent self-renewal of CSCs that contain the MGMT gene [110-112]. A potential strategy would be the use of PARPis to enhance apoptosis under genotoxic damage [102]. Additionally, glioma CSCs reprogram their metabolic machinery and preferentially take up glucose to survive in environments with limited nutrients, through the expression of the high-affinity isoform of glucose transporter 3. The membrane protein glucose transporter 3 therefore represents a promising therapeutic target for potential selective inhibition of CSCs. The inability of standard cancer therapies to efficaciously eliminate CSCs has led to a myriad of studies to identify novel selective inhibitors of these cells. Salinomycin, an ionophoric peptide, was subsequently found to be a potent anti-cancer agent as it inhibits the growth of various immortalized cancer cells both *in vivo* and *in vitro*. In effect, salinomycin reduced the fraction of CSCs by >100-fold compared to paclitaxel (PTX) [113]. However, the underlying mechanisms of action of this compound are yet to be fully understood, although Wnt suppression, p-glycoprotein inhibition, and reactive oxygen species production have been associated with salinomycin-mediated anti-cancer effects [114]. The promising attributes salinomycin brings to the fight against cancer has led to intensive research in investigating the antineoplastic effects of this molecule and its potential clinical use for the treatment of GBM [115].

Breaking the barrier to the brain

The BBB, or more specifically – crossing the BBB – is another major hurdle for effective treatment in GBM. As the appellation suggests, the BBB is a “barrier”, through which only small (< 500 Daltons), lipid soluble molecules can readily penetrate into the CNS [116]. Some drugs appear to penetrate the CNS at high levels, such as TMZ or the nitrosoureas carmustine, lomustine, and semustine. Low to moderate CNS penetration could be partially overcome by administering higher systemic doses, although extracranial toxicity limits the use of this strategy [42]. Strategies to circumvent the BBB have been developed and are continuously studied, the most promising of which are described below.

Direct delivery of therapeutics to the brain can be achieved through convection enhanced delivery (CED), a technique which allows the delivery of drugs directly to the tumour and the surrounding interstitium via a catheter inserted into the tumour under stereotactic guidance. Therapeutic agents can then be infused into the brain tissue under positive

pressure. Even though technological limitations currently prevent CED from being reliable and reproducible, advancements in catheter design and placement as well as in imaging techniques are being made, and with phase III clinical trials underway, CED may yet find a routine place in treating GBM [117].

The use of ultrasound to disrupt the BBB in a non-invasive manner, although not a novel concept [118], is also being investigated for mediating drug delivery. Focused ultrasound sonication in the presence of a bolus of microbubbles has been shown to temporarily open the BBB, allowing entry of systematically administered agents into the brain [119]. Indeed, focused ultrasound was recently shown to enhance delivery of Bevacizumab into the CNS in an animal model of GBM [120]. In addition, the interim results of an ongoing phase 1/2a clinical trial investigating the repeated opening of the BBB using ultrasound, in conjunction with systemic microbubble injections, show that the procedure is both safe and well tolerated in patients with recurrent GBM [121]. The potential to optimise chemotherapy delivery to the brain is evident, although the methodologies still need a little more development before introduction into the clinic.

Peptide carrier-mediated delivery of anti-cancer agents to the CNS has also been under investigation. Peptide carriers, such as K16ApoE, are able to transport various anti-cancer agents to the brain by mimicking a ligand-receptor system. A transient BBB permeability is induced by the peptide carrier, which in turn is used for the non-covalent delivery of chemotherapeutic drugs. This particular strategy offers an avenue for preclinical evaluation of drugs presenting a low to moderate CNS penetration [122]. Certain carriers may also offer significant advantages, such as enhanced drug solubility, more efficient biodistribution, reduced side effects through controlled release, as well as cost effective benefits [123].

Another strategy, which represents the most innovative medical approach today is nanomedicines (see section 2.2). Numerous studies have demonstrated the advantages of nanomedicines in the diagnosis and therapy of cancer. Nanomedicines, usually referred to as nanoparticles, which have the ability to carry drugs across the BBB, and can be lipid based, polymeric, and inorganic in nature [124, 125]. The encapsulation of anti-cancer agents into nanomedicines, offers significant advantages such as increased solubility, extended retention time and stability, controlled release, selective targeting, and reduced side effects [126]. Nanomedicines can be administered either locally or intravenously. Local

administration is usually performed via the CED technique, as diffusion and convection take place simultaneously with this method. By using convection to supplement simple diffusion, an enhanced distribution of small and large molecules can be obtained in the brain, while achieving greater than systemic levels of drug concentrations [127]. For intravenous administration, nanoparticle surface modifications are needed to facilitate crossing the BBB. In some cases, nanomedicine can form a hydrogel, allowing it to be delivered directly into the resection cavity [128].

A strategy that has been extensively studied and that has shown potential is the use of hydrogels, as their unique properties make them ideal candidates for local delivery of anti-cancer agents (see section 2.1). Hydrogels are three-dimensional, cross-linked networks of water soluble polymers that are able to imbibe large amounts of water or biological fluid without the dissolution of the polymer – an attribute due to their hydrophilic but cross-linked structure [129]. Loaded hydrogels can be administered directly into the brain following craniotomy via intracerebral implantation or intracerebroventricular injection, either within the tumour or following resection [130-132].

Overcoming the resistance

Crossing the BBB and delivering the appropriate chemotherapeutic agent is one thing, but another issue of GBM also poses an obstacle in effective treatment – therapeutic resistance. Although the mechanisms remain unclear, three repair systems – MGMT, mismatch repair, and base excision repair – have been associated with ineffective GBM treatment with TMZ [133, 134]. MGMT gene silencing, through methylation, has been correlated with TMZ treatment outcome [111]. Approximately 40% of GBM have a methylated MGMT promoter, which in effect turns of the MGMT gene, resulting in loss of protein expression, and thus higher levels of O_6-methylated guanine causing tumour cell death [135]. Methylated MGMT tumours have an elevated sensitivity to TMZ [111]. Median survival time is significantly higher for MGMT methylated versus unmethylated tumours [42, 136]. As 60% of patients present an unmethylated MGMT gene, there is great interest in developing novel methods to sensitise these tumours through MGMT inhibition. Clinical studies suggest that MGMT inhibitors, such as O^6-benzylguanine, and the more recent O^6-(4-bromotenyl) guanine, or anti-MGMT small interfering Ribonucleic Acid (siRNA) [137], could be administered to re-sensitise tumour cells prior to alkylator therapies [133, 138]. Currently, two TMZ analogues,

the imidazotetrazines DP68 and DP86, are in development and show anti-glioma activity which is independent of MGMT status [139].

In the majority of GBM, aberrant epidermal growth factor receptor (EGFR) activity through overexpression, amplification or mutation of this receptor can be observed. EGFR expression has been linked to an increased proliferation, resistance to chemotherapy, invasion, and apoptosis, and consequently to a decreased patient survival [140]. Several small-molecule adenosine triphosphate mimetics that inhibit EGFR-associated kinase activity have been identified, such as erlotinib, gefitinib, GW572016 and AEE788. Clinical trials involving gefitinib and erlotinib have been conducted, however both compounds failed to demonstrate any correlation between EGFR expression and treatment response or resistance. Additional strategies that inhibit EGFR are currently being evaluated in preclinical studies, such as transforming growth factor alpha-*Pseudonomas* exotoxin, cetuximab, ABX-EGF, EMD720000 and h-R3, Y10 and Mab 806 antibodies [140]. Preclinical studies investigating anti-EGFR siRNA strategies also seem to hold promise [127].

Increased malignancy in human astrocytic tumours – ranging from low-grade astrocytoma to malignant glioma – was shown to be correlated with increased expression of galectin-1. This glycan-binding protein promotes GBM aggressiveness in part by stimulating angiogenesis, and in part by its role in tumour-mediated immune evasion and its expression on tumour-associated endothelial cells [141]. Galectin-1 expression was observed to be significantly higher in high-grade astrocytomas of patients with short-term survival periods compared to patients who lived longer [142]. Furthermore, it has been shown that radiotherapy stimulates galectin-1 expression in GBM cells, while hypoxic conditions also promote an increase of expression. Galectin-1 is negatively regulated by p53, which triggers an apoptotic response to cellular stress such as chemotherapy, but could lead to chemoresistance if p53 functionality is lost. Studies involving anti-galectin-1 siRNAs to knock down its expression are currently being conducted *in vitro* and *in vivo*, with results showing that silencing tumour-derived galactin-1 promising and realistic adjuvant treatment modality [127, 141, 143].

2. LOCAL DELIVERY AND NANOMEDICINES FOR GLIOBLASTOMA TREATMENT

Among central nervous system tumors, GBM is the most common, aggressive and neurological destructive primary brain tumor in adults. Standard care therapy for GBM consists in surgical resection of the accessible tumor (without causing neurological damage) followed by chemoradiation. However, several obstacles limit the assessment of tumor response and the delivery of cytotoxic agents at the tumor site, leading to a lack of effectiveness of conventional treatments against GBM and fatal outcome. As previously cited in section 1 of this chapter, many drugs have been tested *in vitro* on GBM cell lines for their use against GBM. However, some of them have failed in showing clinical success because their CNS concentrations after rate-limiting systemic dose administration is too low. This is one of the reasons why the number of compounds on the market for the management of GBM is limited. Among the strategies that have been adopted in the last two decades to find new and efficacious therapies and drug delivery strategies for the treatment of GBM, the local delivery of chemotherapeutic drugs in the tumor resection cavity and the use of nanomedicines emerged. These two approaches might increase the local concentration at the tumor side reducing systemic side effects, opening the doors for many more drugs to be used against GBM.

In this chapter, our aim is to provide an overview on hydrogels loaded with anticancer drugs and lipid nanocapsules loaded with anticancer drugs for the treatment of GBM recently used in preclinical and clinical studies.

2.1. LOCAL DELIVERY

2.1.1. Local delivery for the treatment of glioblastoma

Brain is a soft tissue characterized by a unique microenvironment maintained by internal and external mechanisms of defense (skull and vertebral column, meninges, cerebrospinal fluid (CSF), CNS barriers) [2]. Many strategies have been developed to circumvent the CNS barriers and reach therapeutic concentrations of chemotherapeutic drugs in brain tumors. Among them, small lipophilic drugs have been used to passively pass the BBB while others

have tried to modify the BBB permeability or used focused ultrasounds to transiently open the BBB for drug delivery [144]. Active compounds have also been modified or incorporated into nanocarriers in order to reach the brain parenchyma by passive targeting or active targeting of the BBB endothelial cells [145]. The passive targeting is the transport of nanocarriers through leaky tumor capillary fenestrations into the tumor interstitium and cells by convection or passive diffusion, followed by their selective accumulation thanks to the enhanced permeability and retention (EPR) effect [146]. The active targeting consists in the use of ligands grafted to the surface of the nanocarriers to bind selectively receptors that are overexpressed in tumor cells or tumor vasculature and not expressed by normal cells [146].

Among the strategies that have been adopted in the last two decades, there is the local delivery of chemotherapeutic drugs in the tumor resection cavity. Local drug delivery, using implantable or injectable systems with sustained drug release characteristics, aims at preventing the growth of cancer cells that cannot be resected by surgery [147]. GBM cells are highly infiltrative throughout the brain but they do not disseminate via the lymphatic system meaning that they are unable to metastases outside the CNS [5]. In more than 90% of cases the formation of recurrences appears in the resection margins or within several cm of the resection cavity [148]. For these reasons the use of local delivery strategies that increase the drug concentrations at the tumor site avoiding systemic side effects without interacting and/or interfering with the CNS barriers and without modifying the drug chemical structure and pharmacological properties is a promising strategy for the treatment of GBM.

Direct injection of chemotherapeutics into the tumor resection cavity, surrounding brain parenchyma and/or into the ventricle via repeated needle-based injection or catheter implants connected to a reservoir was the earliest strategy used for GBM local drug delivery. This method is simple and can be easily repeated, large volumes of drugs can be injected with minimal systemic toxicity and can be adapted for continued delivery of chemotherapeutics [27]. However, the depth of distribution of the drug from the injection site is often very limited (<3 mm) and repeated surgeries are needed, leading to an increased risk of local side effects (e.g. intracranial hemorrhage, infections). Another approach that has been widely studied for the local treatment of GBM is the convection-enhanced delivery

(CED). This consists in direct continuous infusion of an agent in the brain parenchyma using a micro-catheter connected to a pumping device. This device is able to create a pressure gradient that allows the drug to distribute further in the brain tissue compared to the method previously described (2-3 cm) [27, 149], and for this reason is the preferred administration pathway for the local delivery of nanomedicines [150]. However, its reservoir needs to be continually refilled and the drug distribution depends on the infusion parameters (volume, rate and duration of infusion), the device design and the drug characteristics. Moreover, neurotoxicity can be induced by the infusate backflow in the catheter or by the leakage of the therapeutic agent out of the brain parenchyma into the cerebrospinal fluid [27, 151, 152].

Another approach is the craniotomy-based drug delivery. This consists in the use of drug-impregnated gels, nanoparticles or polymeric-based delivery systems (such as films, disks, rods or wafers) that can be implanted or injected in the resection cavity and are able to guarantee a sustained release of the drug in the surrounding brain tissue by degradation (if biodegradable) or diffusion (if non-biodegradable) [153].

The most-successful drug delivery implant, and the only one approved by the regulatory agencies for the treatment of newly-diagnosed and recurrent GBM, is the Gliadel® wafer. This is a biodegradable co-polymer formed of 1,3-bis-(p-carboxyphenoxy)propane and sebacic acid (SA) in a 20:80 ratio (polifeprosan 20) impregnated with the chemotherapeutic drug BCNU [153]. Polifeprosan 20 is able to protect BCNU from degradation and release it over time. The recommended dose of BCNU is 61.6 mg, represented by 8 wafers (7.7 mg BCNU each) that are implanted intracranially to fill the resection cavity. The integration of BCNU into a controlled-delivery wafer allows to circumvent the BBB and release high drug concentrations in the resection cavity [154]. Prolonged overall survival was observed with Gliadel® compared to placebo-treated patients (13.9 months *vs* 11.6 months, respectively), and low systemic toxicities were observed (gastrointestinal disorders, asthenia, fever and depression). On the other side, serious local side effects include seizures, intracranial hypertension, meningitis, cerebral edema, impaired neurosurgical wound healing, wafer migration [155-157]. Gliadel® wafers release the drug in approximately three weeks, but *in vivo* studies in mammalian models showed that the majority of the drug release takes place in the first 5-7 days [155]. For what concerns the drug penetration depth, in different animal

models, high concentrations of drug were observed adjacent to the polifeprosan 20 implants (3-6 mm from the polymer/tissue interface during the first 7 days, 2-3 mm for the next two weeks) while low drug concentrations were observed in distant regions of the brain [158-160]. The use of Gliadel® wafers in the clinics is controversial and its potential benefit in terms of life expectancy must be balanced to its potential toxicity and cost-effectiveness [154].

Since only one third of GBM patients are responsive to alkylating agents [161] and Gliadel® wafers show some inconvenients (poor drug diffusion and fast drug release, one-drug system, implant dislodgement, big resection cavity size needed), several groups tried to improve the efficacy of polymer-mediated implants for the controlled release of other chemotherapeutic drugs in the GBM resection cavity (Table 3). For example, polyanhydride polymers (pCPP:SA at different ratios) wafers were loaded with paclitaxel (PTX), mitoxantrone, camptothecin, doxorubicin, minocycline and, more recently, riluzole and memantine. They were safely and effectively delivered intracranially in animal models and their efficacy has been tested in different GBM models [162-167]. Rapamycin was incorporated into biodegradable caprolactone-glycolide polymer beads and tested *in vivo* in combination with radiotherapy for the local treatment of GBM [168]. Manome *et al.* developed and tested an implantable drug-conjugated device of doxorubicin-PLGA [169] while Von Eckardstein *et al*. developed a PTX/carboplatin liquid crystalline cubic phases and implanted it in the surgical resection cavity of GBM patients in a pilot study that showed its feasibility and safety. Another pilot study has been realized on GBM patients using 6-carboxylcellulose plates loaded with cisplatin, however the clinical benefit of these two last approaches remain to be examined in further clinical studies [170, 171]. A controlled-release ethylene-vinyl acetate co-polymer has been loaded with camptothecin and showed a controlled release over at least 21 days. Due to its low solubility, the efficacy of camptothecin in a GBM model was greatly enhanced by intracerebral implantation using this polymeric delivery system [172].

Table 3. Examples of polymeric implants developed for intracranial implantation and tested for the local treatment of GBM in preclinical and clinical studies

Local delivery system	Drug	Clinical stage	Reference
pCPP:SA wafer	BCNU	FDA approved	[156]
	PTX	Preclinical	[163]
	mitoxantrone	Preclinical	[162]
	DOX	Preclinical	[165]
	camptothecin	Preclinical	[164]
	minocycline	Preclinical	[166]
	riluzole + memantine	Preclinical	[167]
6-carboxylcellulose plates	cisplatin	Pilot study	[171]
open cell polylactic acid solution	cisplatin	Preclinical	[173]
caprolactone-glycolide polymer beads	rapamycin	Preclinical	[168]
Drug-PLGA implant	DOX	Preclinical	[169]
Liquid crystalline cubic phases	PTX + carboplatin	Pilot study	[170]
EVAc polymer	camptothecin	Preclinical	[172]
PLGA wafer	BCNU	Preclinical	[174]
PLGA microassemblies implants	PTX	Preclinical	[175-178]
	PTX + etanidazole	Preclinical	[179]
	5-FU	Phase II	[180]
	Carboplatin	Preclinical	[181]
	BCNU	Preclinical	[181]
Nanofiber membranes	BCNU + irinotecan + cisplatin	Preclinical	[182]

Legend: pCCP:SA: 1,3-bis-(p-carboxyphenoxy)propane and sebacic acid; EVAc: ethylene-vinyl acetate co-polymer; PLGA: poly(lactic-co-glycolic acid); BCNU: carmustine; PTX: paclitaxel; DOX: doxorubicin

On the other side, a wide range of active compounds (both liphophilic and hydrophilic) has been incorporated in degradable polymeric microspheres and extensively studied for the local treatment of GBM. In particular, promising preclinical studies were obtained using microspheres encapsulated with PTX, 5-Fluorouracil, Carboplatin or BCNU following direct intracranial injection (peritumorally, intratumorally or in the tumor resection cavity) or pressed into disks or wafers for implantation in the resection cavity [175, 176, 183-186]. PTX has also been loaded in PLGA microfiber disks, sheets, foams or wafers with different form and geometry alone or in combination with Etanidazole, obtaining good pharmacokinetic and diffusion profiles and promising preliminary efficacy results *in vivo* [174, 177-179]. The 5-Fluorouracil encapsulated PLGA microspheres injected locally with concomitant radiotherapy reached good results in phase I and II clinical trials. However, the median overall survival between groups was not sufficiently different as to show a significant result [180, 187]. Other chemotherapeutic polymer-based systems have also been developed to be injected as solutions peritumorally or in the resection cavity or to be placed on top of the cerebral cortex [173, 174, 181, 182, 188, 189].

Many interesting reviews have been recently published related to many different aspects of GBM management, challenges and future options [27, 30, 144, 145, 183, 190-193]. Here, we will focus on a relatively novel approach that, we believe, holds great potential: the hydrogels, conceived as chemotherapeutic drugs reservoirs and delivery platforms for the local treatment of GBM.

2.1.2. Hydrogels for the treatment of glioblastoma

Hydrogels are three-dimensional (3D) polymeric and hydrophilic networks able to imbibe large amounts of water or biological fluid without the dissolution of the polymer due to their hydrophilic but crosslinked structure. Hydrogels exhibit a thermodynamic compatibility with water which allows them to swell in aqueous media [194]. Hydrogels are used for numerous applications in the medical and pharmaceutical field, for example as membranes for biosensors, materials for contact lenses or artificial skin, linings for artificial hearts. Moreover, they are used for 3D cell culture and as drug delivery devices [194-196].

Hydrogels also emerged as excellent candidates for controlled release, bioadhesive and/or targeted drug delivery as they are able to encapsulate biomacromolecules including proteins

and DNA as well as hydrophilic or hydrophobic drugs [197]. Hydrogel-based drug delivery systems can be used for oral, rectal, ocular, epidermal, and subcutaneous applications [194]. A key point in the success of hydrogels development is the *in situ* gelation. This can be achieved by ultraviolet (UV) polymerization, introducing non-reversible covalent bonds, or via self-assembly by either reversible interactions or non-reversible chemical reactions. The gelation can also be time-dependent or be triggered by specific stimulus (e.g. pH, temperature, light, etc.) [198].

In the field of GBM, hydrogels have been used i) as mimicking platforms in 3D *in vitro* tumor microenvironment models to study the tumor cells biology, motility, migration and angiogenesis behavior [2, 199, 200]; ii) as tools for preclinical screening to grow *ex vivo* cultures of GBM and assess their sensitivity to radiation and drugs [201] iii) as anticancer drug delivery systems for the treatment of GBM.

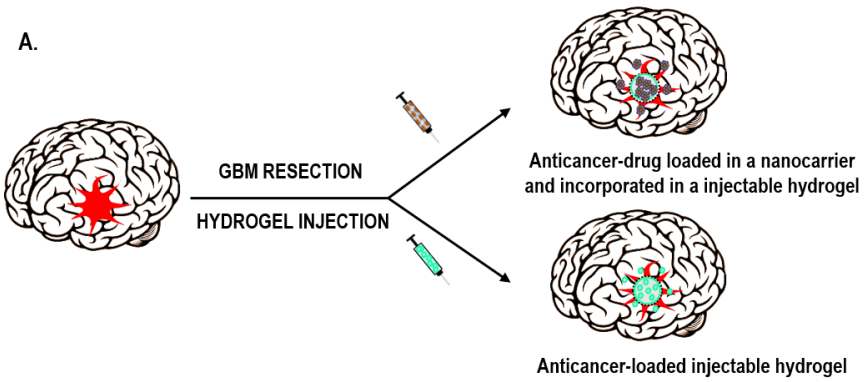

B. IDEAL DRUG-LOADED HYDROGEL FOR THE TREATMENT OF GBM

- Sterile
- Injectable and implantable *in situ*
- Rheological properties close to brain modulus and able to mechanically mime CNS microenvironment
- Adhesion to resection cavity border
- Sustained drug release over one month with initial controlled burst effect
- Biocompatible, non-immunogenic and biodegradable within 6 to 12 months
- Do not allow cell infiltration

Figure 5: **(A)** Schematic representation of the use of anticancer-loaded hydrogels for the treatment of GBM; **(B)** Optimal characteristics that a hydrogel should possess to be efficiently used as treatment for GBM

In this chapter, we will focus on the description of anticancer drug-loaded hydrogels for the treatment of GBM. These systems are directly administered in the brain after a craniotomy via intracerebral implantation or intracerebroventricular injection. They can be administered intratumorally or in the surgical resection cavity [145]. In some cases, the drug is directly loaded in the hydrogel matrix while some authors have incorporated anticancer-loaded nanomedicines into the hydrogels, in order to prolong the sustained release of the drug (Figure 5A). Even if the administration of hydrogels in the GBM resection cavity is very little described in the literature, this route of administration seems very promising due to its clinical relevance. An optimal anticancer-loaded hydrogel for the treatment of GBM should have the characteristics reported in Figure 5B.

Hereunder is presented a non-exhaustive examples list of recent developments in the use of hydrogels for the delivery of anti-cancer drugs in the treatment of GBM (Table 4).

Table 4. Non exhaustive list of anticancer-loaded hydrogels developed for intracranial implantation and tested for the local treatment of GBM

Hydrogel matrix	Active agent	Type of study	Reference
PLGA:plasticizers (40:60)	TMZ	C6 rat glioma resection model	[202]
ReGel™	PTX	Phase 1/2 dose escalation study	[203, 204]
PLGA/PEG microparticles	Trichostatin A, etoposide, methotrexate	*In vitro* studies	[205]
PEG-DMA and water (75:25)	TMZ	U-87 MG subcutaneous GBM xenograft model	[206]
Poly(organophosphazene) hydrogel	Irinotecan	U-87 MG orthotopic GBM xenograft model	[207]
Mebiol™Gel	Free or encapsulated DOX	U-87 MG subcutaneous GBM xenograft model	[208, 209]
	Campthotecin-loaded PLGA microspheres	C6 rat glioma orthotopic and resection models	[210, 211]
Polyvinyl alcohol hydrogel with sulfonate groups and 0.6 % alginate solution	DOX	9L rat orthotopic glioma model	[212]
Alginate	PTX-loaded PLGA microspheres	U-87 MG-luc2 orthotopic GBM xenograft model	[213, 214]
Vesicular phospholipid gels	Cytarabine	U-87 MG subcutaneous GBM xenograft model	[215]
Phospholipid gel	PTX	C6 rat glioma orthotopic model	[216]
Chitosan/β-glycerophosphate hydrogel	Ellagic acid	*In vitro* studies	[217]
PEG-*g*-Chitosan hydrogel	T lymphocytes	*In vitro* studies	[218]
PEG diacrylate-based hydrogel	Peptide-cisplatin prodrug	*In vitro* studies	[219]
PEG-MMA / PEG-DMA hydrogel	PTX-loaded iron oxide nanoparticles	*In vitro* studies	[220]
Monomethoxy PEG-PLGA nanocomposite hydrogel	PTX and TMZ	*In vitro* studies	[221]

Legend: PLGA: poly(lactide-co-glycolide; PEG: polyethylene glycol; PEG-DMA: polyethylene glycol dimethacrylate; PEG-MMA: polyethylene glycol methacrylate; TMZ: temozolomide; PTX: paclitaxel; DOX: doxorubicin; $GemC_{12}$: lauroyl-gemcitabine.

PLGA-based hydrogels

Hydrophobic polymeric networks can be constructed with poly(lactic acid) PLA or poly(lactide-co-glycolide) PLGA. PLGA is one of the most successfully used biodegradable polymers because its hydrolysis leads to the formation of lactic acid and glycolic acid. These two monomers are endogenous and easily metabolized by the body via the Krebs cycle, therefore minimal systemic toxicity is associated with the use of PLGA for drug delivery or biomaterial applications. PLGA is approved by the FDA and EMA in various parenteral drug delivery systems in humans and the polymers are commercially available with different molecular weights and copolymers composition. Nevertheless, PLGA-based hydrogels have limited water absorption capabilities (<5-10 wt.%) [222, 223].

A biodegradable gel matrix for the delivery of TMZ constituted by PLGA:plasticizers (40:60) was developed by Akbar *et* al. The plasticizers were acetyl triethyl citrate and triethyl citrate (30:30). To test their drug delivery system in a clinically relevant model, this group developed a surgical resection model for intracranial C6-green fluorescent protein glioma in rats. A significant reduction of tumor load was observed in the 30% TMZ group compared to blank control (94% reduction in tumor load) [202].

OncoGel™ was tested as adjuvant to radiation therapy in an intracranial 9L gliosarcoma model, alone or in combination with temozolomide and radiation therapy by Tyler *et* al. [203, 204]. OncoGel™ is a non-Cremophor® EL based formulation of PTX in ReGel™, designed for the local delivery of PTX for the treatment of solid tumors. ReGel™ is a copolymer of PLGA and polyethylene glycol (PEG) and it is an environmentally-sensitive controlled release delivery system. Indeed, ReGel™ is a low viscous solution at temperatures between 2 and 15 °C and become a viscous, water insoluble biodegradable controlled-release gel at body temperature. Its biocompatibility has been extensively demonstrated using different preclinical settings (three animal species, various tissues and administration pathways). OncoGel™ can be injected in the proximity of the tumor (e.g. via intralesional injection or placement into the tumor cavity) and offers a controlled release of PTX during 6 weeks maintaining high local concentrations. OncoGel™ has been evaluated in three completed clinical studies in superficially accessible solid tumors and in combination with radiotherapy in esophageal cancer [224]. An interventional study started in 2007 in order to evaluate the

safety and tolerability of this system in the GBM tumor resection cavity (Phase 1/2 dose escalation study of locally-administered OncoGel™ in subjects with recurrent glioma) but it has been terminated for sponsor business decision.

A novel thermosensitive formulation of chemotherapeutic drug-loaded PLGA/PEG microparticles able to form matrices that mold around the resection cavity walls was developed by Rahman *et* al*.* These microparticles have the consistency of a free-flowing powder at room temperature but they create a paste when mixed with a saline-based carrier solution. Although the formed matrices cannot be really defined as hydrogels, we believe that this system can be taken into account in this section due to its physico-chemical properties and use. Indeed, the formulation can be injected or pasted at room temperature until it gradually solidifies into a solid, porous matrix at body temperature. The *in vitro* release kinetics of different drugs (Trichostatin A, etoposide and methotrexate) suggest that they could gradually release the active ingredients over time. Moreover, the matrices properties are not affected by irradiation meaning that they could be used in a combination regimen and no *in vitro* cytotoxicity was observed with drug-free matrices [205].

Photo-polymerizable hydrogels

Photopolymerization is a technique that uses light (visible or UV) to initiate and propagate a polymerization reaction to form a linear or crosslinked polymer structure. The use of photopolymerization has thus been proposed for the production of biomaterial-based polymer networks for specific biomedical applications (e.g. drug delivery) [225]. In particular, photopolymerized polymer networks can be used in tissue engineering due to their capacity to entrap a wide range of substances and cells [226].

A photopolymerizable hydrogel was developed for the delivery of TMZ as a possible local treatment for GBM. This injectable hydrogel consisted in a mixture of PEG dimethacrylate (PEG-DMA) and water (75:25), while 0.5% of Lucirin-TPO® was used as photoinitiator. When this solution was irradiated with a light at 400 nm during 15 s, the hydrogel was rapidly formed (<2 min) and presented a viscous modulus (≈ 10 kPa). The TMZ *in vitro* release kinetics was characterized by a linear burst release of 45% of TMZ during the first 24h, followed by a logarithmic release of 20% over the first week. An *in vivo* short-term tolerability study showed that the unloaded hydrogel did not induce apoptosis in mice brains nor increased microglial activation. The anti-tumor efficacy of this hydrogel was evaluated in

nude mice on a subcutaneous human GBM model, which showed that the tumor growth of mice treated with the photopolymerized TMZ hydrogel significantly decreased compared to the controls [206].

Theranostic hydrogels

Hydrogels constitute excellent candidates for theranostic applications. Indeed, the combination of treatments within an imaging platform, could allow to (*i*) assess noninvasively the biodistribution and target site accumulation of the drug, (*ii*) control the drug release, (*iii*) enhance the therapeutic efficacy via triggered drug release and (*iv*) predict the therapeutic response [227]. Extensive research attempts to monitor the drug delivery to brain tumors using MRI. For this reason, hydrogels containing MRI contrast agents have been developed to monitor the drug response or to improve the tumor delineation before surgical resection [228]. For instance, Kim *et* al. designed an injectable 'MRI-monitored long-term therapeutic hydrogel' for brain tumors (MLTH) [207, 229]. Authors synthesized a thermosensitive/magnetic poly(organophosphazene) hydrogel containing both an anticancer drug (the active metabolite of irinotecan SN-38) and a hydrophobic $CoFe_2O_3$ magnetic core. Using the MLTH, authors succeeded in delivering SN-38 to rodent U-87 MG brain tumors. MRI experiments at 7 Tesla allowed distinguishing MLTH-treated and non-treated areas of brain tumor regions. Moreover, the *in vivo* long-term inhibition tendency of tumor growth demonstrated the potential of the MLTH system as MRI-monitored therapeutic agent [207].

Another example of theranostic hydrogel is the pH/temperature sensitive magnetic nanogel containing contrast agents for MR and fluorescence imaging. This nanogel, developed by Jian *et* al., is intended for systemic use but has the ability to accumulate in the rat brain acidic tumor microenvironment [230]. Indeed, superparamagnetic iron oxide (SPIO) nanoparticles loaded poly(N-isopropylacrilamide-*co*-acrylic acid) nanogels were conjugated with Cy5.5-lactoferrin for targeting *in vivo* rat C6 glioma tumors. The grafted Cy5.5 fluorophore allowed fluorescence imaging, SPIO allowed the MR detection of nanoparticle accumulation in brain tumors, while the lactoferrin is a ligand of low-density lipoprotein receptor-related protein 1 (LRP-1), which is overexpressed in GBM [231].

Other types of anticancer drug-loaded hydrogels

Some groups used the thermoreversible gelation polymer (TPG) as a novel drug delivery system for the local treatment of GBM. TPG hydrogel (Mebiol^{TM}Gel), which is a gel at body temperature but a solution at room temperature, is composed of PEG conjugated with the thermoresponsive polymer poly-N-isopropylamide. Arai *et* al. evaluated the antitumor activity of TPG loaded with free or encapsulated doxorubicin (in PLGA microspheres or liposomes) in a subcutaneous human GBM xenograft model showing a significant inhibition in tumor growth when the drug is encapsulated [208, 209]. Ozeki *et* al. developed a campthotecin-loaded PLGA microspheres-containing TPG hydrogel and evaluated its therapeutic efficacy (comparison of survival) in a C6 rat glioma model and in a resection model of this tumor [210, 211]. The treatment with campthotecin/PLGA/TPG formulation exhibited significant survival compared with the untreated rats (26 *vs* 18 days respectively). Similar therapeutic effects were observed in the groups treated with campthotecin/PLGA/TPG alone and surgical tumor resection plus campthotecin/PLGA/TPG, but some long-term survivors (>60 days) were observed in this last group, meaning that the combination therapy could be a good strategy for this hydrogel [210].

In another study, doxorubicin eluting beads (CM-BC1) have been evaluated for their safety and efficacy in a 9L glioma model. The bead microspheres were produced from a polyvinyl alcohol hydrogel modified with sulfonate groups and mixed with 0.6 % alginate solution. This system shows a controlled loading and delivery of doxorubicin. The beads with a low dose of drug (1 mg/ml) showed to be well tolerated *in vivo* long term studies (6 months). *In vivo* efficacy studies of the beads administered alone or in combination with radiotherapy (3×6 Gy whole-brain irradiation) gave significant results compared to the untreated animals in terms of survival (44, 54 *vs* 26 days respectively). Interestingly, this system could be loaded with other therapeutic agents such as irinotecan, topotecan and mitoxantrone [212].

Alginate has been used to entrap PLGA-PTX microspheres in a solid hydrogel matrix in order to avoid initial burst effect and control the drug release from the microcarriers. This hydrogel has been designed and characterized, tested *in vitro* for its release pharmacockinetis and cytotoxicity and *in vivo* in a subcutaneous tumor study showing promising results. Moreover, using an intracranial human GBM xenograft model this hydrogel showed to significantly

inhibit tumor growth and the drug penetrates up to 5 mm from the implant site until 42 days post implantation [213, 214].

Vesicular phospholipid gels (VPGs) were loaded with cytarabine and characterized as local delivery depots for GBM treatment [215, 232]. These are phospholipid semi-solid dispersions made of numerous vesicles or liposomes that are tightly packed between each other's entrapping the aqueous phase in a reduced space, conferring the system a gel-like rheological behavior. Compared to conventional liposomes, the drug in the VPGs is distributed between inter- and intra-vesicles without concentration gradient, leading to high encapsulation efficiency. Moreover, VPGs have showed high stability to autoclave, responding to one of the main requisites of hydrogels for brain cancer use: the sterility [232]. The *in vivo* release of cytarabine from the gel was demonstrated for at least 28 days with a good drug bio-distribution profile and penetration depth after intracerebral injection. Moreover, the efficacy of this system has been tested in a human subcutaneous GBM model showing a good tumor-suppression compared to the free drug [215]. Recently, Chen *et* al. also used a phospholipid-based hydrogel to deliver PTX after intratumoral administration in rat brains. They proved a sustained release of the drug over time and superior anti-tumor efficacy compared to the free drug [216].

Another study developed a body temperature gelling chitosan/β-glycerophosphate hydrogel loaded with ellagic acid. Its biocompatibility and anti-tumor effect was tested *in vitro* on GBM cell lines (U-87 MG and C6 cells) to suggest its use as GBM treatment option [217]. A thermoreversible PEG-*g*-Chitosan hydrogel could serve as depot for the delivery of T lymphocytes for localized GBM immunotherapy, as suggested by Tsao *et al.* When implanted intratumorally, or in the resection cavity, the released T cells could come into contact with GBM cells and selectively kill them [218]. Another approach for the local treatment of GBM is the use of a PEG diacrylate-based hydrogel complexed with a peptide-cisplatin prodrug. Here, the linking peptide can be selectively cleaved by the matrix metalloproteases, which are highly expressed in GBM cells, releasing the active drug from the hydrogel in a controlled manner. When administered locally, this system is able to deliver a higher dose of the drug selectively to the most invasive portion of the tumor, which is where the matrix metalloproteases are located [219]. Alternatively, PEG methyl ether methacrylate / PEG dimethacrylate magnetic hydrogel containing iron oxide nanoparticles loaded with PTX was

synthesized and tested *in vitro* on M059K GBM cells as a proof of concept for its use as hyperthermia local treatment [220]. Xu *et* al. developed a PTX and TMZ-loaded polymer monomethoxy PEG-PLGA nanocomposite under the form of a thermosensitive gel. This gel presents optimal gelation and rheological properties for a local application in the brain and possesses much higher growth-inhibiting effect and apoptosis-inducing rate in U-87 MG and C6 cells compared to the controls [221]. However, the *in vivo* tolerability, biocompatibility and anti-tumor efficacy studies using established GBM animal models still need to be performed for these last systems. Moreover, a tunable diblock copolypeptide hydrogel and has been developed for the delivery of hydrophobic compounds and studied for local application in restricted sites of the CNS. Also if its application has not been tested specifically for the local treatment of GBM (nor *in vitro* or *in vivo*), its ability to incorporate TMZ could suggest its use for this purpose [233].

2.2. NANOMEDICINES

2.2.1. Nanomedicines for the treatment of glioblastoma

Nanotechnology concerns the use of systems or materials able to exhibit physical, chemical or biological effects thanks to their dimension, which is included in the nanoscale range [234]. Nanomedicine is the application of nanotechnology to medicine [235]. Nanomedicine involves the use of nanocarriers – systems of nano-sized scale able to entrap, load, conjugate or simply deliver one or multiple active agents – to face the challenges related to the delivery of these agents aiming at solving unmet medical and pharmaceutical needs.

In the past two decades, many papers have been published describing a wide variety of nanocarriers as delivery tools for the treatment of GBM (Figure 6) and some are currently on clinical trials [236]. Several parameters are crucial in the development of nanocarriers for drug delivery in the brain. The carrier should be biodegradable, biocompatible, non-toxic and its size should be lower than 100 nm. Surfactants or hydrophilic polymer coatings (e.g. PEG) can be grafted on the nanocarrier surface to prevent opsonization by plasma membranes, avoid clearance by the reticuloendothelial system and to prolong the plasma circulating time. However, the physicochemical properties must be controlled to prevent

immunological responses. Finally, the nanocarrier should be able to protect its content from degradation and release it in a sustained manner [145, 236].

Nanocarriers as delivery tools for the treatment of Glioblastoma:

Nanocarrier	Drug	Approach
Liposomes Polymeric micelles Polymeric nanoparticles Gold nanoparticles Solid lipid nanoparticles Lipid nanocapsules Aptamers Dendrimers Microspheres Micelles Nanoribbons Nanodisk particles Lipoprotein particles Nanoparticle conjugates	Alisertib, Bevacizumab, Carmustine, Cisplatin, Curcumin, Daunorubicin, Docetaxel, Doxorubicin, Etoposide, Ferulic acid, Ferrociphenol, 5-Fluorouracil, Gemcitabine, Indomethacin, Lucanthone, Paclitaxel, Salinomycin, siRNA, Silver, Spherical nucleic acid, Tamoxifen, Temozolomide	Local delivery Passive targeting Active targeting of the blood brain barrier Active targeting of tumor cells Dual active targeting

Figure 6. Examples of nanocarriers used as delivery tools for the delivery of different drugs against GBM. The total number of articles found on pubmed.gov with the search parameter "nanomedicine glioblastoma" was 190 on date 02.11.2017

Nanomedicines can (*i*) be locally administered in the brain; (*ii*) spontaneously reach the tumor environment thanks to their favorable size, surface charge, coating, hydrophobicity and to the BBB leaky fenestrations in high grade gliomas (e.g. [237-240]); (*iii*) be surface-grafted to reach the brain after systemic administration or to selectively kill GBM cells through active binding to overexpressed receptors (active targeting; e.g. Table 5).

Table 5. Examples of nanocarriers designed and tested in preclinical models for the active targeting of the blood-brain barrier, the GBM cells or both.

Nanocarrier	Targeting ligand	Binding molecule	Reference
Micelles	RGD peptide	$\alpha_v\beta_3$ integrins on GBM cells	[241, 242]
Liposomes	WGA	Adsorptive endocytosis in the BBB, receptor mediated endocytosis on GBM cells	[243]
Nanodisk particles	ApoE	Low density lipoprotein receptors and heparin sulphate proteoglycans	[244]
Polymeric NP	Tf	TfR on GBM cells	[245, 246]
	Chlorotoxin peptide	MMP-2 on GBM cells	[247, 248]
	ALMWP	MMP-2 and MMP-9 on GBM cells	[249]
	AS1411 aptamer	Necleolin protein on GBM cells	[250]
	IL-13p, RGD peptide	IL13Rα2 on GBM cells, αvβ3 integrins on neovasculature	[251]
	ITEM4 mAb	Fn14R in GBM cells	[252, 253]
Lipid nanocapsules	OX26 mAb	TfR on cerebral endothelium	[254, 255]
	NFL	Tubulin-binding sites of GBM cells	[256, 257]
Solid lipid NP	Anti-EGFR	EGFR on GBM cells	[258]
	APMP, folic acid	Glucose transporter 1 on BBB cells, folate receptor on GBM cells	[259]
Lipoprotein NP	LDL binding domain	LDR on GBM cells	[260]
Dendrimers	Tf, WGA	Tf receptor or adsorptive endocytosis on BMVECs and GBM cells	[261]

Legend: NP: nanoparticles; Tf: transferrin; TfR: transferrin receptor; WGA: wheat germ agglutinin; MMP: Matrix metalloproteinasis; ALMWP: activable low molecular weight protamine; IL-13p: Interleukin-13 peptide; Fn14R: fibroblast growth factor-inducible 14 receptor; mAb: monoclonal antibody; NFL: neurofilament light subunit-tubulin-binding site 40-63 peptide; APMP: p-aminophenyl-α-D-manno-pyranoside; LDLR: low density lipoprotein receptor; BMVECs: brain microvascular endothelial cells

Therefore, nanomedicine may offer significant advantages over conventional therapies by:

- hosting one or multiple active agents (e.g. chemotherapeutic drugs, nucleic acids, proteins, radiosensitizers or diagnosic tools),
- increasing the solubility and pharmacokinetic profile of the drug,
- protecting the active agent from degradation,
- delivering the drug by passing through the BBB,
- targeting specifically tumoral cells, reducing systemic side effects and protecting normal tissues from direct contact with the drug,
- improving tumor drug distribution and increase the local concentration of the drug in the tumor tissue,
- bypassing drug resistance mechanisms.

Some examples of nanocarriers and drugs used in preclinical or clinical trials for GBM are reported in Figure 6, but examining them all is beyond the scope of this chapter as literature is filled with systematic reviews on this subject (e.g. [125, 145, 191, 236, 262-265]). What is important to highlight is the extreme versatility of nanocarriers - in terms of variety of structures (e.g. components, surface characteristics, loading capacity), diversity of drugs that can be loaded, therapeutic approaches - which allows them to adapt to the needs required to face GBM challenges. Here, we want to focus on a class of nanocarriers that has been extensively reported as a promising delivery strategy for GBM treatment, lipid nanocapsules (LNC).

2.2.2. Lipid nanocapsules for the treatment of glioblastoma

LNC are hybrid biomimetic nanocarriers with a structure that resembles liposomes and polymeric nanocapsules, and able to mimic lipoproteins [145]. They have been developed and patented by Prof. Benoit Group (University of Angers) in 2000 and have been widely used and studied as drug delivery systems since then.

LNC are composed of three components: 1) an oily liquid core made of medium-chain triglycerides (Labrafac®); 2) a rigid shell of nonionic surfactant (e.g. Kolliphor® HS15) with PEG chain oriented towards the water phase and a small proportion of lipophilic surfactant (e.g. lecithin: Lipoid®; Span80®) anchored in the oily phase; 3) an aqueous phase made of water and sodium chloride. The proportion of each component plays an important role in the

formulation process parameters and it defines the physicochemical properties and stability of the final product [266, 267].

LNC are made of FDA-approved components by a solvent-free, soft-energy preparation procedure called “phase-inversion technique” process (Figure 7). This method is based on the changes in solubility of the nonionic surfactant, which becomes less hydrophilic at temperatures higher than the phase inversion zone (PIZ) leading to water in oil (W/O) emulsion (conductivity ~ 0 mS/cm), and more hydrophilic at temperatures lower than PIZ, leading O/W emulsion (conductivity ~ 35 mS/cm) [268, 269]. The phase inversion temperature is the temperature in which the hydrophilic and lipophilic properties of a nonionic surfactant balance [266].

The phase-inversion process consists in two steps: step 1 involves mixing all the components and heat them from room temperature to a pre-fixed temperature <PIZ to obtain a W/O emulsion. Then, three cooling/heating cycles are repeated between the maximum and minimum temperatures (~15°C higher and lower than the phase inversion temperature). The temperature range strongly depends on the salinity of the medium and must be chosen considering the thermostability of the drug to be encapsulated, to avoid its degradation during the formulation process. Step 2 involves an irreversible shock dilution during the last cooling process, induced by adding water to the formulation at a temperature ~1-3°C from the beginning of the O/W emulsion, followed by 5 min stirring. This dilution breaks the microemulsion system and leads to the formation of stable LNC [268].

LNC are colloidal monodispersed systems, with spherical shape and size in the 20-100 nm range. They generally present high encapsulation rates and long-term physical stability (~ 18 months at 4°C) [263, 268]. LNC can incorporate lipophilic and amphiphilic molecules, reversed micelles containing hydrophilic drugs, lipoplexes containing nuceic acids or radiopharmaceuticals and provide a sustained release of the active agents [263, 270]. The size and surface characteristics of LNC can be adapted to prolong their plasma half-life after systemic administration for passive targeting, to specifically recognize receptors for active targeting, or to be used for oral administration and local delivery of active agents [145].

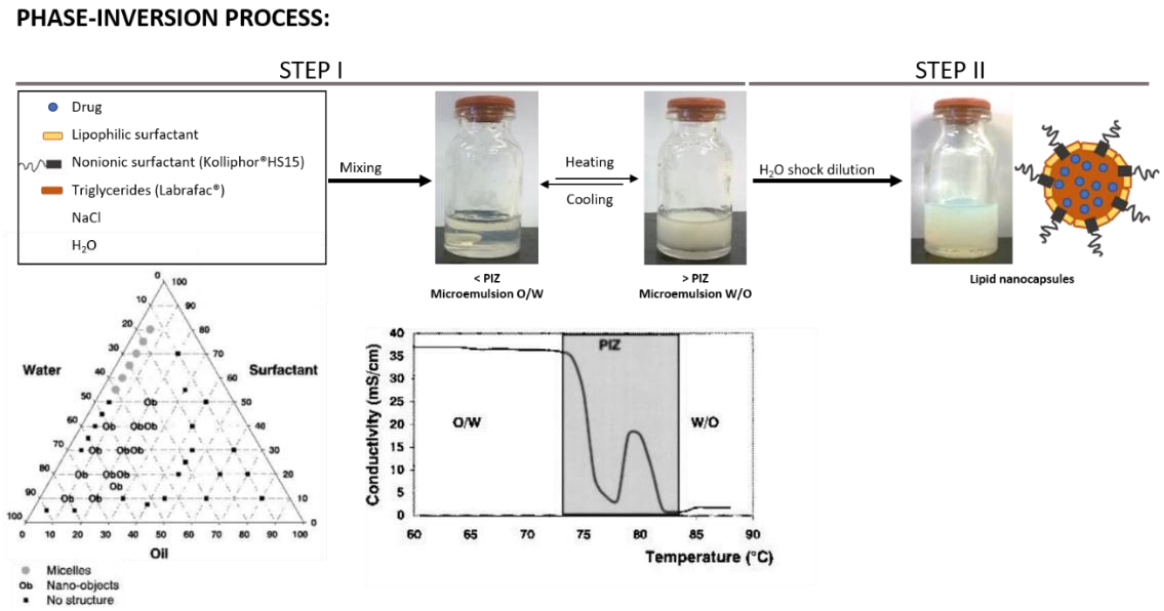

Figure 7. Lipid nanocapsules are prepared by a phase-inversion technique process. The components are mixed and heated under magnetic stirring from room temperature up to a fixed temperature above the phase-inversion zone (PIZ). Three cycles of cooling and heating are performed in the prefixed temperature range before inducing an irreversible shock by dilution with water during the last cooling process which leads to the formation of LNC. The lower images, adapted from [268], represent: the ternary diagram which represents the proportions of components (hydrophilic surfactant, water and oil) required to obtain the LNC with the phase-inversion process (left image); the evolution of the conductivity as a function of the temperature during the cooling/heating cycles (right image).

Several LNC formulations have been developed and studied for the treatment of GBM at preclinical stage (Table 6): LNC have been used as delivery systems for local or systemic administration of drugs (e.g. PTX; ferrociphenol – Fc-diOH), to deliver radionuclides able to induce internal radiation ([271-273]) or, more recently, as nanotheranostic tools to study how the *in vitro* cell conditions impact the tumor microenvironment *in vivo* ([274, 275]).

Table 6. Non-exhaustive list of preclinical *in vivo* studies involving the use of lipid nanocapsules as delivery tools for GBM treatment

Formulation	Active agent	Administration pathway	*In vivo* model	Reference
LNC	PTX	it injection or CED administration	F98 sc and 9L ort	[276, 277]
	^{188}Re-SSS	CED administration or it injection + CED	9L ort and Lab1 ort	[271-273]
	Fc-diOH	it injection or CED administration	9L sc and ort	[278, 279]
	Ansa-Fc-diOH	iv injection, multiple treatment	9L sc	[280]
	PFCE	it injection	U-87 MG ort	[274, 275]
DSPE-mPEG-LNC	Fc-diOH	iv injection or intra-carotid injection	9L sc and ort	[237, 281]
PEG-LAA-LNC	PTX	sc administration	9L sc	[282]
MIAMI-LNC	Fc-diOH	it injection	U-87 MG sc and ort	[283, 284]
NFL-LNC	Fc-diOH	intra-carotid treatment or CED administration	9L ort	[257]
	PTX	CED administration	GL261 ort	[256]
CS-LNC	anti-EGFR + anti-Galectin1 siRNA	CED administration	U-87 MG ort	[127]
	PTX + CpG	CED administration	GL261 ort	[285]

Legend: DSPE-mPEG2000: 1,2-Distearoyl-sn-glycero-3-phospho-ethanolamine N-methoxy-polyethylene glycol; PEG-LAA: carboxy-poly(ethylene glycol)-2000 2-alkyl-lipoamino acid derivative; MIAMI cells: marrow isolated adult multilineage inducible cells; NFL: neurofilament light subunit-tubulin-binding site 40-63 peptide; LNA: nuclease-resistant locked nucleic acid; CS: chitosan;PTX: Paclitaxel; ^{188}Re-SSS: bis-(perthiobenzoato) (dithiobenzoato) rhenium (III); Fc-diOH: ferrociphenol; siRNA: small interfering ribonucleic acid; EGFR: epidermal growth factor receptor; PFCE: Perfluoro-15-crown-5-ether; CED: convection-enhanced delivery; it: intratumoral; iv: intravenous; sc: subcutaneous model; ort: orthotopic model.

Lamprecht *et* al. and Garcion *et* al. were the first ones to show that Kolliphor® HS15-based lipid nanocapsules can reverse multidrug resistance mechanisms by interacting intracellularly with P-glycoprotein-related efflux pumps thus improving anticancer drug delivery [276, 286]. They also showed that LNC are rapidly (from 2 min exposure) accumulated in 9L and F98 GBM cells, through an active and saturating mechanism involving endogenous cholesterol (clathrin/caveolae-independent endocytosis pathway). The LNC

were firstly localized in the early endosome (2 minute esxposure) and then in the Golgi network (30-120 minutes exposure) while the presence in the lysosomes was weak, suggesting that they might distrupt the lysosomes integrity. No signs of LNC were found in the nucleus [276, 287]. Garcion *et* al. also encapsulated PTX in the oily core of LNC and showed, *in vitro* and *in vivo*, that the anti-tumor activity of PTX-LNC is significant increased compared to the free drug and that this effect can be enhanced by combination with radiation therapy [276, 277]. Basile *et* al. conjugated carboxy-PEG lipoamino acid residues to the PTX-LNC surface to increase their plasma half-life and they showed a reduced tumor growth *in vivo* with this system after subcutaneous injection in a 9L model [282]. The encapsulation of PTX into LNC was also shown to be promising by Lollo *et* al., who used multifunctional chitosan-coated LNC for the concomitant delivery of PTX (located in the oily core of the nanocarrier) and immunostimulator CpG (located onto the nanocarrier surface). This system showed enhanced apoptotic effect *in vitro* and increased animal survival *in vivo* after CED administration of the formulation in a GL261 orthotopic model [285]. Chitosan-LNC were also used for the delivery of anti-EGFR siRNA (alone or in combination with anti-Galectin-1 siRNA) showing good EGFR and Galectin-1 expression knockdown and increased sensitivity to TMZ *in vitro* (U-87 MG cell line) and *in vivo* after CED administration in a U-87 MG orthotopic model [70, 137].

Balzeau *et* al. demonstrated that the adsorbtion of neurofilament light subunit-tubulin-binding site 40-63 peptide (NFL) on the LNC increased the nanocarrier cellular uptake and reduced cell proliferation *in vitro*. The CED administration of NFL-PTX-LNC *in vivo* resulted in an increased reduction of glioma growth compared to PTX-LNC [256]. NFL-LNC were also used to deliver the tamoxifen derivative Ferrociphenol (Fc-diOH). Fc-diOH was firstly loaded into ungrafted LNC by Allard *et* al. who showed good cytotoxic effect *in vitro* (IC_{50} 0.6 µM) and specificity against tumor cells. *In vivo*, Fc-diOH–LNC showed ability to slow tumor growth after CED administration in combination with radiotherapy in a 9L orthotopic model [278, 279]. NFL-Fc-diOH-LNC failed to demonstrate an enhanced *in vitro* or *in vivo* activity compared to ungrafted Fc-diOH-LNC or OX26 murine monoclonal antibodies-grafted LNC (OX-26 mAb-Fc-diOH-LNC) after CED administration in a 9L orthotopic model. However, increased animal survival was observed after intra-carotid treatment with NFL-Fc-diOH–LNC [257]. A similar result was shown by Huynh *et* al., who showed enhanced survival after intra-

carotid injection of DSPE-mPEG surface coated Fc-diOH-LNC due to enhanced accumulation in the tumor zone but not after CED administration. They also showed increased plasma half-life and reduced tumor growth by passive targeting after intravenous injection in 9L models [237, 281]. These result highlights the importance of the administration pathway for peripheral drug delivery systems to achieve maximum effective dose at the tumor site reducing the toxicity of the implanted system.

Roger *et* al. and Clavreul *et* al. incorporated Fc-diOH-LNC into mesenchymal stromal (MIAMI) cells and showed that this complex had cytotoxic effect *in vitro* and was able to specifically target brain tumors, ensuring extensive intratumoral distribution and reducing tumor growth *in vivo* after intratumoral injection [283, 284]. This approach is very promising as it allows to combine the advantages of stem cell therapy and nanotechnology to target brain tumors and increase the anticancer drugs local distribution.

More recently another tamoxifen derivative, ansa-Fc-diOH, showed enhanced *in vitro* cytotoxic effect compared to Fc-diOH (IC_{50} 0.1 µM) on glioma cells, which was associated to an oxidative stress and a dose dependent alteration of the cell cycle. Significant tumor growth inhibition and no liver damage were observed after multiple intravenous injections of ansa-Fc-diOH-LNC on a 9L subcutaneous model after [280].

3. GEMCITABINE & GLIOBLASTOMA: CHALLENGES AND FUTURE PERSPECTIVES

Gemcitabine is a nucleoside analogue currently used for the treatment of various solid tumors, as single agent or in combination with other chemotherapeutic drugs. Its use against highly aggressive brain tumors such GBM has been evaluated in preclinical and clinical trials leading to controversial results. Gemcitabine can inhibit DNA chain elongation, is a potent radiosensitizer, and it may enhance antitumor immune activity, but it also presents some drawbacks (short half-life, side effects, chemoresistance). The aim of this chapter is to discuss the challenges related to the use of gemcitabine for glioblastoma and to report recent studies which may overcome these obstacles opening new perspectives for its use in this field (e.g. Gemcitabine derivatives and/or nanomedicines).

3.1. INTRODUCTION

The standard of care treatment of GBM includes surgical resection followed by RT and concomitant plus adjuvant chemotherapy with TMZ [23]. After oral administration, TMZ is spontaneously converted into its active metabolite methyltriazeno-imidazole-carboximide (MTIC) at physiological conditions. This shows excellent bioavailability, is able to pass the BBB and quickly degrades into methyldiazonium ion, which is a potent methylating agent [288]. The DNA methylation leads to mismatch repair system failure (due to the impossibility of finding complementary bases for methylated adducts), inhibition of cell replication and apoptosis (Figure 8A) [289]. The use of TMZ as standard therapy for GBM in combination with RT is the result of a successful clinical trial published by Stupp *et al*. that proved modest survival improvement compared to RT alone and lead to FDA approval on newly diagnosed GBM in 2005. However, despite the aggressive therapeutic regimen, most GBM patients quickly develop tumor recurrences that inevitably lead to death (median survival 14.6 months; 5-year survival rate < 10%) [290]. Some intrinsic characteristics of GBM limit the effectiveness of chemotherapeutics. These include GBM anatomic location (BBB) and unique microenvironment (extracellular matrix, nutrition, oxygenation pH value), GBM cell heterogeneity (e.g. cancer stem cells, tumor microtubes), high proliferation rate (variation in cell cycle distribution, cell-cell contact), angiogenesis and chemoresistance [291, 292].

Resistance to alkylating agents can be due to intrinsic resistance caused by alteration of MGMT expression and/or acquired resistance caused by mutations in DNA mismatch repair enzymes [293]. MGMT is a DNA repair enzyme able to transfer the alkyl group at the O^6 position of guanine to the active site of the enzyme therefore reversing the DNA alkylation produced by TMZ. A correlation has been found between MGMT promoter methylation status (that leads to MGMT gene silencing and lower MGMT expression) and increased survival in GBM patients treated with TMZ [68, 294].

As an attempt to ameliorate the management of GBM patients, increasing their survival rate and quality of life, many researchers have tried to explore different strategies (e.g. local delivery of chemotherapeutics, nanomedicines, gene therapy etc. [295]). Choosing the correct drug or combination (e.g. single or multimodal chemotherapy, combination of chemotherapy and RT), the proper doses, timing of administration and delivery route is crucial for GBM investigators. Historically, the tangible increase in GBM patients' survival was observed when RT was included as standard treatment following surgical resection in the 1970s, shifting the median survival from 3-6 to 9-12 months [296]. The study of radiosensitizing molecules that could enhance RT efficacy leading to a reduction of recurrences has ever since been of great interest. This section focuses on the use of Gemcitabine (2',2'-Difluoro-deoxycytidine; Gem) - a potent chemotherapeutic and radiosensitizing agent acting through a MGMT-independent mechanism of action - for the treatment of GBM, defining its historical background, potential, challenges and current applications.

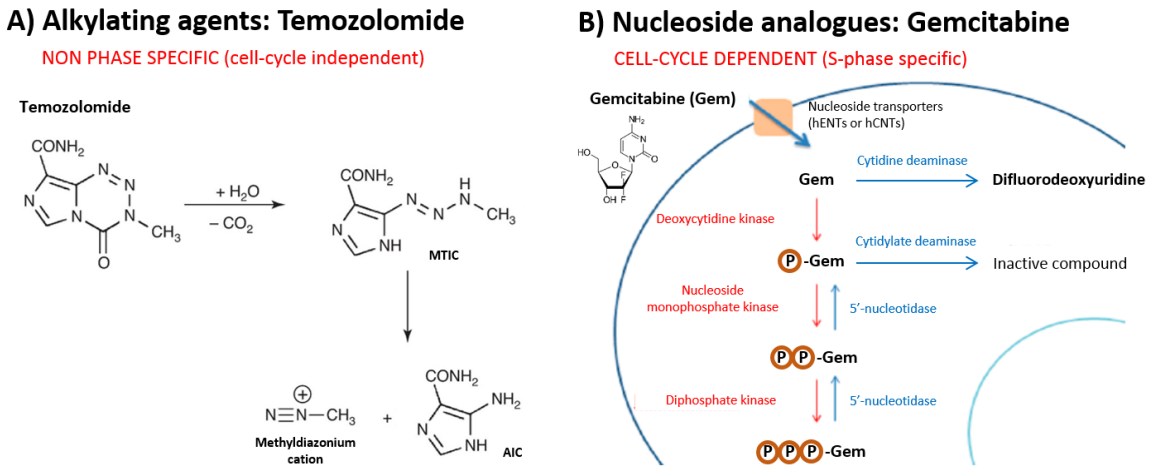

Figure 8. Schematic representation of mechanism of action of TMZ and Gem, adapted with permission from [7] and [297]. **(A)** TMZ is spontaneously hydrolyzed into the active metabolite methyltriazeno-imidazole-carboximide (MTIC) at physiological conditions. MTIC degrades into methyldiazonium cation (methylating agent) and AIC (degradation product). Methyldiazonium cation interacts with DNA producing O^6-methylguanine, N^7-methylguanine, O^3-methyladenine adducts. Alkylated azotate basis lead to DNA mismatch repair events, DNA-strand break and apoptosis. **(B)** Gem uptake is mediated by nucleoside transporters and followed by a series of three phosphorilations. Gem diphosphate inhibits ribonucleotide reductase reducing the concentration of deoxycytidine triphosphate (selfpotentiation). Gem triphosphate incorporates into DNA during replication acting as competitive substrate of deoxycytidine triphosphate, leading to irreversible inhibition of DNA polymerases and block of DNA chain elongation (masked chain termination).

3.2. GEMCITABINE

Gem is a nucleoside analogue currently approved for the treatment of various solid tumors (pancreatic, non-small-cell lung, breast and ovarian cancers), as single agent or in combination with other chemotherapeutic drugs. Gem is generally administered once per week by intravenous infusion over 30 minutes, at a maximum dosage of 1250 mg/m^2, for 21-day cycles (longer administration cycles for pancreatic cancer). Gem is a prodrug, as it needs to be transported into the cells through nucleoside transporters (mainly hENT1, hCNT1 and hCNT3) where it undergoes sequential phosphorylation by deoxycytidine kinase (DCK) in order to be active (Figure 8B). Gem triphosphate acts as deoxycytidine triphosphate competitive substrate, it is incorporated into DNA during replication, inhibiting DNA chain elongation by "mask chain termination". The formation of Gem-induced DNA fragments leads to cell death by apoptosis [298]. At the same time, Gem diphosphate inhibits ribonucleotide reductase, an enzyme of DNA synthesis, depleting the biosynthesis of the deoxyribonucleoside triphosphate precursors and avoiding the intracellular inactivation of Gem monophosphate thus "self-potentiating" its own concentration and cytotoxic activity

[299]. It has been recently hypothesized that Gem and its metabolites can passively diffuse in good communicating cells through gap junctions (composed of connexin proteins). Even if the connexins expression and function in GBM is not well known yet [300], it has been demonstrated *in vitro* on different GBM cell lines that Gem-mediated toxicity can diffuse and can be transferred between cells by a phenomenon called “bystander effect” [301].

Gem is a powerful radiation sensitizer at non-cytotoxic concentrations even after a brief exposure time [302, 303]. Moreover difluorodeoxyuridine, one of Gem metabolites, can act as radiosensitizer and shows cytotoxic activity at concentrations that are easily reached in plasma [304, 305]. Even if the mechanism involved is still unclear, it is believed that the main factors contributing to Gem-radioenhancing activity are depletion of phosphorylated deoxynucleotides (especially deoxyadenosine triphosphate) and Gem-induced cell cycle redistribution into the S-phase [306-310].

Gem presents significant immunomodulatory activity in different animal tumor models, independently of its cytotoxic effect. Indeed, Gem has shown to selectively deplete B-lymphocytes, myeloid derived suppressor cells and regulatory T cells in tumor-bearing animals [311-314].

Gem is an attractive molecule for the treatment of GBM (Figure 9A). Indeed, as previously mentioned, it is a powerful chemotherapeutic and radiosensitizing agent acting through a MGMT-independent mechanism, which could avoid crossed-linked resistance with TMZ. Its toxicity is probably mediated through gap junctions suggesting that it could be a useful agent in tumors displaying gap junctions and expressing different type of connexins, such as GBM. Even if Gem’s ability to pass the BBB is modest, it has shown to pass the blood-tumor barrier in GBM patients at concentrations high enough to enable radiosensitization. Moreover, the clinical use of Gem has shown its ability to act in synergy not only with RT but also with other chemotherapeutic agents (e.g. carboplatin, cisplatin, paclitaxel). Finally, the immunomodulating capacities of Gem might be useful for its use against GBM in combination with immunotherapies [315]. Due to the aggressiveness and the unique characteristics of GBM, the rationale for the use of such a versatile molecule and the combination of multiple therapeutic strategies is high.

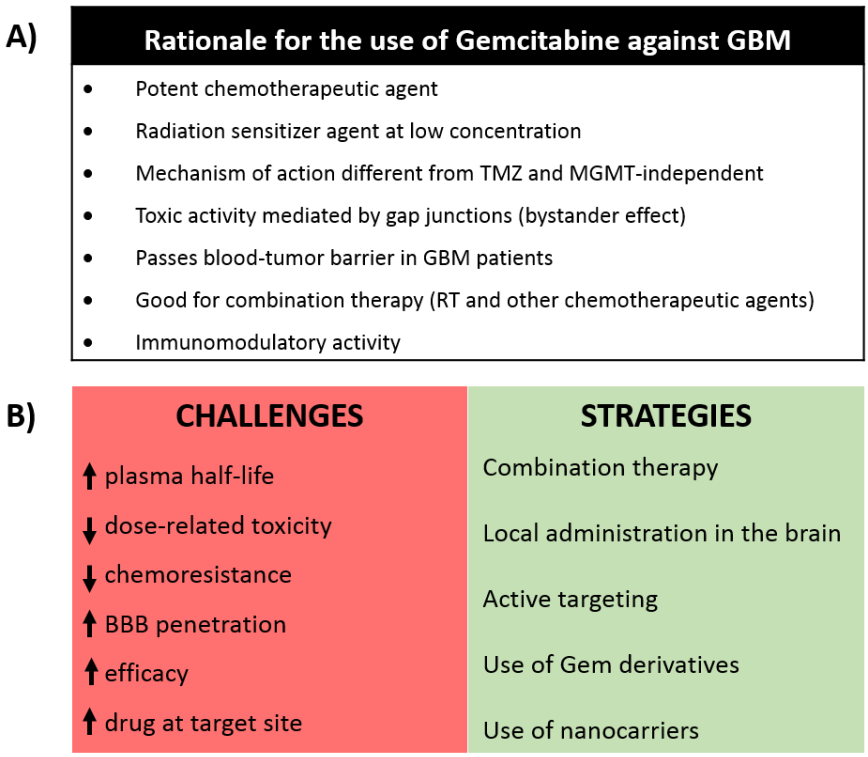

Figure 9. List of the advantages (A) and challenges (B) related to the use of Gem for the treatment of GBM and some strategies that have been developed to overcome them.

3.3. GEMCITABINE FOR THE TREATMENT OF GLIOBLASTOMA

3.3.1. Gemcitabine followed by radiation therapy for the treatment of glioblastoma

The first study suggesting the use of Gem for the treatment of GBM was published by Rieger *et al.* in 1999 [316] (Table 7), the same year that TMZ received accelerated approval for use in anaplastic astrocytoma. In this work, the authors studied the effect of Gem on 12 human malignant GBM cell lines *in vitro*, showing them to be susceptible to the cytotoxic and anticlonogenic action of Gem. Gem was 100-fold more potent than its related agent Cytarabine. Interestingly, it was demonstrated that pre-exposure of the cells to dexamethasone (a steroid drug commonly used for the control of cerebral edema in GBM patients) moderately reduced the cytotoxic effect of Gem, as previously shown with other anti-cancer drugs. Subsequently, the same group performed a Phase II clinical trial enrolling 21 patients with newly diagnosed GBM to evaluate the therapeutic efficacy of pre-irradiation Gem chemotherapy followed by standard RT [317]. Patients were administered 1000 mg/m^2 intravenously on days 1, 8 and 15 of each one-month cycle and for a maximum of four

cycles. Radiotherapy was then administered two weeks after the last dose of Gem. The regimen used in the study resulted to be safe but didn't improve survival compared to RT alone. In the same period, another group performed a Phase II clinical trial on patients with anaplastic astrocytoma or GBM at first relapse showing similar results [318]. Indeed, no objective response was obtained from this study. Authors suggested that selection bias might have confounded results as patients could start the treatment only two-months after prior RT, leaving time for the disease to progress. Moreover, the concomitant use of anticonvulsants and steroids might have reduced the effect of Gem. Another Phase II clinical study reported the combination of Gem and treosulfan as pre-irradiating chemotherapy regimen before standard RT in newly diagnosed GBM patients [319]. The doses used (days 1 and 8: 3500 mg/m^2 Treosulfan, 1000 mg/m^2 Gem per cycle, intravenous administration) had been established based on a previous phase I trial in various solid tumors (not GBM), which showed beneficial palliative effects and minimal toxicity due to the chemotherapy combination [320]. However, on GBM patients this regimen produced some deep venous thrombosis and hematological toxicities, and no survival increase was reported compared to RT alone [319].

Despite the promising *in vitro* results, these clinical trials unequivocally showed that pretreatment with Gem followed by RT weeks after the completion of the chemotherapy was not an efficient strategy for the management of GBM. Several factors can explain this lack of efficacy. For example, the cytotoxic action of Gem is S-phase dependent. Indeed, it is likely that Gem optimal cytotoxic activity is achieved in rapidly growing tumors with concomitant RT (e.g. recurrent tumors developing after surgery) instead of established GBM tumors with a large population of non-proliferating cells and weeks before RT [321, 322]. Moreover, Gem is hydrophilic meaning that its penetration through the BBB is low [323-325]. Its concentration in the brain is maximal two hours after intravenous administration and then rapidly decrease in healthy animals [323]. In tumor-bearing models as well as in GBM patients the BBB is partially disrupted and Gem uptake can increase reaching concentrations high enough to enable radiosensitization [325, 326]. As radiosensitization depends on the length of interval between drug treatment and radiation [327], choosing the correct timing between Gem administration and RT is crucial.

3.3.2. Combination of gemcitabine and concomitant radiation therapy for the treatment of glioblastoma

As a way to exploit Gem potential in the treatment of GBM, the first strategy was to study the radiosensitizing activity of Gem in GBM (*in vitro* and *in vivo*) in order to optimize the combination regimen between Gem and RT (Table 7).

On GBM cell lines, it has been shown that Gem radiosensitization is highly dependent on the cell line and its cell cycle progression after Gem+RT treatment [309]. Ostruzka *et al.* reported that U251 cells (presenting mutant p53) accumulate in S-phase after incubation with Gem and ionizing radiation and S-phase-specific cell death was induced. At the same treatment conditions, D54 cells (presenting wild-type p53) showed G1 block with fewer cells in S-phase and absence of S-phase-specific cell death induction [309]. Another study, performed by Genc *et al.* on Gli-6 cells, showed that Gem is able to induce radiosensitization in exponentially growing cells and small spheroids (Ø 250-400 µm) but not in confluent cell cultures and large spheroids (Ø 400-500 µm). This may be due to changes in cell cycle distribution, cell-cell contact, nutrient and drug diffusion, metabolism in the different conditions [321]. Fehlauer *et al.* evaluated the cytotoxic and radiosensitizing effect of Gem *in vitro* on GaMG and U-87 MG spheroids and on organotypic multicellular spheroids derived from GBM patients [322]. Their results showed migration inhibition and proliferation inhibition in the two-established cell-lines following combination therapy (Gem+RT). The response in organotypic multicellular spheroids was more heterogeneous, with no obvious changes in volume or histological damage but decrease in proliferating cells and alterations of protein expression levels (MIB-1, p21 and p53). Carpinelli *et al.* tested Gem activity in C6 rat malignant gliomas, to evaluate its effects on cell cycle phase distribution, apoptosis and its efficacy *in vivo* [308]. They showed that Gem induces accumulation in S-phase and apoptosis in C6 cell line. Moreover, a significant reduction in tumor volume was observed in rats after intraperitoneal Gem administration, as well as perturbation in cell cycle progression and increase in apoptosis. These studies confirmed the potential interest of using Gem in combination with radiotherapy for the treatment of GBM.

Gem radiosensitization *in vitro* can be achieved either by long exposure to low drug concentrations or brief treatment with higher but clinically relevant concentrations (radiosensitization detectable 4h after treatment and can last for 2 days), therefore defining

Gem administration schedule is essential for its effect [327, 328]. Maraveyas *et al.* thought that in humans a twice weekly dosing or a slower rate of infusion would be preferable as radiosensitization strategy and they evaluated the maximum tolerated dose for the concomitant use of Gem and RT in carcinoma patients with brain metastasis in a clinical phase I study. Subsequently, a phase I study was designed by Fabi *et al.* to test Gem with concomitant RT in newly diagnosed GBM patients [329]. As a difference compared to the previously described clinical studies, patients were enrolled in the study within 40 days after surgery. From 24 to 72 hours before the first RT session and then once weekly, patients received Gem intravenously at a fixed-dose rate of 10 mg/m^2/min. RT (involved field irradiation, 2.0 Gys) was given daily, five days per week over six weeks. The aim of the study was to identify the dose-limiting toxicity and maximum tolerated dose, which were found at 175 mg/m^2/weekly. Subsequently, a phase II study was conducted to evaluate the activity of Gem as radiosensitizer for newly diagnosed GBM [330]. Patients received standard cranial irradiation and concomitant fixed dose rate intravenous Gem (175 mg/m^2 weekly for six weeks). Irrespective of tumor response, no later than 6 weeks after chemo-RT, patients were treated with TMZ. As Gem has a different mechanism of action compared to TMZ (Figure 8), it can be useful for patients with unmethylated MGMT status which are expected to respond in a lesser extent to alkylating agents. This study showed that Gem administered concurrently with RT is safe and clinically active as radiosensitizer in GBM patients, and its effect is achieved irrespective of the methylation status of the MGMT promoter.

Kim *et al.* recently published the long-term results of a Phase I dose-escalation study on Gem plus RT for newly diagnosed high grade gliomas (grade 3 or 4 supratentorial glioma) patients [331]. The maximum tolerated dose was 750 mg/m^2/week during the last 4 weeks of radiation. This regimen was well tolerated and the survival results were promising for further studies, particularly on poor prognosis patient subgroups.

The efficacy of Gem in combination with RT was also reported in a preclinical study performed by Galbàn *et al*., showing reduction of tumor burden and increased survival after treatment in a proneural PDGF GBM subtype mouse model [332].

3.3.3. Alternative delivery strategies for gemcitabine in the treatment of glioblastoma

Gem is a strong chemotherapeutic and radiosensitizing agent but presents some drawbacks. Firstly, it has a short-term plasma half-life due to extensive degradation by cytidine deaminase in the liver [299]. Secondly, side effects can be observed due to high drug doses, frequent administration schedules or combination with other drugs (myelosuppression, thrombocytopenia, edema, cutaneous toxicity) [299, 333]. Also, limited Gem penetration through solid tumors such as GBM may result in reduced efficacy and increased resistance [334, 335]. Genomic alteration can induce cell resistance to antimetabolic drugs such Gem. In this sense, a decreased expression of nucleoside transporters could block the cellular uptake of Gem, while reduced levels or alteration of deoxycytidine kinase would block its phosphorylation leading to inactivity of the drug. Overexpression of cytidine deaminase leads to irreversible hydrolytic deamination of Gem and its inactivation in blood, liver and kidney. High levels of enzymes able to reduce Gem monophosphate and triphosphate (5'-nucleotidase) would also reduce the cells sensitivity to the drug. Finally, aberrant expression of genes associated with cellular survival and apoptosis or overexpression of ribonucleotide reductase able to convert ribonucleosides in deoxyribonucleosides triphosphates are also involved in the resistance to Gem [304]. To increase Gem delivery to the target site and enhance the chemotherapeutic and/or radiosensitizing properties of Gem against GBM, researchers have studied different delivery strategies including active targeting to pass the BBB or target GBM cells, local delivery of Gem, encapsulation of Gem or its derivatives in nanomedicines or combinational strategies (Figure 9B; Table 7).

Guo *et al.*, who developed peripherial benzodiazepine receptors (PBR) ligand-Gem conjugate system to target selectively the PBR receptors (overexpressed in brain tumors), were the first to change the delivery strategy to increase Gem efficacy in GBM [336]. The tumor target selectivity was significantly increased after intravenous administration of PBR-Gem conjugate in orthotopic SF188/VEGF^{+} model in rats compared to native Gem. This approach would allow to increase the concentration at the target site, enhancing drug efficacy and reducing side effects.

Table 7. Preclinical studies and clinical trials using Gem as therapeutic strategy for GBM treatment

Therapeutic strategy		Characteristics of the study	Main results	Ref.
Preclinical studies				
	Gem	Cytotoxicity studies (LN-18, U138MG, U87MG, LN-428, D247MG, T98G, LN-319, LN-229, A172, U251MG, U373MG, LN-308 cells)	GBM cells sensitive to cytotoxic and anticlonogenic action of Gem	[316]
C	Gem -/+ RT	Cytotoxicity and radiosensitivity studies (U251, D54 GBM cells)	Progression of cells in S-phase after Gem treatment influences radiosensitization	[309]
C	Gem -/+ RT	Cytotoxicity and radiosensitivity studies on Gli-6 monolayers and spheroids	Effect depends on the state of the cells and the size of the spheroids	[321]
	Gem	Cytotoxicity *in vitro* and efficacy *in vivo* (C6 model)	Reduction in tumor volume, alteration of cell cycle progression and increase of apoptosis	[308]
C	Gem + RT	Cytotoxic and radiosensitivity on GBM spheroids (GaMG, U87MG) and patient-derived OMS	Good efficacy in cell-lines spheroids; heterogeneous response in OMS	[322]
	Gem	Gem mechanism of action *in vitro* (U87MG, SKI-1 cells)	Gem toxicity can diffuse through gap junctions inducing bystander effect	[301]
N	Gem-PBCA-NP	Cytotoxicity *in vitro* and efficacy *in vivo* (C6 model)	Inhibit cell growth *in vitro*, reduce tumor growth *in vivo*	[339]
L	Gem	Safety and efficacy of CED delivery (9L model)	Increased animal survival	[337]
T	PBR-Gem conjugate	Efficacy of active targeting (pharmacokinetics, distribution)	Increased tumor target selectivity against PBR	[336]
C	Gem + RT	Efficacy in proneural PDGF GBM subtype mouse model	Reduction of tumor burden and increased survival	[332]
C	Gem + DCK + RT	Cytotoxic and radiosensitivity studies *in vitro* and *in vivo* (GI261, U373, C6)	Increased efficacy with the triple combination	[338]
C, N	PEG-lipo-CD133-Gem -/+ BV	Efficacy in GBM stem cells *in vitro* and sc GBM model *in vivo*	Enhanced anti-tumor effect, increased survival; synergy between the drugs	[340,341]
N, T	IONP-Gem- CTX	Stability, cellular uptake (SF-763, U-118 MG cells), active targeting	Good cellular uptake, prolonged blood circulation, ability to cross BBB	[342]
C, L, D, N	PEG- SQ-Gem-NP +/- RT	Cytotoxicity *in vitro* and efficacy *in vivo* (GR2 model)	Good distribution in the brain and increased animals survival	343]
Clinical studies				
	Gem; followed by RT	Phase II on ND GBM	Safe but not effective	[317]
	Gem; followed by RT	Phase II on R GBM	Safe but not effective	[318]
C	Gem + Treosulfan; followed by RT	Phase II on ND GBM	Not effective, some hematological toxicities and thrombosis	[319]
	Sugery + Gem	Phase 0	Gem and its metabolite dFdU can pass blood-tumor barrier and be uptaken by tumor cells in GBM patients reaching radiosensitizing concentrations	[326]
C	Gem + RT; followed by TMZ	Phase I and II on ND GBM	Safe and effective regimen	[329,330]
C	Gem + RT	Phase I on ND HGG	Safe and promising regimen, expecially for poor prognosis patients subgroups	[331]

Therapeutic strategies: **C**: combination therapy (e.g. with RT, chemotherapeutic agents etc.); **L**: local administration; **D**: use of Gem derivatives; **N**: use of nanocarriers; Abbreviations: OMS: organotypic multicellular spheroids; PBR: peripheral benzodiazepine receptor; PBCA: Polybutylcyanoacrylate; NP: nanoparticles; PEG: polyethylene glycol; lipo: liposomes ; BV: Bevacizumab; IONP: iron oxide nanoparticle ; CTX : chlorotoxin; SQ-Gem: squalenoyl-gemcitabine; ND: newly diagnosed patients; R: recurrent patients; HGG: high-grade glioma patients.

On the other side, Diegen et al. delivered Gem directly into the CNS by CED in rats [337]. CED efficiently distributes infusate throughout the interstitial spaces of neural parenchyma by bulk-flow, allowing the drug delivery across the BBB. In the aggressive 9L glioma model, the CED delivery of Gem showed reduction in tumor volume compared to intraperitoneal administration of Gem, and long-term survival of some animals.

A rather different strategy was used by Szatmári *et al.*, who used a gene therapy approach to increase the toxic and radiosensitizing effect of Gem in different *in vitro* and *in vivo* glioma models [338]. They introduced an adenovirus vector encoding for the human deoxycytidine kinase gene into glioma cells and transplanted them in rodent brains. Their results show that the combination of deoxycytidine kinase overexpression, Gem treatment and irradiation significantly increased the toxic and radiosensitizing effects of Gem *in vitro*, and the animal survival *in vivo* (even if in a different extent for the two models).

Wang *et al*. were the first ones to use nanoparticles (NP) for the delivery of Gem in GBM [339]. Polybutylcyanoacrylate NP were loaded with Gem, coated with polysorbate-80 to increase their ability to pass the BBB and tested on C6 glioma cells. The results show that this Gem-polybutylcyanoacrylate-NP can effectively inhibit the growth of C6 cells *in vitro* and enhance anti-tumor activity on brain tumors *in vivo* after intravenous administration.

Shin *et al.* encapsulated Gem in PEGylated liposomes conjugated to anti-CD133 monoclonal antibody as an attempt to increase drug penetration into the tumor, reduce systemic toxicity and target GBM stem cells overexpressing CD133 surface marker to increase its therapeutic efficacy. In their first study, the authors demonstrated that PEG-lipo-CD133-Gem were stable, with long circulating time *in vivo* after intravenous administration and were able to reduce toxicity and exert significant anti-tumor efficacy in a subcutaneous tumor model [340]. In a second study, a synergistic effect was observed between PEG-lipo-CD133-Gem and the anti-angiogenic drug Bevacizumab, allowing to achieve good anti-tumoral response reducing the drug doses and the side effects [341].

To increase Gem circulation time and overcome the BBB, Mu *et al*. developed a Gem-loaded iron oxide NP (IONP) and conjugated it *via* hyaluronic acid to chlorotoxin, a peptide able to cross the BBB and target brain tumor cells [342]. The IONP-HA-Gem- chlorotoxin formulation showed cellular uptake in SF-763 and U-118 MG cells, prolonged blood circulation and ability to cross the BBB in healthy mice after intravenous administration.

Gaudin *et al.* have bioconjugated Gem with liquid squalene producing squalenoyl-gemcitabine, a prodrug that spontaneously form NPs [343]. Squalenoylation of nucleoside analogues has been extensively reported in the literature as a way able to protect the drug from degradation, bypass resistance mechanisms and improve their anticancer activity [344]. In GBM, the CED administration of PEGylated SQ-Gem allowed widespread distribution in the brain and increased animals' survival in rats bearing intracranial RG2 tumors compared to free Gem, when used alone or in combination with RT [343].

4. REFERENCES

[1] A. Omuro, L.M. DeAngelis, Glioblastoma and other malignant gliomas: a clinical review, JAMA, 310 (2013) 1842-1850.

[2] T.A. Ulrich, E.M. de Juan Pardo, S. Kumar The mechanical rigidity of the extracellular matrix regulates the structure, motility, and proliferation of glioma cells, Cancer Res 69 (2009) 4167-74.

[3] I. Fischer, J.P. Gagner, M. Law, E.W. Newcomb, D. Zagzag, Angiogenesis in gliomas: biology and molecular pathophysiology, Brain Pathol, 15 (2005) 297-310.

[4] N.A. Bush, S.M. Chang, M.S. Berger, Current and future strategies for treatment of glioma, Neurosurg Rev, 40 (2017) 1-14.

[5] F.B. Furnari, T. Fenton, R.M. Bachoo, A. Mukasa, J.M. Stommel, A. Stegh, W.C. Hahn, K.L. Ligon, D.N. Louis, C. Brennan, L. Chin, R.A. DePinho, W.K. Cavenee, Malignant astrocytic glioma: genetics, biology, and paths to treatment, Genes Dev, 21 (2007) 2683-2710.

[6] S.A. Grossman, J.F. Batara, Current management of glioblastoma multiforme, Semin Oncol, 31 (2004) 635-644.

[7] S. Tsigkos, S. Mariz, J. Llinares, L. Fregonese, S. Aarum, N.W. Frauke, K. Westermark, B. Sepodes, Establishing medical plausibility in the context of orphan medicines designation in the European Union, Orphanet J Rare Dis, 9 (2014) 175.

[8] J. Bianco, C. Bastiancich, A. Jankovski, A. des Rieux, V. Preat, F. Danhier, On glioblastoma and the search for a cure: where do we stand?, Cell Mol Life Sci,74 (2017) 2451-2466.

[9] T.R. Jue, K.L. McDonald, The challenges associated with molecular targeted therapies for glioblastoma, J Neurooncol, 127 (2016) 427-434.

[10] N.R. Parker, A.L. Hudson, P. Khong, J.F. Parkinson, T. Dwight, R.J. Ikin, Y. Zhu, Z.J. Cheng, F. Vafaee, J. Chen, H.R. Wheeler, V.M. Howell, Intratumoral heterogeneity identified at the epigenetic, genetic and transcriptional level in glioblastoma, Sci Rep, 6 (2016) 22477.

[11] T. Yamahara, Y. Numa, T. Oishi, T. Kawaguchi, T. Seno, A. Asai, K. Kawamoto, Morphological and flow cytometric analysis of cell infiltration in glioblastoma: a comparison of autopsy brain and neuroimaging, Brain Tumor Pathol, 27 (2010) 81-87.

[12] S.M. Robbins, D.L. Senger, Assessing Mechanisms of Glioblastoma Invasion, in: R. Martínez Murillo, A. Martínez (Eds.) Animal Models of Brain Tumors, Humana Press, Totowa, NJ, 2013, pp. 275-298.

[13] P.G. Fisher, P.A. Buffler, Malignant gliomas in 2005: where to GO from here?, JAMA, 293 (2005) 615-617.

[14] T. Denysenko, L. Gennero, M.A. Roos, A. Melcarne, C. Juenemann, G. Faccani, I. Morra, G. Cavallo, S. Reguzzi, G. Pescarmona, A. Ponzetto, Glioblastoma cancer stem cells: heterogeneity, microenvironment and related therapeutic strategies, Cell Biochem Funct, 28 (2010) 343-351.

[15] T. Smets, T.M. Lawson, C. Grandin, A. Jankovski, C. Raftopoulos, Immediate post-operative MRI suggestive of the site and timing of glioblastoma recurrence after gross total resection: a retrospective longitudinal preliminary study, Eur Radiol, 23 (2013) 1467-1477.

[16] M.C. Mabray, R.F. Barajas, Jr., S. Cha, Modern brain tumor imaging, Brain Tumor Res Treat, 3 (2015) 8-23.

[17] V. Cuccarini, A. Erbetta, M. Farinotti, L. Cuppini, F. Ghielmetti, B. Pollo, F. Di Meco, M. Grisoli, G. Filippini, G. Finocchiaro, M.G. Bruzzone, M. Eoli M, Advanced MRI may complement histological diagnosis of lower grade gliomas and help in predicting survival, J Neurooncol, 126 (2016) 279-88.

[18] H.W. Kao, S.W. Chiang, H.W. Chung, F.Y. Tsai, C.Y. Chen, Advanced MR imaging of gliomas: an update, Biomed Res Int, 2013 (2013) 970586.

[19] T. Kazda, M. Bulik, P. Pospisil, R. Lakomy, M. Smrcka, P. Slampa, R. Jancalek, Advanced MRI increases the diagnostic accuracy of recurrent glioblastoma: Single institution thresholds and validation of MR spectroscopy and diffusion weighted MR imaging, Neuroimage Clin, 11 (2016) 316-321.

[20] D. Treister, S. Kingston, K.E. Hoque, M. Law, M.S. Shiroishi, Multimodal magnetic resonance imaging evaluation of primary brain tumors, Semin Oncol, 41 (2014) 478-495.

[21] R. Altieri, F. Zenga, M.M. Fontanella, F. Cofano, A. Agnoletti, G. Spena, E. Crobeddu, R. Fornaro, A. Ducati, D. Garbossa, Glioma Surgery: Technological Advances to Achieve a Maximal Safe Resection, Surg Technol Int, 27 (2015) 297-302.

[22] J. Buckner, P. Brown, B. O'Neill, F. Meyer, C. Wetmore, J. Uhm, Central nervous system tumors, Mayo Clin Proc, 82 (2007) 1271-1286.

[23] R. Stupp, M. Brada, M.J. van den Bent, J.C. Tonn, G. Pentheroudakis, High-grade glioma: ESMO Clinical Practice Guidelines for diagnosis, treatment and follow-up, Ann Oncol, 25 Suppl 3 (2014) iii93-101.
[24] P.D. Delgado-Lopez, E.M. Corrales-Garcia, Survival in glioblastoma: a review on the impact of treatment modalities, Clin Transl Oncol, 18 (2016) 1062-1071.
[25] M. Jansen, S. Yip, D.N. Louis, Molecular pathology in adult neuro-oncology: an update on diagnostic, prognostic and predictive markers, Lancet Neurol, 9 (2010) 717-726.
[26] K.L. Chaichana, M.J. McGirt, J. Frazier, F. Attenello, H. Guerrero-Cazares, A. Quinones-Hinojosa, Relationship of glioblastoma multiforme to the lateral ventricles predicts survival following tumor resection, J Neurooncol, 89 (2008) 219-224.
[27] K.L. Chaichana, L. Pinheiro, H. Brem, Delivery of local therapeutics to the brain: working toward advancing treatment for malignant gliomas, Ther Deliv, 6 (2015) 353-369.
[28] A.F. Hottinger, K.J. Abdullah, R. Stupp, Current standard of care in glioblastoma therapy, in: S. Brem K. G. Abdullah (Ed.) Glioblastoma, Elsevier, 2017.
[29] N.R. Smoll, K. Schaller, O.P. Gautschi, Long-term survival of patients with glioblastoma multiforme (GBM), J Clin Neurosci, 20 (2013) 670-675.
[30] J.G. Wolbers, Novel strategies in glioblastoma surgery aim at safe, supra-maximum resection in conjunction with local therapies, Chin J Cancer, 33 (2014) 8-15.
[31] K.R. Yabroff, L. Harlan, C. Zeruto, J. Abrams, B. Mann, Patterns of care and survival for patients with glioblastoma multiforme diagnosed during 2006, Neuro Oncol, 14 (2012) 351-359.
[32] W. Dandy, Removal of right cerebral hemisphere for certain tumors with hemiplegia: Preliminary report, J Amer Med Assoc, 90 (1928) 823-825.
[33] J. Wright, J. Chugh, C. Wright, F. Alonso, A. Hdeib, H. Gittleman, J. Barnholtz-Sloan, A. Sloan, Laser interstitial thermal therapy followed by minimal-access transsulcal resection for the treatment of large and difficult to access brain tumors, Neurosurg Focus, 41 (2016) e14.
[34] S.L. Hervey-Jumper, M.S. Berger, Maximizing safe resection of low- and high-grade glioma, J Neurooncol, 130 (2016) 269-282.
[35] R.L. Yong, R.R. Lonser, Surgery for glioblastoma multiforme: striking a balance, World neurosurgery, 76 (2011) 528-530.
[36] R. Young, A. Jamshidi, G. Davis, J. Sherman, Current trends in the surgical management and treatment of adult glioblastoma, Ann Transl Med, 3 (2015) 121.
[37] M. Lacroix, D. Abi-Said, D.R. Fourney, Z.L. Gokaslan, W. Shi, F. DeMonte, F.F. Lang, I.E. McCutcheon, S.J. Hassenbusch, E. Holland, K. Hess, C. Michael, D. Miller, R. Sawaya, A multivariate analysis of 416 patients with glioblastoma multiforme: prognosis, extent of resection, and survival, J Neurosurg, 95 (2001) 190-198.
[38] D.M. Patel, N. Agarwal, K.L. Tomei, D.R. Hansberry, I.M. Goldstein, Optimal Timing of Whole-Brain Radiation Therapy Following Craniotomy for Cerebral Malignancies, World Neurosurg, 84 (2015) 412-419.
[39] R. Mirimanoff, T. Gorlia, W. Mason, M. van den Bent, R. Kortmann, B. Fisher, M. Reni, A. Brandes, J. Curschmann, S. Villa, G. Cairncross, A. Allgeier, D. Lacombe, R. Stupp, Radiotherapy and temozolomide for newly diagnosed glioblastoma: recursive partitioning analysis of the EORTC 26981/22981-NCIC CE3 phase III randomized trial, J Clin Oncol, 24 (2006) 2563-2569.
[40] D. Patel, N. Agarwal, K. Tomei, D. Hansberry, I. Goldstein, Optimal timing of whole-brain radiation therapy following craniotomy for cerebral malignancies, World Neurosurg, 84 (2015) 412-419.
[41] R. Stupp, M. Brada, M. van den Bent, J. Tonn, G. Pentheroudakis, High-grade glioma: ESMO Clinical Practice Guidelines for diagnosis, treatment and follow-up, Ann Oncol, 25 (2014) 93-101.
[42] C. Corso, R. Bindra, Success and failures of combined modalities in glioblastoma multiforme: Old problems and new directions, Semin Radiat Oncol, 26 (2016) 281-298.
[43] P. Ehrlich, Address in pathology on chemotherapeutics: Scientific principles, methods, and results, Lancet, 2 (1913) 445–451.
[44] E. Krumbhaar, H. Krunbhaar, The blood and bone barrow in yelloe cross gas (mustard gas) poisoning, J Med Res, 40 (1919) 497-508.
[45] E. Krumbhaar, Rôle of the blood and bone marrow in certain forms of gas poisoning: I. Peripheral blood changes and their significance, J Amer Med Assoc, 72 (1919) 39-41.
[46] J. Fenn, R. Udelsman, First use of intravenous chemotherapy cancer treatment: rectifying the record, J Am Coll Surg, 212 (2011) 413-417.
[47] R. Thomas, L. Recht, S. Nagpal, Advances in the management of glioblastoma: the role of temozolomide and MGMT testing, Clin Pharmacol, 5 (2013) 1-9.

[48] T. Connors, Anticancer drug development: The way forward, Oncologist, 1 (1996) 180-181.
[49] G.F. Woodworth, G.P. Dunn, E.A. Nance, J. Hanes, H. Brem. Emerging insights into barriers to effective brain tumor therapeutics. Front Oncol. (2014) 4:126.
[50] O. van Tellingen, B. Yetkin-Arik, M.C. de Gooijer, P. Wesseling, T. Wurdinger, H.E. de Vries. Overcoming the blood-brain tumor barrier for effective glioblastoma treatment. Drug Resist Updat. 19 (2015) 1-12.
[51] P. Rubin, D. Gash, J. Hansen, D. Nelson, J. Williams, Disruption of the blood-brain barrier as the primary effect of CNS irradiation, Radiother Oncol, 31 (1994) 51-60.
[52] Peereboom, E. Neuwelt, Chemotherapy delivery issues in central nervous system malignancy: a reality check, J Clin Oncol, 25 (2007) 2295-2305.
[53] M. Cohen, Y. Shen, P. Keegan, R. Pazdur, FDA drug approval summary: bevacizumab (Avastin) as treatment of recurrent glioblastoma multiforme, Oncologist, 14 (2009) 1131-1138.
[54] L. Ashby, K. Smith, B. Stea, Gliadel wafer implantation combined with standard radiotherapy and concurrent followed by adjuvant temozolomide for treatment of newly diagnosed high-grade glioma: a systematic literature review, World J Surg Oncol, 14 (2016) 225.
[55] M. Westphal, D. Hilt, E. Bortey, P. Delavault, R. Olivares, P. Warnke, I. Whittle, J. Jääskeläinen, Z. Ram, A phase 3 trial of local chemotherapy with biodegradable carmustine (BCNU) wafers (Gliadel wafers) in patients with primary malignant glioma, Neuro Oncol, 5 (2003) 79-88.
[56] H. Bock, M. Puchner, F. Lohmann, M. Schütze, S. Koll, R. Ketter, R. Buchalla, N. Rainov, S. Kantelhardt, V. Rohde, A. Giese, First-line treatment of malignant glioma with carmustine implants followed by concomitant radiochemotherapy: a multicenter experience, Neurosurg Rev, 33 (2010) 441-449.
[57] H. Brem, S. Piantadosi, P. Burger, M. Walker, R. Selker, N. Vick, K. Black, M. Sisti, S. Brem, G. Mohr, P. Muller, R. Morawetz, S. Clifford Schold, P.-B.T.T. Group, Placebo-controlled trial of safety and efficacy of intraoperative controlled delivery by biodegradable polymers of chemotherapy for recurrent gliomas. The Polymer-brain Tumor Treatment Group, Lancet, 345 (1995) 1008-1012.
[58] M. Borner, W. Scheithauer, C. Twelves, J. Maroun, H. Wilke, Answering patients' needs: oral alternatives to intravenous therapy, Oncologist, 6 (2001) 12-16.
[59] G. Liu, E. Franssen, M. Fitch, E. Warner, Patient preferences for oral versus intravenous palliative chemotherapy, J Clin Oncol, 15 (1997) 110-115.
[60] M. Brada, S. Stenning, R. Gabe, L. Thompson, D. Levy, R. Rampling, S. Erridge, F. Saran, R. Gattamaneni, K. Hopkins, S. Beall, V. Collins, S. Lee, Temozolomide versus procarbazine, lomustine, and vincristine in recurrent high-grade glioma, J Clin Oncol, 28 (2010) 4601-4608.
[61] J. Silber, M. Bobola, A. Blank, M. Chamberlain, O(6)-methylguanine-DNA methyltransferase in glioma therapy: promise and problems, Biochim Biophys Acta, 1826 (2012) 71-82.
[62] A. Davies, U. Weinberg, Y. Palti, Tumor treating fields: a new frontier in cancer therapy, Ann N Y Acad Sci, 1291 (2013) 86-95.
[63] S. Taillibert, E. Le Rhun, M. Chamberlain, Tumor treating fields: a new standard treatment for glioblastoma?, Curr Opin Neurol, 28 (2015) 659-664.
[64] E. Domingo-Musibay, E. Galanis, What next for newly diagnosed glioblastoma?, Future Oncol, 11 (2015) 3273-3283.
[65] R. Stupp, E. Wong, A. Kanner, D. Steinberg, H. Engelhard, V. Heidecke, E. Kirson, S. Taillibert, F. Liebermann, V. Dbalý, Z. Ram, J. Villano, N. Rainov, U. Weinberg, D. Schiff, L. Kunschner, J. Raizer, J. Honnorat, A. Sloan, M. Malkin, J. Landolfi, F. Payer, M. Mehdorn, R. Weil, S. Pannullo, M. Westphal, M. Smrcka, L. Chin, H. Kostron, S. Hofer, J. Bruce, R. Cosgrove, N. Paleologous, Y. Palti, P. Gutin, NovoTTF-100A versus physician's choice chemotherapy in recurrent glioblastoma: a randomised phase III trial of a novel treatment modality, Eur J Cancer, 48 (2012) 2192-2202.
[66] M.D. Prados, S.A. Byron, N.L. Tran, J.J. Phillips, A.M. Molinaro, K.L. Ligon, P.Y. Wen, J.G. Kuhn, I.K. Mellinghoff, J.F. de Groot, H. Colman, T.F. Cloughesy, S.M. Chang, T.C. Ryken, W.D. Tembe, J.A. Kiefer, M.E. Berens, D.W. Craig, J.D. Carpten, J.M. Trent, Toward precision medicine in glioblastoma: the promise and the challenges, Neur Oncol, 17 (2015) 1051-1063.
[67] M. Brada, S. Stenning, R. Gabe, L.C. Thompson, D. Levy, R. Rampling, S. Erridge, F. Saran, R. Gattamaneni, K. Hopkins, S. Beall, V.P. Collins, S.M. Lee, Temozolomide versus procarbazine, lomustine, and vincristine in recurrent high-grade glioma, J Clin Oncol, 28 (2010) 4601-4608.
[68] M. Weller, R. Stupp, G. Reifenberger, A.A. Brandes, M.J. van den Bent, W. Wick, M.E. Hegi, MGMT promoter methylation in malignant gliomas: ready for personalized medicine?, Nat Rev Neurol, 6 (2010) 39-51.
[69] J.N. Sarkaria, G.J. Kitange, C.D. James, R. Plummer, H. Calvert, M. Weller, W. Wick, Mechanisms of chemoresistance to alkylating agents in malignant glioma, Clin Cancer Res, 14 (2008) 2900-2908.

[70] F. Danhier, K. Messaoudi, L. Lemaire, J.P. Benoit, F. Lagarce, Combined anti-Galectin-1 and anti-EGFR siRNA-loaded chitosan-lipid nanocapsules decrease temozolomide resistance in glioblastoma: in vivo evaluation, Int J Pharm, 481 (2015) 154-161.
[71] J.J. Vredenburgh, A. Desjardins, J.E. Herndon, 2nd, J. Marcello, D.A. Reardon, J.A. Quinn, J.N. Rich, S. Sathornsumetee, S. Gururangan, J. Sampson, M. Wagner, L. Bailey, D.D. Bigner, A.H. Friedman, H.S. Friedman, Bevacizumab plus irinotecan in recurrent glioblastoma multiforme, J Clin Oncol, 25 (2007) 4722-4729.
[72] H.S. Friedman, M.D. Prados, P.Y. Wen, T. Mikkelsen, D. Schiff, L.E. Abrey, W.K. Yung, N. Paleologos, M.K. Nicholas, R. Jensen, J. Vredenburgh, J. Huang, M. Zheng, T. Cloughesy, Bevacizumab alone and in combination with irinotecan in recurrent glioblastoma, J Clin Oncol, 27 (2009) 4733-4740.
[73] P. Fu, Y.S. He, Q. Huang, T. Ding, Y.C. Cen, H.Y. Zhao, X. Wei, Bevacizumab treatment for newly diagnosed glioblastoma: Systematic review and meta-analysis of clinical trials, Mol Clin Oncol, 4 (2016) 833-838.
[74] A. Narayana, P. Kelly, J. Golfinos, E. Parker, G. Johnson, E. Knopp, D. Zagzag, I. Fischer, S. Raza, P. Medabalmi, P. Eagan, M.L. Gruber, Antiangiogenic therapy using bevacizumab in recurrent high-grade glioma: impact on local control and patient survival, J Neurosurg, 110 (2009) 173-180.
[75] D.R. Johnson, H.E. Leeper, J.H. Uhm, Glioblastoma survival in the United States improved after Food and Drug Administration approval of bevacizumab: a population-based analysis, Cancer, 119 (2013) 3489-3495.
[76] W. Wick, M. Weller, M. van den Bent, R. Stupp, Bevacizumab and recurrent malignant gliomas: a European perspective, J Clin Oncol, 28 (2010) 188-189.
[77] A. Desjardins, Neuro-oncology: What is the optimal use of bevacizumab in glioblastoma?, Nat Rev Neurol, 11 (2015) 429-430.
[78] M. Gilbert, J. Dignam, T. Armstrong, J. Wefel, D. Blumenthal, M. Vogelbaum, H. Colman, A. Chakravarti, S. Pugh, M. Won, R. Jeraj, P. Brown, K. Jaeckle, D. Schiff, V. Stieber, D. Brachman, M. Werner-Wasik, I. Tremont-Lukats, E. Sulman, K. Aldape, W.J. Curran, M. Mehta, A randomized trial of bevacizumab for newly diagnosed glioblastoma, N Engl J Med, 370 (2014) 699-708.
[79] O. Chinot, W. Wick, W. Mason, R. Henriksson, F. Saran, R. Nishikawa, A. Carpentier, K. Hoang-Xuan, F. Kavan, D. Cernea, A. Brandes, M. Hilton, L. Abrey, T. Cloughesy, Bevacizumab plus radiotherapy-temozolomide for newly diagnosed glioblastoma, N Engl J Med, 370 (2014) 709-722.
[80] W. Wick, O. Chinot, M. Bendszus, W. Mason, R. Henriksson, F. Saran, R. Nishikawa, C. Revil, Y. Kerloeguen, T. Cloughesy, Evaluation of pseudoprogression rates and tumor progression patterns in a phase III trial of bevacizumab plus radiotherapy/temozolomide for newly diagnosed glioblastoma, Neuro Oncol, 18 (2016) 1434-1441.
[81] O. Chinot, R. Nishikawa, W. Mason, R. Henriksson, F. Saran, T. Cloughesy, J. Garcia, C. Revil, L. Abrey, W. Wick, Upfront bevacizumab may extend survival for glioblastoma patients who do not receive second-line therapy: an exploratory analysis of AVAglio, Neuro Oncol, 18 (2016) 1313-1318.
[82] S. Rose, FDA pulls approval for Avastin in breast cancer, Cancer Discov, 1 (2011) 1-2.
[83] B. Kovic, F. Xie, Economic evaluation of bevacizumab for the first-line treatment of newly diagnosed glioblastoma multiforme, J Clin Oncol, 33 (2015) 2296-2302.
[84] B. Campos, L. Olsen, T. Urup, H. Poulsen, A comprehensive profile of recurrent glioblastoma, Oncogene, 35 (2016) 5819-5825.
[85] H. Sun, S. Du, G. Liao, X. Xie, C. Ren, Y. Yuan, Do glioma patients derive any therapeutic benefit from taking a higher cumulative dose of temozolomide regimens?: a meta-analysis, Medicine, 94 (2015) e827.
[86] A. Tosoni, E. Franceschi, R. Poggi, A. Brandes, Relapsed glioblastoma: treatment strategies for initial and subsequent recurrences, Curr Treat Options Oncol, 17 (2016) 49.
[87] A. Yin, J. Cheng, X. Zhang, B. Liu, The treatment of glioblastomas: a systematic update on clinical Phase III trials, Crit Rev Oncol Hematol, 87 (2013) 265-282.
[88] clinicaltrials.gov, in 2017, National Library of Medicine (US).
[89] E.C. Holland, Glioblastoma multiforme: the terminator, Proc Natl Acad Sci U S A, 97 (2000) 6242-6244.
[90] L. Tavano, R. Muzzalupo, Multi-functional vesicles for cancer therapy: The ultimate magic bullet, Colloids Surf B Biointerfaces, 147 (2016) 161-171.
[91] G. Bradač, U. Büll, R. Fahlbusch, T. Grumme, E. Kazner, K. Kretzschmar, W. Lanksch, W. Meese, J. Schramm, H. Steinhoff, O. Stochdorph, S. Wende, Computed Tomography in Intracranial Tumors: Differential Diagnosis and Clinical Aspects, Springer-Verlag, Berlin, 1982.
[92] R. Stupp, M. Hegi, W. Mason, M. van den Bent, M. Taphoorn, R. Janzer, S. Ludwin, A. Allgeier, B. Fisher, K. Belanger, P. Hau, A. Brandes, J. Gijtenbeek, C. Marosi, C. Vecht, K. Mokhtari, P. Wesseling, S. Villa, E.

Eisenhauer, T. Gorlia, M. Weller, D. Lacombe, J. Cairncross, R. Mirimanoff, E.O.f.R.a.T.o.C.B.T.a.R.O. Groups, N.C.I.o.C.C.T. Group, Effects of radiotherapy with concomitant and adjuvant temozolomide versus radiotherapy alone on survival in glioblastoma in a randomised phase III study: 5-year analysis of the EORTC-NCIC trial, Lancet Oncol, 10 (2009) 459-466.

[93] J. Scott, L. Bauchet, T. Fraum, L. Nayak, A. Cooper, S. Chao, J. Suh, M. Vogelbaum, D. Peereboom, S. Zouaoui, H. Mathieu-Daudé, P. Fabbro-Peray, V. Rigau, L. Taillandier, L. Abrey, L. DeAngelis, J. Shih, F. Iwamoto, Recursive partitioning analysis of prognostic factors for glioblastoma patients aged 70 years or older, Cancer, 118 (2012) 5595-5600.

[94] M. Neagu, D. Reardon, An update on the role of immunotherapy and vaccine strategies for primary brain tumors, Curr Treat Options Oncol, 16 (2015) 54.

[95] J. Sampson, D. Mitchell, Vaccination strategies for neuro-oncology, Neuro Oncol, 17 (2015) 15-25.

[96] H. Ardon, S. Van Gool, I. Lopes, W. Maes, R. Sciot, G. Wilms, P. Demaerel, P. Bijttebier, L. Claes, J. Goffin, F. Van Calenbergh, S. De Vleeschouwer, Integration of autologous dendritic cell-based immunotherapy in the primary treatment for patients with newly diagnosed glioblastoma multiforme: a pilot study, J Neurooncol, 99 (2010) 261-272.

[97] V. Schijns, C. Pretto, L. Devillers, D. Pierre, F. Hofman, T. Chen, P. Mespouille, P. Hantos, P. Glorieux, D. Bota, A. Stathopoulos, First clinical results of a personalized immunotherapeutic vaccine against recurrent, incompletely resected, treatment-resistant glioblastoma multiforme (GBM) tumors, based on combined allo- and auto-immune tumor reactivity, Vaccine, 33 (2015) 269--2696.

[98] J. Reijneveld, E. Voest, M. Taphoorn, Angiogenesis in malignant primary and metastatic brain tumors, J Neurol, 247 (2000) 597-608.

[99] C. Scaringi, R. Enrici, G. Minniti, Combining molecular targeted agents with radiation therapy for malignant gliomas, Onco Targets Ther, 6 (2013) 1079-1095.

[100] M. McGee, J. Hamner, R. Williams, S. Rosati, T. Sims, C. Ng, M. Gaber, C. Calabrese, J. Wu, A. Nathwani, C. Duntsch, T. Merchant, A. Davidoff, Improved intratumoral oxygenation through vascular normalization increases glioma sensitivity to ionizing radiation, Int J Radiat Oncol Biol Phys, 76 (2010) 1537-1545.

[101] V. Gupta, N. Jaskowiak, M. Beckett, H. Mauceri, J. Grunstein, R. Johnson, D. Calvin, E. Nodzenski, M. Pejovic, D. Kufe, M. Posner, R. Weichselbaum, Vascular endothelial growth factor enhances endothelial cell survival and tumor radioresistance, Cancer J, 8 (2002) 47-54.

[102] E. Bolderson, D. Richard, B. Zhou, K. Khanna, Recent advances in cancer therapy targeting proteins involved in DNA double-strand break repair, Clin Cancer Res, 15 (2009) 6314-6320.

[103] M. Rouleau, A. Patel, M. Hendzel, S. Kaufmann, G. Poirier, PARP inhibition: PARP1 and beyond, Nat Rev Cancer, 10 (2010) 293-301.

[104] H. Bryant, N. Schultz, H. Thomas, K. Parker, D. Flower, E. Lopez, S. Kyle, M. Meuth, N. Curtin, T. Helleday, Specific killing of BRCA2-deficient tumours with inhibitors of poly(ADP-ribose) polymerase, Nature, 434 (2005) 913-917.

[105] H. Farmer, N. McCabe, C. Lord, A. Tutt, D. Johnson, T. Richardson, M. Santarosa, K. Dillon, I. Hickson, C. Knights, N. Martin, S. Jackson, G. Smith, A. Ashworth, Targeting the DNA repair defect in BRCA mutant cells as a therapeutic strategy, Nature, 434 (2005) 917-921.

[106] C. Powell, C. Mikropoulos, S. Kaye, C. Nutting, S. Bhide, K. Newbold, K. Harrington, Pre-clinical and clinical evaluation of PARP inhibitors as tumour-specific radiosensitisers, Cancer Treat Rev, 36 (2010) 566-575.

[107] J. Senra, B. Telfer, K. Cherry, C. McCrudden, D. Hirst, M. O'Connor, S. Wedge, I. Stratford, Inhibition of PARP-1 by olaparib (AZD2281) increases the radiosensitivity of a lung tumor xenograft, Mol Cancer Ther, 10 (2011) 1949-1958.

[108] D. Bonnet, J. Dick, Human acute myeloid leukemia is organized as a hierarchy that originates from a primitive hematopoietic cell, Nature Med, 3 (1997) 730-737.

[109] R. Galli, E. Binda, U. Orfanelli, B. Cipelletti, A. Gritti, S. De Vitis, R. Fiocco, C. Foroni, F. Dimeco, A. Vescovi, Isolation and characterization of tumorigenic, stem-like neural precursors from human glioblastoma, Cancer Res, 64 (2004) 7011-7021.

[110] D. Beier, S. Röhrl, D. Pillai, S. Schwarz, L. Kunz-Schughart, P. Leukel, M. Proescholdt, A. Brawanski, U. Bogdahn, A. Trampe-Kieslich, B. Giebel, J. Wischhusen, G. Reifenberger, P. Hau, C. Beier, Temozolomide preferentially depletes cancer stem cells in glioblastoma, Cancer Res, 68 (2008) 5706-5715.

[111] M. Hegi, A. Diserens, T. Gorlia, M. Hamou, N. de Tribolet, M. Weller, J. Kros, J. Hainfellner, W. Mason, L. Mariani, J. Bromberg, P. Hau, R. Mirimanoff, J. Cairncross, R. Janzer, R. Stupp, MGMT gene silencing and benefit from temozolomide in glioblastoma, N Engl J Med, 352 (2005) 997-1003.

[112] J. Lathia, S. Mack, E. Mulkearns-Hubert, C. Valentim, J. Rich, Cancer stem cells in glioblastoma, Genes Dev, 29 (2015) 1203-1217.
[113] P. Gupta, T. Onder, G. Jiang, K. Tao, C. Kuperwasser, R. Weinberg, E. Lander, Identification of selective inhibitors of cancer stem cells by high-throughput screening, Cell, 138 (2009) 645-659.
[114] L. Qin, P. Jia, Z. Zhang, S. Zhang, ROS-p53-cyclophilin-D signaling mediates salinomycin-induced glioma cell necrosis, J Exp Clin Canc Res, 34 (2015) 57.
[115] A. Calzolari, E. Saulle, M. De Angelis, L. Pasquini, A. Boe, F. Pelacchi, L. Ricci-Vitiani, M. Baiocchi, U. Testa, Salinomycin potentiates the cytotoxic effects of TRAIL on glioblastoma cell lines, PLoS One, 9 (2014) e94438.
[116] W. Pardridge, Blood-brain barrier delivery, Drug Discov Today, 12 (2007) 54-61.
[117] M. Vogelbaum, M. Aghi, Convection-enhanced delivery for the treatment of glioblastoma, Neuro Oncol, 17 (2015) 3-8.
[118] K. Hynynen, N. McDannold, N. Vykhodtseva, F. Jolesz, Non-invasive opening of BBB by focused ultrasound, Acta Neurochir Suppl, 86 (2003) 555-558.
[119] J. Choi, J. Feshitan, B. Baseri, S. Wang, Y. Tung, M. Borden, E. Konofagou, Microbubble-size dependence of focused ultrasound-induced blood-brain barrier opening in mice in vivo, IEEE Trans Biomed Eng, 57 (2010) 145-154.
[120] H. Liu, P. Hsu, C. Lin, C. Huang, W. Chai, P. Chu, C. Huang, P. Chen, L. Yang, J. Kuo, K. Wei, Focused ultrasound enhances central nervous system delivery of bevacizumab for malignant glioma treatment, Radiology, 281 (2016) 99-108.
[121] A. Carpentier, M. Canney, A. Vignot, V. Reina, K. Beccaria, C. Horodyckid, C. Karachi, D. Leclercq, C. Lafon, J. Chapelon, L. Capelle, P. Cornu, M. Sanson, K. Hoang-Xuan, J. Delattre, A. Idbaih, Clinical trial of blood-brain barrier disruption by pulsed ultrasound, Sci Transl Med, 8 (2016) 343re342.
[122] G. Sarkar, G. Curran, J. Sarkaria, V. Lowe, R. Jenkins, Peptide carrier-mediated non-covalent delivery of unmodified cisplatin, methotrexate and other agents via intravenous route to the brain, PLoS One, 9 (2014) e97655.
[123] T. Allen, P. Cullis, Drug delivery systems: entering the mainstream, Science, 303 (2004) 1818-1822.
[124] D. Peer, J. Karp, S. Hong, O. Farokhzad, R. Margalit, R. Langer, Nanocarriers as an emerging platform for cancer therapy, Nat Nanotech, 2 (2007) 751-760.
[125] A. Gutkin, Z. Cohen, D. Peer, Harnessing nanomedicine for therapeutic intervention in glioblastoma, Expert Opin Drug Deliv, 13 (2016) 1573-1582.
[126] S. Kim, J. Harford, K. Pirollo, E. Chang, Effective treatment of glioblastoma requires crossing the blood-brain barrier and targeting tumors including cancer stem cells: The promise of nanomedicine, Biochem Biophys Res Commun, 468 (2015) 485-489.
[127] F. Danhier, K. Messaoudi, L. Lemaire, J. Benoit, F. Lagarce, Combined anti-Galectin-1 and anti-EGFR siRNA-loaded chitosan-lipid nanocapsules decrease temozolomide resistance in glioblastoma: in vivo evaluation, Int J Pharm, 481 (2015) 154-161.
[128] C. Bastiancich, K. Vanvarenberg, B. Ucakar, M. Pitorre, G. Bastiat, F. Lagarce, V. Préat, F. Danhier, Lauroyl-gemcitabine-loaded lipid nanocapsule hydrogel for the treatment of glioblastoma, J Control Release, 225 (2016) 283-293.
[129] T. Hoare, K. DS, Hydrogels in drug delivery: Progress and challenges, Polymer, 49 (2008) 1993-2007.
[130] C. Bastiancich, P. Danhier, V. Préat, F. Danhier, Anticancer drug-loaded hydrogels as drug delivery systems for the local treatment of glioblastoma, J Control Release, 243 (2016) 29-42.
[131] A. Vellimana, V. Recinos, L. Hwang, K. Fowers, K. Li, Y. Zhang, S. Okonma, C. Eberhart, H. Brem, B. Tyler, Combination of paclitaxel thermal gel depot with temozolomide and radiotherapy significantly prolongs survival in an experimental rodent glioma model, J Neurooncol, 111 (2013) 229-236.
[132] T. Fourniols, L. Randolph, A. Staub, K. Vanvarenberg, J. Leprince, V. Préat, A. des Rieux, F. Danhier, Temozolomide-loaded photopolymerizable PEG-DMA-based hydrogel for the treatment of glioblastoma, J Control Release, 210 (2015) 95-104.
[133] F. Marchesi, M. Turriziani, G. Tortorelli, G. Avvisati, F. Torino, L. De Vecchis, Triazene compounds: mechanism of action and related DNA repair systems, Pharmacol Res, 56 (2007) 275-287.
[134] G. Perazzoli, J. Prados, R. Ortiz, O. Caba, L. Cabeza, M. Berdasco, B. Gónzalez, C. Melguizo, Temozolomide resistance in glioblastoma cell lines: Implication of MGMT, MMR, P-glycoprotein and CD133 expression, PLoS One, 10 (2015) e0140131.
[135] M. Weller, R. Stupp, G. Reifenberger, A. Brandes, M. van den Bent, W. Wick, M. Hegi, MGMT promoter methylation in malignant gliomas: ready for personalized medicine?, Nat Rev Neurol, 6 (2010) 39-51.

[136] N. Parker, P. Khong, J. Parkinson, V. Howell, H. Wheeler, Molecular heterogeneity in glioblastoma: potential clinical implications, Front Oncol, 5 (2015) 55.
[137] K. Messaoudi, C. Clavreul, F. Danhier, P. Saulnier, J.-P. Benoît, F. Lagarce, Combined silencing expression of MGMT with EGFR or galectin-1 enhances the sensitivity of glioblastoma to temozolomide, Eur J Nanomed, 7 (2015) 97-107.
[138] B. Kaina, G. Margison, M. Christmann, Targeting O^6-methylguanine-DNA methyltransferase with specific inhibitors as a strategy in cancer therapy, Cell Mol Life Sci, 67 (2010) 3663-3681.
[139] Y. Ramirez, A. Mladek, R. Phillips, M. Gynther, J. Rautio, A. Ross, R. Wheelhouse, J. Sakaria, Evaluation of novel imidazotetrazine analogues designed to overcome temozolomide resistance and glioblastoma regrowth, Mol Cancer Ther, 14 (2015) 111-119.
[140] J. Rich, D. Bigner, Development of novel targeted therapies in the treatment of malignant glioma, Nat Rev Drug Discov, 3 (2004) 430-446.
[141] T. Verschuere, J. Toelen, W. Maes, F. Poirier, L. Boon, T. Tousseyn, T. Mathivet, H. Gerhardt, V. Mathieu, R. Kiss, F. Lefranc, S. Van Gool, S. De Vleeschouwer, Glioma-derived galectin-1 regulates innate and adaptive antitumor immunity, Int J Cancer, 134 (2014) 873-884.
[142] M. Le Mercier, S. Fortin, V. Mathieu, R. Kiss, F. Lefranc, Galectins and gliomas, Brain Pathol, 20 (2010) 17-27.
[143] I. Camby, C. Decaestecker, F. Lefranc, H. Kaltner, H. Gabius, R. Kiss, Galectin-1 knocking down in human U87 glioblastoma cells alters their gene expression pattern, Biochem Biophys Res Commun, 335 (2005) 27-35.
[144] A. Burgess, K. Shah, O. Hough, K. Hynynen, Focused ultrasound-mediated drug delivery through the blood-brain barrier, Expert Rev Neurother, 15 (2015) 477-491.
[145] R. Karim, C. Palazzo, B. Evrard, G. Piel, Nanocarriers for the treatment of glioblastoma multiforme: Current state-of-the-art, J Control Release, 227 (2016) 23-37.
[146] F. Danhier, O. Feron, V. Preat, To exploit the tumor microenvironment: Passive and active tumor targeting of nanocarriers for anti-cancer drug delivery, J Control Release, 148 (2010) 135-146.
[147] M. Singh, S. Kundu, M.A. Reddy, V. Sreekanth, R.K. Motiani, S. Sengupta, A. Srivastava, A. Bajaj, Injectable small molecule hydrogel as a potential nanocarrier for localized and sustained in vivo delivery of doxorubicin, Nanoscale, 6 (2014) 12849-12855.
[148] M. Westphal, D.C. Hilt, E. Bortey, P. Delavault, R. Olivares, P.C. Warnke, I.R. Whittle, J. Jaaskelainen, Z. Ram, A phase 3 trial of local chemotherapy with biodegradable carmustine (BCNU) wafers (Gliadel wafers) in patients with primary malignant glioma, Neuro Oncol, 5 (2003) 79-88.
[149] B.K. Hendricks, A.A. Cohen-Gadol, J.C. Miller, Novel delivery methods bypassing the blood-brain and blood-tumor barriers, Neurosurgical focus, 38 (2015) E10.
[150] T. Garg, S. Bhandari, G. Rath, A.K. Goyal, Current strategies for targeted delivery of bio-active drug molecules in the treatment of brain tumor, J Drug Targ, 23 (2015) 865-887.
[151] V. Varenika, P. Dickinson, J. Bringas, R. LeCouteur, R. Higgins, J. Park, M. Fiandaca, M. Berger, J. Sampson, K. Bankiewicz, Detection of infusate leakage in the brain using real-time imaging of convection-enhanced delivery, J Neurosurg, 109 (2008) 874-880.
[152] J.B. Wolinsky, Y.L. Colson, M.W. Grinstaff, Local drug delivery strategies for cancer treatment: gels, nanoparticles, polymeric films, rods, and wafers, J Control Release, 159 (2012) 14-26.
[153] T.A. Juratli, G. Schackert, D. Krex, Current status of local therapy in malignant gliomas--a clinical review of three selected approaches, Pharmacol Ther, 139 (2013) 341-358.
[154] K.G. Abdullah, J.A Burdick. Local Drug Delivery in the Treatment of Glioblastoma, in: S. Brem K. G. Abdullah (Ed.) Glioblastoma, Elsevier, 2017.
[155] D.A. Bota, A. Desjardins, J.A. Quinn, M.L. Affronti, H.S. Friedman, Interstitial chemotherapy with biodegradable BCNU (Gliadel) wafers in the treatment of malignant gliomas, Ther Clin Risk Manag, 3 (2007) 707-715.
[156] Food and Drug administration webpage, www.fda.gov, in, 2013, pp. Reference ID 3358686.
[157] J. Perry, A. Chambers, K. Spithoff, N. Laperriere, Gliadel wafers in the treatment of malignant glioma: a systematic review, Curr Oncol, 14 (2007) 189-194.
[158] S.A. Grossman, C. Reinhard, O.M. Colvin, M. Chasin, R. Brundrett, R.J. Tamargo, H. Brem, The intracerebral distribution of BCNU delivered by surgically implanted biodegradable polymers, J Neurosurg, 76 (1992) 640-647.
[159] L.K. Fung, M.G. Ewend, A. Sills, E.P. Sipos, R. Thompson, M. Watts, O.M. Colvin, H. Brem, W.M. Saltzman, Pharmacokinetics of interstitial delivery of carmustine, 4-hydroperoxycyclophosphamide, and paclitaxel from a biodegradable polymer implant in the monkey brain, Cancer Res, 58 (1998) 672-684.

[160] A.B. Fleming, W.M. Saltzman, Pharmacokinetics of the carmustine implant, Clin Pharmacokinet, 41 (2002) 403-419.
[161] J.R. Silber, M.S. Bobola, A. Blank, M.C. Chamberlain, O(6)-methylguanine-DNA methyltransferase in glioma therapy: promise and problems, Biochim Biophys Acta, 1826 (2012) 71-82.
[162] F. DiMeco, K.W. Li, B.M. Tyler, A.S. Wolf, H. Brem, A. Olivi, Local delivery of mitoxantrone for the treatment of malignant brain tumors in rats, J Neurosurg, 97 (2002) 1173-1178.
[163] K.A. Walter, M.A. Cahan, A. Gur, B. Tyler, J. Hilton, O.M. Colvin, P.C. Burger, A. Domb, H. Brem, Interstitial taxol delivered from a biodegradable polymer implant against experimental malignant glioma, Cancer Res, 54 (1994) 2207-2212.
[164] P.B. Storm, J.L. Moriarity, B. Tyler, P.C. Burger, H. Brem, J. Weingart, Polymer delivery of camptothecin against 9L gliosarcoma: release, distribution, and efficacy, J neurooncol, 56 (2002) 209-217.
[165] M.S. Lesniak, U. Upadhyay, R. Goodwin, B. Tyler, H. Brem, Local Delivery of Doxorubicin for the Treatment of Malignant Brain Tumors in Rats, Anticancer Res, 25 (2005) 3825-3831.
[166] H. Bow, L.S. Hwang, N. Schildhaus, J. Xing, L. Murray, Q. Salditch, X. Ye, Y. Zhang, J. Weingart, H. Brem, B. Tyler, Local delivery of angiogenesis-inhibitor minocycline combined with radiotherapy and oral temozolomide chemotherapy in 9L glioma, J Neurosurg, 120 (2014) 662-669.
[167] K. Yohay, B. Tyler, K.D. Weaver, A.C. Pardo, D. Gincel, J. Blakeley, H. Brem, J.D. Rothstein, Efficacy of local polymer-based and systemic delivery of the anti-glutamatergic agents riluzole and memantine in rat glioma models, J Neurosurg, 120 (2014) 854-863.
[168] B. Tyler, S. Wadsworth, V. Recinos, V. Mehta, A. Vellimana, K. Li, J. Rosenblatt, H. Do, G.L. Gallia, I.M. Siu, R.T. Wicks, M.A. Rudek, M. Zhao, H. Brem, Local delivery of rapamycin: a toxicity and efficacy study in an experimental malignant glioma model in rats, Neuro Oncol, 13 (2011) 700-709.
[169] Y. Manome, T. Kobayashi, M. Mori, R. Suzuki, N. Funamizu, N. Akiyama, S. Inoue, Y. Tabata, M. Watanabe, Local delivery of doxorubicin for malignant glioma by a biodegradable PLGA polymer sheet, Anticancer Res, 26 (2006) 3317-3326.
[170] K.L. von Eckardstein, R. Reszka, J.C. Kiwit, Intracavitary chemotherapy (paclitaxel/carboplatin liquid crystalline cubic phases) for recurrent glioblastoma -- clinical observations, J Neurooncol, 74 (2005) 305-309.
[171] S.V. Sheleg, E.A. Korotkevich, E.A. Zhavrid, G.V. Muravskaya, A.F. Smeyanovich, Y.G. Shanko, T.L. Yurkshtovich, P.B. Bychkovsky, S.A. Belyaev, Local chemotherapy with cisplatin-depot for glioblastoma multiforme, J Neurooncol, 60 (2002) 53-59.
[172] J.D. Weingart, R.C. Thompson, B. Tyler, O.M. Colvin, H. Brem, Local delivery of the topoisomerase I inhibitor camptothecin sodium prolongs survival in the rat intracranial 9L gliosarcoma model, Intl J cancer, 62 (1995) 605-609.
[173] K.O. Lillehei, Q. Kong, S.J. Withrow, B. Kleinschmidt-DeMasters, Efficacy of intralesionally administered cisplatin-impregnated biodegradable polymer for the treatment of 9L gliosarcoma in the rat, Neurosurgery, 39 (1996) 1191-1199.
[174] J.S. Lee, T.K. An, G.S. Chae, J.K. Jeong, S.H. Cho, H.B. Lee, G. Khang, Evaluation of in vitro and in vivo antitumor activity of BCNU-loaded PLGA wafer against 9L gliosarcoma, Eur J Pharm Biopharm, 59 (2005) 169-175.
[175] K.W. Li, W. Dang, B.M. Tyler, G. Troiano, T. Tihan, H. Brem, K.A. Walter, Polilactofate microspheres for Paclitaxel delivery to central nervous system malignancies, Clin Cancer Res, 9 (2003) 3441-3447.
[176] G. Pradilla, P.P. Wang, P. Gabikian, K. Li, C.A. Magee, K.A. Walter, H. Brem, Local intracerebral administration of Paclitaxel with the paclimer delivery system: toxicity study in a canine model, J neurooncol, 76 (2006) 131-138.
[177] B.Y. Ong, S.H. Ranganath, L.Y. Lee, F. Lu, H.S. Lee, N.V. Sahinidis, C.H. Wang, Paclitaxel delivery from PLGA foams for controlled release in post-surgical chemotherapy against glioblastoma multiforme, Biomaterials, 30 (2009) 3189-3196.
[178] S.H. Ranganath, C.-H. Wang, Biodegradable microfiber implants delivering paclitaxel for post-surgical chemotherapy against malignant glioma, Biomaterials, 29 (2008) 2996-3003.
[179] P. Kumar Naraharisetti, B. Yung Sheng Ong, J. Wei Xie, T. Kam Yiu Lee, C.-H. Wang, N.V. Sahinidis, In vivo performance of implantable biodegradable preparations delivering Paclitaxel and Etanidazole for the treatment of glioma, Biomaterials, 28 (2007) 886-894.
[180] P. Menei, L. Capelle, J. Guyotat, S. Fuentes, R. Assaker, B. Bataille, P. Francois, D. Dorwling-Carter, P. Paquis, L. Bauchet, F. Parker, J. Sabatier, N. Faisant, J.P. Benoit, Local and sustained delivery of 5-fluorouracil from biodegradable microspheres for the radiosensitization of malignant glioma: a randomized phase II trial, Neurosurgery, 56 (2005) 242-248; discussion 242-248.

[181] D.F. Emerich, S.R. Winn, P. Snodgrass, D. LaFreniere, M. Agostino, T. Wiens, H. Xiong, R.T. Bartus, Injectable chemotherapeutic microspheres and glioma II: enhanced survival following implantation into deep inoperable tumors, Pharm Res, 17 (2000) 776-781.
[182] Y.Y. Tseng, Y.C. Wang, C.H. Su, T.C. Yang, T.M. Chang, Y.C. Kau, S.J. Liu, Concurrent delivery of carmustine, irinotecan, and cisplatin to the cerebral cavity using biodegradable nanofibers: In vitro and in vivo studies, Colloids Surf B Biointerfaces, 134 (2015) 254-261.
[183] J.A. Floyd, A. Galperin, B.D. Ratner, Drug encapsulated polymeric microspheres for intracranial tumor therapy: A review of the literature, Adv Drug Deliv Rev, 91 (2015) 23-37.
[184] P. Menei, M. Boisdron-Celle, A. Croue, G. Guy, J.P. Benoit, Effect of stereotactic implantation of biodegradable 5-fluorouracil-loaded microspheres in healthy and C6 glioma-bearing rats, Neurosurgery, 39 (1996) 117-123; discussion 123-114.
[185] L. Lemaire, V.G. Roullin, F. Franconi, M.C. Venier-Julienne, P. Menei, P. Jallet, J.J. Le Jeune, J.P. Benoit, Therapeutic efficacy of 5-fluorouracil-loaded microspheres on rat glioma: a magnetic resonance imaging study, NMR Biomed, 14 (2001) 360-366.
[186] D.F. Emerich, S.R. Winn, Y. Hu, J. Marsh, P. Snodgrass, D. LaFreniere, T. Wiens, B.P. Hasler, R.T. Bartus, Injectable chemotherapeutic microspheres and glioma I: enhanced survival following implantation into the cavity wall of debulked tumors, Pharm Res, 17 (2000) 767-775.
[187] P. Menei, E. Jadaud, N. Faisant, M. Boisdron-Celle, S. Michalak, D. Fournier, M. Delhaye, J.P. Benoit, Stereotaxic implantation of 5-fluorouracil-releasing microspheres in malignant glioma, Cancer, 100 (2004) 405-410.
[188] Y.H. Zhang, H. Zhang, J.M. Liu, Z.J. Yue, Temozolomide/PLGA microparticles: a new protocol for treatment of glioma in rats, Med oncol, 28 (2011) 901-906.
[189] X. Zhang, S. Yao, C. Liu, Y. Jiang, Tumor tropic delivery of doxorubicin-polymer conjugates using mesenchymal stem cells for glioma therapy, Biomaterials, 39 (2015) 269-281.
[190] Y.Y. Tseng, Y.C. Kau, S.J. Liu, Advanced interstitial chemotherapy for treating malignant glioma, Expert Opin Drug Deliv, 13 (2016) 1533-1544.
[191] A. Mangraviti, D. Gullotti, B. Tyler, H. Brem, Nanobiotechnology-based delivery strategies: New frontiers in brain tumor targeted therapies, J Control Release, 240 (2016) 443-453 .
[192] A. Mangraviti, B. Tyler, H. Brem, Interstitial chemotherapy for malignant glioma: Future prospects in the era of multimodal therapy, Surg Neurol Int, 6 (2015) S78-84.
[193] G. Orive, O.A. Ali, E. Anitua, J.L. Pedraz, D.F. Emerich, Biomaterial-based technologies for brain anti-cancer therapeutics and imaging, Biochim Biophys Acta, 1806 (2010) 96-107.
[194] N.A. Peppas, P. Bures, W. Leobandung, H. Ichikawa, Hydrogels in pharmaceutical formulations, Eur J Pharm Biopharm, 50 (2000) 27-46.
[195] N.A. Peppas, R. Langer, New challenges in biomaterials, Science, 263 (1994) 1715-1720.
[196] B.D.H. Ratner, A.S., Synthetic hydrogels for biomedical applications., in: A.S. Series (Ed.) Hydrogels for Medical and Related Applications, American Chemical Society, Washington DC, 1976, pp. 1-36.
[197] C.C. Lin, A.T. Metters, Hydrogels in controlled release formulations: network design and mathematical modeling, Adv Drug Deliv Rev, 58 (2006) 1379-1408.
[198] S.R. Van Tomme, G. Storm, W.E. Hennink, In situ gelling hydrogels for pharmaceutical and biomedical applications, Int J Pharm, 355 (2008) 1-18.
[199] C. Wang, X. Tong, F. Yang, Bioengineered 3D brain tumor model to elucidate the effects of matrix stiffness on glioblastoma cell behavior using PEG-based hydrogels, Mol Pharm, 11 (2014) 2115-2125.
[200] S.S. Rao, J. Dejesus, A.R. Short, J.J. Otero, A. Sarkar, J.O. Winter, Glioblastoma behaviors in three-dimensional collagen-hyaluronan composite hydrogels, ACS Appl Mater Interfaces, 5 (2013) 9276-9284.
[201] C. Jiguet Jiglaire, N. Baeza-Kallee, E. Denicolai, D. Barets, P. Metellus, L. Padovani, O. Chinot, D. Figarella-Branger, C. Fernandez, Ex vivo cultures of glioblastoma in three-dimensional hydrogel maintain the original tumor growth behavior and are suitable for preclinical drug and radiation sensitivity screening, Exp Cell Res, 321 (2014) 99-108.
[202] U. Akbar, T. Jones, J. Winestone, M. Michael, A. Shukla, Y. Sun, C. Duntsch, Delivery of temozolomide to the tumor bed via biodegradable gel matrices in a novel model of intracranial glioma with resection, J Neurooncol, 94 (2009) 203-212.
[203] A.K. Vellimana, V.R. Recinos, L. Hwang, K.D. Fowers, K.W. Li, Y. Zhang, S. Okonma, C.G. Eberhart, H. Brem, B.M. Tyler, Combination of paclitaxel thermal gel depot with temozolomide and radiotherapy significantly prolongs survival in an experimental rodent glioma model, J Neurooncol, 111 (2013) 229-236.

[204] B. Tyler, K.D. Fowers, K.W. Li, V.R. Recinos, J.M. Caplan, A. Hdeib, R. Grossman, L. Basaldella, K. Bekelis, G. Pradilla, F. Legnani, H. Brem, A thermal gel depot for local delivery of paclitaxel to treat experimental brain tumors in rats, J Neurosurg, 113 (2010) 210-217.
[205] C.V. Rahman, S.J. Smith, P.S. Morgan, K.A. Langmack, P.A. Clarke, A.A. Ritchie, D.C. Macarthur, F.R. Rose, K.M. Shakesheff, R.G. Grundy, R. Rahman, Adjuvant chemotherapy for brain tumors delivered via a novel intra-cavity moldable polymer matrix, PloS one, 8 (2013) e77435.
[206] T. Fourniols, L.D. Randolph, A. Staub, K. Vanvarenberg, J.G. Leprince, V. Preat, A. des Rieux, F. Danhier, Temozolomide-loaded photopolymerizable PEG-DMA-based hydrogel for the treatment of glioblastoma, J Control Release, 210 (2015) 95-104.
[207] J.I. Kim, B. Kim, C. Chun, S.H. Lee, S.C. Song, MRI-monitored long-term therapeutic hydrogel system for brain tumors without surgical resection, Biomaterials, 33 (2012) 4836-4842.
[208] T. Arai, T. Joki, M. Akiyama, M. Agawa, Y. Mori, H. Yoshioka, T. Abe, Novel drug delivery system using thermoreversible gelation polymer for malignant glioma, J Neurooncol, 77 (2006) 9-15.
[209] T. Arai, O. Benny, T. Joki, L.G. Menon, M. Machluf, T. Abe, R.S. Carroll, P.M. Black, Novel local drug delivery system using thermoreversible gel in combination with polymeric microspheres or liposomes, Anticancer Res, 30 (2010) 1057-1064.
[210] T. Ozeki, D. Kaneko, K. Hashizawa, Y. Imai, T. Tagami, H. Okada, Combination therapy of surgical tumor resection with implantation of a hydrogel containing camptothecin-loaded poly(lactic-co-glycolic acid) microspheres in a C6 rat glioma model, Biol Pharm Bull, 35 (2012) 545-550.
[211] T. Ozeki, K. Hashizawa, D. Kaneko, Y. Imai, H. Okada, Treatment of rat brain tumors using sustained-release of camptothecin from poly(lactic-co-glycolic acid) microspheres in a thermoreversible hydrogel, Chem Pharm Bull, 58 (2010) 1142-1147.
[212] S. Vinchon-Petit, D. Jarnet, S. Michalak, A. Lewis, J.P. Benoit, P. Menei, Local implantation of doxorubicin drug eluting beads in rat glioma, Int J Pharm, 402 (2010) 184-189.
[213] S.H. Ranganath, I. Kee, W.B. Krantz, P.K. Chow, C.H. Wang, Hydrogel matrix entrapping PLGA-paclitaxel microspheres: drug delivery with near zero-order release and implantability advantages for malignant brain tumour chemotherapy, Pharm Res, 26 (2009) 2101-2114.
[214] S.H. Ranganath, Y. Fu, D.Y. Arifin, I. Kee, L. Zheng, H.S. Lee, P.K. Chow, C.H. Wang, The use of submicron/nanoscale PLGA implants to deliver paclitaxel with enhanced pharmacokinetics and therapeutic efficacy in intracranial glioblastoma in mice, Biomaterials, 31 (2010) 5199-5207.
[215] N. Qi, C. Cai, W. Zhang, Y. Niu, J. Yang, L. Wang, B. Tian, X. Liu, X. Lin, Y. Zhang, Y. Zhang, H. He, K. Chen, X. Tang, Sustained delivery of cytarabine-loaded vesicular phospholipid gels for treatment of xenografted glioma, Int J Pharm, 472 (2014) 48-55.
[216] T. Chen, T. Gong, T. Zhao, X. Liu, Y. Fu, Z. Zhang, T. Gong, Paclitaxel loaded phospholipid-based gel as a drug delivery system for local treatment of glioma, Int J Pharm, 528 (2017) 127-132.
[217] S. Kim, S.K. Nishimoto, J.D. Bumgardner, W.O. Haggard, M.W. Gaber, Y. Yang, A chitosan/beta-glycerophosphate thermo-sensitive gel for the delivery of ellagic acid for the treatment of brain cancer, Biomaterials, 31 (2010) 4157-4166.
[218] C.T. Tsao, F.M. Kievit, A. Ravanpay, A.E. Erickson, M.C. Jensen, R.G. Ellenbogen, M. Zhang, Thermoreversible poly(ethylene glycol)-g-chitosan hydrogel as a therapeutic T lymphocyte depot for localized glioblastoma immunotherapy, Biomacromolecules, 15 (2014) 2656-2662.
[219] J.R. Tauro, R.A. Gemeinhart, Matrix metalloprotease triggered delivery of cancer chemotherapeutics from hydrogel matrixes, Bioconj Chem, 16 (2005) 1133-1139.
[220] S.A. Meenach, J.M. Shapiro, J.Z. Hilt, K.W. Anderson, Characterization of PEG-iron oxide hydrogel nanocomposites for dual hyperthermia and paclitaxel delivery, J Biomat Sci. Polymer edition, 24 (2013) 1112-1126.
[221] Y. Xu, M. Shen, Y. Sun, P. Gao, Y. Duan, Polymer Nanocomposites Based Thermo-Sensitive Gel for Paclitaxel and Temozolomide Co-Delivery to Glioblastoma Cells, J Nanosci Nanotech, 15 (2015) 9777-9787.
[222] F. Danhier, E. Ansorena, J.M. Silva, R. Coco, A. Le Breton, V. Preat, PLGA-based nanoparticles: an overview of biomedical applications, J Control Release, 161 (2012) 505-522.
[223] A. Alexander, Ajazuddin, J. Khan, S. Saraf, S. Saraf, Poly(ethylene glycol)-poly(lactic-co-glycolic acid) based thermosensitive injectable hydrogels for biomedical applications, J Control Release, 172 (2013) 715-729.
[224] N.L. Elstad, K.D. Fowers, OncoGel (ReGel/paclitaxel)--clinical applications for a novel paclitaxel delivery system, Adv Drug Deliv Rev, 61 (2009) 785-794.

[225] B. Baroli, Photopolymerization of biomaterials: issues and potentialities in drug delivery, tissue engineering, and cell encapsulation applications, J Chem Tech Biotech, 81 (2006) 491-499.
[226] K.T. Nguyen, J.L. West, Photopolymerizable hydrogels for tissue engineering applications, Biomaterials, 23 (2002) 4307-4314.
[227] N. Schleich, F. Danhier, V. Preat, Iron oxide-loaded nanotheranostics: major obstacles to in vivo studies and clinical translation, J Control Release, 198 (2015) 35-54.
[228] L. Sun, D.Y. Joh, A. Al-Zaki, M. Stangl, S. Murty, J.J. Davis, B.C. Baumann, M. Alonso-Basanta, G.D. Kaol, A. Tsourkas, J.F. Dorsey, Theranostic Application of Mixed Gold and Superparamagnetic Iron Oxide Nanoparticle Micelles in Glioblastoma Multiforme, J Biomed Nanotech, 12 (2016) 347-356.
[229] J.I. Kim, C. Chun, B. Kim, J.M. Hong, J.K. Cho, S.H. Lee, S.C. Song, Thermosensitive/magnetic poly(organophosphazene) hydrogel as a long-term magnetic resonance contrast platform, Biomaterials, 33 (2012) 218-224.
[230] L. Jiang, Q. Zhou, K. Mu, H. Xie, Y. Zhu, W. Zhu, Y. Zhao, H. Xu, X. Yang, pH/temperature sensitive magnetic nanogels conjugated with Cy5.5-labled lactoferrin for MR and fluorescence imaging of glioma in rats, Biomaterials, 34 (2013) 7418-7428.
[231] H. Xie, Y. Zhu, W. Jiang, Q. Zhou, H. Yang, N. Gu, Y. Zhang, H. Xu, H. Xu, X. Yang, Lactoferrin-conjugated superparamagnetic iron oxide nanoparticles as a specific MRI contrast agent for detection of brain glioma in vivo, Biomaterials, 32 (2011) 495-502.
[232] N. Qi, X. Tang, X. Lin, P. Gu, C. Cai, H. Xu, H. He, Y. Zhang, Sterilization stability of vesicular phospholipid gels loaded with cytarabine for brain implant, Int J Pharm, 427 (2012) 234-241.
[233] S. Zhang, M.A. Anderson, Y. Ao, B.S. Khakh, J. Fan, T.J. Deming, M.V. Sofroniew, Tunable diblock copolypeptide hydrogel depots for local delivery of hydrophobic molecules in healthy and injured central nervous system, Biomaterials, 35 (2014) 1989-2000.
[234] K. Park, The drug delivery field at the inflection point: Time to fight its way out of the egg, Journal of Controlled Release, 267 (2017) 2-14.
[235] K. Riehemann, S.W. Schneider, T.A. Luger, B. Godin, M. Ferrari, H. Fuchs, Nanomedicine – challenge and perspectives, Angew Chem Int Ed Engl, 48 (2009) 872-897.
[236] A. Miranda, M.J. Blanco-Prieto, J. Sousa, A. Pais, C. Vitorino, Breaching barriers in glioblastoma. Part II: Targeted drug delivery and lipid nanoparticles, Int J Pharm, 531 (2017) 389-410.
[237] N.T. Huynh, M. Morille, J. Bejaud, P. Legras, A. Vessieres, G. Jaouen, J.P. Benoit, C. Passirani, Treatment of 9L gliosarcoma in rats by ferrociphenol-loaded lipid nanocapsules based on a passive targeting strategy via the EPR effect, Pharm Res, 28 (2011) 3189-3198.
[238] M.I. Koukourakis, S. Koukouraki, I. Fezoulidis, N. Kelekis, G. Kyrias, S. Archimandritis, N. Karkavitsas, High intratumoural accumulation of stealth liposomal doxorubicin (Caelyx) in glioblastomas and in metastatic brain tumours, Brit J Cancer, 83 (2000) 1281-1286.
[239] T. Siegal, A. Horowitz, A. Gabizon, Doxorubicin encapsulated in sterically stabilized liposomes for the treatment of a brain tumor model: biodistribution and therapeutic efficacy, J Neurosurg, 83 (1995) 1029-1037.
[240] A. Bernardi, E. Braganhol, E. Jager, F. Figueiro, M.I. Edelweiss, A.R. Pohlmann, S.S. Guterres, A.M. Battastini, Indomethacin-loaded nanocapsules treatment reduces in vivo glioblastoma growth in a rat glioma model, Cancer Lett, 281 (2009) 53-63.
[241] X. Liu, W. Cui, B. Li, Z. Hong, Targeted therapy for glioma using cyclic RGD-entrapped polyionic complex nanomicelles, Int J Nanomed, 7 (2012) 2853-2862.
[242] C. Zhan, B. Gu, C. Xie, J. Li, Y. Liu, W. Lu, Cyclic RGD conjugated poly(ethylene glycol)-co-poly(lactic acid) micelle enhances paclitaxel anti-glioblastoma effect, J Control Release, 143 (2010) 136-142.
[243] J. Du, W.L. Lu, X. Ying, Y. Liu, P. Du, W. Tian, Y. Men, J. Guo, Y. Zhang, R.J. Li, J. Zhou, J.N. Lou, J.C. Wang, X. Zhang, Q. Zhang, Dual-targeting topotecan liposomes modified with tamoxifen and wheat germ agglutinin significantly improve drug transport across the blood-brain barrier and survival of brain tumor-bearing animals, Mol Pharm, 6 (2009) 905-917.
[244] M. Ghosh, R.O. Ryan, ApoE enhances nanodisk-mediated curcumin delivery to glioblastoma multiforme cells, Nanomedicine (London), 9 (2014) 763-771.
[245] J. Chang, A. Paillard, C. Passirani, M. Morille, J.P. Benoit, D. Betbeder, E. Garcion, Transferrin adsorption onto PLGA nanoparticles governs their interaction with biological systems from blood circulation to brain cancer cells, Pharm Res, 29 (2012) 1495-1505.
[246] W.H. Ren, J. Chang, C.H. Yan, X.M. Qian, L.X. Long, B. He, X.B. Yuan, C.S. Kang, D. Betbeder, J. Sheng, P.Y. Pu, Development of transferrin functionalized poly(ethylene glycol)/poly(lactic acid) amphiphilic block

copolymeric micelles as a potential delivery system targeting brain glioma, J Mater Sci Mater Med, 21 (2010) 2673-2681.
[247] E. Locatelli, M. Naddaka, C. Uboldi, G. Loudos, E. Fragogeorgi, V. Molinari, A. Pucci, T. Tsotakos, D. Psimadas, J. Ponti, M.C. Franchini, Targeted delivery of silver nanoparticles and alisertib: in vitro and in vivo synergistic effect against glioblastoma, Nanomedicine (London, England), 9 (2014) 839-849.
[248] C. Fang, K. Wang, Z.R. Stephen, Q. Mu, F.M. Kievit, D.T. Chiu, O.W. Press, M. Zhang, Temozolomide nanoparticles for targeted glioblastoma therapy, ACS Appl Mater Interfaces, 7 (2015) 6674-6682.
[249] G. Gu, H. Xia, Q. Hu, Z. Liu, M. Jiang, T. Kang, D. Miao, Y. Tu, Z. Pang, Q. Song, L. Yao, H. Chen, X. Gao, J. Chen, PEG-co-PCL nanoparticles modified with MMP-2/9 activatable low molecular weight protamine for enhanced targeted glioblastoma therapy, Biomaterials, 34 (2013) 196-208.
[250] J. Guo, X. Gao, L. Su, H. Xia, G. Gu, Z. Pang, X. Jiang, L. Yao, J. Chen, H. Chen, Aptamer-functionalized PEG-PLGA nanoparticles for enhanced anti-glioma drug delivery, Biomaterials, 32 (2011) 8010-8020.
[251] H. Gao, Z. Yang, S. Cao, Y. Xiong, S. Zhang, Z. Pang, X. Jiang, Tumor cells and neovasculature dual targeting delivery for glioblastoma treatment, Biomaterials, 35 (2014) 2374-2382.
[252] C.S. Schneider, J.G. Perez, E. Cheng, C. Zhang, P. Mastorakos, J. Hanes, J.A. Winkles, G.F. Woodworth, A.J. Kim, Minimizing the non-specific binding of nanoparticles to the brain enables active targeting of Fn14-positive glioblastoma cells, Biomaterials, 42 (2015) 42-51.
[253] A.S. Wadajkar, J.G. Dancy, N.B. Roberts, N.P. Connolly, D.K. Strickland, J.A. Winkles, G.F. Woodworth, A.J. Kim, Decreased non-specific adhesivity, receptor targeted (DART) nanoparticles exhibit improved dispersion, cellular uptake, and tumor retention in invasive gliomas, J Control Release, 267 (2017) 144-153 .
[254] A. Beduneau, F. Hindre, A. Clavreul, J.C. Leroux, P. Saulnier, J.P. Benoit, Brain targeting using novel lipid nanovectors, J Control Release, 126 (2008) 44-49.
[255] A. Beduneau, P. Saulnier, F. Hindre, A. Clavreul, J.C. Leroux, J.P. Benoit, Design of targeted lipid nanocapsules by conjugation of whole antibodies and antibody Fab' fragments, Biomaterials, 28 (2007) 4978-4990.
[256] J. Balzeau, M. Pinier, R. Berges, P. Saulnier, J.-P. Benoit, J. Eyer, The effect of functionalizing lipid nanocapsules with NFL-TBS.40-63 peptide on their uptake by glioblastoma cells, Biomaterials, 34 (2013) 3381-3389.
[257] A.-L. Laine, N.T. Huynh, A. Clavreul, J. Balzeau, J. Béjaud, A. Vessieres, J.-P. Benoit, J. Eyer, C. Passirani, Brain tumour targeting strategies via coated ferrociphenol lipid nanocapsules, Eur J Pharm Biopharm, 81 (2012) 690-693.
[258] Y.C. Kuo, C.T. Liang, Inhibition of human brain malignant glioblastoma cells using carmustine-loaded catanionic solid lipid nanoparticles with surface anti-epithelial growth factor receptor, Biomaterials, 32 (2011) 3340-3350.
[259] Y.C. Kuo, C.H. Lee, Inhibition against growth of glioblastoma multiforme in vitro using etoposide-loaded solid lipid nanoparticles with p-aminophenyl-alpha-D-manno-pyranoside and folic acid, J Pharm Sci, 104 (2015) 1804-1814.
[260] M. Nikanjam, A.R. Gibbs, C.A. Hunt, T.F. Budinger, T.M. Forte, Synthetic nano-LDL with paclitaxel oleate as a targeted drug delivery vehicle for glioblastoma multiforme, J Control Release, 124 (2007) 163-171.
[261] H. He, Y. Li, X.R. Jia, J. Du, X. Ying, W.L. Lu, J.N. Lou, Y. Wei, PEGylated Poly(amidoamine) dendrimer-based dual-targeting carrier for treating brain tumors, Biomaterials, 32 (2011) 478-487.
[262] P. Jativa, V. Cena, Use of nanoparticles for glioblastoma treatment: a new approach, Nanomedicine (London), 12 (2017) 2533-2554.
[263] J. Aparicio-Blanco, A.I. Torres-Suarez, Glioblastoma Multiforme and Lipid Nanocapsules: A Review, J Biomed Nanotechnol, 11 (2015) 1283-1311.
[264] A.S. Wadajkar, J.G. Dancy, D.S. Hersh, P. Anastasiadis, N.L. Tran, G.F. Woodworth, J.A. Winkles, A.J. Kim, Tumor-targeted nanotherapeutics: overcoming treatment barriers for glioblastoma, Wiley Interdiscip Rev Nanomed Nanobiotechnol, 9 (2017) 4.
[265] P.A. Chiarelli, F.M. Kievit, M. Zhang, R.G. Ellenbogen, Bionanotechnology and the future of glioma, Surg Neurol Int, 6 (2015) S45-58.
[266] N.T. Huynh, C. Passirani, P. Saulnier, J.P. Benoit, Lipid nanocapsules: a new platform for nanomedicine, Int J Pharm, 379 (2009) 201-209.
[267] E. Moysan, Y. Gonzalez-Fernandez, N. Lautram, J. Bejaud, G. Bastiat, J.P. Benoit, An innovative hydrogel of gemcitabine-loaded lipid nanocapsules: when the drug is a key player of the nanomedicine structure, Soft matter, 10 (2014) 1767-1777.

[268] B. Heurtault, P. Saulnier, B. Pech, J.E. Proust, J.P. Benoit, A novel phase inversion-based process for the preparation of lipid nanocarriers, Pharm Res, 19 (2002) 875-880.
[269] N. Anton, P. Gayet, J.P. Benoit, P. Saulnier, Nano-emulsions and nanocapsules by the PIT method: an investigation on the role of the temperature cycling on the emulsion phase inversion, Int J Pharm, 344 (2007) 44-52.
[270] F. Lagarce, C. Passirani, Nucleic-Acid Delivery Using Lipid Nanocapsules, Curr Pharma Biotech, 17 (2016) 723-727.
[271] E. Allard, F. Hindre, C. Passirani, L. Lemaire, N. Lepareur, N. Noiret, P. Menei, J.-P. Benoit, 188Re-loaded lipid nanocapsules as a promising radiopharmaceutical carrier for internal radiotherapy of malignant gliomas, Eur J Nucl Med Mol Imaging, 35 (2008) 1838-1846.
[272] C. Vanpouille-Box, F. Lacoeuille, C. Belloche, N. Lepareur, L. Lemaire, J.J. LeJeune, J.P. Benoit, P. Menei, O.F. Couturier, E. Garcion, F. Hindre, Tumor eradication in rat glioma and bypass of immunosuppressive barriers using internal radiation with (188)Re-lipid nanocapsules, Biomaterials, 32 (2011) 6781-6790.
[273] A. Cikankowitz, A. Clavreul, C. Tétaud, L. Lemaire, A. Rousseau, N. Lepareur, D. Dabli, F. Bouchet, E. Garcion, P. Menei, O. Couturier, F. Hindré, Characterization of the distribution, retention, and efficacy of internal radiation of 188Re-lipid nanocapsules in an immunocompromised human glioblastoma model, J neurooncol, 131 (2017) 49-58.
[274] L. Lemaire, G. Bastiat, F. Franconi, N. Lautram, T. Duong Thi Dan, E. Garcion, P. Saulnier, J.P. Benoit, Perfluorocarbon-loaded lipid nanocapsules as oxygen sensors for tumor tissue pO2 assessment, Eur J Pharm Biopharm, 84 (2013) 479-486.
[275] L. Lemaire, J. Nel, F. Franconi, G. Bastiat, P. Saulnier, Perfluorocarbon-Loaded Lipid Nanocapsules to Assess the Dependence of U87-Human Glioblastoma Tumor pO2 on In Vitro Expansion Conditions, PloS one, 11 (2016) e0165479.
[276] E. Garcion, A. Lamprecht, B. Heurtault, A. Paillard, A. Aubert-Pouessel, B. Denizot, P. Menei, J.P. Benoit, A new generation of anticancer, drug-loaded, colloidal vectors reverses multidrug resistance in glioma and reduces tumor progression in rats, Mol Cancer Ther, 5 (2006) 1710-1722.
[277] S. Vinchon-Petit, D. Jarnet, A. Paillard, J.-P. Benoit, E. Garcion, P. Menei, In vivo evaluation of intracellular drug-nanocarriers infused into intracranial tumours by convection-enhanced delivery: distribution and radiosensitisation efficacy, J neurooncol, 97 (2010) 195-205.
[278] E. Allard, D. Jarnet, A. Vessières, S. Vinchon-Petit, G. Jaouen, J.-P. Benoit, C. Passirani, Local Delivery of Ferrociphenol Lipid Nanocapsules Followed by External Radiotherapy as a Synergistic Treatment Against Intracranial 9L Glioma Xenograft, Pharm Res, 27 (2009) 56.
[279] E. Allard, C. Passirani, E. Garcion, P. Pigeon, A. Vessières, G. Jaouen, J.-P. Benoit, Lipid nanocapsules loaded with an organometallic tamoxifen derivative as a novel drug-carrier system for experimental malignant gliomas, J Control Release, 130 (2008) 146-153.
[280] A.-L. Lainé, A. Clavreul, A. Rousseau, C. Tétaud, A. Vessieres, E. Garcion, G. Jaouen, L. Aubert, M. Guilbert, J.-P. Benoit, R.-A. Toillon, C. Passirani, Inhibition of ectopic glioma tumor growth by a potent ferrocenyl drug loaded into stealth lipid nanocapsules, Nanomedicine, 10 (2014) 1667-1677.
[281] N.T. Huynh, C. Passirani, E. Allard-Vannier, L. Lemaire, J. Roux, E. Garcion, A. Vessieres, J.-P. Benoit, Administration-dependent efficacy of ferrociphenol lipid nanocapsules for the treatment of intracranial 9L rat gliosarcoma, Int J Pharm, 423 (2012) 55-62.
[282] L. Basile, C. Passirani, N.-T. Huynh, J. Béjaud, J.-P. Benoit, G. Puglisi, R. Pignatello, Serum-stable, long-circulating paclitaxel-loaded colloidal carriers decorated with a new amphiphilic PEG derivative, Int J Pharm, 426 (2012) 231-238.
[283] M. Roger, A. Clavreul, N.T. Huynh, C. Passirani, P. Schiller, A. Vessières, C. Montero-Menei, P. Menei, Ferrociphenol lipid nanocapsule delivery by mesenchymal stromal cells in brain tumor therapy, Int J Pharm, 423 (2012) 63-68.
[284] A. Clavreul, A. Montagu, A.L. Laine, C. Tetaud, N. Lautram, F. Franconi, C. Passirani, A. Vessieres, C.N. Montero-Menei, P. Menei, Targeting and treatment of glioblastomas with human mesenchymal stem cells carrying ferrociphenol lipid nanocapsules, Int J Nanomed, 10 (2015) 1259-1271.
[285] G. Lollo, M. Vincent, G. Ullio-Gamboa, L. Lemaire, F. Franconi, D. Couez, J.-P. Benoit, Development of multifunctional lipid nanocapsules for the co-delivery of paclitaxel and CpG-ODN in the treatment of glioblastoma, Int J Pharm, 495 (2015) 972-980.
[286] A. Lamprecht, J.P. Benoit, Etoposide nanocarriers suppress glioma cell growth by intracellular drug delivery and simultaneous P-glycoprotein inhibition, J Control Release, 112 (2006) 208-213.
[287] A. Paillard, F. Hindre, C. Vignes-Colombeix, J.P. Benoit, E. Garcion, The importance of endo-lysosomal escape with lipid nanocapsules for drug subcellular bioavailability, Biomaterials, 31 (2010) 7542-7554.

[288] E.S. Newlands, M.F. Stevens, S.R. Wedge, R.T. Wheelhouse, C. Brock, Temozolomide: a review of its discovery, chemical properties, pre-clinical development and clinical trials, Cancer Treatment Rev, 23 (1997) 35-61.
[289] H.S. Friedman, T. Kerby, H. Calvert, Temozolomide and treatment of malignant glioma, Clin Cancer Res, 6 (2000) 2585-2597.
[290] R. Stupp, M.E. Hegi, W.P. Mason, M.J. van den Bent, M.J. Taphoorn, R.C. Janzer, S.K. Ludwin, A. Allgeier, B. Fisher, K. Belanger, P. Hau, A.A. Brandes, J. Gijtenbeek, C. Marosi, C.J. Vecht, K. Mokhtari, P. Wesseling, S. Villa, E. Eisenhauer, T. Gorlia, M. Weller, D. Lacombe, J.G. Cairncross, R.O. Mirimanoff, Effects of radiotherapy with concomitant and adjuvant temozolomide versus radiotherapy alone on survival in glioblastoma in a randomised phase III study: 5-year analysis of the EORTC-NCIC trial, The Lancet Oncol, 10 (2009) 459-466.
[291] R.D. Kortmann, B. Jeremic, M. Weller, L. Plasswilm, M. Bamberg, Radiochemotherapy of malignant glioma in adults. Clinical experiences, Strahlenther Onkol, 179 (2003) 219-232.
[292] C. Bastiancich, P. Danhier, V. Preat, F. Danhier, Anticancer drug-loaded hydrogels as drug delivery systems for the local treatment of glioblastoma, J Control Release, 243 (2016) 29-42.
[293] K. Messaoudi, A. Clavreul, F. Lagarce, Toward an effective strategy in glioblastoma treatment. Part I: resistance mechanisms and strategies to overcome resistance of glioblastoma to temozolomide, Drug Discov Today, 20 (2015) 899-905.
[294] W. Wick, M. Weller, M. van den Bent, M. Sanson, M. Weiler, A. von Deimling, C. Plass, M. Hegi, M. Platten, G. Reifenberger, MGMT testing--the challenges for biomarker-based glioma treatment, Nat Rev Neurol, 10 (2014) 372-385.
[295] J. Bianco, C. Bastiancich, A. Jankovski, A. des Rieux, V. Preat, F. Danhier, On glioblastoma and the search for a cure: where do we stand?, Cell Mol Life Sci, 74 (2017) 2451-2466.
[296] E.C. Jung, J; Chao, ST; Murphy, ES; Suh, JH., Principles and Tenets of Radiation Treatment in Glioblastoma, in: S. Brem K. G. Abdullah (Ed.) Glioblastoma, Elsevier, 2017.
[297] E. Moysan, G. Bastiat, J.P. Benoit, Gemcitabine versus Modified Gemcitabine: a review of several promising chemical modifications, Mol Pharm, 10 (2013) 430-444.
[298] P. Huang, W. Plunkett, Induction of apoptosis by gemcitabine, Seminars in oncology, 22 (1995) 19-25.
[299] H.J. Guchelaar, D.J. Richel, A. van Knapen, Clinical, toxicological and pharmacological aspects of gemcitabine, Cancer Treat Rev, 22 (1996) 15-31.
[300] L.J. Sinyuk M., Connexins: Bridging the gap between cancer cell communication in glioblastoma, in: M. Kandouz (Ed.) Intercellular Communication in Cancer, Springer, 2015.
[301] S. Cottin, K. Ghani, P.O. de Campos-Lima, M. Caruso, Gemcitabine intercellular diffusion mediated by gap junctions: new implications for cancer therapy, Mol Cancer, 9 (2010) 141.
[302] D.S. Shewach, T.S. Lawrence, Gemcitabine and radiosensitization in human tumor cells, Invest New Drugs, 14 (1996) 257-263.
[303] T.S. Lawrence, E.Y. Chang, T.M. Hahn, D.S. Shewach, Delayed radiosensitization of human colon carcinoma cells after a brief exposure to 2',2'-difluoro-2'-deoxycytidine (Gemcitabine), Clin Cancer Res, 3 (1997) 777-782.
[304] A.M. Bergman, H.M. Pinedo, G.J. Peters, Determinants of resistance to 2',2'-difluorodeoxycytidine (gemcitabine), Drug Resist Updat, 5 (2002) 19-33.
[305] B. Pauwels, A.E. Korst, H.A. Lambrechts, G.G. Pattyn, C.M. de Pooter, F. Lardon, J.B. Vermorken, The radiosensitising effect of difluorodeoxyuridine, a metabolite of gemcitabine, in vitro, Cancer Chemother Pharmacol, 58 (2006) 219-228.
[306] T.S. Lawrence, A.W. Blackstock, C. McGinn, The mechanism of action of radiosensitization of conventional chemotherapeutic agents, Sem Radiat Oncol, 13 (2003) 13-21.
[307] B. Pauwels, A.E.C. Korst, G.G.O. Pattyn, H.A.J. Lambrechts, D.R. Van Bockstaele, K. Vermeulen, M. Lenjou, C.M.J. de Pooter, J.B. Vermorken, F. Lardon, Cell cycle effect of gemcitabine and its role in the radiosensitizing mechanism in vitro, Int J Radiat Oncol Biol Phys, 57 (2003) 1075-1083.
[308] G. Carpinelli, B. Bucci, I. D'Agnano, R. Canese, F. Caroli, L. Raus, E. Brunetti, D. Giannarelli, F. Podo, C.M. Carapella, Gemcitabine treatment of experimental C6 glioma: the effects on cell cycle and apoptotic rate, Anticancer Res, 26 (2006) 3017-3024.
[309] L.J. Ostruszka, D.S. Shewach, The role of cell cycle progression in radiosensitization by 2',2'-difluoro-2'-deoxycytidine, Cancer Res, 60 (2000) 6080-6088.
[310] D. Latz, K. Fleckenstein, M. Eble, J. Blatter, M. Wannenmacher, K.J. Weber, Radiosensitizing potential of gemcitabine (2',2'-difluoro-2'-deoxycytidine) within the cell cycle in vitro, Int J Radiat Oncol Biol Phys, 41 (1998) 875-882.

[311] A.K. Nowak, B.W. Robinson, R.A. Lake, Gemcitabine exerts a selective effect on the humoral immune response: implications for combination chemo-immunotherapy, Cancer Res, 62 (2002) 2353-2358.
[312] E. Suzuki, V. Kapoor, A.S. Jassar, L.R. Kaiser, S.M. Albelda, Gemcitabine selectively eliminates splenic Gr-1+/CD11b+ myeloid suppressor cells in tumor-bearing animals and enhances antitumor immune activity, Clin Cancer Res, 11 (2005) 6713-6721.
[313] E. Suzuki, J. Sun, V. Kapoor, A.S. Jassar, S.M. Albelda, Gemcitabine has significant immunomodulatory activity in murine tumor models independent of its cytotoxic effects, Cancer Biol Ther, 6 (2007) 880-885.
[314] I. Shevchenko, S. Karakhanova, S. Soltek, J. Link, J. Bayry, J. Werner, V. Umansky, A.V. Bazhin, Low-dose gemcitabine depletes regulatory T cells and improves survival in the orthotopic Panc02 model of pancreatic cancer, Int J Cancer, 133 (2013) 98-107.
[315] A.A. Thomas, M.S. Ernstoff, C.E. Fadul, Immunotherapy for the Treatment of Glioblastoma, Cancer J, 18 (2012) 59-68.
[316] J. Rieger, S. Durka, J. Streffer, J. Dichgans, M. Weller, Gemcitabine cytotoxicity of human malignant glioma cells: modulation by antioxidants, BCL-2 and dexamethasone, Eur J Pharm, 365 (1999) 301-308.
[317] M. Weller, J. Streffer, W. Wick, R.D. Kortmann, E. Heiss, W. Kuker, R. Meyermann, J. Dichgans, M. Bamberg, Preirradiation gemcitabine chemotherapy for newly diagnosed glioblastoma. A phase II study, Cancer, 91 (2001) 423-427.
[318] S.Z. Gertler, D. MacDonald, M. Goodyear, P. Forsyth, D.J. Stewart, K. Belanger, J. Perry, D. Fulton, W. Steward, N. Wainman, L. Seymour, NCIC-CTG phase II study of gemcitabine in patients with malignant glioma (IND.94), Ann Oncol, 11 (2000) 315-318.
[319] W. Wick, M. Hermisson, R.D. Kortmann, W.M. Kuker, F. Duffner, J. Dichgans, M. Bamberg, M. Weller, Neoadjuvant gemcitabine/treosulfan chemotherapy for newly diagnosed glioblastoma: a phase II study, J Neurooncol, 59 (2002) 151-155.
[320] H. Szelenyi, E. Thiel, N. Niederle, U. Keilholz, A Phase I trial of gemcitabine and treosulfan (GeT) to overcome multidrug resistance in patients with advanced solid tumors, in: Proc Am Soc Clin Oncol, 1999, pp. 228a.
[321] M. Genc, N. Castro Kreder, A. Barten-van Rijbroek, L.J. Stalpers, J. Haveman, Enhancement of effects of irradiation by gemcitabine in a glioblastoma cell line and cell line spheroids, J Cancer Res Clin Oncol, 130 (2004) 45-51.
[322] F. Fehlauer, M. Muench, E.J. Smid, B. Slotman, E. Richter, P. Van der Valk, P. Sminia, Combined modality therapy of gemcitabine and irradiation on human glioma spheroids derived from cell lines and biopsy tissue, Oncol Rep, 15 (2006) 97-105.
[323] Y. Esumi, K. Mitsugi, A. Takao, H. Seki, M. Kawai, Disposition of gemcitabine in rat and dog after single and multiple dosings, Xenobiotica, 24 (1994) 805-817.
[324] J.Z. Kerr, S.L. Berg, R. Dauser, J. Nuchtern, M.J. Egorin, L. McGuffey, A. Aleksic, S. Blaney, Plasma and cerebrospinal fluid pharmacokinetics of gemcitabine after intravenous administration in nonhuman primates, Cancer Chemother Pharmacol, 47 (2001) 411-414.
[325] S.K. Apparaju, G.A. Gudelsky, P.B. Desai, Pharmacokinetics of gemcitabine in tumor and non-tumor extracellular fluid of brain: an in vivo assessment in rats employing intracerebral microdialysis, Cancer Chemother Pharmacol, 61 (2008) 223-229.
[326] J. Sigmond, R.J. Honeywell, T.J. Postma, C.M. Dirven, S.M. de Lange, K. van der Born, A.C. Laan, J.C. Baayen, C.J. Van Groeningen, A.M. Bergman, G. Giaccone, G.J. Peters, Gemcitabine uptake in glioblastoma multiforme: potential as a radiosensitizer, Ann Oncol, 20 (2009) 182-187.
[327] T.S. Lawrence, A. Eisbruch, D.S. Shewach, Gemcitabine-mediated radiosensitization, Semin Oncol, 24 (1997) S7-24-s27-28.
[328] A. Maraveyas, J. Sgouros, S. Upadhyay, A.H. Abdel-Hamid, M. Holmes, M. Lind, Gemcitabine twice weekly as a radiosensitiser for the treatment of brain metastases in patients with carcinoma: a phase I study, Br J Cancer, 92 (2005) 815-819.
[329] A. Fabi, A. Mirri, A. Felici, A. Vidiri, A. Pace, E. Occhipinti, F. Cognetti, G. Arcangeli, B. Iandolo, M.A. Carosi, G. Metro, C.M. Carapella, Fixed dose-rate gemcitabine as radiosensitizer for newly diagnosed glioblastoma: a dose-finding study, J Neurooncol, 87 (2008) 79-84.
[330] G. Metro, A. Fabi, M.A. Mirri, A. Vidiri, A. Pace, M. Carosi, M. Russillo, M. Maschio, D. Giannarelli, D. Pellegrini, A. Pompili, F. Cognetti, C.M. Carapella, Phase II study of fixed dose rate gemcitabine as radiosensitizer for newly diagnosed glioblastoma multiforme, Cancer Chemother Pharmacol, 65 (2010) 391-397.
[331] M.M. Kim, S. Camelo-Piragua, M. Schipper, Y. Tao, D. Normolle, L. Junck, A. Mammoser, B.L. Betz, Y. Cao, C.J. Kim, J. Heth, O. Sagher, T.S. Lawrence, C.I. Tsien, Gemcitabine Plus Radiation Therapy for High-Grade

Glioma: Long-Term Results of a Phase 1 Dose-Escalation Study, Int J Radiat Oncol Biol Phys, 94 (2016) 305-311.
[332] S. Galban, B. Lemasson, T.M. Williams, F. Li, K.A. Heist, T.D. Johnson, J.S. Leopold, T.L. Chenevert, T.S. Lawrence, A. Rehemtulla, T. Mikkelsen, E.C. Holland, C.J. Galban, B.D. Ross, DW-MRI as a biomarker to compare therapeutic outcomes in radiotherapy regimens incorporating temozolomide or gemcitabine in glioblastoma, PloS one, 7 (2012) e35857.
[333] L. Toschi, G. Finocchiaro, S. Bartolini, V. Gioia, F. Cappuzzo, Role of gemcitabine in cancer therapy, Fut Oncol (London), 1 (2005) 7-17.
[334] I.F. Tannock, C.M. Lee, J.K. Tunggal, D.S.M. Cowan, M.J. Egorin, Limited Penetration of Anticancer Drugs through Tumor Tissue, A Potential Cause of Resistance of Solid Tumors to Chemotherapy, Clin Cancer Res 8 (2002) 878-884.
[335] L.A. Huxham, A.H. Kyle, J.H. Baker, L.K. Nykilchuk, A.I. Minchinton, Microregional effects of gemcitabine in HCT-116 xenografts, Cancer Res, 64 (2004) 6537-6541.
[336] P. Guo, J. Ma, S. Li, Z. Guo, A.L. Adams, J.M. Gallo, Targeted delivery of a peripheral benzodiazepine receptor ligand-gemcitabine conjugate to brain tumors in a xenograft model, Cancer Chemother Pharmacol, 48 (2001) 169-176.
[337] J.W. Degen, S. Walbridge, A.O. Vortmeyer, E.H. Oldfield, R.R. Lonser, Safety and efficacy of convection-enhanced delivery of gemcitabine or carboplatin in a malignant glioma model in rats, J Neurosurg, 99 (2003) 893-898.
[338] T. Szatmari, G. Huszty, S. Desaknai, T. Spasokoukotskaja, M. Sasvari-Szekely, M. Staub, O. Esik, G. Safrany, K. Lumniczky, Adenoviral vector transduction of the human deoxycytidine kinase gene enhances the cytotoxic and radiosensitizing effect of gemcitabine on experimental gliomas, Cancer Gene Ther, 15 (2008) 154-164.
[339] C.X. Wang, L.S. Huang, L.B. Hou, L. Jiang, Z.T. Yan, Y.L. Wang, Z.L. Chen, Antitumor effects of polysorbate-80 coated gemcitabine polybutylcyanoacrylate nanoparticles in vitro and its pharmacodynamics in vivo on C6 glioma cells of a brain tumor model, Brain Res, 1261 (2009) 91-99.
[340] D.H. Shin, S. Xuan, W.-Y. Kim, G.-U. Bae, J.-S. Kim, CD133 antibody-conjugated immunoliposomes encapsulating gemcitabine for targeting glioblastoma stem cells, J Mat Chem B, 2 (2014) 3771-3781.
[341] D.H. Shin, S.J. Lee, J.S. Kim, J.H. Ryu, J.S. Kim, Synergistic Effect of Immunoliposomal Gemcitabine and Bevacizumab in Glioblastoma Stem Cell-Targeted Therapy, J Biomed Nanotech, 11 (2015) 1989-2002.
[342] Q. Mu, G. Lin, V.K. Patton, K. Wang, O.W. Press, M. Zhang, Gemcitabine and chlorotoxin conjugated iron oxide nanoparticles for glioblastoma therapy, J Mat Chem B, 4 (2016) 32-36.
[343] A. Gaudin, E. Song, A.R. King, J.K. Saucier-Sawyer, R. Bindra, D. Desmaele, P. Couvreur, W.M. Saltzman, PEGylated squalenoyl-gemcitabine nanoparticles for the treatment of glioblastoma, Biomaterials, 105 (2016) 136-144.
[344] P. Couvreur, B. Stella, L.H. Reddy, H. Hillaireau, C. Dubernet, D. Desmaele, S. Lepetre-Mouelhi, F. Rocco, N. Dereuddre-Bosquet, P. Clayette, V. Rosilio, V. Marsaud, J.M. Renoir, L. Cattel, Squalenoyl nanomedicines as potential therapeutics, Nano letters, 6 (2006) 2544-2548.

CHAPTER II.
AIM OF THE THESIS

AIM OF THE THESIS

Glioblastoma (GBM) is the most common, aggressive and malignant brain tumor in adults. Surgical debulking of the tumor followed, several weeks later, by radiotherapy and concomitant chemotherapy with Temozolomide (TMZ) is the standard of care treatment for GBM patients. However, GBM intrinsic characteristic – including infiltrative capacity, high proliferation rate, presence of the BBB, chemoresistance - always lead to the formation of recurrences, which arise around the resection cavity borders (90% of the cases) and inevitably result in patient's death. Indeed, despite the tremendous technological advancements and progress in GBM knowledge, its prognosis is still very low. New, specific and more effective drugs and/or multi-drug synergistic approaches that allow to target different tumorigenic pathways, as well as more efficient drug delivery strategies need to be discovered and tested to resolve GBM unmet medical needs.

This project is based on the hypothesis that an anticancer drug-loaded hydrogel directly delivered in the resection cavity after surgery, and able to sustainably release one or multiple active agents over time, could contribute to the cure of GBM by reducing the formation of local recurrences. In this study, an injectable hydrogel formed of lipid nanocapsules and the drug lauroyl-gemcitabine ($GemC_{12}$-LNC) was used to test this assumption (Figure 1).

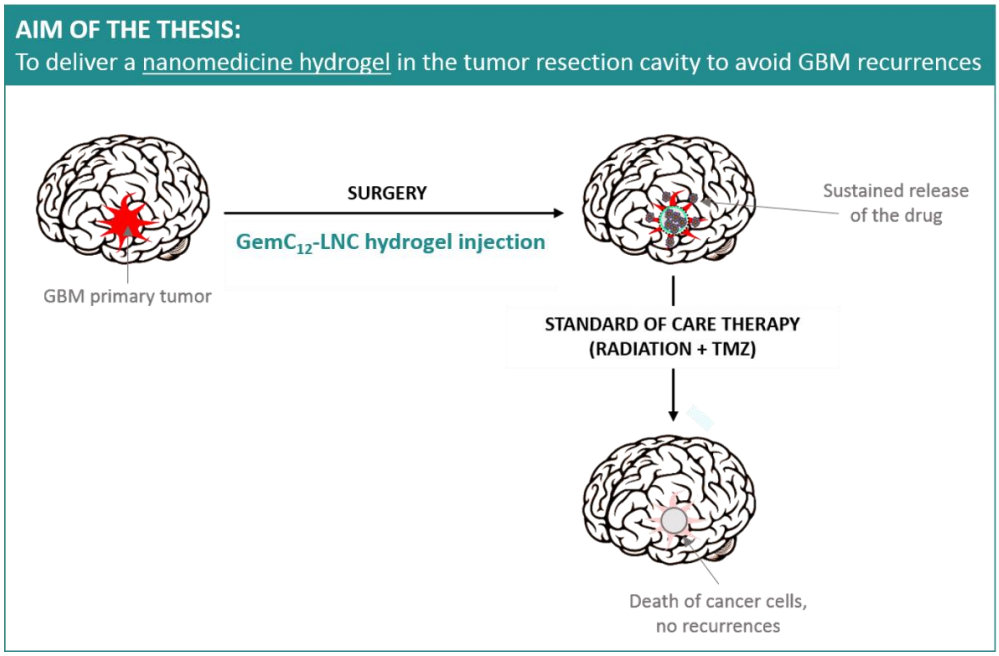

Figure 1. Schematic image representing the aim of this PhD Thesis.

$GemC_{12}$-LNC is a unique nanomedicine hydrogel formed of prodrug lauroyl-gemcitabine ($GemC_{12}$) and lipid nanocapsules (LNC) that has been developed by Benoit group (Université d'Angers). $GemC_{12}$ is an amphiphilic derivative of Gem that shows improved stability in plasma and improved cytotoxicity in different cell lines. LNC are biocompatible and biomimetic nanocarriers obtained by a phase-inversion process, formed of an oily core surrounded by a highly organized membrane of low molecular weight surfactants. When $GemC_{12}$ is encapsulated in LNC, the formulation spontaneously forms a hydrogel thanks to an inter-nanoparticle association of $GemC_{12}$-LNC, without the addition of polymers, gelling agents or external stimuli.

The delivery of $GemC_{12}$-LNC hydrogel in the tumor resection cavity would allow to combine the advantages of the local delivery of chemotherapeutic agents and nanomedicine filling the gap time between the GBM resection and the chemoradiation. $GemC_{12}$ has a different mechanism of action compared to TMZ, meaning that its local delivery should not increase GBM cells chemoresistance against alkylating agents.

The innovative aspects of this study are: (*i*) the use of a gemcitabine derivative against GBM (*ii*) the use of a gel-delivery system uniquely formed of a safe and well-known nanocarrier and a cytotoxic drug for the treatment of GBM; (*iii*) the development of a surgical procedure able to mimic the clinical conditions to test the hydrogel efficacy.

The specific objectives of this work are:

1. Identification of the $GemC_{12}$-LNC hydrogel parameters that could allow its use as sustained drug delivery depot in the brain (Chapter III)

2. Identification of an appropriate rodent model or surgical procedures able to mimic the clinical conditions and test the anti-tumor efficacy of local delivery systems (Chapter IV and VI)

3. Evaluation of the feasibility, tolerability and efficacy of the $GemC_{12}$-LNC hydrogel as a local delivery treatment for GBM (Chapter III, V and VI)

The surgical procedure developed here could be used by others to test different local delivery systems in rodents. Moreover, this work will expand the knowledge about the use of gemcitabine derivatives against GBM providing a new therapeutic strategy for this tumor. Ultimately, we hope that our results will contribute to the development of materials able to benefit the survival and quality of life of operable GBM patients.

CHAPTER III.

LAUROYL-GEMCITABINE LOADED LIPID NANOCAPSULE HYDROGEL FOR THE TREATMENT OF GLIOBLASTOMA: PROOF OF CONCEPT

Adapted from:
Bastiancich C, Vanvarenberg K, Ucakar B, Pitorre M, Bastiat G, Lagarce F, Préat V, Danhier F. Lauroyl-gemcitabine-loaded lipid nanocapsule hydrogel for the treatment of glioblastoma. *J Controlled Release* 225:283-93 (2016).

ABSTRACT

The local delivery of chemotherapeutic agents is a very promising strategy for the treatment of Glioblastoma (GBM). Gemcitabine is a chemotherapeutic agent that has a different mechanism of action compared to alkylating agents and shows excellent radio-sensitizing properties. So, we developed an injectable gel-like nanodelivery system consisting in lipid nanocapsules loaded with anticancer prodrug lauroyl-gemcitabine ($GemC_{12}$-LNC) to obtain a sustained and local delivery of this drug in the brain. In this study, the $GemC_{12}$-LNC have been formulated and characterized and the viscoelastic properties of the hydrogel were evaluated after extrusion from 30 G needles. This system showed a sustained and prolonged in vitro release of the drug over one month. $GemC_{12}$ and the $GemC_{12}$-LNC have shown increased in vitro cytotoxic activity on U-87 MG glioma cells compared to the parent hydrophilic drug. The $GemC_{12}$-LNC hydrogel reduced significantly the size of a subcutaneous human GBM tumor model compared to the drug and short-term tolerability studies showed that this system is suitable for local treatment in the brain. In conclusion, this proof-of-concept study demonstrated the feasibility, safety and efficiency of the injectable $GemC_{12}$-LNC hydrogel for the local treatment of GBM.

KEYWORDS

Lipid nanocapsules, Gemcitabine, Hydrogel, Nanomedicine, Glioblastoma

TABLE OF CONTENTS

1. INTRODUCTION

Glioblastoma (GBM), a grade IV astrocytoma (WHO classification of Glioma), is the most common, malignant and aggressive brain tumor in adults [1] and affects 3 in 10,000 persons in the European Union and about the same number in the United States [2, 3]. GBM is characterized by rapid proliferation and propensity to infiltrate in healthy brain tissues, and causes chronical debilitation, neurologic deficits and death [2, 4]. Despite the efforts that have been made in the last decades to treat and prolong the overall survival of patients affected by GBM, this tumor remains currently incurable. The standard-of-care therapy includes surgical resection combined with radiotherapy and/or concomitant chemotherapy with Carmustine (BCNU) or Temozolomide (TMZ) but the median survival after the treatment is still very low (12-15 months, with a 2-year survival rate of 27%) [1, 5, 6].

There are several problems that lead to such a low therapeutic efficacy: (i) the central nervous system is isolated from the systemic circulation by the blood-brain barrier (BBB). This is a physiological and pharmacological barrier that makes it impossible to many chemotherapeutic agents to reach the brain and the tumor site at therapeutic doses, therefore limiting the therapeutic options [7]. (ii) GBM have a high tendency to form recurrences after surgical resection due to the presence of disseminated malignant cells that form micro-metastasis that are undetectable by magnetic resonance imaging (MRI). Moreover, due to the position of the tumor in the brain it is almost impossible to completely eradicate it by surgical resection without damaging functional brain tissue [7, 8]. (iii) GBM cells show intrinsic or acquired chemoresistance to alkylating agents: one of the major mechanisms of resistance is mediated by the enzyme O_6-methylguanine methyltransferase (MGMT). This DNA repair enzyme is able to remove the alkyl groups from the O_6 position of guanine reversing the methylation action of TMZ. Other mechanisms include the mismatch repair and the base excision repair pathways, the deregulation of apoptosis-regulating genes and proteins and the overexpression of proteins such as Galectin-1 or Epidermal Growth Factor Receptor (EGFR) by tumor cells [9-12].

The unmet medical needs related to GBM and its devastating and incurable effects bring to an urgent necessity to find new treatment strategies, which represent a great challenge for researchers and clinicians. In the last few years, many papers have been published

concerning different nanodelivery platforms that could allow chemotherapeutic drugs to reach the tumor by active or passive targeting [13, 14]. Among others, lipid-nanocapsules (LNC) are biomimetic carriers composed of an oily core and surrounded by a shell of sufactants which are obtained by a solvent-free, cost-effective soft-energy procedure. LNC are made up of biocompatible, biodegradable and FDA approved constituents and have shown high drug-loading capacity, long physical stability [15]. They are considered as one of the most promising platforms for the central nervous system (CNS) drug delivery for their ability to enter in glioma cells, prevent opsonization and macrophage uptake and inhibit the efflux pumps at the blood-CNS barriers. LNC encapsulated with drugs such as Ferrociphenol or Paclitaxel have been already tested in preclinical studies for the treatment of GBM showing promising results [16].

As surgical resection has a critical role in the GBM therapy and the 80-90% of its recurrences are localized within 2 cm of the original site of the tumor, the local delivery of chemotherapeutic agents into the resection cavity is a very promising strategy [7, 17, 18]. In 1996, the FDA approved the first implant for the intracerebral treatment of GBM, a biodegradable wafer impregnated in BCNU (Gliadel®) which showed interesting results in terms of prolonging overall survival and a reduction in systemic toxicities [1, 6, 18]. However, even if Gliadel® showed its safety and its modest efficacy in terms of post-operative survival time, it produces post-implant complications including intracranial abscess, meningitis, impaired wound healing, cerebrospinal fluid leak, seizures and tumor cyst formation. Moreover, neurosurgeons find it difficult to adjust the wafers to the resection cavity and some fragments seem to migrate from the implantation site. Additionally, the drug penetration depth is very limited and the drug release very fast (one week) [19-21]. Despite these inconvenients, the local drug delivery of cytotoxic agents seems very promising for the treatment of GBM as it allows to bypass the CNS barriers by direct administration of the drug into the brain. Moreover, it allows to obtain a long and sustained release of the active molecule reaching therapeutic concentrations at the tumor site without involving other organs. Many researchers have focused their attention on this administration pathway by producing different types of physical implants or hydrogels able to deliver the treatment at the tumor site or in the tumor resection cavity [7, 22-27]. Recently, our group has developed a TMZ-loaded photopolymerizable PEG-DMA based hydrogel in order to overcome some of

the drawbacks that have been reported for Gliadel® aiming at obtaining an effective and prolonged treatment for GBM [28]. In the present study, we developed a hydrogel formed from an innovative nanodelivery system loaded with the anticancer drug gemcitabine (Gem), which has a different mechanism of action compared to alkylating agents. Gem is a nucleoside analogue used in the treatment of various solid tumors (non-small-cell lung cancer, pancreatic cancer, breast and ovarian cancer) that irreversibly inhibits the production of nucleic acids and it is also a potent radiosensitizer agent [29, 30]. As it shows a short plasma half-life and some mechanisms of resistance related to its transport into cancer cells, some prodrugs have been synthesized in order to improve its metabolic stability and cytotoxicity [30, 31]. In particular, the group of Benoit *et al.* has recently developed a nanomedicine directly forming a hydrogel by the incorporation of 4-(N)-lauroyl-gemcitabine ($GemC_{12}$) into LNC (Figure 1) [32].

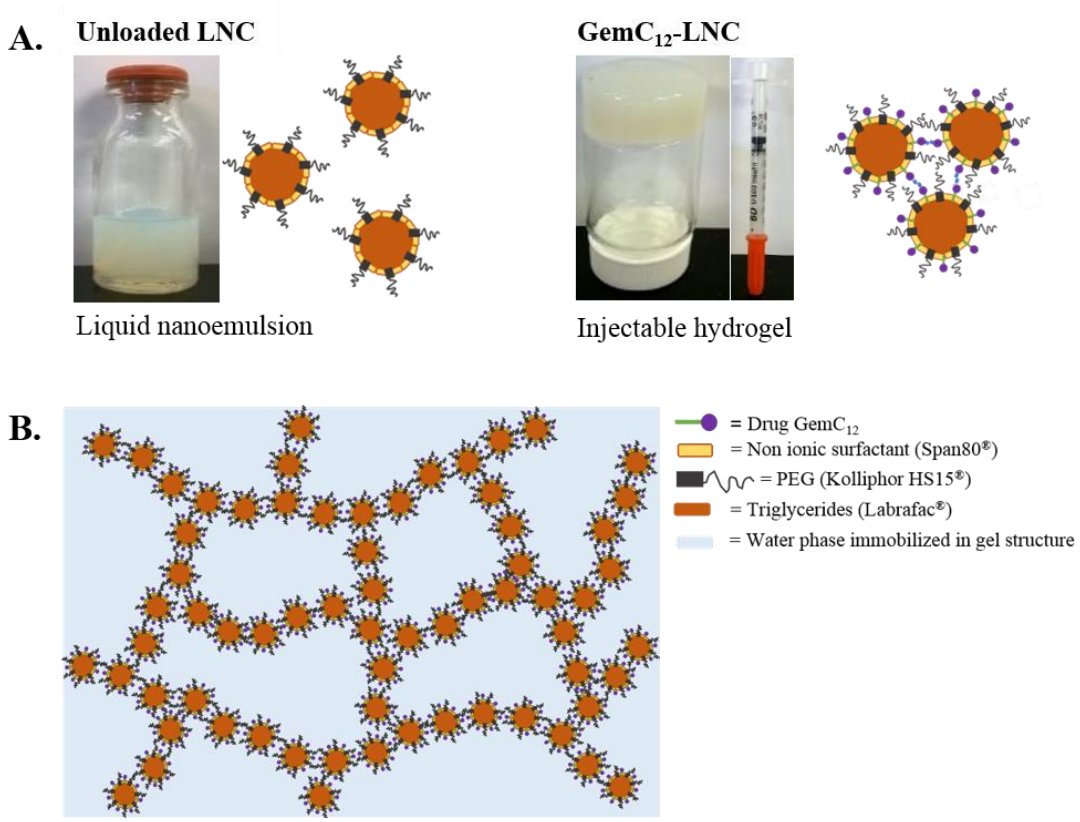

Figure 1. Pictures taken during the experiments and schematic representation of unloaded LNC (A, left image) and $GemC_{12}$-LNC hydrogel (A, right image; B). LNC are formed of an oily core of tryglicerides (Labrafac®) surrounded by a shell formed of hydrophilic and nonionic surfactants (Kolliphor HS15® and Span80®, respectively). When the drug $GemC_{12}$ is incorporated in the formulation, the alkyl chain of the drug is inserted in the LNC structure while the active part of the molecule is oriented toward the water phase forming H-bond cross linkings that are able to immobilize the water phase forming a gel. This hydrogel is injectable through insulin syringes.

As Gem has a MGMT-independent mechanism of action, show excellent radio-sensitizing properties and have been shown to pass the blood-tumor barrier in GBM patients [33], we hypothesized to deliver its lipophilic prodrug $GemC_{12}$ inside the tumor or in the tumor resection cavity in order to avoid GBM recurrences.

Altogether, the main advantages of $GemC_{12}$-LNC hydrogel to fulfill the requirements of GBM treatment are: *(i)* the hydrogel is injectable and only formed of LNC and the drug; the formulation is simple, easy to scale up and all the components are biocompatible and biodegradable. *(ii)* Compared to other systems, no polymer, gelling agent (e.g. Ca++) or external stimuli (e.g. irradiation) are needed for the gelification. *(iii)* Due its different mechanism of action compared to alkylating agents, Gem has the potent to overcome the resistance of GBM to conventional chemotherapy. *(iv)* Gem presents radiosentizing properties, allowing its combination with radiotherapy. *(v)* No studies have been published using 4-(N)-acyl-Gem derivatives for the treatment of GBM.

The aim of this study was to “proof the concept” of the feasibility, safety and efficiency of the injectable $GemC_{12}$-LNC hydrogel for the local treatment of GBM. This gel could adapt to the resection cavity and adhere to the brain parenchyma in order to kill the tumor infiltrating cells. Hence, we formulated a $GemC_{12}$-LNC hydrogel and evaluated its physiochemical and viscoelastic properties after extrusion from 30 G needles. We evaluated the $GemC_{12}$ *in vitro* release kinetics in artificial cerebrospinal fluid and the *in vitro* cytotoxicity. The anti-tumor efficacy and short-term tolerability were also evaluated *in vivo*, on a subcutaneous human GBM tumor model and in the brain, respectively.

2. MATERIALS AND METHODS

2.1. SYNTHESIS OF GEMC12

$GemC_{12}$ has been synthesized as previously reported [31, 32]. Briefly, 100 mL of dioxane (Sigma-Aldrich, France) and 5 g of dodecanoic anhydride (2 mmol; Sigma-Aldrich, France) were added to an aqueous solution of Gem base (1.958 g Gem in 39 mL of water, 1 mmol; Carbosynth, United Kingdom) and stirred at 50°C for 48 hours monitoring the reaction by thin-layer chromatography. The reaction solvents were then eliminated by evaporation under vacuum and the residues were purified by silica gel column flash chromatography (elution in dichloromethane-ethanol 96:4 v/v; Fisher Scientific, United Kingdom). $GemC_{12}$ was recovered as main product, in the form of a white powder with molecular weight of about 446 g/mol. The chemical stability of this compound has been tested by Immordino *et al.*, who showed that the amide linkage of $GemC_{12}$ is stable in the pH range 4-9 [31].

^{1}H-NMR ($(CD_3)_2SO$): 10.99 (1H, s, NHCO), 8.22 (1H, d, 6-CH), 7.27 (1H, d, 5-CH), 6.33 (1H, m, 10 -CH), 4.16 (1H, m, 30 -CH), 3.88–3.78 (2H, m, 50 -CH), 3.65 (1H, m, 40 -CH), 2.39 (1H, t, CO– CH_2), 1.52 (2H, t, CO–CH_2–CH_2), 1.22 (16H, m, $CH_2(CH_2)_8CH_3$), 0.84 (3H, t, CH_3).

2.2. FORMULATION OF LIPID NANOCAPSULES (LNC)

LNC were prepared using a phase-inversion process reported in the literature [34, 35]. To obtain the gel $GemC_{12}$-LNC, 0.093 g of $GemC_{12}$, 1.24 g of Labrafac® (Gattefosse, France) and 0.25 g of Span80® (Sigma-Aldrich, USA) were weighed and stirred in a water bath at 50°C with 200 µL of acetone (VWR Chemicals, Belgium) until complete dissolution of the drug. The acetone was then let to evaporate and 0.967 g of Kolliphor® (Sigma-Aldrich, Germany), 0.045 g of Sodium Chloride (VWR Chemicals, Belgium) and 1.02 g of water for injections (Braun, Germany) were added to the formulation. Three cycles of heating and cooling were performed under magnetic stirring (500 rpm) between 40 and 70°C. During the last cooling cycle, at the temperature corresponding to the phase-inversion zone (around 53-55°C), 2.12 g of water for injections were added and stirred for one more minute. After the last cooling process and shock dilution the $GemC_{12}$-LNC formulations were inserted in insulin syringes (BD Micro-Fine™ needle 0.30 mm (Ø 30 G) x 8 mm; Becton Dickinson, France) in order to

form the gel directly inside the syringes and stored at 4°C until further use. The unloaded LNC were obtained using the same method without adding the active compound and then stored at 4°C until further use. The formulations were obtained working under aseptic conditions.

2.3. PHYSICOCHEMICAL CHARACTERIZATION

2.3.1. Size and Zeta Potential

Unloaded LNC and $GemC_{12}$-LNC average particle sizes and polydispersity indexes were measured using a dynamic laser light scattering apparatus Zetasizer NanoZS (Malvern Instruments, UK). Zeta potential measurements were performed by laser Doppler velocimetry. For the measurement, each sample was suitably diluted in a ratio of 1:60 with MilliQ water (Merck-Millipore, Germany) (N=4 *n*=4).

2.3.2. Quantitative determinations of $GemC_{12}$ content in the hydrogel

The quantitative determinations of $GemC_{12}$ were measured by High Performance Liquid Chromatography (HPLC) analysis using an Agilent Technologies instrument Agilent 1100 series, under isocratic conditions. The separation was carried out using a Thermo Scientific BDS Hypersil C18 (100 x 4,6 mm; particle size 3 µm) column, with a mobile phase containing methanol (VWR Chemicals, France) and MilliQ water in a ratio of 90:10 (v/v) as previously reported [31, 36]. The detection wavelength was set at 248 nm and the flow rate was maintained at 0.8 mL/min. Under these conditions, the retention time of $GemC_{12}$ was about 2.3 minutes. A calibration curve was obtained by diluting $GemC_{12}$ in methanol at concentrations included between 1 and 150 µg/mL (correlation coefficient of R^2=0.9994). The limit of quantification was 1 µg/mL. The coefficients of variation were all within 10 %. The total drug content of $GemC_{12}$ loaded in the hydrogel was evaluated by dissolution of an amount of $GemC_{12}$-LNC in methanol (dilution ratio 1:240) and quantification by HPLC. The encapsulation efficiency (EE) of $GemC_{12}$ in the LNC was calculated as the ratio between the total drug content and the initial amount of drug weighed for the formulation. The drug loading was evaluated as the ratio between the total $GemC_{12}$ content and the content of the oil component (Labrafac®) in the formulation (w/w) [37].

$$EE\ (\%) = \frac{Total\ content\ of\ GemC_{12}\ in\ hydrogel}{Initial\ amount\ of\ GemC_{12}} \times 100$$

$$Drug\ loading = \frac{Total\ content\ of\ GemC_{12}\ in\ hydrogel}{Amount\ of\ oil\ component\ in\ hydrogel} \times 100$$

2.4. RHEOLOGICAL PROPERTIES OF GEMC12-LNC HYDROGEL EXTRUDED FROM SYRINGES

The viscoelastic properties of unloaded LNC and $GemC_{12}$-LNC hydrogel extruded from 30 G needles were measured at 25°C using a Modular Compact Rheometer MCR 102 (Anton Paar, Austria), with a cone plate geometry (diameter 50 mm, angle: 0.5). At 0.1% constant strain, storage modulus G' and loss modulus G" were measured as a function of the angular frequency (0.1-10 Hz) (*n*=3 N=3).

2.5. *IN VITRO* STUDIES

2.5.1. In vitro release of GemC12 from the drug-loaded lipid nanocapsules hydrogel

The *in vitro* release of $GemC_{12}$-LNC from the hydrogel was obtained during a period of one month. 200 µL of gel were placed at the bottom of a 5 mL glass tube and 300 µL of artificial cerebrospinal fluid (pH 7.35; see composition in section S1 [38]) were added. The tubes were incubated at 37°C and, at fixed time intervals, 100 µL of supernatant were collected and replaced by 100 µL of fresh medium. The samples were then diluted in methanol (1:1 v/v) and stored at -20°C until further use. For the quantification, the samples were suitably diluted in methanol (minimum dilution of 1:20 v/v in order to disrupt the LNC structure) and centrifuged at 15,000 rpm for 15 minutes to precipitate the protein residues and avoid interferences. The supernatant was then injected in HPLC using the previously described method. After incubation at 37°C for one month the supernatant was removed and the gel was recovered, weighed and appropriately diluted in methanol to obtain the amount of drug still present in the gel structure (N=4, *n*=12).

2.5.2. Cell cultures

U-87 MG glioma cells (ATTC, USA) were cultured in Eagle's Minimum Essential Medium (EMEM; ATTC, USA) supplemented with 10% Bovine Fetal Serum (Gibco, Life Technologies USA), 100 U/mL penicillin G sodium and 100 µg/mL streptomycin sulfate (Gibco, Life Technologies, USA). Cells were subcultured in 75 cm^2 culture flasks (Corning® T-75, Sigma-Aldrich, USA) and incubated at 37°C and 5% CO_2.

2.5.3. MTT colorimetric assay

U-87 MG cell viability was measured by the MTT (Thiazolyl Blue Tetrazolium Bromide) assay which allows to quantify the metabolic activity of the living cells. Cells were seeded at a density of $5x10^3$ cells/well in 96-well plates previously coated with poly(D)lysine (0.1 mg/mL per well and washed three times with PBS; Sigma-Aldrich, USA) and incubated at 37°C and 5% CO_2. Then, they were either incubated with Triton X-100 (Sigma-Aldrich, USA), different concentrations of gemcitabine hydrochloride (GemHCl; Sigma-Aldrich, China), $GemC_{12}$, $GemC_{12}$-LNC, unloaded LNC, or left untreated. The treatments were dissolved in PBS (GemHCl, $GemC_{12}$-LNC and unloaded LNC) or in Water/Ethanol/Tween®80 6.9/87.6/5.5 v/v ($GemC_{12}$) and then suitably diluted in complete culture medium. The concentration of active drug ranged between 0.01 and 100 µM. After 6, 24 or 48 h of incubation cells were rinsed with PBS and incubated 3 h with 200 µL of MTT solution (0.5 mg/mL; Sigma-Aldrich, USA). Formazan salts were then solubilized in dimethyl sulfoxide (Merck, USA) and spectrophotometric readings were performed at 560 nm with a MultiSkan EX plate reader (Thermo Fisher Scientific, USA). Cells cultured with complete culture medium or Triton X-100 were considered as negative and positive controls, respectively. The results are expressed as relative percentage of living cells compared to the negative control (untreated cells) (N=3, *n*=14).

2.6. *IN-VIVO* STUDIES

All experiments were performed following the Belgian national regulations guidelines and were approved by the ethical committee for animal care of the faculty of medicine of the

Université Catholique de Louvain (2014/UCL/MD/004). Animals had free access to water and food.

2.6.1. Anti-tumor efficacy on subcutaneous human glioblastoma tumor model

Eight-week-old female NMRI nude mice (Janvier, France) were anesthetized by intraperitoneal injection of ketamine/xylazine (66.6 and 8.6 mg/kg, respectively) and U-87 MG glioma cells were injected subcutaneously in their right flank (2 x 10^6 cells/mouse). Tumors were allowed to grow and their initial volume was measured using an electronic caliper using the formula corresponding to a prolate ellipsoid: volume = Π/6 × length × width^2. When the tumors reached the volume of about 35 mm^3, mice were randomized in 4 groups and treatments were injected intratumorally. As the hydrogel covered the tumor, daily measurements of the tumor growth was impossible. Hence, after 8 days mice were sacrificed and tumors were extracted and weighed. As the density of the tumor had been previously reported as equal to 1 [28] the initial volumes and the final weights were compared to evaluate the effect of the treatment on the tumor growth. Group 1: control group (no treatment) (*n*=7); Group 2: unloaded LNC (*n*=7); Group 3: $GemC_{12}$ dissolved in Water/Ethanol/Tween®80 (6.9/87.6/5.5 v/v) (*n*=8); Group 4: $GemC_{12}$-LNC gel (*n*=10).The dose injected in mice of groups 3 and 4 was 19.5 mg of $GemC_{12}$ per kilogram of body weight (equivalent to 13.1 mg of GemHCl per kg of body weight). The LNC delivered dose of unloaded LNC was the same as $GemC_{12}$-LNC (40 µl).

2.6.2. Short-term tolerability assay

Eight-week-old female NMRI mice (Janvier, France) were hazardously divided in 4 groups. On day one, mice were anesthetized by intraperitoneal injection of ketamine/xylazine (66.6 and 8.6 mg/kg, respectively) and a hole was created into the skull at the left frontal lobe using a drill. Ten µL of either NaCl 0.9% solution, unloaded LNC, $GemC_{12}$ (dissolved in Water/Ethanol/Tween®80 6.9/87.6/5.5 v/v) or $GemC_{12}$-LNC hydrogel were injected in the hole using 0.5 mL syringes with 30 G needles. The amount of drug administered in these two groups corresponded to 5.5 mg of $GemC_{12}$ per kilogram of body weight. Mice were then sutured and observed for one week. On day eight, mice were sacrificed and brains were removed and fixed in 10% formalin solution (Merck, Germany) for 24 h and then in PBS at

4°C for at least two days. Brains were then embedded in paraffin, sectioned in 10 µm sections using a MICROM 17M325 microtome (Thermo Fischer Scientific, USA) and collected on super-frost plus glass slides [39]. Slides were incubated at 37°C overnight and then stored at room temperature until further use.

For the histological analysis and evaluation of the cellular inflammatory response the samples were deparaffinized and stained with haematoxylin and eosin (H&E) (*n*=3, N=3).

For the TUNEL assay, the Dual End Fluorometric TUNEL System kit ® (Promega, USA) was used following supplier instructions and nuclei were stained using DAPI (Sigma Aldrich, USA). Slides were mounted with Vectashield (Vector Laboratories, USA) and examined under an inverted fluorescent microscope (Apotome, Zeiss, Belgium) with 350 nm (blue, DAPI) and 748-789 nm (green, TUNEL) excitation filters (*n*=3, N=3).

The microglia activation was evaluated by Iba-1 immunostaining. Slides were deparaffinized, the endogenous peroxydases were blocked with hydrogen peroxide (30% v/v) and left for 1h and 30min in citrate buffer in a water bath at 100°C. Sections were then incubated for 30 min with 10% normal horse serum to block non-specific binding sites before incubation with a goat anti-human Iba-1 antibody (1:1000; Novus Biologicals, USA) overnight at room temperature. Slides were washed and incubated for 60 min at room temperature with rabbit anti-goat IgG biotinylated antibody (1:200; Vector Laboratories, USA). Sections were then counterstained with hematoxylin, dehydrated and mounted with DPX neutral mounting medium (Prosan, Belgium). Slides were scanned using a SCN400 Leica slide scanner and image analysis was performed with Digital Image Hub (Leica, Germany) (*n*=3, N=3).

2.7. STATISTICAL ANALYSIS

The number of samples used in each experiment was expressed as N while the number of replicates for each experiment was expressed as *n*. Results were expressed as mean ± standard deviation (SD) for the *in vitro* experiments (Table 1; Figures 2, 3 and 4) and as mean ± standard error of the mean (SEM) for the *in vivo* experiments (Figure 5). Two-way ANOVA test with Bonferroni post-tests and unpaired t-test were performed using the software GraphPad Prism to demonstrate statistical differences between groups for the MTT assays and *in vivo* efficacy assay, respectively.

3. RESULTS AND DISCUSSION

3.1. PHYSICOCHEMICAL CHARACTERIZATION AND RHEOLOGICAL PROPERTIES OF THE UNLOADED AND GEMC12-LOADED LNC

The formulation of unloaded LNC and GemC12-LNC have been prepared by phase-inversion technique. As previously reported by Moysan *et al.* [32], the GemC12-LNC formulation rapidly acquired the consistency of a gel and for this reason it was necessary to store the formulations inside syringes in order to be able to use them afterwards. The filling of the syringes has to be done between 1 and 5 minutes after the shock dilution, in order to let the formulation gelifying inside the syringes. On the contrary, the unloaded LNC maintained a liquid state also after the shock dilution with water. The unloaded LNC and GemC12-LNC formulations were characterized in terms of physicochemical properties and loading capacity, and the results are reported in Table 1. The size of the LNC in both formulations was around 68 nm, the polydispersity indexes showed a narrow size distribution and the zeta potential values were slightly negative. The GemC12 encapsulation efficiency and drug loading were evaluated after disruption of the LNC in methanol and HPLC analysis, and were around 98% and 7.3%, respectively. Regarding the literature, our system present a low drug loading: among others, Mesoporous silica-loaded nanoparticles (NP) present a Gem loading of 40% [40], albumin NP allows for a Gem loading of 10% [41] and PLA-NP present a Gem loading of 22% [42]. Nevertheless, Moysan *et al.* have been previously reported that, when the drug loading is higher than 7.5% in our system the gelation process was instantaneous after the shock dilution, so it is impossible to fill the syringes at higher drug loading values [32]. Additionally, even if the drug loading is low, this system allows the delivery of therapeutic concentrations. For example, 10 µl (injectable volume in the mice brain) allows the delivery of around 5.5 mg/kg of GemC12, which corresponds to a therapeutic dose for local treatment [43].

In this study LNC have been used as nanodelivery system for the drug GemC12 not only to deliver and protect the active molecule but also for the innovative and unique property of forming a product with gel-like consistency when the drug is incorporated in the LNC structure (Figure 1) [32]. In this system, the drug actively participate in the structure of the gel: indeed, the hydrogel is formed by an interparticulate association of GemC12-LNC in

which the Gem moieties of $GemC_{12}$ located at the oil–water interface of LNC form H-bond cross-linkings and thus immobilize the water phase. Nanoparticle hydrogels have been made with liposomes, solid lipid NP and micelles [44-46]. Nevertheless, in these systems the loaded nanocarriers were dispersed in polymer matrices responsible for the gelation. In a "single gel", the main advantage consists in the fact that the degradation of the gel corresponds to the LNC release, as no other components (synthetic or natural polymers, gelling agents, external stimuli) are able to induce additional side effects, influence the activity or the release of the drug have been added to the formulation.

Table 1. Physicochemical characterization and loading efficacy of $GemC_{12}$-loaded lipid nanocapsules (N=4 *n* =4; mean ± SD)

	Size (nm)	**Polydispersity index**	**Zeta Potetial (mV)**	**Encapsulation efficiency (%)**	**Drug Loading (%)**
Unloaded LNC	68 ± 5	0.12 ± 0.08	- 1.9 ± 0.1	-	-
$GemC_{12}$-LNC	69 ± 4	0.27 ± 0.05	- 2.5 ± 0.2	98 ± 11	7.3 ± 0.8

Rheological studies (viscoelastic property determination) were conducted on the unloaded LNC and $GemC_{12}$-LNC formulations after extrusion from an insulin syringe with 30 G needle. The results of the unloaded LNC *vs* $GemC_{12}$-LNC (7.3% $GemC_{12}$/Labrafac® w/w) profiles, illustrated in Figure 2, confirmed that the unloaded formulation showed no gelation or elastic behavior while $GemC_{12}$-LNC showed gel properties. These results confirmed what was previously reported by Moysan *et al.* [32] which demonstrated that, when the drug loading of the system is between 5 to 10 % ($GemC_{12}$/Labrafac® w/w), the formulation acquires a gel-like consistency because $GemC_{12}$ actively participates in the gel structure. The drug is located at the oil-water interface of the LNC and forms 3D-pearl necklace of $GemC_{12}$-LNC. Indeed, the alkyl chain is inserted in LNC structure while the Gem structure is oriented toward the water phase forming H-bond cross linkings and immobilizing the water phase to form a gel. Moysan *et al*. have also demonstrated that this hydrogel can be injected using a syringe with 18 G and 21 G needles without any loss of viscoelastic properties [32]. As the hydrogel modulus is similar to the brain tissue modulus under shear deformation (± 1 kPa), $GemC_{12}$-LNC mechanical properties of are adapted for brain implantation [47].

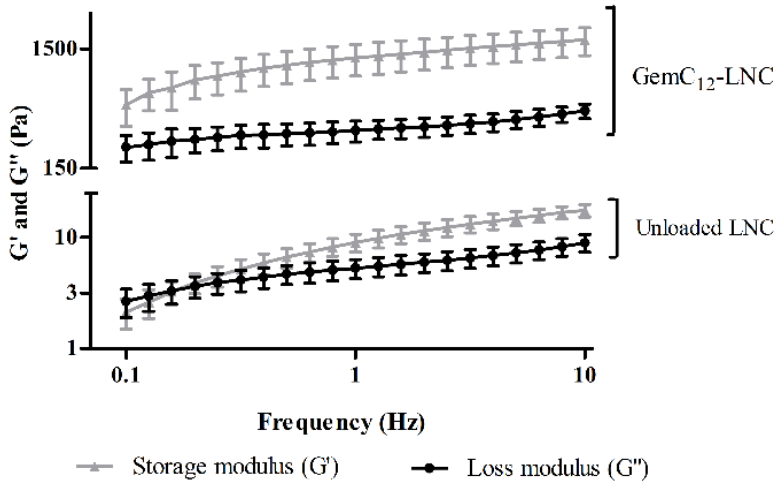

Figure 2. Viscoelastic property profiles of unloaded LNC and GemC$_{12}$-LNC (7.3% GemC$_{12}$/Labrafac® w/w): storage modulus G' (triangles, grey lines) and loss modulus G" (circles, black lines) *vs* frequency for unloaded LNC and GemC$_{12}$-LNC. (mean ± SD; N=3 *n*=3)

3.2. *IN VITRO* RELEASE OF GEMC$_{12}$ FROM THE DRUG-LOADED LNC HYDROGEL

In this study, we have decided to use the GemC$_{12}$-LNC with a drug loading of approximately 7.5% because previous *in vitro* hydrogel dissolution studies conducted in PBS for one week showed a slower dissolution compared to the 5% hydrogel [32]. As the goal of our study was to obtain a hydrogel that could be injected in the tumor resection cavity and slowly release the drug in order to kill the residual infiltrating GBM cells, the *in vitro* release kinetics of our GemC$_{12}$-LNC hydrogel has been evaluated after incubation at 37°C in artificial cerebrospinal fluid. Figure 3 shows an initial drug release of 56 ± 9 % in the first 48 hours followed by sustained release of the drug from the hydrogel with an almost zero-order release rate (R^2 = 0.95). After one month of incubation almost 77 ± 8 % of GemC$_{12}$ was released from the gel (N=4, *n*=12). As the gel is only formed of GemC$_{12}$ and LNC the release of the drug corresponds to the degradation of the gel. After one month of incubation the gel was still present at the bottom of the tubes, indicating that the drug was not totally released yet. Indeed, when the supernatant was removed and the gel structure disrupted by dilution with methanol the 8 ± 3 % of drug was recovered. We believe that the initial burst effect followed by slow and sustained release of the drug from the gel seem very promising for further *in vivo* studies as it could allow to deliver a higher dose in the first two days to kill the residual GBM cells and then slow down the drug release to maintain the cytotoxic effect. *In vivo* the release of the drug will depend on many factors including the LCR flow and clearance [48]

which are supposed to accelerate the drug release but good results have been reported for GBM treatment using 5-Fluorouracil microspheres showing these *in-vitro* release patterns [27, 49].

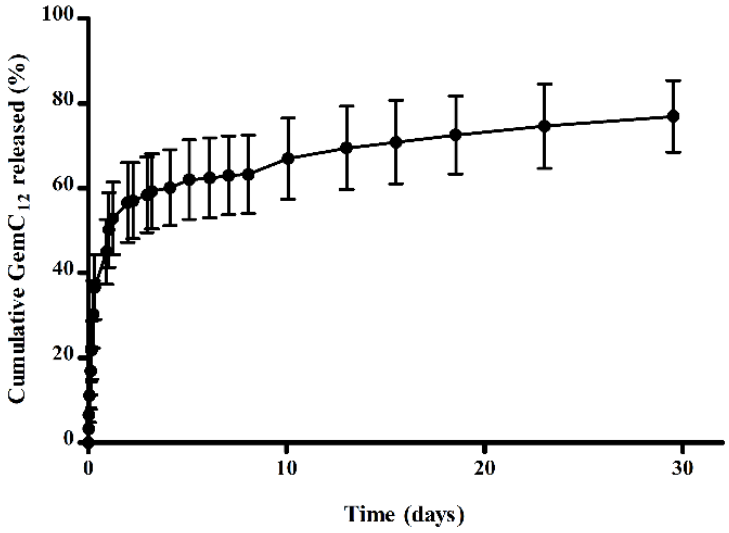

Figure 3. *In vitro* cumulative release of $GemC_{12}$-LNC from the hydrogel. The release study was performed in artificial cerebrospinal fluid (pH 7.4) at 37°C over one month and $GemC_{12}$ was quantified by HPLC (N=4 *n* =12; mean ± SD).

3.3. CYTOTOXICITY ASSAYS

To evaluate the cytotoxicity of $GemC_{12}$-LNC, MTT assays were conducted on U-87 MG GBM cell line after 6, 24 or 48 h of incubation at different concentrations of GemHCl, $GemC_{12}$ or $GemC_{12}$-LNC (0.01, 1, 10, 100 µM). Results are illustrated in Figure 4. After 6 h no changes in the percentage of cell survival was observed neither for GemHCl, $GemC_{12}$ or $GemC_{12}$-LNC compared to the untreated cells (data not shown). After 24 h of incubation, the unloaded LNC showed absence of cytotoxicity at all concentrations tested (data not shown) while the three formulations of Gem showed low toxicity at concentrations within 0.01 and 10 µM and increased cytotoxic effect at 100 µM. At this concentration, $GemC_{12}$ showed a percentage of cell survival significantly lower compared to GemHCl (p<0.001) while $GemC_{12}$-LNC was significantly more cytotoxic compared to $GemC_{12}$ and GemHCl (p<0.001). After 48 h of incubation the treatment with $GemC_{12}$ showed a significant higher cytotoxic effect compared to GemHCl at concentrations of 0.01, 10 and 100 µM (p<0.001, p<0.05, p<0.001 respectively) and compared to $GemC_{12}$-LNC at concentration of 0.01 µM (p<0.001). At this incubation time, $GemC_{12}$-LNC was significantly more cytotoxic than GemHCl and $GemC_{12}$ at concentration of 100 µM (p<0.001 and p<0.05 respectively). The IC_{50} values, obtained after

48 h of incubation at 6 different concentrations of drug (0.01, 0.1, 1, 5, 10 and 100 µM), are 12.06 µM, 0.18 µM and 0.56 µM for GemHCl, $GemC_{12}$ and $GemC_{12}$-LNC, respectively.

Some authors have previously evaluated the cytotoxic effect of Gem on different glioma cells [50-55]. Also, it has been previously reported that 4(N)-modifications in the Gem structure allowed to increase its plasma stability and consequently the drug half-life by reducing the deamination process produced by cytidine deaminase [30, 31]. Moreover, the lipophilic prodrugs, alone or incorporated in carriers such as liposomes or NP, have shown increased anticancer activity both *in vitro* and *in vivo* on different tumor models [31, 56-58]. $GemC_{12}$-LNC have been previously tested *in vitro* on human lung and pancreatic cancer cell lines and *in vivo* in a metastatic model of human non-small-cell lung cancer showing higher anticancer activity and reduced side effects compared to Gem [32, 59]. In accordance with previous reports in the literature, our results show that the encapsulation of $GemC_{12}$ in the LNC did not modify the cytotoxic activity of $GemC_{12}$, which is higher than that of the parent drug GemHCl. The different cell uptake mechanisms of $GemC_{12}$ and $GemC_{12}$-LNC could explain the different cytotoxic effects of the two treatments at equivalent incubation times (e.g. 48 h) and the fact that an enhanced cytotoxic activity of $GemC_{12}$-LNC is only observed at high concentrations. The cell internalization of the unloaded drug is mediated by nucleoside transporters [30] while the $GemC_{12}$-LNC uptake might be mediated by endocytosis as previously reported by Garcion *et al.* for LNC on 9L and F98 cells glioma cell lines [60, 61]. Hence, at higher concentrations the nucleoside transporters should be saturated while the endocytosis GemC12-LNC remains efficient. Moreover, the $GemC_{12}$ could be released from the nanocarrier outside the cell and then being internalized by nucleoside transporters. The exact mechanism of uptake of our $GemC_{12}$-LNC drug-nanocarrier complex still remains unknown and will be subject of future studies. To our knowledge, no pharmacokinetics or quantitative biodistribution studies have been published after local administration of 4-(N)-acyl-Gem-loaded NP. Hence, it is impossible for us to compare our *in vitro* results with *in vivo* drug tissue distribution. However, indubitably, these *in vitro* results should be modestly taken into account. Indeed, the sustained release of the drug as well as the gel consistency of our system (and their related advantages for *in vivo* studies) are not represented in the *in vitro* studies.

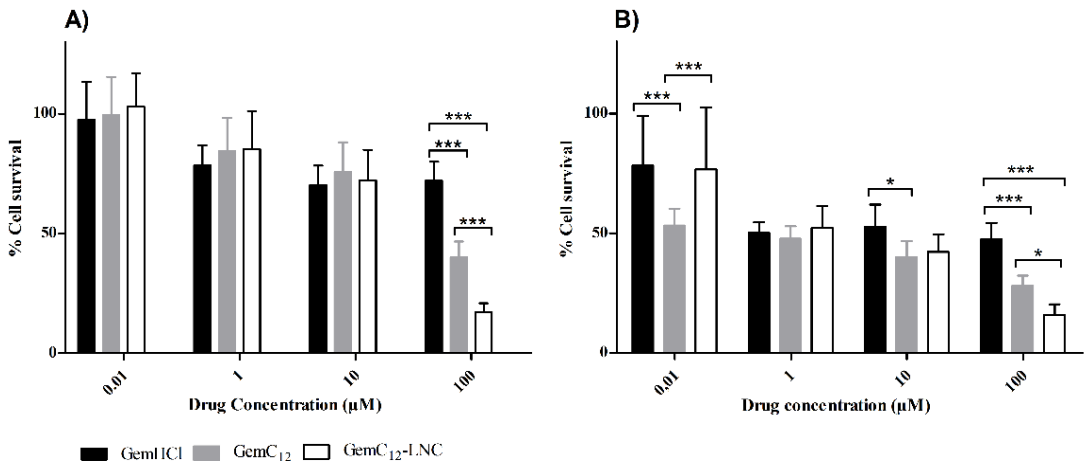

Figure 4. *In vitro* cytotoxicity studies: U-87 MG glioma cells were treated with GemHCl, $GemC_{12}$ or $GemC_{12}$-LNC for 24 h (A) and 48 h (B). The cytotoxic effect of the treatments was assessed by MTT assay. Data are presented as percentage of cell survival (untreated cells assumed as 100%) (N= 3 *n*=14; mean ± SD). **p* <0.05 and ****p*< 0.001

3.4. *IN VIVO* STUDIES: ANTI-TUMOR EFFICACY ON SUBCUTANEOUS HUMAN GLIOBLASTOMA TUMOR MODEL

To test whether the $GemC_{12}$-LNC hydrogel is suitable for the treatment of GBM we have performed an *in vivo* anti-tumor efficacy study using a subcutaneous human GBM tumor model as previously reported by Fourniols *et al.* [28]. Mice were injected subcutaneously with U-87 MG glioma cells in their flank and tumor was let to grow until reaching a measurable size. Then, different treatments (no treatment, unloaded LNC, $GemC_{12}$ and $GemC_{12}$-LNC) were injected inside the tumor and mice were sacrificed after eight days to evaluate the tumor response to the treatment. Results are illustrated in Figure 5. In mice treated with $GemC_{12}$ (Groups 3) no significant reduction was observed compared to the control groups 1 and 2 (no treatment and unloaded LNC). Interestingly, a significant reduction of the tumor weight was observed in the mice injected with the $GemC_{12}$-LNC hydrogel (Group 4) compared to the controls and $GemC_{12}$ (groups 1, 2 and 3; **p*<0.05). At the moment of tumor extraction the tumors were significantly reduced (4 animals) or disappeared (3 animals) and the gel was still present at the injection site indicating that it a suitable system to obtain a slow and prolonged release of the drug over time. For the group treated with $GemC_{12}$ (Group 3) the tumor increase is less pronounced than for the untreated group. No inflammation was observed at the site of injection in the unloaded LNC group compared to the animals treated with $GemC_{12}$: in this group local toxicity (strong inflammation and necrosis) was observed immediately after the injection of the drug and

persisted until the sacrifice of the animals. Moreover, three animals died at day 3 after injection. The intratumoral injection of the $GemC_{12}$-LNC hydrogel produced only sporadic inflammation starting from day 4 after injection but all mice lost body weight at day 3 and three animals died. The others (seven animals) quickly recuperate their initial body weight. Although the dose injected was similar compared to previous studies involving the use of Gem or its derivatives for local administration [43, 56, 59, 62], we hypothesize that the side effects observed in mice treated with the drug and $GemC_{12}$-LNC are due to the high dose injected. The maximum volume at which tumor can be resected in a orthotopic GBM tumor model is 10 mm^3 [11] and, as the tumor is located in the brain and the intracranial pressure needs to be controlled, 10 µl will be the maximum volume of treatment that can be injected for this type of tumor model [63, 64]. This volume would correspond, in the case of $GemC_{12}$-LNC hydrogel, to 5.5 mg $GemC_{12}$ per kg of body weight. However, the tumor volume in a subcutaneous human GBM tumor model at the moment of treatment injection is around 35 mm^3 [43, 62]. For this reason, we have adapted the dose of $GemC_{12}$ for this proof-of-concept anti-tumor efficacy study to 19.5 mg per kg of body weight, which is three times the dose injectable in the brain and it is in accordance with the literature for subcutaneous tumors locally treated with Gem [43, 56, 62]. Hence; the observed toxicity in this study has to be nuanced since this dose is much higher than the one that can be used for the orthotopic model. When we have injected in the brain, for the tolerability studies, 10 µl of $GemC_{12}$-LNC (5.5 mg $GemC_{12}$ per kg of body weight) no side effects or abnormal behavior were observed (as reported in the next section).

Some authors have previously published pre-clinical studies related to the use of Gem for GBM. For example, Carpinelli *et al.* and Wang *et al*. had previously showed a significant reduction of the tumor growth in rats after systemic administration of Gem in a C6 Glioma model while Galban *et al*. evaluated in mice the use of Gem in combination with radiotherapy as an alternative treatment for GBM patients who fail to respond to conventional treatment [33, 54, 55]. More recently, Shin *et al.* have encapsulated Gem and bevacizumab in immunoliposomes while Mu *et al.* have formulated Gem and chlorotoxin-conjugated iron oxide NP, and both have obtained promising results [65, 66]. Moreover, some clinical studies have been carried on to evaluate if the radiosenziting properties of Gem could have a positive impact on the treatment of GBM, obtaining controversial results

[29, 67-71]. To our knowledge, no studies have been published until now using 4-(N)-acyl-Gem derivatives *in vitro* on GBM cell lines or *in vivo* for the local treatment of GBM as an alternative strategy for tumors resistant to alkylating agents. Our results indicate that $GemC_{12}$-LNC is an injectable nanodelivery system able to induce significant reduction or disappearance of the tumor. The subcutaneous U-87 MG model was used to establish the proof-of-concept of our system and to evaluate its impact on tumor growth. Since we have demonstrated a significant tumor reduction when treated with $GemC_{12}$-LNC, further studies will be conducted in an orthotopic model of GBM over a longer period of time as well as in a tumor resection model.

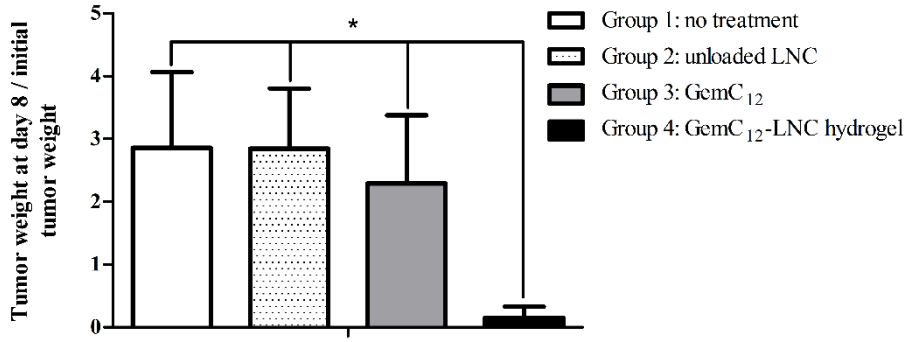

Figure 5. Anti-tumor efficacy of $GemC_{12}$-LNC hydrogel in a subcutaneous GBM model. Ratios between tumor weights 8 days after treatment and initial tumor weights of xenografted human U-87 MG tumor-bearing nude mice untreated (control), treated with unloaded LNC, $GemC_{12}$ or $GemC_{12}$-LNC hydrogel. The dose was 19.5 mg of $GemC_{12}$ per kilogram of body weight. Results are expressed as the tumor weight at day 8/initial tumor weight ratio ± SEM, *p <0.05 (*n*=7 for groups 1, 2, 4; *n*=5 for group 3).

3.5. *IN-VIVO* STUDIES: SHORT-TERM TOLERABILITY ASSAY

The short-term *in vivo* tolerability assays were assessed to test whether the $GemC_{12}$-LNC gel is suitable for local application in the brain. The inflammatory response, apoptosis and microglia activation of the brain tissue were evaluated at the injection site one week after the administration in the cortex of either PBS, unloaded LNC, $GemC_{12}$ or $GemC_{12}$-LNC. After the sacrifice of the mice, brains were removed, processed and the cellular response was evaluated by H&E coloration, TUNEL assay and iba-1 immunostaining on the brain tissue sections. The injected volume corresponds to the maximal amount allowed for intracerebral injection in mice (10 µl) [72]. The dose administered was 5.5 mg of $GemC_{12}$ per kg of body

weight. All mice survived to the day of their sacrifice and no abnormal behavior was observed in any group.

The images of the H&E staining (Figure 6) showed no significant inflammation in the brain tissue seven days after the injection of the PBS or unloaded LNC while the $GemC_{12}$ induced an inflammation at the site of injection. This was expected as it is a cytotoxic agent. The TUNEL assay (Figure 7) showed agglomeration of apoptotic cells in the $GemC_{12}$ sections at the site of injection. This result was also expected, as Gem have shown to induce apoptosis in different tumor cell lines [50, 54]. More interestingly, the H&E staining and the TUNEL assays of the $GemC_{12}$-LNC sections showed less inflammatory or apoptotic response and at the site of injection compared to $GemC_{12}$, suggesting that the gel structure could protect the tissue from the direct contact with high concentrations of the drug and release the drug slowly over time. Indeed, only singular apoptotic cells were observed in the $GemC_{12}$-LNC sections of Figure 7, probably due to the released molecules of $GemC_{12}$. As the cellular response observed in the H&E staining of $GemC_{12}$-LNC sections is comparable with the controls (PBS and unloaded LNC), we assume that the mechanical trauma of the surgery and injection induced the response more than the gel itself, as previously reported in literature [73]. Microglia are specialized macrophages of the brain that responds immediately to any minor brain damage [74, 75]. Their response over time is frequently used to assess the neuroinflammation at the injection site of hydrogels or biodegradable implants [76]. As their presence peaks at seven days, represents a standard response after injury and does not indicate irreversible damage [75] we were not surprised to observe microglial activation in all groups (Figure 8). However, we observed significantly higher microglia activation in the $GemC_{12}$ sections compared to other groups.

In conclusion, our data showed that one week after the injection of the gel no increase of inflammation, apoptosis or microglia activation was observed in the $GemC_{12}$-LNC tissues, compared to the PBS and unloaded LNC sections, indicating that the gel is well tolerated in mice brain in the short-term. Further assays will be performed in a long-term period to see how the brain tissue will respond to the slow degradation of the gel and the release of the drug.

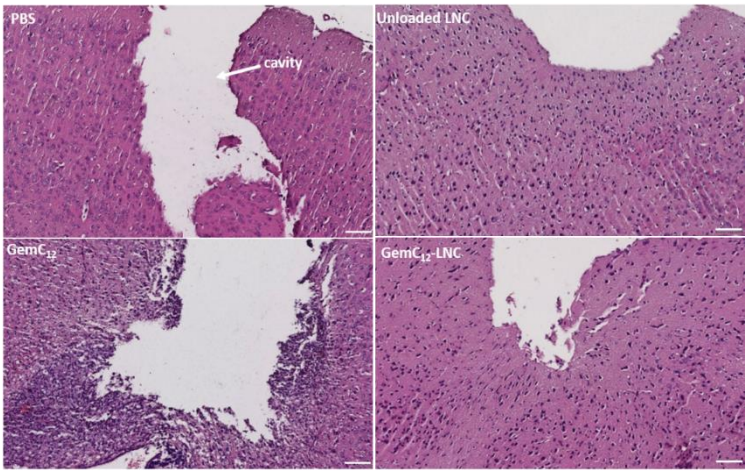

Figure 6. *In vivo* short-term tolerability assay: evaluation of the inflammatory response in the brain tissue after injection of PBS, unloaded LNC, $GemC_{12}$, and $GemC_{12}$-LNC. The amount of $GemC_{12}$ administered was 0.16 mg per mouse. Brains were extracted 7 days post-surgery and stained with H&E (N=3 *n*=3). Scale bar: 100 µm.

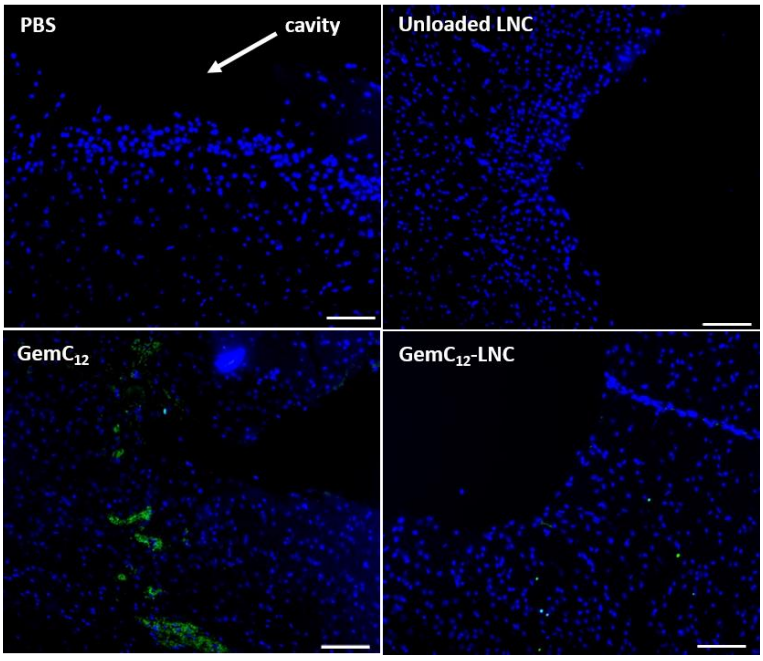

Figure 7. *In vivo* short-term tolerability assay: evaluation of the cell apoptosis in the brain tissue after injection of PBS, unloaded LNC, $GemC_{12}$, and $GemC_{12}$-LNC. The amount of $GemC_{12}$ administered was 0.16 mg per mouse. Brains were extracted 7 days post-surgery and treated for TUNEL (N=3 *n*=3). Blue: living nuclei (DAPI); Green: apoptotic cells (TUNEL). Scale bar: 100 µm

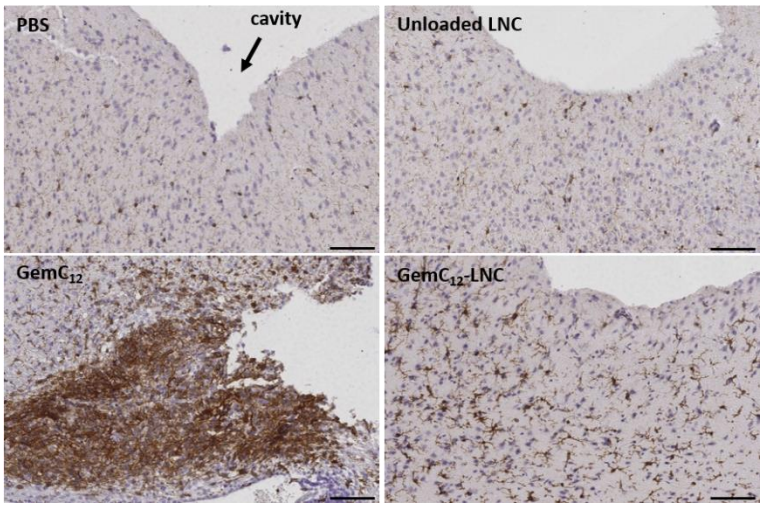

Figure 8. *In vivo* short-term tolerability assay: evaluation of the microglia activation in the brain tissue after injection of PBS, unloaded LNC, $GemC_{12}$, and $GemC_{12}$-LNC. The amount of $GemC_{12}$ administered was 0.16 mg per mouse. Brains were extracted 7 days post-surgery and treated for immunohistochemistry. Microglia activation was assessed by Iba-1 staining and sections were counterstained with hematoxylin (N=3 *n*=3). Scale bar: 100 µm

4. CONCLUSIONS

In this study we have demonstrated the feasibility, safety and efficiency of our injectable $GemC_{12}$-LNC hydrogel for the local treatment of GBM.

This system, which has a very simple formulation that avoids the use of solvents during the preparation and the presence of polymers or gelling agents in the hydrogel, has been demonstrated to be: *i)* directly injectable in the brain using 30-G needles syringes, *ii)* to have mechanical properties compatible with brain implantation, *iii)* to release the drug *in-vitro* in a sustained and prolonged manner during one month, *iv)* to reduce the tumor growth in a subcutaneous human GBM tumor model, *v)* to have a good short-term tolerability in brain tissue.

In conclusion, this proof-of concept study demonstrated that $GemC_{12}$-LNC hydrogel could be considered as a promising platform for the delivery of $GemC_{12}$ for the local treatment of GBM.

5. REFERENCES

[1] K.A. Batich, J.H. Sampson, Standard of care and future pharmacological treatment options for malignant glioma: an urgent need for screening and identification of novel tumor-specific antigens, Expert Opin Pharmacother, 15 (2014) 2047-2061.

[2] S. Tsigkos, S. Mariz, J. Llinares, L. Fregonese, S. Aarum, N.W. Frauke, K. Westermark, B. Sepodes, Establishing medical plausibility in the context of orphan medicines designation in the European Union, Orphanet J Rare Dis, 9 (2014) 175.

[3] Q.T. Ostrom, H. Gittleman, P. Farah, A. Ondracek, Y. Chen, Y. Wolinsky, N.E. Stroup, C. Kruchko, J.S. Barnholtz-Sloan, CBTRUS statistical report: Primary brain and central nervous system tumors diagnosed in the United States in 2006-2010, Neuro Oncol, 15 Suppl 2 (2013) ii1-56.

[4] S.A. Grossman, X. Ye, S. Piantadosi, S. Desideri, L.B. Nabors, M. Rosenfeld, J. Fisher, Survival of patients with newly diagnosed glioblastoma treated with radiation and temozolomide in research studies in the United States, Clin Cancer Res, 16 (2010) 2443-2449.

[5] R.D. Kortmann, B. Jeremic, M. Weller, L. Plasswilm, M. Bamberg, Radiochemotherapy of malignant glioma in adults. Clinical experiences, Strahlenther Onkol, 179 (2003) 219-232.

[6] R. Stupp, M. Brada, M.J. van den Bent, J.C. Tonn, G. Pentheroudakis, High-grade glioma: ESMO Clinical Practice Guidelines for diagnosis, treatment and follow-up, Ann Oncol, 25 Suppl 3 (2014) iii93-101.

[7] P.P. Wang, J. Frazier, H. Brem, Local drug delivery to the brain, Adv Drug Deliv Rev, 54 (2002) 987-1013.

[8] S.A. Grossman, J.F. Batara, Current management of glioblastoma multiforme, Semin Oncol, 31 (2004) 635-644.

[9] Q. Pan, X.J. Yang, H.M. Wang, X.T. Dong, W. Wang, Y. Li, J.M. Li, Chemoresistance to temozolomide in human glioma cell line U251 is associated with increased activity of O6-methylguanine-DNA methyltransferase and can be overcome by metronomic temozolomide regimen, Cell Biochem Biophys, 62 (2012) 185-191.

[10] J.N. Sarkaria, G.J. Kitange, C.D. James, R. Plummer, H. Calvert, M. Weller, W. Wick, Mechanisms of chemoresistance to alkylating agents in malignant glioma, Clin Cancer Res, 14 (2008) 2900-2908.

[11] F. Danhier, K. Messaoudi, L. Lemaire, J.P. Benoit, F. Lagarce, Combined anti-Galectin-1 and anti-EGFR siRNA-loaded chitosan-lipid nanocapsules decrease temozolomide resistance in glioblastoma: in vivo evaluation, Int J Pharm, 481 (2015) 154-161.

[12] K. Messaoudi, A. Clavreul, F. Lagarce, Toward an effective strategy in glioblastoma treatment. Part I: resistance mechanisms and strategies to overcome resistance of glioblastoma to temozolomide, Drug Discov Today, 20 (2015) 899-905.

[13] F. Danhier, O. Feron, V. Preat, To exploit the tumor microenvironment: Passive and active tumor targeting of nanocarriers for anti-cancer drug delivery, J Control Release, 148 (2010) 135-146.

[14] F. Danhier, A. Le Breton, V. Preat, RGD-based strategies to target alpha(v) beta(3) integrin in cancer therapy and diagnosis, Mol Pharm, 9 (2012) 2961-2973.

[15] N.T. Huynh, C. Passirani, P. Saulnier, J.P. Benoit, Lipid nanocapsules: a new platform for nanomedicine, Int J Pharm, 379 (2009) 201-209.

[16] J. Aparicio-Blanco, A.I. Torres-Suarez, Glioblastoma Multiforme and Lipid Nanocapsules: A Review, J biomed nanotechnol, 11 (2015) 1283-1311.

[17] F.H. Hochberg, A. Pruitt, Assumptions in the radiotherapy of glioblastoma, Neurology, 30 (1980) 907-911.

[18] M. Westphal, D.C. Hilt, E. Bortey, P. Delavault, R. Olivares, P.C. Warnke, I.R. Whittle, J. Jaaskelainen, Z. Ram, A phase 3 trial of local chemotherapy with biodegradable carmustine (BCNU) wafers (Gliadel wafers) in patients with primary malignant glioma, Neuro Oncol, 5 (2003) 79-88.

[19] H.H. Engelhard, The role of interstitial BCNU chemotherapy in the treatment of malignant glioma, Surg Neurol, 53 (2000) 458-464.

[20] D.A. Bota, A. Desjardins, J.A. Quinn, M.L. Affronti, H.S. Friedman, Interstitial chemotherapy with biodegradable BCNU (Gliadel) wafers in the treatment of malignant gliomas, Ther Clin Risk Manag, 3 (2007) 707-715.

[21] T.A. Juratli, G. Schackert, D. Krex, Current status of local therapy in malignant gliomas--a clinical review of three selected approaches, Pharmacol Ther, 139 (2013) 341-358.

[22] S. Brem, B. Tyler, K. Li, G. Pradilla, F. Legnani, J. Caplan, H. Brem, Local delivery of temozolomide by biodegradable polymers is superior to oral administration in a rodent glioma model, Cancer Chemother Pharmacol, 60 (2007) 643-650.
[23] B. Tyler, K.D. Fowers, K.W. Li, V.R. Recinos, J.M. Caplan, A. Hdeib, R. Grossman, L. Basaldella, K. Bekelis, G. Pradilla, F. Legnani, H. Brem, A thermal gel depot for local delivery of paclitaxel to treat experimental brain tumors in rats, J Neurosurg, 113 (2010) 210-217.
[24] T. Ozeki, D. Kaneko, K. Hashizawa, Y. Imai, T. Tagami, H. Okada, Combination therapy of surgical tumor resection with implantation of a hydrogel containing camptothecin-loaded poly(lactic-co-glycolic acid) microspheres in a C6 rat glioma model, Biol Pharm Bull, 35 (2012) 545-550.
[25] B.Y. Ong, S.H. Ranganath, L.Y. Lee, F. Lu, H.S. Lee, N.V. Sahinidis, C.H. Wang, Paclitaxel delivery from PLGA foams for controlled release in post-surgical chemotherapy against glioblastoma multiforme, Biomaterials, 30 (2009) 3189-3196.
[26] A.K. Vellimana, V.R. Recinos, L. Hwang, K.D. Fowers, K.W. Li, Y. Zhang, S. Okonma, C.G. Eberhart, H. Brem, B.M. Tyler, Combination of paclitaxel thermal gel depot with temozolomide and radiotherapy significantly prolongs survival in an experimental rodent glioma model, J Neurooncol, 111 (2013) 229-236.
[27] P. Menei, L. Capelle, J. Guyotat, S. Fuentes, R. Assaker, B. Bataille, P. Francois, D. Dorwling-Carter, P. Paquis, L. Bauchet, F. Parker, J. Sabatier, N. Faisant, J.P. Benoit, Local and sustained delivery of 5-fluorouracil from biodegradable microspheres for the radiosensitization of malignant glioma: a randomized phase II trial, Neurosurgery, 56 (2005) 242-248.
[28] T. Fourniols, L.D. Randolph, A. Staub, K. Vanvarenberg, J.G. Leprince, V. Preat, A. des Rieux, F. Danhier, Temozolomide-loaded photopolymerizable PEG-DMA-based hydrogel for the treatment of glioblastoma, J Control Release, 210 (2015) 95-104.
[29] J. Sigmond, R.J. Honeywell, T.J. Postma, C.M. Dirven, S.M. de Lange, K. van der Born, A.C. Laan, J.C. Baayen, C.J. Van Groeningen, A.M. Bergman, G. Giaccone, G.J. Peters, Gemcitabine uptake in glioblastoma multiforme: potential as a radiosensitizer, Ann Oncol, 20 (2009) 182-187.
[30] E. Moysan, G. Bastiat, J.P. Benoit, Gemcitabine versus Modified Gemcitabine: a review of several promising chemical modifications, Mol Pharm, 10 (2013) 430-444.
[31] M.L. Immordino, P. Brusa, F. Rocco, S. Arpicco, M. Ceruti, L. Cattel, Preparation, characterization, cytotoxicity and pharmacokinetics of liposomes containing lipophilic gemcitabine prodrugs, J Control Release, 100 (2004) 331-346.
[32] E. Moysan, Y. Gonzalez-Fernandez, N. Lautram, J. Bejaud, G. Bastiat, J.P. Benoit, An innovative hydrogel of gemcitabine-loaded lipid nanocapsules: when the drug is a key player of the nanomedicine structure, Soft Matter, 10 (2014) 1767-1777.
[33] S. Galban, B. Lemasson, T.M. Williams, F. Li, K.A. Heist, T.D. Johnson, J.S. Leopold, T.L. Chenevert, T.S. Lawrence, A. Rehemtulla, T. Mikkelsen, E.C. Holland, C.J. Galban, B.D. Ross, DW-MRI as a biomarker to compare therapeutic outcomes in radiotherapy regimens incorporating temozolomide or gemcitabine in glioblastoma, PLoS One, 7 (2012) e35857.
[34] S.P. Heurtault B, Pech B, Proust JE, Richard J, Benoit JP, Lipidic nanocapsules, formulation process and use as a drug delivery system, in, 2001.
[35] B. Heurtault, P. Saulnier, B. Pech, J.E. Proust, J.P. Benoit, A novel phase inversion-based process for the preparation of lipid nanocarriers, Pharm Res, 19 (2002) 875-880.
[36] S. Arpicco, C. Lerda, E. Dalla Pozza, C. Costanzo, N. Tsapis, B. Stella, M. Donadelli, I. Dando, E. Fattal, L. Cattel, M. Palmieri, Hyaluronic acid-coated liposomes for active targeting of gemcitabine, Eur J Pharm Biopharm, 85 (2013) 373-380.
[37] A. Beloqui, M.A. Solinis, A.R. Gascon, A. del Pozo-Rodriguez, A. des Rieux, V. Preat, Mechanism of transport of saquinavir-loaded nanostructured lipid carriers across the intestinal barrier, J Control Release, 166 (2013) 115-123.
[38] N. Hajos, I. Mody, Establishing a physiological environment for visualized in vitro brain slice recordings by increasing oxygen supply and modifying aCSF content, J Neurosci Methods, 183 (2009) 107-113.
[39] K.K. Chereddy, A. Lopes, S. Koussoroplis, V. Payen, C. Moia, H. Zhu, P. Sonveaux, P. Carmeliet, A. des Rieux, G. Vandermeulen, V. Preat, Combined effects of PLGA and vascular endothelial growth factor promote the healing of non-diabetic and diabetic wounds, Nanomedicine, 11 (2015) 1975-1984.
[40] H. Meng, M. Wang, H. Liu, X. Liu, A. Situ, B. Wu, Z. Ji, C.H. Chang, A.E. Nel, Use of a lipid-coated mesoporous silica nanoparticle platform for synergistic gemcitabine and paclitaxel delivery to human pancreatic cancer in mice, ACS nano, 9 (2015) 3540-3557.

[41] X. Yu, Y. Di, C. Xie, Y. Song, H. He, H. Li, X. Pu, W. Lu, D. Fu, C. Jin, An in vitro and in vivo study of gemcitabine-loaded albumin nanoparticles in a pancreatic cancer cell line, Int J Nanomedicine, 10 (2015) 6825-6834.

[42] D. Cosco, D. Paolino, F. De Angelis, F. Cilurzo, C. Celia, L. Di Marzio, D. Russo, N. Tsapis, E. Fattal, M. Fresta, Aqueous-core PEG-coated PLA nanocapsules for an efficient entrapment of water soluble anticancer drugs and a smart therapeutic response, Eur J Pharm Biopharm, 89 (2015) 30-39.

[43] T. Manabe, H. Okino, R. Maeyama, K. Mizumoto, M. Tanaka, T. Matsuda, New infusion device for trans-tissue, sustained local delivery of anticancer agent to surgically resected tissue: potential use for suppression of local recurrence of pancreatic cancer, J Biomed Mater Res B Appl Biomater, 73 (2005) 203-207.

[44] S. Bobone, E. Miele, B. Cerroni, D. Roversi, A. Bocedi, E. Nicolai, A. Di Venere, E. Placidi, G. Ricci, N. Rosato, L. Stella, Liposome-Templated Hydrogel Nanoparticles as Vehicles for Enzyme-Based Therapies, Langmuir, 31 (2015) 7572-7580.

[45] J. Hao, X. Wang, Y. Bi, Y. Teng, J. Wang, F. Li, Q. Li, J. Zhang, F. Guo, J. Liu, Fabrication of a composite system combining solid lipid nanoparticles and thermosensitive hydrogel for challenging ophthalmic drug delivery, Colloids Surf B Biointerfaces, 114 (2014) 111-120.

[46] A.C. Santos Akkari, E.V. Ramos Campos, A.F. Keppler, L.F. Fraceto, E. de Paula, G.R. Tofoli, D.R. de Araujo, Budesonide-hydroxypropyl-beta-cyclodextrin inclusion complex in binary poloxamer 407/403 system for ulcerative colitis treatment: A physico-chemical study from micelles to hydrogels, Colloids Surf B Biointerfaces, 138 (2016) 138-147.

[47] S. Chatelin, A. Constantinesco, R. Willinger, Fifty years of brain tissue mechanical testing: from in vitro to in vivo investigations, Biorheology, 47 (2010) 255-276.

[48] J.J. Iliff, M. Wang, Y. Liao, B.A. Plogg, W. Peng, G.A. Gundersen, H. Benveniste, G.E. Vates, R. Deane, S.A. Goldman, E.A. Nagelhus, M. Nedergaard, A paravascular pathway facilitates CSF flow through the brain parenchyma and the clearance of interstitial solutes, including amyloid beta, Sci Transl Med, 4 (2012) 147ra111.

[49] P. Menei, E. Jadaud, N. Faisant, M. Boisdron-Celle, S. Michalak, D. Fournier, M. Delhaye, J.P. Benoit, Stereotaxic implantation of 5-fluorouracil-releasing microspheres in malignant glioma, Cancer, 100 (2004) 405-410.

[50] J. Rieger, S. Durka, J. Streffer, J. Dichgans, M. Weller, Gemcitabine cytotoxicity of human malignant glioma cells: modulation by antioxidants, BCL-2 and dexamethasone, Eur J Pharmacol, 365 (1999) 301-308.

[51] L.J. Ostruszka, D.S. Shewach, The role of cell cycle progression in radiosensitization by 2',2'-difluoro-2'-deoxycytidine, Cancer Res, 60 (2000) 6080-6088.

[52] P. Guo, J. Ma, S. Li, Z. Guo, A.L. Adams, J.M. Gallo, Targeted delivery of a peripheral benzodiazepine receptor ligand-gemcitabine conjugate to brain tumors in a xenograft model, Cancer Chemother Pharmacol, 48 (2001) 169-176.

[53] M. Genc, N. Castro Kreder, A. Barten-van Rijbroek, L.J. Stalpers, J. Haveman, Enhancement of effects of irradiation by gemcitabine in a glioblastoma cell line and cell line spheroids, J Cancer Res Clin Oncol, 130 (2004) 45-51.

[54] G. Carpinelli, B. Bucci, I. D'Agnano, R. Canese, F. Caroli, L. Raus, E. Brunetti, D. Giannarelli, F. Podo, C.M. Carapella, Gemcitabine treatment of experimental C6 glioma: the effects on cell cycle and apoptotic rate, Anticancer Res, 26 (2006) 3017-3024.

[55] C.X. Wang, L.S. Huang, L.B. Hou, L. Jiang, Z.T. Yan, Y.L. Wang, Z.L. Chen, Antitumor effects of polysorbate-80 coated gemcitabine polybutylcyanoacrylate nanoparticles in vitro and its pharmacodynamics in vivo on C6 glioma cells of a brain tumor model, Brain Res, 1261 (2009) 91-99.

[56] P. Brusa, M.L. Immordino, F. Rocco, L. Cattel, Antitumor activity and pharmacokinetics of liposomes containing lipophilic gemcitabine prodrugs, Anticancer Res, 27 (2007) 195-199.

[57] W.G. Chung, M.A. Sandoval, B.R. Sloat, P.D. Lansakara, Z. Cui, Stearoyl gemcitabine nanoparticles overcome resistance related to the over-expression of ribonucleotide reductase subunit M1, J Control Release, 157 (2012) 132-140.

[58] B.R. Sloat, M.A. Sandoval, D. Li, W.G. Chung, P.D. Lansakara, P.J. Proteau, K. Kiguchi, J. DiGiovanni, Z. Cui, In vitro and in vivo anti-tumor activities of a gemcitabine derivative carried by nanoparticles, Int J Pharm, 409 (2011) 278-288.

[59] N. Wauthoz, G. Bastiat, E. Moysan, A. Cieslak, K. Kondo, M. Zandecki, V. Moal, M.C. Rousselet, J. Hureaux, J.P. Benoit, Safe lipid nanocapsule-based gel technology to target lymph nodes and combat

mediastinal metastases from an orthotopic non-small-cell lung cancer model in SCID-CB17 mice, Nanomedicine, 11 (2015) 1237-1245.
[60] E. Garcion, A. Lamprecht, B. Heurtault, A. Paillard, A. Aubert-Pouessel, B. Denizot, P. Menei, J.P. Benoit, A new generation of anticancer, drug-loaded, colloidal vectors reverses multidrug resistance in glioma and reduces tumor progression in rats, Molecular cancer therapeutics, 5 (2006) 1710-1722.
[61] A. Paillard, F. Hindre, C. Vignes-Colombeix, J.P. Benoit, E. Garcion, The importance of endo-lysosomal escape with lipid nanocapsules for drug subcellular bioavailability, Biomaterials, 31 (2010) 7542-7554.
[62] H. Okino, R. Maeyama, T. Manabe, T. Matsuda, M. Tanaka, Trans-tissue, sustained release of gemcitabine from photocured gelatin gel inhibits the growth of heterotopic human pancreatic tumor in nude mice, Clin Cancer Res, 9 (2003) 5786-5793.
[63] O. Benny, S.K. Kim, K. Gvili, I.S. Radzishevsky, A. Mor, L. Verduzco, L.G. Menon, P.M. Black, M. Machluf, R.S. Carroll, In vivo fate and therapeutic efficacy of PF-4/CTF microspheres in an orthotopic human glioblastoma model, FASEB J, 22 (2008) 488-499.
[64] J.T. Dilworth, S.A. Krueger, M. Dabjan, I.S. Grills, J. Torma, G.D. Wilson, B. Marples, Pulsed low-dose irradiation of orthotopic glioblastoma multiforme (GBM) in a pre-clinical model: Effects on vascularization and tumor control, Radiotherapy and Oncology, 108 (2013) 149-154.
[65] Q. Mu, G. Lin, V.K. Patton, K. Wang, O.W. Press, M. Zhang, Gemcitabine and chlorotoxin conjugated iron oxide nanoparticles for glioblastoma therapy, J Mater Chem B Mater Biol Med, 4 (2016) 32-36.
[66] D.H. Shin, S.J. Lee, J.S. Kim, J.H. Ryu, J.S. Kim, Synergistic Effect of Immunoliposomal Gemcitabine and Bevacizumab in Glioblastoma Stem Cell-Targeted Therapy, J Biomed Nanotechnol, 11 (2015) 1989-2002.
[67] S.Z. Gertler, D. MacDonald, M. Goodyear, P. Forsyth, D.J. Stewart, K. Belanger, J. Perry, D. Fulton, W. Steward, N. Wainman, L. Seymour, NCIC-CTG phase II study of gemcitabine in patients with malignant glioma (IND.94), Ann Oncol, 11 (2000) 315-318.
[68] M. Weller, J. Streffer, W. Wick, R.D. Kortmann, E. Heiss, W. Kuker, R. Meyermann, J. Dichgans, M. Bamberg, Preirradiation gemcitabine chemotherapy for newly diagnosed glioblastoma. A phase II study, Cancer, 91 (2001) 423-427.
[69] A. Fabi, A. Mirri, A. Felici, A. Vidiri, A. Pace, E. Occhipinti, F. Cognetti, G. Arcangeli, B. Iandolo, M.A. Carosi, G. Metro, C.M. Carapella, Fixed dose-rate gemcitabine as radiosensitizer for newly diagnosed glioblastoma: a dose-finding study, J Neurooncol, 87 (2008) 79-84.
[70] G. Metro, A. Fabi, M.A. Mirri, A. Vidiri, A. Pace, M. Carosi, M. Russillo, M. Maschio, D. Giannarelli, D. Pellegrini, A. Pompili, F. Cognetti, C.M. Carapella, Phase II study of fixed dose rate gemcitabine as radiosensitizer for newly diagnosed glioblastoma multiforme, Cancer Chemother Pharmacol, 65 (2010) 391-397.
[71] W. Wick, M. Hermisson, R.D. Kortmann, W.M. Kuker, F. Duffner, J. Dichgans, M. Bamberg, M. Weller, Neoadjuvant gemcitabine/treosulfan chemotherapy for newly diagnosed glioblastoma: a phase II study, J Neurooncol, 59 (2002) 151-155.
[72] Shimizu, Routes of administration, in: H.J. Hedrich (Ed.) The Laboratory Mouse (Handbook of Experimental Animals) Elsevier, 2004, pp. 527-541.
[73] E. Fournier, C. Passirani, C.N. Montero-Menei, J.P. Benoit, Biocompatibility of implantable synthetic polymeric drug carriers: focus on brain biocompatibility, Biomaterials, 24 (2003) 3311-3331.
[74] D. Ito, Y. Imai, K. Ohsawa, K. Nakajima, Y. Fukuuchi, S. Kohsaka, Microglia-specific localisation of a novel calcium binding protein, Iba1, Brain Res Mol Brain Res, 57 (1998) 1-9.
[75] K.B. Bjugstad, K. Lampe, D.S. Kern, M. Mahoney, Biocompatibility of poly(ethylene glycol)-based hydrogels in the brain: an analysis of the glial response across space and time, J Biomed Mater Res A, 95 (2010) 79-91.
[76] M.T. Giordana, A. Attanasio, P. Cavalla, A. Migheli, M.C. Vigliani, D. Schiffer, Reactive cell proliferation and microglia following injury to the rat brain, Neuropathology and applied neurobiology, 20 (1994) 163-174.

6. SUPPLEMENTARY MATERIALS

6.1. COMPOSITION OF ARTIFICIAL CEREBROSPINAL FLUID

To prepare 500 mL of artificial cerebrospinal fluid, Sodium Chloride (3.07 g), Potassium Chloride (0.11 g; VWR Chemicals, Belgium), Magnesium Chloride (0.22 g; Sigma-Aldrich, USA), Calcium Chloride (0.13 g; Sigma-Aldrich, China), Sodium Carbonate (3 g; Merck, Germany), Disodium hydrogen phosphate dehydrate (0.03 g; Merck, Germany), D-glucose (0.30 g; Sigma-Aldrich, USA), L-Ascorbic acid (0.1 g; Sigma-Aldrich, China) and Bovine Serum Albumin (0.15 g; Sigma-Aldrich, USA) were weighed. MilliQ water was added and pH was adjusted to 7.35 ± 0.05 with concentrated Hydrochloric acid (VWR Chemicals, France).

CHAPTER IV.

DEVELOPMENT OF A SURGICAL GLIOBLASTOMA RESECTION PROCEDURE IN MICE

Adapted from:

Bastiancich C*, Bianco J*, Joudiou N, Gallez B, des Rieux A, Danhier F. Novel model of orthotopic U-87 MG glioblastoma resection in athymic nude mice. *J Neuroscience Methods* 284:96-102 (2017).

ABSTRACT

In vitro and in vivo models of experimental glioma are useful tools to gain a better understanding of glioblastoma (GBM) and to investigate novel treatment strategies. However, the majority of preclinical models focus on treating solid intracranial tumours, despite surgical resection being the mainstay in the standard care of patients with GBM today. The lack of resection and recurrence models therefore has undermined efforts in finding a treatment for this disease. Here we present a novel orthotopic tumour resection and recurrence model that has potential for the investigation of local delivery strategies in the treatment of GBM. The model presented is simple to achieve through the use of a biopsy punch, is reproducible, does not require specific or expensive equipment, and results in a resection cavity suitable for local drug delivery systems, such as the implantation or injection of hydrogels. We show that tumour resection is well tolerated, does not induce deleterious neurological deficits, and significantly prolongs survival of mice bearing U-87 MG GBM tumours. In addition, the resulting cavity could accommodate adequate amounts of hydrogels for local delivery of chemotherapeutic agents to eliminate residual tumour cells that can induce tumour recurrence.

KEYWORDS

Glioblastoma, tumour, resection, recurrence, local drug delivery

TABLE OF CONTENTS

1. INTRODUCTION

Glioblastoma (GBM) is the most common and aggressive malignant tumour of the central nervous system in adults. These tumours show a high proliferation rate with diffuse infiltration of adjacent brain tissue [1]. Conventional therapeutic procedures, aiming at increasing patient life expectancy, focus on maximal surgical resection combined with adjuvant radiotherapy and/or chemotherapy by oral delivery of Temozolomide (TMZ) [2]. However, tumour recurrences due to residual infiltrative cells at the resection margin are inevitable, leading to a median survival of about 14 months, with a 5 year-life expectancy of less than 10% [3]. In consequence, there is a much unmet medical need that necessitates solving. Innovative drug delivery systems aiming at delivering drugs to the tumour site present a promising approach in treating this disease [4]. The local drug delivery of cytotoxic agents, using injectable systems in the tumour resection cavity with sustained drug release characteristics, aims at preventing the growth of cancer cells that cannot be resected during surgery.

Local delivery seems very promising for the treatment of GBM for a number of reasons. One is that it allows for bypassing the blood brain barrier through direct administration of a drug into the brain. Another is that sustained drug release, reaching therapeutic concentrations at the tumour site without involving other organs, can be obtained [4]. The rationale for the use of local delivery strategies in GBM treatment has been highlighted by approval of Gliadel® by the FDA. However, due to some conflicting results being obtained with the use of Gliadel®, and limitations in current treatment options available, novel avenues of treating GBM through local drug delivery strategies need to be investigated [5, 6].

To evaluate the efficacy of these drug delivery systems on GBM recurrence, a clinically relevant tumour resection model is needed. Despite many preclinical studies, most *in vivo* GBM models do not mimic the clinical scenario of surgical debulking and instead focus on treating solid intact intracranial tumours. Therefore, in light of the central role of tumour resection in clinical therapy, development of rodent models of GBM resection and recurrence are a necessity [7], and indeed, several models do currently exist. Akbar and colleagues were the first to perform an intracranial resection in a rat model of C6–green

fluorescent protein intracranial glioma model. Through the use of a fluorescent dissecting microscope, they were able to detect the tumour and subsequently guide a suction tip that allowed for the precise microsurgical resection of the tumour [8]. This method was also reproduced in nude rats by Denbo and colleagues [9], while Kauer and colleagues further modified it to develop an efficient GBM subtotal resection model in nude mice [7]. A simplified technique, using mere aspiration for 5 seconds to remove a GBM tumour in rats, has also been reported, although it was found less effective in completely or efficiently resecting the tumour tissue, with no difference in survival observed between resected and control animals [10]. Nevertheless, the drawback of these techniques is the need of specific or expensive equipment that are not always available.

To provide a clinically relevant model for studying GBM treatments, we developed a novel approach for resection of U-87 MG mouse intracranial GBM in a validated and reproducible manner, using a biopsy punch. The advantages that our resection technique provides include simplicity, reproducibility, and the lack of necessity for any specific or expensive equipment.

2. MATERIALS AND METHODS

2.1. ANIMALS

All experiments were conducted on six week old, female, specific opportunistic pathogen-free (SPOF) NMRI nude mice (Janvier, France) in accordance with Belgian national regulation guidelines as well as with EU Directive 2010/63/EU. All experiments were approved by the ethical committee of the Université catholique de Louvain (2014/UCL/MD/004). Mice were maintained on standard laboratory food and water *ad libitum*, with a 12 hour artificial light/dark cycle.

2.2. CELL CULTURE

U-87 MG glioma cells (ATTC, USA) were cultured in Eagle's Minimum Essential Medium (EMEM; ATTC, USA), supplemented with 10% foetal bovine serum (Gibco, USA), 100 U/mL penicillin and 100 µg/mL streptomycin (Gibco, USA). Cells were cultured as monolayers in 75 cm^2 culture flasks (Sigma, USA) and maintained at 37°C/5% CO_2.

2.3. ORTHOTOPIC U-87 MG HUMAN GLIOBLASTOMA TUMOUR MODEL

For the intracranial glioma model, animals were anesthetised by intraperitoneal injection of ketamine/xylazine (100 and 13 mg/kg, respectively) and positioned in a stereotactic frame. Once immobile, an incision 5 mm long was made along the midline. A burr hole was drilled into the skull at the right frontal lobe, 0.5 mm posterior and 2.1 mm lateral to the bregma using a high-speed drill (Dremel Inc., USA). A 5 µL Hamilton syringe fitted with a 26 gauge needle was used to inject 2.5 µL of complete culture medium containing 3 x 10^4 U-87 MG glioma cells at the junction between the cortex and striatum at a depth of 2.5 – 3.0 mm from the outer border of the cranium over a five minute period. After injection, the needle was kept in place for 5 minutes before slowly being extracted to prevent a vacuum and cell build-up into the needle track. The wound was then sutured and the animals were allowed to awaken under an infrared heating lamp [11]. No post-surgery analgesics were administered following the procedure. Animals awoke and were active between 1 and 2 hours following surgery and did not display any signs of distress. The presence, volume and localisation of

tumours was determined by Magnetic Resonance Imaging (MRI) between day 9 and 12 post inoculation of the U-87 MG cells. Animals were killed when they presented ≥ 20% body weight loss or 10% body weight loss plus clinical signs of distress (paralysis, arched back, lack of movement).

2.4. MAGNETIC RESONANCE IMAGING

MRI was performed using a 11.7 T Bruker Biospec MRI system (Bruker, Germany) equipped with a 1 H quadrature transmit/receive surface cryoprobe after anesthetising animals with 1% isoflurane mixed with air (2.5% for induction, 1% for maintenance). Respiration was continuously monitored while animal core temperature was maintained throughout the experiment by hot water circulation in the cradle. Tumour volume was assessed using rapid acquisition with relaxation enhancement (RARE) sequence (TR = 2500 ms; effective echo time (TE_{eff}) = 30 ms; RARE factor = 8; FOV = 2 x 2 cm; matrix 256 x 256; twenty-five contiguous slices of 0.3 mm, $N_{average}$ = 4). Volumes were calculated from manually drawn region of interest (ROI).

2.5. BIOPSY PUNCH RESECTION OF TUMOUR MASS

On the 13th day post-inoculation of the tumour, mice were randomly assigned into control (no resection, no treatment) or resection (resection, no treatment) groups (*n* = 11 in each group). For intracranial glioma resection, animals were anaesthetised with ketamine/xylazine as described above before being immobilised in a stereotactic frame. A 7 mm incision was made in the midline along the previous surgical scar. The periosteum was removed revealing the bregma and previous burr hole. A high-speed drill was used to thin the skull area centred around the burr hole, after which fine tip tweezers (Dumont, Switzerland) were used to obtain a 2.1 diameter circular cranial window exposing the brain. A biopsy punch (7 mm long, 2 mm Ø, Kai Medical, Germany) was limited to and inserted 3 mm deep and twisted for 15 seconds to cut the brain/tumour tissue. Once withdrawn, a Pasteur pipette connected to a diaphragm vacuum pump (Vaccubrand GMBH + CO KG, Germany) was used to remove the explant and blood build up. Residual blood was removed by allowing an absorbable haemostatic triangle (Fine Science Tools, Germany) to rest in the formed cavity. Once stabilised, the dural window was repaired by covering with a 4 mm x 4

mm square piece of Neuro-Patch® (Aesculap, Germany) impregnated with a reconstituted fibrin hydrogel (25 mg/mL fibrin, 10 IU/mL thrombin, equal volumes; Baxter Innovations, Austria). The wound was closed with 3-0 Vicryl sutures and the animals allowed to recover. No post-surgery analgesics were administered following the procedure. Animals awoke and were active between 1 and 2 hours following surgery and did not display any signs of distress. Each step of the biopsy punch resection procedure is outlined in Figure 1. Weight and behaviour were monitored over time as described above. To evaluate tumour growth and the efficacy of tumour resection, at least 3 mice were sacrificed at day 13 before and after resection. Once experimental endpoints of survival had been reached, the brains were extracted and fixed in 10% formalin solution (Merck, Germany) overnight. The brains were then rinsed in PBS, cryoprotected with 30% sucrose solution for 24 hours, snap frozen and stored at -20^{o}C until analysed.

2.6. HISTOLOGICAL ANALYSIS OF RECURRENT TUMOURS

Brains were sectioned at 12 µm using a Leica CM 1950 cryostat (Leica Biosystems Nussloch GmbH, Germany) and stored at -20^{o}C until used. For histological analysis, slides were allowed to dry at room temperature overnight before being subjected to haematoxylin & eosin (H&E) staining or immunofluorescence. For H&E staining, samples were processed using a Sakura DRS 601 automated slide stainer (Sakura Finetek Europe, The Netherlands). For immunofluorescence, brain sections were rehydrated and blocked for 1 hour at room temperature in a blocking solution consisting of 10% normal goat serum, 2% bovine serum albumin, and 0.01% Triton X-100 in PBS. A rabbit polyclonal anti-Glial fibrillary acidic protein (GFAP) (1:800 in blocking solution, Abcam, UK) antibody was used to identify normal brain tissue, while a mouse monoclonal anti-human mitochondria (1:800 in blocking solution, Abcam, UK) antibody was used to identify U-87 MG cells by incubation for 1 hour at room temperature. Sections were then rinsed with PBS (3 x 5 minute washes) after which Alexafluor antihost IgG antibodies (1:400 in PBS containing 0.5% bovine serum albumin, Invitrogen, USA) were applied for 1 hour at room temperature and away from light. Sections were rinsed again with PBS (3 x 5 minute washes) before cell nuclei were counterstained through staining with DAPI (1µM in PBS, Sigma, USA) for 10 minutes and away from light following the secondary antibodies. Sections were mounted with Vectashield hard set

mounting medium (without DAPI, Vector Laboratories) and stored away from light until analysed. Digital images were acquired using an EVOS fluorescent microscope. For survival, statistical significance was analysed using the Wilcoxon test in GraphPad Prism (GraphPad Software, USA) and determined based on $p < 0.05$. Images were processed using Adobe Photoshop.

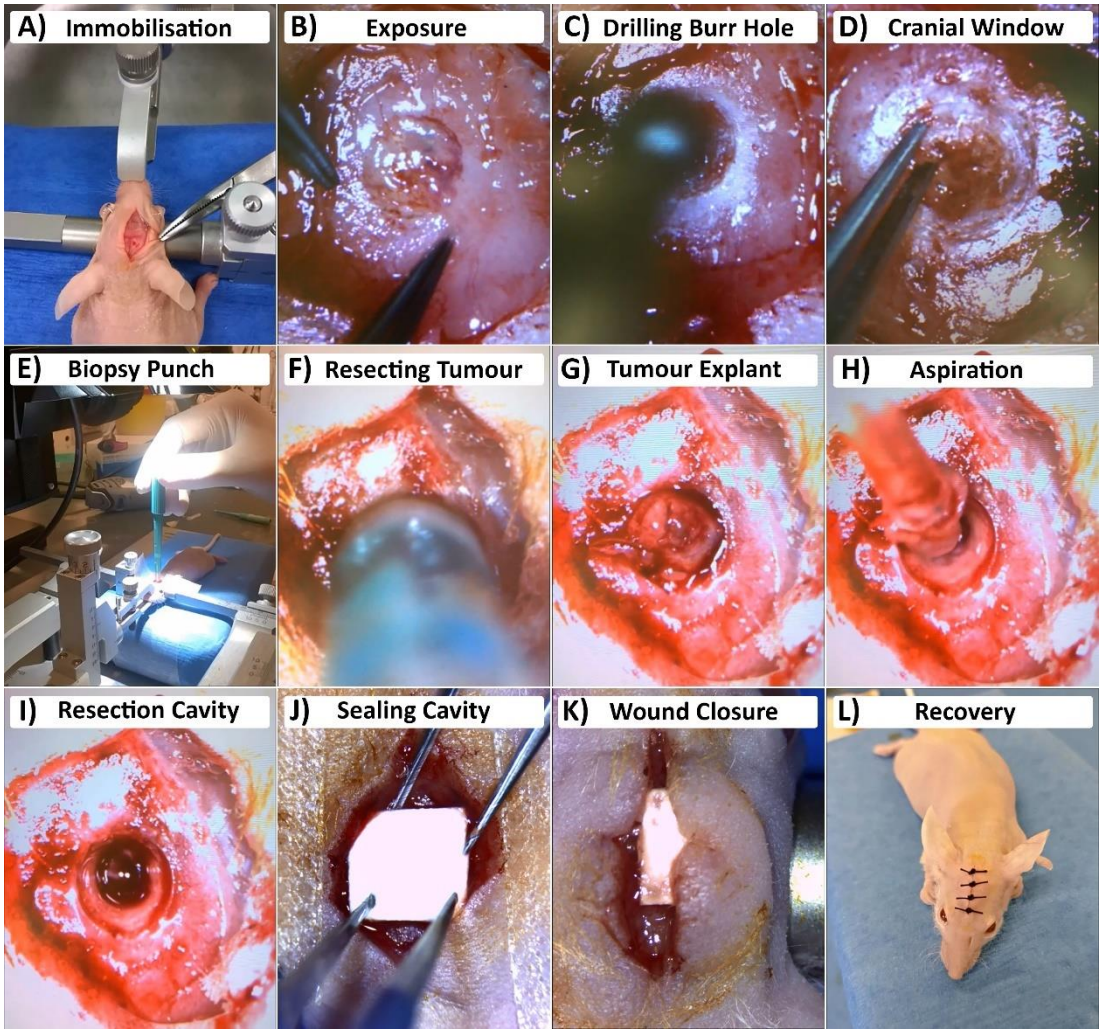

Figure 1: Orthotopic U-87 MG tumour resection using a 2 mm biopsy punch. **A:** Immobilised mouse on a stereotactic frame; **B:** Previous burr hole; **C:** Drill-assisted widening of previous burr hole; **D:** Manually expanding cranial window to a 2.1 mm diameter; **E:** Insertion of biopsy punch, 3 mm deep; **F:** Resection by twisting for 15 seconds; **G:** Tumour explant; **H:** Aspiration of resected tumour tissue; **I:** Resection cavity; **J:** Sealing of cavity with Neuro-Patch®; **K:** Wound closure; **L:** Sutured mouse, recovering.

3. RESULTS

3.1. TUMOUR IMPLANTATION

A modification of a previously described U-87 MG cell inoculation protocol to induce tumours in nude mice was used in this study [11]. MRI analysis of tumours at different time points after cell implantation showed that developing tumours had volumes of 0.2 ± 0.1 µl at day 9, and 0.4 ± 0.2 µl at day 13 (*n* = 11), with a median survival of 24 days being observed in animals in which tumour development was left unhindered. Considering these results, we determined that the optimal day for resection using a 2 mm biopsy punch was 13 days post inoculation. Before day 13, tumours were considered inadequate in size, therefore all tumour tissue could be removed, resulting in tumour recurrences not being visualised. Beyond day 13, the exponential development of tumours resulted in overgrowth that could not be excised adequately, leaving the majority of tumour intact following resection (Figure 2).

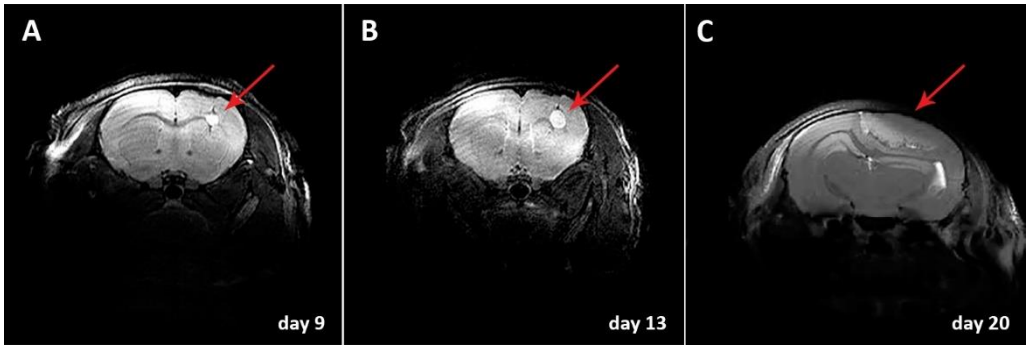

Figure 2: Coronal (T_2-weighted) images of U-87 MG tumours obtained through MRI that monitor tumour growth at day 9 (**A**), day 13 (**B**), and day 20 (**C**) post implantation. Lighter zones indicated by red arrows show tumour location within the brain high in the right striatum and lower cortex of U-87 MG inoculated mice.

3.2. TUMOUR RESECTION USING A BIOPSY PUNCH

The biopsy resection procedure can be fully completed within 25 – 30 minutes per animal. The two main difficulties that could arise during this procedure are swelling of the brain parenchyma, restricting cavity size and formation, and excessive bleeding. Swelling is the brain parenchyma, thus potentially constricting the formed cavity, occurred to varied degrees in all animals undergoing the procedure. Tumour location, and in particular the

presence of large blood vessels usually abated within 2 – 3 minutes following resection. No hemiplegia was observed due to the resection procedure.

3.3. VISUALISATION OF CAVITY POST RESECTION

Following resection, a number of animals were immediately sacrificed to observe cavity formation. We observed that a cavity with clearly defined borders forms (Figure 3A). The theoretical volume of the cavity, when using a 2 mm biopsy punch, equals to 9.42 µL. Once bleeding was abated, 5 µL of liquid or gel could fit adequately within the freshly formed cavity (not shown). Analysis of cryosectioned brains bearing a cavity also confirmed the formation of defined borders and resection volume (Figure 3B). Animals that had undergone resection were also imaged using MRI 7 days after resection (Figure 3C, D). Scans showed that the cavity remained intact, and could be distinguished at 1 week post resection. MRI scans also revealed that fluid accumulation within the cavity can occur in some animals (hypersignal in T_2-weighted image, Figure 3D), although they did not reveal when they commence or if the fluid diffuses back into the surrounding parenchyma. Nevertheless, the presence of fluid did not influence survival or behaviour of the animals, and most importantly, did not influence recurrence.

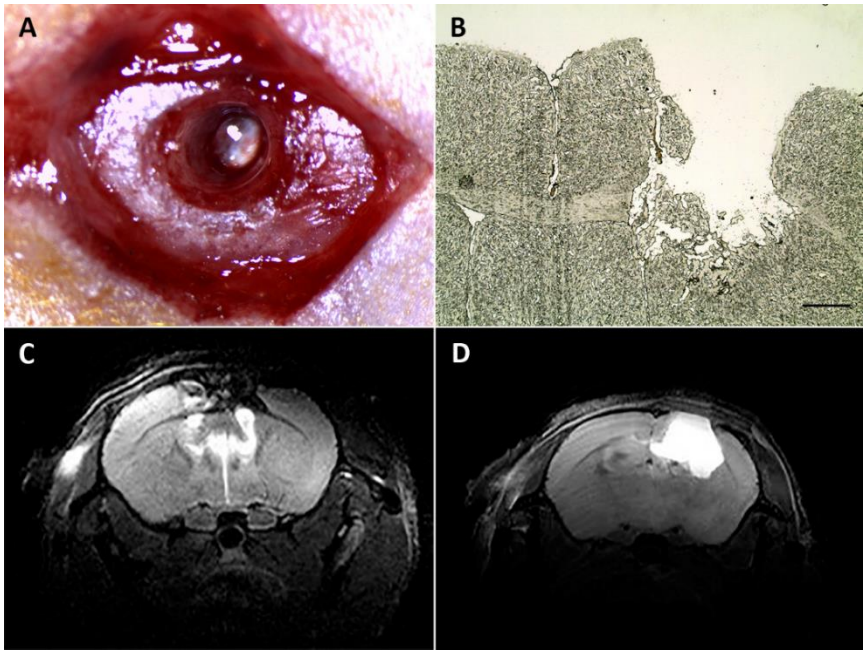

Figure 3: A: Cavity, immediately post-resection and cleared of blood, showing a defined edge; **B:** Cryosectioned brain immediately following resection; **C:** MRI scan following resection at day 7 showing the extent of tissue removal; **D:** MRI scan at day 7 post resection, showing fluid build-up within the resection cavity, indicated by the hypersignal. Scale bar in B = 400 µm

3.4. SURVIVAL FOLLOWING U-87 MG TUMOUR RESECTION

A Kaplan-Meier survival curve showed a significant increase in survival (p = 0.0021) of mice that had undergone biopsy punch resection (median survival 36 days) to those mice not receiving surgical resection (median survival 24 days) following U-87 MG inoculation and tumour formation (Figure 4). Resection did not result in any observable side effects or deficits in neurological function. Once recurrence had taken hold, the health of the animals deteriorated rapidly to include marked weight loss, hunching of the back, disorientation, ultimately resulting in death or sacrifice. Paralysis was observed in a number of mice early during the recurrence growth of the tumour.

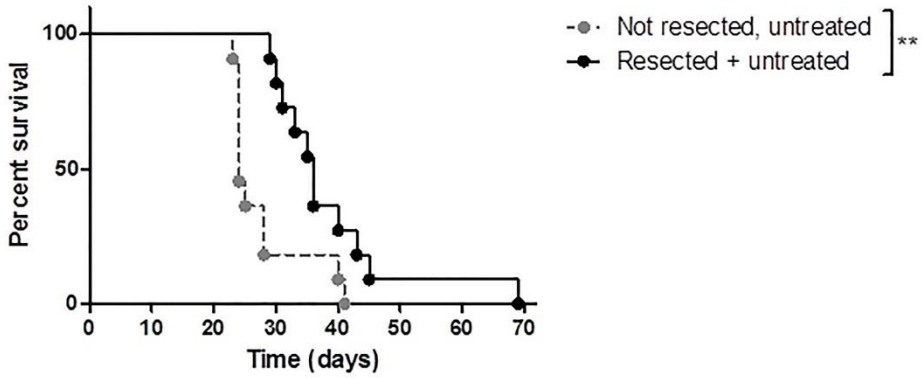

Figure 4: Kaplan-Meier survival curve for resected, untreated animals and non-resected, untreated animals (n = 11 for both groups).

3.5. VISUALISATION OF TUMOUR RECURRENCE

After inoculation with U-87 MG cells, and following 13 days of growth, a thickened and vascularised periosteum could be observed above and around the original burr hole. Upon creation of the cranial window, the majority of animals presented a vascularised growth centred on the injection site that corresponded to the underlying tumour (Figure 5A). A biopsy punch, limited to 3 mm in length with surgical tape (Figure 5B) was then centred above the tumour and used to make the resection cavity. Tumour recurrence, observed in all resected animals, was robust and aggressive, often extending from the resection cavity borders into other brain regions through growth and compression of healthy brain tissue (Figure 5C, D).

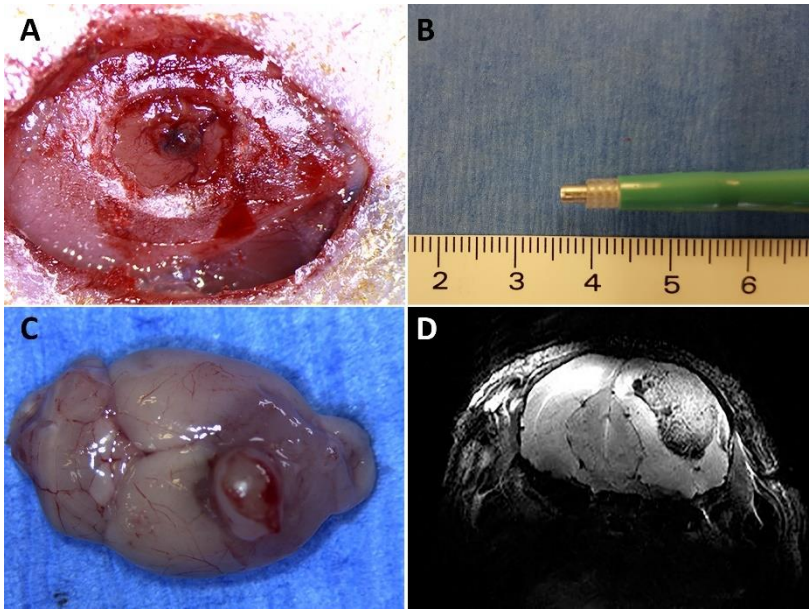

Figure 5: A: A cranial window at 13 days post inoculation. The dark, blood vessel rich central area corresponds to the tumour; **B:** A disposable 2 mm Ø biopsy punch limited to 3 mm in length used for tumour resection; **C:** Tumour recurrence at day 36; **D:** MRI scan showing the extent of recurrence at 31 days post resection.

3.6. HISTOLOGICAL EVALUATION OF U-87 MG ORTHOTOPIC TUMOUR AND RESECTION

H&E and immunofluorescence were used to further confirm the efficiency of resection using a biopsy punch (Figure 6). As U-87 MG tumours lack glial fibrillary acidic protein (GFAP) immunoreactivity, an anti-GFAP antibody was used to distinguish normal brain tissue versus cancerous tissue. The human origin of U-87 MG allowed for the use of an anti-human mitochondria antibody to identify cancerous growth. A clear and distinct border could be seen between normal and cancerous tissue (Figure 6A-C). It is clearly seen that GFAP positive cells are only present in normal brain tissue. Although some auto-fluorescence of the brain tissue is present, human mitochondria stained cells can be seen within the GFAP negative tumour. Cancerous tissue was shown to exhibit distinctly different morphology and density to normal mouse brain tissue, showing profuse human mitochondria staining, while being negative to GFAP (Figure 6D-F). H&E staining did not show presence of tumour at or around the resection site (Figure 6G). Even though U-87 MG is not an invasive cell type [12], sparse staining of anti-human mitochondria cells could be observed at the resection border (Figure 6H), although GFAP staining was abundant (Figure 6I). It could be implied that, even though not invasive, enough U-87 MG cells were left unresected following our resection to induce tumour recurrence in our model.

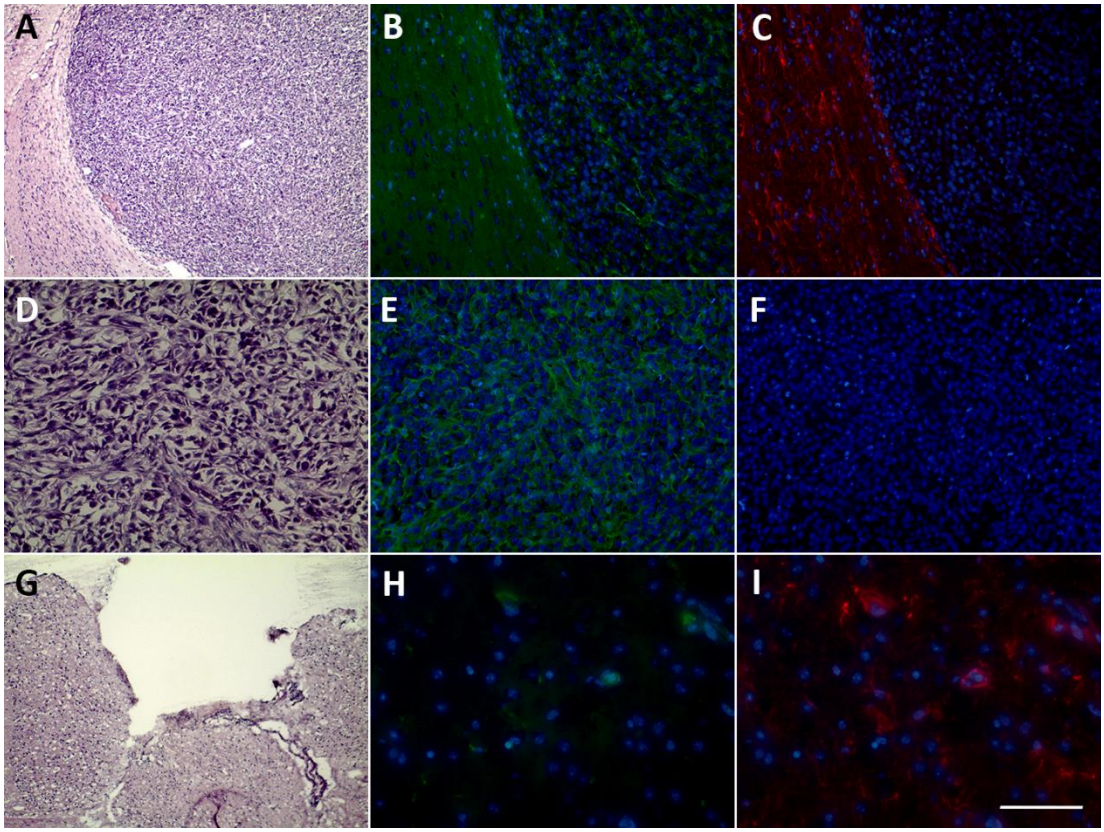

Figure 6: A: H&E staining showing a recurred tumour and the distinct border between cancerous and normal tissue; **B:** Anti-human mitochondria staining of U-87 MG cells within the tumour tissue; **C:** Anti-GFAP staining showing normal brain parenchyma next to the tumour mass; **D:** H&E staining of within the recurred tumour mass; **E:** Anti-human mitochondria staining within the recurred tumour mass; **F:** No GFAP staining observed within the tumour mass; **G:** H&E staining of resected tumour; **H:** Anti-human mitochondria staining of tissue bordering resection cavity; **I:** Anti-GFAP staining of tissue bordering resection cavity. Scale bar: A, G = 400 µm; B, C, E, F = 200 µm; D, H, I = 100 µm.

4. DISCUSSION

Aggressive surgical resection is an important factor for improved outcomes when treating gliomas. Increased volumetric extent of resection has been directly correlated with improved survival in low as well as in high grade gliomas such as GBM [13-15]. To this day, surgical resection remains as the main component in treating GBM. However, the focus of most preclinical models is on treating established tumours, with only a limited number of animal models currently available that focus on resecting tumours. In view of this shortage, we developed a novel, simplified and reproducible intracranial resection mouse model. Even though we used the non-invasive U-87 MG cell for tumour formation, the purpose of this study was to develop a resection and recurrence model that could be implemented in varying treatment modalities for GBM. For example, the resulting resection cavity will allow us to investigate novel treatment strategies based on local delivery of bioactive molecules. One strategy that has shown potential in treating GBM is the use of hydrogels for local delivery of anti-cancer agents, permitted by their unique properties. Because hydrogels have a hydrophilic but cross-linked structure, they are able to absorb large amounts of water or biological fluid without the dissolution of the polymer [16]. Following surgery, drug-loaded hydrogels could be administered directly into the brain, either within the tumour or following resection [4], overcoming technical issues such as the limitations of the blood brain barrier.

It has previously been established that GBM recurs within 2 cm of the resected tumour site in 90% of cases [17]. Our resection model, although not invasive, is subtotal and thus leads to tumour occurrence. We chose to resect at day 13 post inoculation, and observed a median post resection survival of 23 days. If a strategy using bioactive molecules would be investigated, this survival period provides ample time to assess the effects of anticancer drugs in eliminating tumour cells that have remained after resection, in turn delaying tumour recurrence. As mentioned above, U-87 MG cells do not infiltrate deep into the brain after inoculation. However, our model could also be applied to other xenograft models that could mimic a wider range of clinical hallmarks associated with GBM, including brain invasion.

All mice that had a confirmed tumour at day 13, as seen by MRI, achieved 100% recurrence following resection. Given that surgery in GBM patients is clearly beneficial with its primary goal of maximising the extent of resection while minimising injury, mortality and morbidity was not observed in our model during the biopsy punch resection procedure. A few mice died shortly after inoculation with U-87 MG cells within the brain, while one mouse was sacrificed (at day 55 post resection) due to a cutaneous infection not related to the inoculation or resection. Overall, the resection and recurrence model we have developed was well tolerated, and could serve as a template for future studies investigating treatment options for GBM.

5. CONCLUSIONS

We have established a reproducible surgical resection and recurrence mouse model of GBM devoid of injurious neurological outcomes following surgery. This model has applications in investigating intracavity mediated distribution of bioactive materials for local delivery of anticancer agents in the treatment of GBM in a pre-clinical model.

6. REFERENCES

[1] A. Bernardi, E. Braganhol, E. Jäger, F. Figueiró, M. Edelweiss, A. Pohlmann, S. Guterres, A. Battastini, Indomethacin-loaded nanocapsules treatment reduces in vivo glioblastoma growth in a rat glioma model, Cancer Lett, 281 (2009) 53-63.

[2] R. Stupp, W. Mason, M. van den Bent, M. Weller, B. Fisher, M. Taphoorn, K. Belanger, A. Brandes, C. Marosi, U. Bogdahn, J. Curschmann, R. Janzer, S. Ludwin, T. Gorlia, A. Allgeier, D. Lacombe, J. Cairncross, E. Eisenhauer, R. Mirimanoff, E.O.f.R.a.T.o.C.B.T.a.R. Groups, N.C.I.o.C.C.T. Group, Radiotherapy plus concomitant and adjuvant temozolomide for glioblastoma, N Eng J Med, 352 (2005) 987-996.

[3] F. Lefranc, N. Sadeghi, I. Camby, T. Metens, O. Dewitte, R. Kiss, Present and potential future issues in glioblastoma treatmen, Expert Rev Anticancer Ther, 6 (2006) 719-732.

[4] C. Bastiancich, P. Danhier, V. Préat, F. Danhier, Anticancer drug-loaded hydrogels as drug delivery systems for the local treatment of glioblastoma, J Control Release, 243 (2016) 29-42.

[5] H. Bock, M. Puchner, F. Lohmann, M. Schütze, S. Koll, R. Ketter, R. Buchalla, N. Rainov, S. Kantelhardt, V. Rohde, A. Giese, First-line treatment of malignant glioma with carmustine implants followed by concomitant radiochemotherapy: a multicenter experience, Neurosurg Rev, 33 (2010) 441-449.

[6] L. Ashby, K. Smith, B. Stea, Gliadel wafer implantation combined with standard radiotherapy and concurrent followed by adjuvant temozolomide for treatment of newly diagnosed high-grade glioma: a systematic literature review, World J Surg Oncol, 14 (2016) 225.

[7] T. Kauer, J. Figueiredo, S. Hingtgen, K. Shah, Encapsulated therapeutic stem cells implanted in the tumor resection cavity induce cell death in gliomas, Nat Neurosci, 15 (2011) 197-214.

[8] U. Akbar, T. Jones, J. Winestone, M. Michael, A. Shukla, Y. Sun, C. Duntsch, Delivery of temozolomide to the tumor bed via biodegradable gel matrices in a novel model of intracranial glioma with resection, J Neurooncol, 94 (2009) 203-212.

[9] J. Denbo, R. Williams, W. Orr, T. Sims, C. Ng, J. Zhou, Y. Spence, C. Morton, A. Nathwani, C. Duntsch, L. Pfeffer, A. Davidoff, Continuous local delivery of interferon-β stabilizes tumor vasculature in an orthotopic glioblastoma xenograft resection model, Surgery, 150 (2011) 497-504.

[10] T. Ozeki, D. Kaneko, K. Hashizawa, Y. Imai, T. Tagami, H. Okada, Combination therapy of surgical tumor resection with implantation of a hydrogel containing camptothecin-loaded poly(lactic-co-glycolic acid) microspheres in a C6 rat glioma model, Biol Pharm Bull, 35 (2012) 545-550.

[11] F. Danhier, K. Messaoudi, L. Lemaire, J. Benoit, F. Lagarce, Combined anti-Galectin-1 and anti-EGFR siRNA-loaded chitosan-lipid nanocapsules decrease temozolomide resistance in glioblastoma: in vivo evaluation, Int J Pharm, 481 (2015) 154-161.

[12] V. Jacobs, P. Valdes, W. Hickey, J. De Leo, Current review of in vivo GBM rodent models: emphasis on the CNS-1 tumour model, ASN Neuro, 3 (2011) e00063.

[13] K. Chaichana, I. Jusue-Torres, R. Navarro-Ramirez, S. Raza, M. Pascual-Gallego, A. Ibrahim, M. Hernandez-Hermann, L. Gomez, X. Ye, J. Weingart, A. Olivi, J. Blakeley, G. Gallia, M. Lim, H. Brem, A. Quinones-Hinojosa, Establishing percent resection and residual volume thresholds affecting survival and recurrence for patients with newly diagnosed intracranial glioblastoma, Neuro Oncol, 16 (2014) 113-122.

[14] A. Fukui, Y. Muragaki, T. Saito, T. Maruyama, M. Nitta, S. Ikuta, T. Kawamata, Volumetric analysis using low-field intraoperative magnetic resonance imaging for 168 newly diagnosed supratentorial glioblastomas: effects of extent of resection and residual tumor volume on survival and recurrence, World Neurosurg, 98 (2016) 73-80.

[15] N. Sanai, M. Polley, M. McDermott, A. Parsa, M. Berger, An extent of resection threshold for newly diagnosed glioblastomas, J Neurosurg, 115 (2011) 3-8.

[16] T. Hoare, D. Kohane, Hydrogels in drug delivery: Progress and challenges, Polymer, 49 (2008) 1993-2007.

[17] F. Hochberg, A. Pruitt, Assumptions in the radiotherapy of glioblastoma, Neurology, 30 (1980) 907-911.

CHAPTER V.

LAUROYL-GEMCITABINE LOADED LIPID NANOCAPSULE HYDROGEL FOR THE TREATMENT OF GLIOBLASTOMA: LONG-TERM EFFICACY AND TOLERABILITY

Adapted from:

Bastiancich C, Bianco J, Vanvarenberg K, Ucakar B, Joudiou N, Gallez B, Bastiat G, Lagarce F, Préat V, Danhier F. Injectable nanomedicine hydrogel for local chemotherapy of glioblastoma after surgical resection. *J Controlled Release* 264: 45-54 (2017).

ABSTRACT

Glioblastoma (GBM) treatment includes, when possible, surgical resection of the tumor followed by radiotherapy and oral chemotherapy with temozolomide, however recurrences quickly develop around the resection cavity borders leading to patient death. We hypothesize that the local delivery of lauroyl-gemcitabine lipid nanocapsule based hydrogel ($GemC_{12}$-LNC) in the tumor resection cavity of GBM is a promising strategy as it would allow to bypass the blood brain barrier, thus reaching high local concentrations of the drug. The cytotoxicity and internalization pathways of $GemC_{12}$-LNC were studied on different GBM cell lines (U251, T98-G, 9L-LacZ, U-87 MG). The $GemC_{12}$-LNC hydrogel was well tolerated when injected in mouse brain. In an orthotopic xenograft model, after intratumoral administration, $GemC_{12}$-LNC significantly increased mice survival compared to the controls. Moreover, its ability to delay tumor recurrences was demonstrated after perisurgical administration in the resection cavity of the GBM. In conclusion, we demonstrate that $GemC_{12}$-LNC hydrogel could be considered as a promising tool for the post-resection management of GBM, prior to the standard of care chemo-radiation.

KEYWORDS

Lipid nanocapsules, Gemcitabine, Hydrogel, Nanomedicine, Glioblastoma, Local delivery

TABLE OF CONTENTS

1. INTRODUCTION

Glioblastoma (GBM) is the most aggressive and lethal brain tumor in adults. It is a grade IV astrocytoma characterized by rapid proliferation, high infiltration capacity, chemoresistance and ability to quickly form recurrences, even after multiple surgery and treatment [1]. GBM can be divided into IDH-wildtype GBM (90%) which arises in an acute de novo manner without previous lower grade pathology or symptoms, or into IDH-mutant GBM (10%) which derives from the progressive evolution and transformation of lower grade astrocytomas and normally affects younger patients [2]. In both cases, maximal safe surgical resection of the accessible primary tumor is the first and most important step in the management of these tumors, but it can only be applied to 65-75 % of GBM patients [3, 4]. Following resection, GBM patients are generally treated with standard treatment regimens which include radiotherapy plus concomitant and adjuvant oral chemotherapy with the alkylating agent Temozolomide (TMZ) [5]. However, recurrences develop at the resection border margins (90% of cases) or in other regions of the brain within two years leading, in most of the cases, to death [6, 7]. Indeed, despite the efforts of the scientific community, the prognosis for GBM patients remains poor (median survival <15 months), 2- and 4- year survival rates are 27% and 10% respectively and the long-term survivors are nearly inexistent [8, 9].

Limitations in the effectiveness of current standard of care treatments are amplified through the formation of GBM recurrences due to several hurdles. The anatomical location of the tumor interferes with a complete surgical resection while the presence of the blood-brain barrier (BBB) limits the number of cytotoxic drugs that can effectively reach the tumor site at therapeutic concentrations. In addition, GBM cells widely diffuse into the brain parenchyma, and their tendrils are often undetectable by imaging techniques. Moreover, cancer stem cells with high tumorigenic ability, self-renewal potential and strong resistance to radio and chemotherapy have been recognized in gliomas [10-13]. As chemoradiation can have an impact on the wound healing process, GBM patients generally follow the standard radio- and chemotherapy regimen several weeks after surgery, once the wound has healed [14]. During this time gap, the residual tumor cells can proliferate around the resection cavity borders. Further difficulties in treatment are brought about by the high heterogeneity of GBM cells

combined to their innate and acquired chemoresistance, reducing the efficacy of TMZ. Indeed, only one third of GBM patients are responsive to alkylating agents [13, 15, 16].

In the last decades, many strategies have been adopted to increase the therapeutic efficacy and survival rate of GBM patients (e.g. gene therapy, immunotherapy, targeted therapy, nanomedicines, ultrasounds, etc) [17-22]. Among them, the local delivery of chemotherapeutic drugs in the tumor resection cavity has shown a promising role [23-25]. This approach aims at increasing the local concentrations of the drugs, subsiding systemic side effects, while also reducing the lapse of time between resection and the chemotherapy which in turn prevents the growth of the remaining cancer cells, often responsible of recurrences. Gliadel®, a carmustine-loaded biodegradable wafer, is the most-successful and the only local delivery implant currently approved by the FDA for GBM [26, 27]. Its use has shown modest effect in prolonging the overall survival of GBM patients but tumor recurrences have been reported in the majority of treated cases. To improve the sustained intracerebral drug release and overcome limitations such as local side effects, poor drug penetration depth and implant dislodgements, many researchers are currently focusing on the local delivery of cytotoxic drugs through different delivery systems (e.g. foams, films, membranes, hydrogels) [25, 28]. Our group is mainly focused on craniotomy-based drug delivery *via* anti-cancer loaded hydrogels [29, 30]. These injectable and adaptable systems can be implanted or injected into the resection cavity immediately after surgery and can guarantee a sustained release of the drug in the surrounding brain tissue over time. Some hydrogels are also administrable intratumorally in non-operable GBM tumors [31]. Several aspects need to be considered when developing an effective anticancer drug loaded hydrogel for the local treatment of GBM. Firstly, choosing a drug that does not interfere with the mechanisms of action or the chemoresistance pathways of TMZ, and could have radiosensitizing and/or synergic properties with the standard treatments is of importance. Secondly, the release profile of the drug from the hydrogel should be controlled and sustained over time. Finally, the system should be injectable, degradable and well tolerated. It should have mechanical properties compatible with the brain tissue and possibly adapt to the resection cavity and adhere to the brain parenchyma [25].

Recently, we proposed the use of an innovative hydrogel uniquely formed of lipid nanocapsules (LNC) and lauroyl-gemcitabine ($GemC_{12}$) for the local treatment of GBM [29].

This injectable nanomedicine hydrogel presents mechanical properties adapted for brain implantation and allows a sustained release of the drug over 1 month *in vitro*. *In vivo*, this system is well tolerated during one week in mouse brain and reduces tumor growth in a subcutaneous human GBM model, when compared to free drug.

In this paper, we hypothesize that $GemC_{12}$-LNC nanomedicine hydrogel could improve the GBM recurrences management when injected in the tumor resection cavity immediately after surgery. Therefore, (i) the *in vitro* cytotoxicity and cellular uptake, (ii) the *in vivo* mid- and long-term tolerability in mouse brain, and (iii) the antitumor efficacy of the after intratumoral injection in an orthotopic human xenograft GBM model and after local injection in the resection cavity in an orthotopic resection model were investigated.

2. MATERIALS AND METHODS

2.1. FORMULATION OF GEMC12 LIPID NANOCAPSULES HYDROGEL (GEMC12-LNC)

The gel formulation $GemC_{12}$-LNC was prepared using a phase-inversion method previously reported in the literature [32]. Briefly, 0.093 g of $GemC_{12}$ (synthesized as previously described [33]), 1.24 g of Labrafac® (Gattefosse, France) and 0.25 g of Span80® (Sigma-Aldrich, USA) were weighed and stirred in a water bath at 50°C with 200 µL of acetone (VWR Chemicals, Belgium) until complete dissolution of the drug. The acetone was then allowed to evaporate and 0.967 g of Kolliphor® (Sigma-Aldrich, Germany), 0.045 g of Sodium Chloride (VWR Chemicals, Belgium) and 1.02 g of injectable water (Braun, Germany) were added to the formulation. Three cycles of heating and cooling were performed under magnetic stirring (500 rpm) between 40 and 70°C. During the last cooling cycle, at the temperature corresponding to the phase-inversion zone, 2.12 g of injectable water was added and the formulation stirred for one more minute. The formulations were then inserted into insulin syringes (BD Micro-Fine™ needle 0.30 ml, Ø 30 G; Becton Dickinson, France) before the gelation process occurred, and stored at 4°C until further use. The unloaded LNC were obtained using the same method without adding the active compound. For the fluorescent-labeled LNC, 83.4 µl of the fluorescent DiD fluorophor (1,1'-Dioctadecyl-3,3,3',3'-Tetramethylindodicarbocyanine 4-Chlorobenzenesulfonate salt, Thermo Fischer Scientific, USA; 1 mg/ml solution in absolute ethanol), were added to the first step of the formulation process, which was then carried on as previously described protected from the light. All the formulations were obtained under aseptic conditions.

2.2. *IN VITRO* CELLULAR STUDIES

U251, T98-G and U-87 MG glioma cells (ATTC, USA) were cultured in Eagle's Minimum Essential Medium (EMEM; ATTC, USA) while 9L-LacZ cells (ATTC, USA) were cultured in Dulbecco's modified Eagle's Medium with 4.5 g/L glucose, 0.58 g/L L-glutamine and 0.11 g/L sodium pyruvate (DMEM; Gibco, Life Technologies, USA). Medias were supplemented with 10% Fetal Bovine Serum (FBS; Gibco, Life Technologies USA), 100 U/mL penicillin G sodium and 100 µg/mL streptomycin sulfate (Gibco, Life Technologies, USA). Cells were subcultured

in 75 cm^2 culture flasks (Corning® T-75, Sigma-Aldrich, USA) and incubated at 37°C and 5% CO_2.

2.2.1. Cytotoxicity studies (Crystal violet assay)

Cytotoxicity assays were performed using crystal violet staining after 48 hours of incubation with different concentrations of GemHCl, $GemC_{12}$ or $GemC_{12}$-LNC with or without the hENT1 transporter inhibitor dypiridamole (Sigma Aldrich, USA). Cells were seeded at a density of 2.5-5 × 10^3 cells/well depending on the cell type in 96-wells plates and incubated at 37°C and 5% CO_2. To obtain a cell monolayer and obtain homogenous adhesion of the cells throughout the wells, for U-87 MG cell line wells were previously coated with poly(D)lysine (0.1 mg/mL per well; Sigma-Aldrich, USA) and then rinsed with phosphate buffered saline (PBS; Gibco, Life Technologies USA) before being plated and incubated at 37 °C and 5% CO_2 [29]. They were then either incubated with Triton X-100 (Sigma-Aldrich, USA), different concentrations of gemcitabine hydrochloride (GemHCl; Sigma-Aldrich, USA), $GemC_{12}$, $GemC_{12}$-LNC, unloaded LNC or left untreated. The treatments were dissolved in PBS (GemHCl, $GemC_{12}$-LNC and unloaded LNC) or in Water/Ethanol/Tween® 80 6.9/87.6/5.5 v/v ($GemC_{12}$; [34]) and then suitably diluted in complete culture medium. The concentration of active drug ranged between 0.01 and 25 µM. To study the effect of nucleoside transport inhibitors on drug sensitivity, cells were exposed to Dyp (10 µM) before and during the treatments incubation to inhibit hENT1 transporters [35]. After 48 h of incubation with the treatments, cells were fixed with 10% formalin solution (Merck, Germany) for 20 minutes and then stained with Crystal violet solution (0.5% in 20% Methanol) for 20 minutes. The plates were then rinsed with distilled water multiple times, air-dried and observed at the microscope. Methanol was added to the wells and spectrophotometric readings were performed after 30 minutes at 560 nm with a MultiSkan EX plate reader (Thermo Fisher Scientific, USA). Cells cultured with complete culture medium or Triton X-100 were considered as negative and positive controls, respectively. Results are expressed as relative percentage of living cells compared to the negative control (untreated cells) (N=3, *n*=18).

2.2.2. Cellular uptake and internalization studies

Cellular uptake of fluorescent-labeled (DiD) unloaded LNC or $GemC_{12}$-LNC (0.06 $mg \cdot g^{-1}$ DiD/Labrafac®) was quantified by flow cytometry. Glioma cell lines were seeded in 12-well plates ($8x10^4$ cells/well for 9L-LacZ cells; $1.2x10^5$ cells/well for U251, T98G and U-87 MG cells) and incubated at 37°C, 5% CO_2 overnight. Cells were then incubated at 4°C or 37°C with Hanks' Balanced Salt Solution (HBSS, control; Gibco, Life Technologies USA), unloaded DiD-LNC or DiD-$GemC_{12}$-LNC (1.21 mg/ml LNC in HBSS) for 1h or 8h. At the end of the incubation time, cells were rinsed with PBS, trypsinized and diluted with medium. After centrifugation (250 ×g, 5 min, 4 °C), the cell pellet was resuspended in 300 µL PBS. Measurements were performed using a FACSscan cytometer (FlowJo software). The procedure was repeated in three independent experiments, and at least 2000 cells were analyzed in each measurement.

Cellular internalization was also observed by fluorescent microscopy. For this experiments, 12 well-plates containing one poly(D)lysine-coated coverslip (as previously described) per well were used. Cells were seeded in the wells ($8x10^4$ cells/well for 9L-LacZ cells; $1.2x10^5$ cells/well for U251, T98G and U-87 MG cells) overnight before being incubated at 4°C or 37°C with unloaded DiD-LNC or DiD-$GemC_{12}$-LNC for 1h or 8h. At the end of the incubation time, cells were fixed with 2% paraformaldehyde (5 minutes, room temperature), rinsed three times with PBS and incubated for 1h at room temperature with Concanavalin A Alexa Fluor® 488 conjugate (ConA) in the dark. Cells were then rinsed three times and coverslips were mounted on slides using Vectashield HardSet mounting medium (with DAPI; Labconsult, Belgium) and stored at -20°C until further use. Slides were examined under an inverted fluorescent microscope (Apotome, Zeiss, Belgium) with 350 nm (blue, DAPI; cell nuclei), 488 nm (green, ConA; cell membranes) and 647 nm (red, DiD; LNC) excitation filters.

2.3. *IN VIVO* STUDIES

All experiments were performed following the Belgian national regulations guidelines as well as in accordance with EU Directive 2010/63/EU, and were approved by the ethical committee for animal care of the faculty of medicine of the Université catholique de Louvain (2014/UCL/MD/004). Animals had free access to water and food. Animal body weight was constantly monitored throughout the experiments.

2.3.1. Mid- and long-term tolerability assays

Seven-week-old female NMRI mice (Janvier, France) were randomly divided into 4 groups. On day one, mice were anesthetized by intraperitoneal injection of ketamine/xylazine (66.6 and 8.6 mg/kg, respectively) and a hole was created in the skull at the left frontal lobe using a high-speed drill (Dremel Inc., USA). Ten µL of either sterile PBS solution, unloaded LNC or $GemC_{12}$-LNC hydrogel was injected in the hole. This volume corresponds to the maximal amount allowed for intracerebral injection in mice. A fourth group included animals administered with 2.5 µL of $GemC_{12}$ (the injected volume was reduced for this group as the drug is dissolved in Water/Ethanol/Tween®80 6.9/87.6/5.5 v/v). The amount of drug administered in the drug treated groups corresponded to 5.5 mg/kg of $GemC_{12}$. Mice were then sutured and observed for two or six months (mid- or long-term, respectively). After this time, mice were sacrificed and brains were removed and fixed in 10% formalin solution (Merck, Germany) for 20 h before being rinsed in PBS and kept at 4°C for at least two days. Brains were then embedded in paraffin, sectioned at 10 µm using a MICROM 17M325 microtome (Thermo Fischer Scientific, USA) and collected on super-frost plus glass slides. Slides were incubated at 37°C overnight before being stored at room temperature until further use.

For the histological analysis and evaluation of the cellular inflammatory response the samples were deparaffinized and stained with haematoxylin and eosin (H&E) (n=5 for mid-term experiments, n=3 for long-term experiments) using a Sakura DRS 601 automated slide stainer (Sukura Finetek Europe, The Netherlands).

For the TUNEL assay, the Dual End Fluorometric TUNEL System kit ® (Promega, USA) was used following manufacturer instructions. Slides were mounted with Vectashield HardSet mounting medium (with DAPI; Vector Laboratories, USA) and examined under an inverted fluorescent microscope (Apotome, Zeiss, Belgium) with 350 nm (blue, DAPI) and 748-789 nm (green, TUNEL) excitation filters (n=5 for mid-term experiments, n=3 for long-term experiments).

Microglia activation was evaluated by Iba-1 immunostaining. Slides were deparaffinized, endogenous peroxidases were blocked with hydrogen peroxide (30% v/v) and then left for 90min in citrate buffer in a water bath at 100°C. Sections were then incubated for 30 min

with 10% normal horse serum to block non-specific binding sites before incubation with a goat anti-human Iba-1 antibody (1:1000; Novus Biologicals, USA) overnight at room temperature. Slides were then rinsed and incubated for 60 min at room temperature with rabbit anti-goat IgG biotinylated antibody (1:200; Vector Laboratories, USA). Sections were then counterstained with hematoxylin, dehydrated and mounted with DPX neutral mounting medium (Prosan, Belgium). Slides were scanned using a SCN400 Leica slide scanner and image analysis was performed with Digital Image Hub (Leica, Germany) (*n*=5 for mid-term experiments, *n*=3 for long-term experiments).

2.3.2. Orthotopic U-87 MG human glioblastoma tumor model

Six-week-old female NMRI nude mice (Janvier, France) were anesthetized by intraperitoneal injection of ketamine/xylazine (100 and 13 mg/kg, respectively), fixed in a stereotactic frame and 3 x 10^4 U-87 MG glioma cells were injected in the right frontal lobe using a Hamilton syringe as previously described [36, 37]. The injection coordinates for the orthotopic model and resection model were 0.5 mm anterior or posterior, 2.1 mm lateral from the bregma and 2.5-3 mm deep from the outer border of the cranium, respectively. The presence, volume and location of the tumors were determined by Magnetic Resonance Imaging (MRI), which was performed for all mice included in the study between day 9 and 13 post tumor cell implantations.

2.3.3. MRI

MRI was performed using a 11.7 T Bruker Biospec MRI system (Bruker, Germany) equipped with a 1 H quadrature transmit/receive surface cryoprobe after anesthetising animals with isoflurane mixed with air (2.5% for induction, 1% for maintenance). Respiration was continuously monitored while animal core temperature was maintained throughout the experiment by hot water circulation in the cradle. Tumor volume was assessed using rapid acquisition with relaxation enhancement (RARE) sequence (TR = 2500 ms; effective echo time (TE_{eff}) = 30 ms; RARE factor = 8; FOV = 2 x 2 cm; matrix 256 x 256; twenty-five contiguous slices of 0.3 mm, NA = 4). Tumor volumes were calculated from a manually drawn region of interest.

2.3.4. Anti-tumor efficacy of GemC12-LNC hydrogel after intratumoral administration in an orthotopic U-87 MG human glioblastoma tumor

At day 15 post-tumor inoculation mice were randomly divided into six groups and treated intratumorally, intravenously or left untreated. For the local treatment, mice were anesthetized, fixed in a stereotactic frame and treatments were injected in the previous burr hole using a 0.3 ml insulin syringe ($GemC_{12}$-LNC hydrogel and unloaded LNC) or a Hamilton syringe fitted with a 32G needle (GemHCl and $GemC_{12}$). For intravenous treatment, mice were injected through the tail vein. **Group 1:** control group (no treatment) (*n*=11); **Group 2:** intratumoral injection of unloaded LNC, 5 µL (*n*=7); **Group 3:** intratumoral injection of GemHCl, 2.5 µL (*n*=7); **Group 4:** intratumoral injection of $GemC_{12}$ dissolved in Water/Ethanol/Tween®80 (6.9/87.6/5.5 v/v), 2.5 µL (*n*=7); **Group 5:** intravenous injection of $GemC_{12}$ solubilised as previously mentioned and diluted in sterile PBS, 100 µL (*n*=7); **Group 6:** intratumoral injection of $GemC_{12}$-LNC gel, 5 µL (*n*=9). The dose of drug injected was 3 mg/kg of $GemC_{12}$. The delivered dose of unloaded LNC was the same as $GemC_{12}$-LNC.

2.3.5. Anti-tumor efficacy of GemC12-LNC hydrogel after peritumoral administration in the U-87 MG tumor resection cavity

At day 13 post-tumor inoculation, the tumor resection was performed using the biopsy-punch resection model, as previously described by Bianco *et* al. [37]. Briefly, animals were anaesthetised with ketamine/xylazine and immobilised in a stereotactic frame. A 7 mm incision was made in the midline along the previous surgical scar and a 2.1 diameter circular cranial window was created around the previous burr hole to expose the brain using a high-speed drill (Dremel Inc., USA). A 2 mm Ø biopsy punch (Kai Medical, Germany) was then inserted 3 mm deep and twisted for 15 seconds to cut the brain/tumour tissue. Once withdrawn, the tumor and brain tissues were aspired using a diaphragm vacuum pump (Vaccubrand GMBH + CO KG, Germany). Between 2.5 to 5 µL of treatment (depending on the group) was placed into the resection cavity before sealing the cranial window with a 4 mm x 4 mm square piece of Neuro-Patch® (Aesculap, Germany) impregnated with a reconstituted fibrin hydrogel (25 mg/mL fibrin, 10 IU/mL thrombin, equal volumes; Baxter Innovations, Austria). **Group 1:** control group (no treatment) (*n*=10); **Group 2:** unloaded LNC, 5 µL (*n*=7); **Group 3:** GemHCl, 2.5 µL (*n*=7); **Group 4:** $GemC_{12}$ dissolved in Water/Ethanol/Tween®80

(6.9/87.6/5.5 v/v), 2.5 µL (*n*=7); **Group 5:** $GemC_{12}$-LNC gel, 5 µL (*n*=7). The dose of drug administered was 3 mg/kg of $GemC_{12}$. The delivered dose of unloaded LNC was the same as $GemC_{12}$-LNC. For both anti-tumor efficacy studies, mice were sacrificed when they presented ≥ 20% body weight loss or 10% body weight loss plus clinical signs of distress (paralysis, arched back, lack of movement).

2.4. STATISTICAL ANALYSIS

Statistical analysis was performed using GraphPad Prism (GraphPad Software, USA) and determined based on $p < 0.05$. For the *in vitro* cytotoxicity studies, Kruskal-Wallis test + Dunn multiple comparison post-test was performed for Fig.1, while two-way ANOVA test with Bonferroni post-test were used for Fig. 2. In these experiments, N corresponds to the number of independent experiments performed while *n* is the number of replicates for each experiment. Results are expressed as mean ± standard deviation (SD) of at least three independent experiments. For the *in vivo* efficacy studies, the statistical analysis was estimated from comparison of Kaplan-Meier survival curves using the log-rank test (Mantel Cox test). Outliers were calculated using GraphPad software (significance level 0.01, two-sided) and removed from the study.

3. RESULTS AND DISCUSSION

3.1. IN VITRO CYTOTOXICITY OF GEMC12-LNC IN GBM CELL LINES WITH OR WITHOUT NUCLEOSIDE TRANSPORTER INHIBITION

We previously demonstrated, using the MTT assay, a higher cytotoxicity of $GemC_{12}$ and $GemC_{12}$-LNC compared to the parent drug GemHCl on the U-87 MG cell line, hypothesizing that this result was due to differences in the internalization mechanisms of the drugs [29]. Gemcitabine is a nucleoside analogue and its cellular uptake requires the presence of specialized plasma membrane nucleoside transporters (NT), either sodium-independent (equilibrative nucleoside transporters hENT1 and hENT2) or sodium-dependent (concentrative nuclear transporters hCNT1, hCNT2 and hCNT3). The different distribution of these NT in cells and tissues as well as their different ability to transport nucleoside analogs is related to the different drug response (e.g. sensibility to the drug, chemoresistance) [35, 38]. Gemcitabine is preferentially directed by hENT1 and several studies have shown that higher levels of this transporter are associated to a better response to the drug [33, 39]. Hence, to evaluate if there is a difference between the internalization pathways of GemHCl, the alkylated drug $GemC_{12}$ and $GemC_{12}$-LNC, we tested if their cytotoxic activity in four GBM cell lines is affected by the inhibition of the hENT1 transporter. We performed crystal violet staining after 48 h of incubation with different concentrations of the drugs, with or without incubation with dypiridamole, which can specifically block the hENT1 transporter [35, 40]. Dyp significantly inhibited GemHCl uptake in U251 (Fig. 1A) and T98G cells (Fig. 1B), as shown by a reduced cytotoxic effect of the drug at concentrations of 0.1, 1 and 10 µM compared to the cells without Dyp (p<0.001, p<0.01, p<0.05 respectively for U251; p<0.001 for T98G cells). On the contrary, this effect was not observed for $GemC_{12}$ and $GemC_{12}$-LNC suggesting that the internalization of these two drugs does not rely on the same adenosine transporters as the commercial drug GemHCl. A similar behavior was also observed for 9L-LacZ (especially at 0.1 µM; Fig. 1C) and U-87 MG cells (Fig. 1D), but to a much lesser extent. Indeed, 9L-LacZ cells are much more sensitive to gemcitabine in all its three forms compared to the other cell lines studied, showing less than 35% survival starting from 0.1 µM in the absence of Dyp (Fig. S1). At this concentration, GemHCl is significantly more cytotoxic than $GemC_{12}$ and $GemC_{12}$-LNC (p<0.01, p<0.001 respectively), while at lower or higher

concentrations no significant difference is observed between the groups. When the transporter inhibitor is added, GemHCl seems less cytotoxic but not in a significant way (Fig. 1C), meaning that in this cell line other transporters are probably involved in the cellular drug uptake. On the other side, U-87 MG cells are less sensitive to GemHCl in the examined concentration range, decreasing the influence of the inhibitor on the drug cytotoxicity (Fig. 1D). Moreover, it has been previously shown that adenosine analogue uptake is only partially inhibited by Dyp in U-87 MG, possibly because of an altered hENT phenotype [41]. Overall, our results are in accordance with other studies performed on non-GBM cell lines who reported that gemcitabine derivatives, alone or in nanoparticles, are less sensitive to the hENT1 inhibition than GemHCl. The improved lipophilicity of Gem derivatives could enhance intracellular uptake via passive pathways or endocytosis.thus improving growth inhibition effects [42-44]. However interestingly, for all cell lines tested in this work, the cytotoxic action of $GemC_{12}$ and $GemC_{12}$-LNC seem potentiated by the presence of Dyp. As hENT are bidirectional, the net drug uptake is represented by the combined contributions of NT-mediated influx and efflux [38, 45]. We hypothesize that the drug effect potentiation could then be correlated to the presence and action of inwardly directed hCNT, which could also be responsible for $GemC_{12}$ and $GemC_{12}$-LNC uptake in these cell lines.

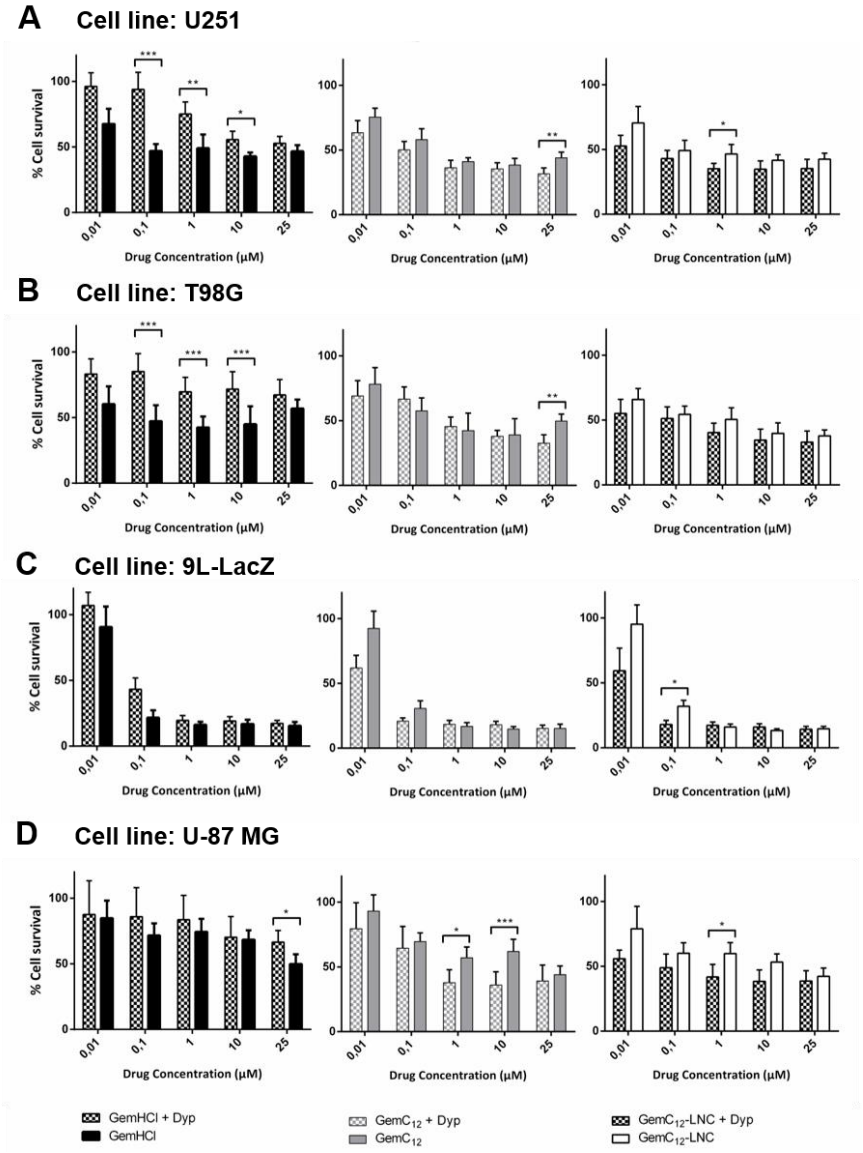

Figure 1. *In vitro* cytotoxicity studies on (**A**) U251, (**B**) T98G, (**C**) 9L-LacZ, and (**D**) U-87 MG glioma cells. Crystal violet staining after 48 hours of incubation of different concentrations of GemHCl (black bar), $GemC_{12}$ (gray bar) or $GemC_{12}$-LNC (white bar) with or without 10 µM of hENT1 transporter inhibitor dypiridamole (squared pattern or filled pattern, respectively). Data are presented as percentage of cell survival (untreated cells assumed as 100%) (N= 3 *n*= 18; mean ± SD). *** $p<0.001$, ** $p<0.01$, * $p<0.05$ by Kruskal-Wallis test + Dunn multiple comparison post-test. Dyp: dypiridamole

3.2. INTERNALIZATION STUDIES OF LNC INTO GBM CELL LINES

Garcion *et* al. and Paillard *et* al. [46, 47] have previously demonstrated, by using the F98 glioma cell line, that LNC internalization is mediated through an active, saturable, clathrin/caveolae-independent endocytosis mechanism involving endogenous cholesterol. To test whether the presence of $GemC_{12}$ at the interface of the LNCs could influence its cellular uptake, we performed internalization studies using LNC labelled with the fluorescent dye DiD using flow cytometry (FACS) and fluorescence microscopy. Therefore, we have

compared the capacity of DiD-LNC and DiD-GemC$_{12}$-LNC to enter U251, T98G, 9L-LacZ and U-87 MG glioma cells after 1h or 8h of incubation at 4°C or 37°C. At 4°C, when energy consumption and active transport processes are minimal [48], increased fluorescence was observed in cells treated with GemC$_{12}$-LNC compared to unloaded LNC (Fig. 2). However, this difference is only significant in 9L-LacZ after 8h (** p<0.01) and in U-87 MG cells after 1h and 8h (* *p*<0.05). At 37°C we observed a significant difference between unloaded LNC and GemC$_{12}$-LNC after 8h in all the cell lines (** *p*<0.01 for U251, T98G; *** *p*<0.001 for U-87 MG respectively) except 9L-LacZ where, at this concentration, both conditions are cytotoxic (data not shown). As it has been previously demonstrated that DiD labelling is irreversible and can be used to confirm the uptake of the LNC in the cells [49], we used fluorescent microscopy to qualitatively confirm the nanocarrier uptake. Figure 3, which represents the U-87 MG cells following 8h of incubation with DiD-LNC and DiD-GemC$_{12}$-LNC, shows absence of DiD signal in the proximity of the cell nuclei for the unloaded LNC at 4°C and low DiD signal at 37°C. Its detection increases for the DiD-GemC$_{12}$-LNC, especially at 37°C confirming that cellular uptake of the drug-loaded nanocarrier is mediated through active transport. These results are in accordance with those of the cytotoxicity studies.

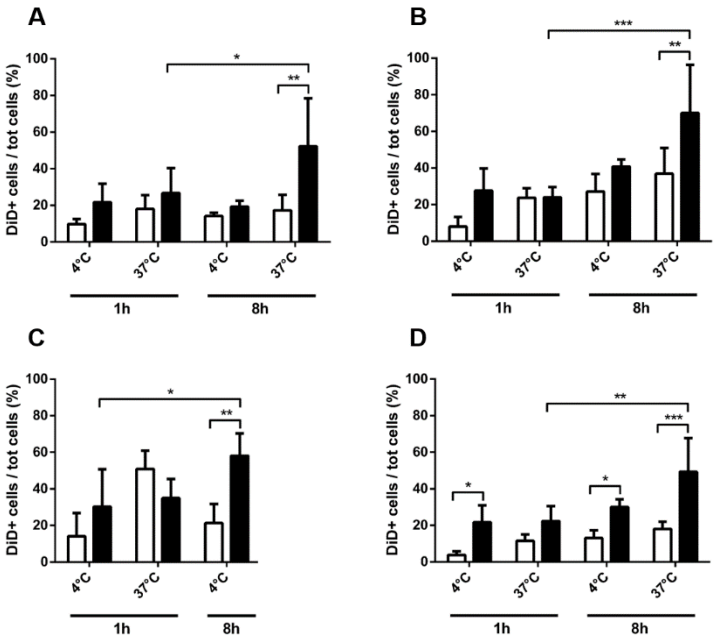

Figure 2. *In vitro* cellular uptake studies: Flow cytometry analysis after 1h or 8h incubation with fluorescent-labeled (DiD) unloaded LNC (white bars) or GemC$_{12}$-LNC (1.21 mg/mL LNC, 100 µM GemC$_{12}$; black bars) of (**A**) U251, (**B**) T98G, (**C**) 9L-LacZ, and (**D**) U-87 MG glioma cells at 4 and 37°C. Percentage of fluorescent cells relative to all cells measured by flow cytometry normalized to each control (HBSS). *** *p*<0.001, ** *p*<0.01, * *p*<0.05 by two-way ANOVA test with Bonferroni post-test (N=3 *n*=3; mean ± SD)

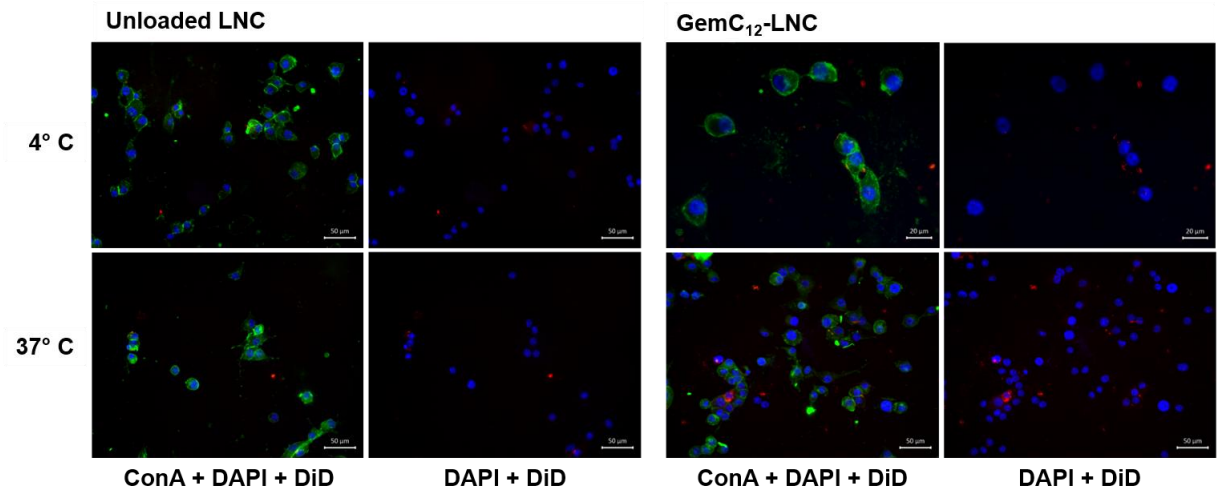

Figure 3. Fluorescence microscopy images of U-87 MG glioma cells after 8h incubation with fluorescent-labeled (DiD) unloaded LNC or $GemC_{12}$-LNC at 4°C and 37°C. Blue: cells nuclei (DAPI); Green: cell membranes (Concanavalin A, Alexa Fluor® 488 Conjugate); Red: LNC (DiD). Microscope images: 20x (scale bar 50 µm) or 40x (scale bar 20 µm).

3.3. MID-TERM AND LONG-TERM TOLERABILITY OF $GEMC_{12}$-LNC IN MOUSE BRAIN

We previously reported that, after one week of exposure, no significant inflammation was observed in the $GemC_{12}$-LNC group compared to the control groups (PBS and unloaded LNC), while some singular apoptotic cells and slight microglia activation were observed [29]. However, it is known that neuroinflammation following injury or administration of implants into the brain can last for a much longer period, and the main actors in this response are activated microglia and astrocytes. The latter can form a gliotic scar, creating a barrier between the affected and the unaffected brain areas [50]. Once the inflammatory response recedes, the tissue is repaired and the damaged areas strengthened, while the cells restore their normal morphology [50].

Therefore, to evaluate the influence of prolonged exposure to $GemC_{12}$-LNC gel in the mouse brain, we evaluated its tolerability after 2 and 6 months. During the study, none of the animals showed behavioral changes, apparent neurological deficits or body weight loss. All the brains had normal morphology and no apparent lesions were visible immediately after extraction and fixation. While sectioning, the hole corresponding to the administration site was easily visualized in almost all the brains. Figure 4 shows brain sections of the PBS and $GemC_{12}$-LNC treated groups. After two months, no increased inflammation, apoptosis or microglia activation was observed in the $GemC_{12}$-LNC group compared to the controls in proximity to the site of injection. Interestingly, in two of the animals treated with $GemC_{12}$-

LNC hydrogel, a cavity was observed below the injection site, which could correspond to the space occupied by the hydrogel (Fig. S2). Around this formed cavity the presence of activated microglia was slightly increased compared to the controls. Their presence could have resulted from the slow degradation of the hydrogel and, therefore, a longer contact of the foreign body (hydrogel) with the tissue compared to the other groups. Indeed, it has been previously shown that slower rates of hydrogel degradation can lead to higher microglial activation as these cells can phagocytose the degradation products [50].

After six months, no increase in inflammation, apoptosis or microglia activation was observed in the $GemC_{12}$-LNC group compared to the controls.

It is important to note that unloaded LNC and $GemC_{12}$ groups exhibited similar results (normal shape, no lesion, no inflammation, no apoptosis; data not shown).

Our results are in accordance with previous tolerability studies on controlled release systems, which showed a typical and mild foreign body reaction being resolved 2 months after implantation [51]. In conclusion, the $GemC_{12}$-LNC can be considered as well tolerated in mouse brain and therefore suitable for local administration into the brain.

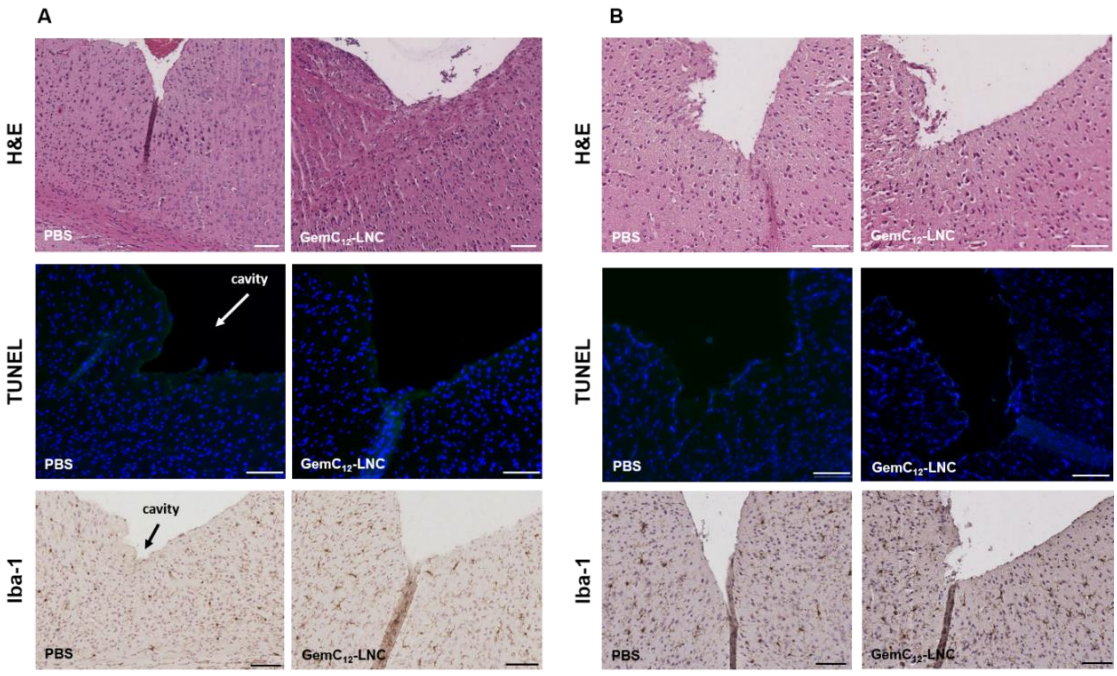

Figure 4. *In vivo* mid-term (**A**) and long-term (**B**) tolerability assay. Evaluation of the inflammatory response (Hematoxylin & Eosin staining, upper panel), cell apoptosis (TUNEL assay, mid panel) and microglia activation (Iba-1 staining, lower panel) in the brain tissue 2 months (mid-term) or 6 months (long-term) after local injection of PBS and $GemC_{12}$-LNC. The amount of $GemC_{12}$ administered was 0.16 mg per mouse. Scale bar: 100 µm (*n*=3-5). TUNEL assay: living nuclei (Blue, DAPI); apoptotic cells (Green, TUNEL). Scale bar: 100 µm.

3.4. ANTI- TUMOR EFFICACY OF GEMC12-LNC HYDROGEL AFTER INTRATUMORAL ADMINISTRATION IN AN ORTHOTOPIC U-87 MG HUMAN GLIOBLASTOMA

To test the antitumor efficacy of the $GemC_{12}$-LNC hydrogel, the U-87 MG human xenograft orthotopic model in nude mice was chosen for its wide use as a preclinical model, good reproducibility, reliable growth and disease progression [52]. These tumors are non-infiltrative, with a well demarcated tumor mass visible both by MRI images and Hematoxylin & Eosin stained sections [37], but present a subpopulation of cancer stem-like cells with self-propagating potential [53]. These features make it a good model for testing the antitumor efficacy after local delivery of a drug into the tumor or in the tumor resection cavity.

U-87 MG cells were injected at the border between the striatum and the cortex of nude mice using a stereotactic frame and the tumor was visualized by MRI. To evaluate the antitumor efficacy of the hydrogel and its capacity to slow down tumor recurrences, treatments were administered intratumorally by stereotactic injection at day 15 post-tumor inoculation (Figure 5).

The survival data of the different groups are summarized in Table 1 and Kaplan-Meier survival curves are shown in Figure 5.

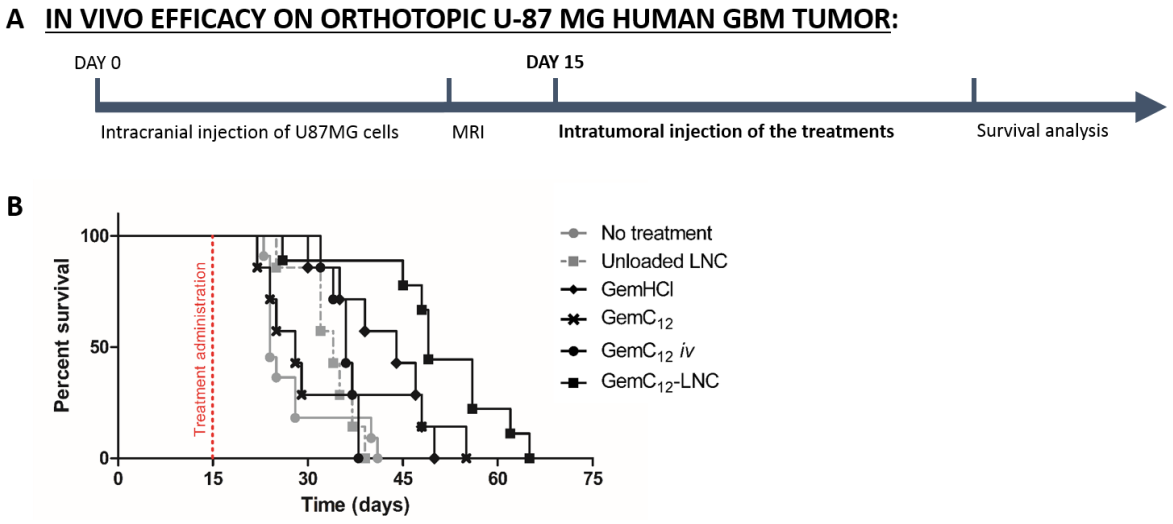

Figure 5. (**A**) Time schedule of the anti-tumor efficacy studies using an orthotopic U-87 MG human GBM tumor model; (**B**) Kaplan-Meier survival curves for animals treated intratumorally with this model. Drug dose administered: 3 mg/kg (*n* = 7-11 for all groups).

In this orthotopic model, the median survival of the $GemC_{12}$-LNC treated mice was compared to all the other groups and a significant improvement in the median survival of mice treated with the hydrogel was observed compared to the other treatments. Interestingly, no differences were observed between the intravenous and intratumoral administration of the free drug $GemC_{12}$, while intratumoral administration of $GemC_{12}$-LNC significantly prolonged animal survival compared to both these groups. These results, which are in accordance with the short-term efficacy studies we have previously reported using $GemC_{12}$-LNC hydrogel in a subcutaneous GBM xenograft tumor model [29], might be explained by the sustained continuous drug release obtained by a gel formulation compared to the unloaded liquid form, and they confirm the rationale for the use of Gem derivatives as a local delivery strategy for GBM. Recently, Gaudin *et* al. also reported an increased survival time of animals treated with squaneoyl-gemcitabine nanoparticles compared to free drug after local administration by CED in an orthotopic RG2 GBM model [54].

Table 1. *In vivo* efficacy studies: Median survival (days) of animals treated intratumorally at day 15 post-cell inoculation (orthotopic model) or locally treated in the tumor resection cavity at day 13 post-cell inoculation (resection model).

Tumor model	**Treatment**	***n***	**Survival time (days)**		**Mantel Cox test (each *vs* $GemC_{12}$-LNC)**
			Range	**Median**	
Orthotopic model	No treatment	11	23-41	24	***
	Unloaded LNC	7	25-39	34	***
	GemHCl	7	30-50	44	*
	$GemC_{12}$	7	22-55	28	*
	$GemC_{12}$ *iv*	7	32-38	36	**
	$GemC_{12}$-LNC	9	26-65	49	
Orthotopic resection model	No treatment	10	29-45	35.5	**
	Unloaded LNC	7	29-51	38	*
	GemHCl	7	29-53	37	*
	$GemC_{12}$	7	28-92	61	n.s.
	$GemC_{12}$-LNC	7	32-92	62	

Legend: *n*: number of animals per group; Mantel Cox test: survival curve comparison between each control group and the $GemC_{12}$-LNC hydrogel (*** $p<0.001$, ** $p<0.01$, * $p<0.05$, n.s. $p>0.05$)

3.5. ANTI- TUMOR EFFICACY OF GEMC12-LNC HYDROGEL AFTER PERISURGICAL ADMINISTRATION IN THE U-87 MG TUMOR RESECTION CAVITY

To better mimic the local delivery clinical scenario, a second anti-tumor efficacy study was performed after perisurgical administration of $GemC_{12}$-LNC within the tumor resection cavity (Figure 6A). For this last purpose, we used a subtotal resection model that we recently developed and validated [37]. Here, U-87 MG cells were injected at the border between the striatum and the cortex of nude mice using a stereotactic frame and the tumor was visualized by MRI. At day 13 post-tumor inoculation, the brain region around the tumor was defined by a 2 mm diameter biopsy punch that was inserted at a depth of 3 mm from the skull border. The resulting explant was then aspired leading to a resection cavity able to host 5 µL of $GemC_{12}$-LNC hydrogel, corresponding to 3 mg/kg (Figure 6B; video S3). Recurrence of the tumors, which lead to mouse death, were observed in all animals where a primary tumor had been detected by MRI but they appeared at different time points depending on the treatment administered (Figure 6C).

As for the previous model, the median survival of the $GemC_{12}$-LNC treated mice was compared to all the other groups (Table 1). Significant improvement in the median survival of mice, and therefore slowdown of tumor recurrences formations, was observed in groups treated with $GemC_{12}$ and $GemC_{12}$-LNC hydrogel compared to the untreated, unloaded LNC and GemHCl-treated animals (Figure 6D). Interestingly, the curves of the $GemC_{12}$ and $GemC_{12}$-LNC groups almost overlap in the orthotopic resection tumor model, while in the orthotopic non-resected tumor model a significant difference between the curves is observed (* $p<0.05$). This different result could be explained by the tumor microenvironment *vs* post-resection tumor microenvironment characteristics [55], the immunostimulatory capacities of gemcitabine [56], and possibly different humoral adaptive and innate immune response of the animals in our two orthotopic tumor models [57]. For example, Sasso *et* al. have recently demonstrated the targeting capacity of $GemC_{12}$-LNC towards the monocytic-myeloid derived suppressor cells (MDSCs) in lymphoma and melanoma mouse models [58]. MDSCs are a heterogeneous population of granulocytic and myeloid cells, highly present in GBM patients, able to accumulate in the tumor-bearing host to support glioma growth, invasion, and vascularization, and differentially mediating immunosuppression depending on their stage [59-61]. The targeted action of $GemC_{12}$-LNC

on these cells could potentially reduce the tumor-associated immunosuppression in the orthotopic tumor model (where the tumor microenvironment is not affected by the resection procedure), thus increasing its efficacy compared to the free drug. This assumption will be subject of further studies in more appropriate immunological rodent models.

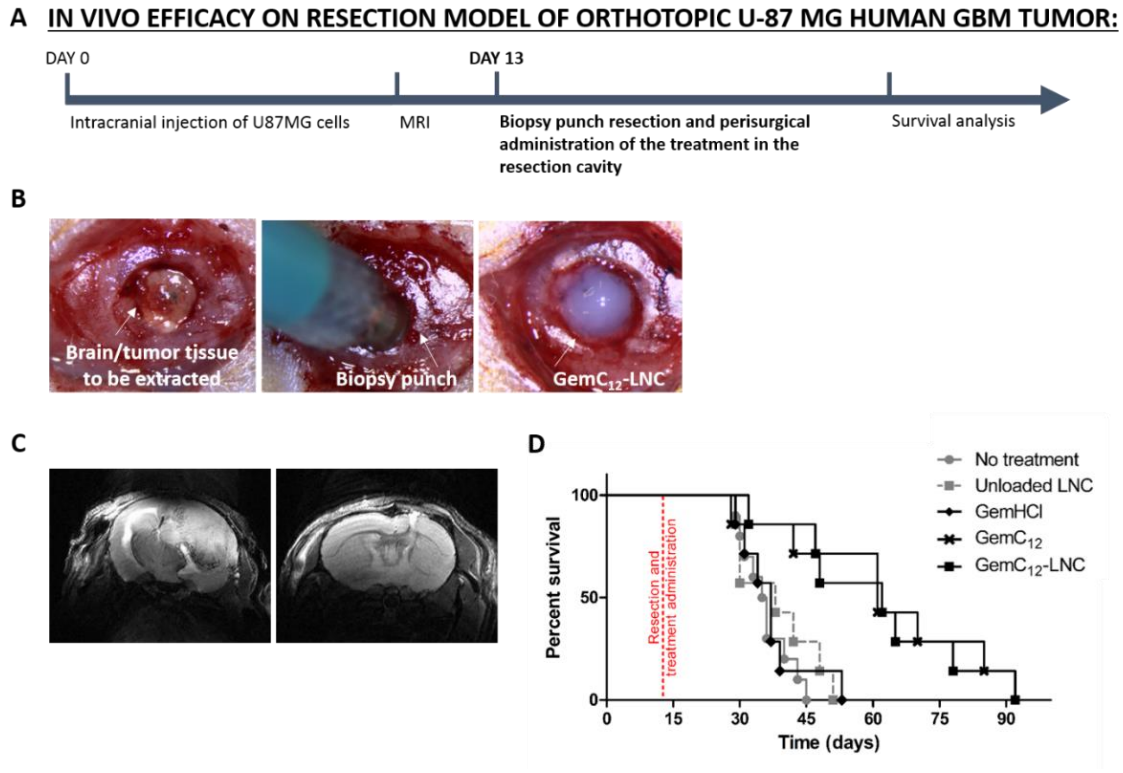

Figure 6. (**A**) Time schedule of the anti-tumor efficacy studies using a resection model of orthotopic U-87 MG human GBM tumor model; (**B**) Images taken during the tumor resection surgeries and treatment administration: tumor tissue visible within the 2x2 mm cranial window (left), biopsy punch twisting (middle) followed by aspiration. $GemC_{12}$-LNC hydrogel (5µL) injected into the resection cavity, and filling it completely (right). (**C**) Axial (T_2-weighted) images of mouse brain following resection: untreated (day 31 post-resection, left) and treated with $GemC_{12}$-LNC (day 61 post-resection, right). (**D**) Kaplan-Meier survival curves for animals treated locally in the resection cavity. Drug dose administered: 3 mg/kg (*n* = 7-11 for all groups).

4. CONCLUSIONS

The objective of this work was to test the cytotoxicity, mid- and long-term tolerability and efficacy of $GemC_{12}$-LNC nanomedicine hydrogel on GBM. We demonstrated that the different cytotoxic effects observed on GBM cells lines for $GemC_{12}$-LNC and the commercial drug GemHCl might be due to different cell transport mechanisms (different adenosine transporters, endocytosis). The $GemC_{12}$-LNC hydrogel is well tolerated in mouse brain after 2 and 6 months of exposure, suggesting that this system is suitable for an application in the brain. Intratumoral administration of the hydrogel in an orthotopic human xenograft GBM model showed a significant increase in the animals' survival compared to the controls. Moreover, using a reproducible U-87 MG GBM tumor resection technique, we demonstrated that $GemC_{12}$-LNC hydrogel slows down recurrences formation after perisurgical administration in the resection cavity. To our knowledge, it is the first time that this surgical resection procedure, which allows to mimic the clinical setting, is used to test local delivery of anticancer drugs in orthotopic GBM mouse models. In conclusion, $GemC_{12}$-LNC nanomedicine-based hydrogel could be considered as a promising strategy for the local treatment of GBM, although further studies need to be performed to show its efficacy in other animal models, and in synergy with other chemotherapeutic agents and/or radiotherapy.

5. REFERENCES

[1] E.C. Holland, Glioblastoma multiforme: the terminator, Proc Natl Acad Sci U S A, 97 (2000) 6242-6244.

[2] D.N. Louis, A. Perry, G. Reifenberger, A. von Deimling, D. Figarella-Branger, W.K. Cavenee, H. Ohgaki, O.D. Wiestler, P. Kleihues, D.W. Ellison, The 2016 World Health Organization Classification of Tumors of the Central Nervous System: a summary, Acta Neuropathol, 131 (2016) 803-820.

[3] R.L. Yong, R.R. Lonser, Surgery for glioblastoma multiforme: striking a balance, World neurosurgery, 76 (2011) 528-530.

[4] K.R. Yabroff, L. Harlan, C. Zeruto, J. Abrams, B. Mann, Patterns of care and survival for patients with glioblastoma multiforme diagnosed during 2006, Neuro-oncology, 14 (2012) 351-359.

[5] R. Stupp, M. Brada, M.J. van den Bent, J.C. Tonn, G. Pentheroudakis, High-grade glioma: ESMO Clinical Practice Guidelines for diagnosis, treatment and follow-up, Ann Oncol, 25 Suppl 3 (2014) iii93-101.

[6] F.H. Hochberg, A. Pruitt, Assumptions in the radiotherapy of glioblastoma, Neurology, 30 (1980) 907-911.

[7] S. Roy, D. Lahiri, T. Maji, J. Biswas, Recurrent Glioblastoma: Where we stand, South Asian J Cancer, 4 (2015) 163-173.

[8] R. Stupp, M.E. Hegi, W.P. Mason, M.J. van den Bent, M.J. Taphoorn, R.C. Janzer, S.K. Ludwin, A. Allgeier, B. Fisher, K. Belanger, P. Hau, A.A. Brandes, J. Gijtenbeek, C. Marosi, C.J. Vecht, K. Mokhtari, P. Wesseling, S. Villa, E. Eisenhauer, T. Gorlia, M. Weller, D. Lacombe, J.G. Cairncross, R.O. Mirimanoff, Effects of radiotherapy with concomitant and adjuvant temozolomide versus radiotherapy alone on survival in glioblastoma in a randomised phase III study: 5-year analysis of the EORTC-NCIC trial, The Lancet. Oncology, 10 (2009) 459-466.

[9] N.R. Smoll, K. Schaller, O.P. Gautschi, Long-term survival of patients with glioblastoma multiforme (GBM), J Clin Neurosci, 20 (2013) 670-675.

[10] T. Yamahara, Y. Numa, T. Oishi, T. Kawaguchi, T. Seno, A. Asai, K. Kawamoto, Morphological and flow cytometric analysis of cell infiltration in glioblastoma: a comparison of autopsy brain and neuroimaging, Brain Tumor Pathol, 27 (2010) 81-87.

[11] T. Denysenko, L. Gennero, M.A. Roos, A. Melcarne, C. Juenemann, G. Faccani, I. Morra, G. Cavallo, S. Reguzzi, G. Pescarmona, A. Ponzetto, Glioblastoma cancer stem cells: heterogeneity, microenvironment and related therapeutic strategies, Cell biochemistry and function, 28 (2010) 343-351.

[12] D. Treister, S. Kingston, K.E. Hoque, M. Law, M.S. Shiroishi, Multimodal magnetic resonance imaging evaluation of primary brain tumors, Semin Oncol, 41 (2014) 478-495.

[13] S. Osuka, E.G. Van Meir, Overcoming therapeutic resistance in glioblastoma: the way forward, J Clin Invest, 127 (2017) 415-426.

[14] D.M. Patel, N. Agarwal, K.L. Tomei, D.R. Hansberry, I.M. Goldstein, Optimal Timing of Whole-Brain Radiation Therapy Following Craniotomy for Cerebral Malignancies, World neurosurgery, 84 (2015) 412-419.

[15] J.R. Silber, M.S. Bobola, A. Blank, M.C. Chamberlain, O(6)-methylguanine-DNA methyltransferase in glioma therapy: promise and problems, Biochim Biophys Acta, 1826 (2012) 71-82.

[16] N.R. Parker, A.L. Hudson, P. Khong, J.F. Parkinson, T. Dwight, R.J. Ikin, Y. Zhu, Z.J. Cheng, F. Vafaee, J. Chen, H.R. Wheeler, V.M. Howell, Intratumoral heterogeneity identified at the epigenetic, genetic and transcriptional level in glioblastoma, Sci rep, 6 (2016) 22477.

[17] H. Okura, C.A. Smith, J.T. Rutka, Gene therapy for malignant glioma, Mol Cell Ther, 2 (2014) 21.

[18] A. Tivnan, T. Heilinger, E.C. Lavelle, J.H. Prehn, Advances in immunotherapy for the treatment of glioblastoma, J Neurooncol, 131 (2017) 1-9.

[19] A. Mangraviti, D. Gullotti, B. Tyler, H. Brem, Nanobiotechnology-based delivery strategies: New frontiers in brain tumor targeted therapies, J Control Release, 240 (2016) 443-453.

[20] R. Karim, C. Palazzo, B. Evrard, G. Piel, Nanocarriers for the treatment of glioblastoma multiforme: Current state-of-the-art, J Control Release, 227 (2016) 23-37.

[21] A. Burgess, K. Shah, O. Hough, K. Hynynen, Focused ultrasound-mediated drug delivery through the blood-brain barrier, Expert Rev Neurother, 15 (2015) 477-491.

[22] J. Bianco, C. Bastiancich, A. Jankovski, A. des Rieux, V. Preat, F. Danhier, On glioblastoma and the search for a cure: where do we stand?, Cell Mol Life Sci, (2017).

[23] M. Westphal, Z. Ram, V. Riddle, D. Hilt, E. Bortey, Gliadel wafer in initial surgery for malignant glioma: long-term follow-up of a multicenter controlled trial, Acta Neurochir (Wien), 148 (2006) 269-275; discussion 275.
[24] P. Menei, L. Capelle, J. Guyotat, S. Fuentes, R. Assaker, B. Bataille, P. Francois, D. Dorwling-Carter, P. Paquis, L. Bauchet, F. Parker, J. Sabatier, N. Faisant, J.P. Benoit, Local and sustained delivery of 5-fluorouracil from biodegradable microspheres for the radiosensitization of malignant glioma: a randomized phase II trial, Neurosurgery, 56 (2005) 242-248; discussion 242-248.
[25] C. Bastiancich, P. Danhier, V. Preat, F. Danhier, Anticancer drug-loaded hydrogels as drug delivery systems for the local treatment of glioblastoma, J Control Release, 243 (2016) 29-42.
[26] D.A. Bota, A. Desjardins, J.A. Quinn, M.L. Affronti, H.S. Friedman, Interstitial chemotherapy with biodegradable BCNU (Gliadel) wafers in the treatment of malignant gliomas, Ther Clin Risk Manag, 3 (2007) 707-715.
[27] M. Westphal, D.C. Hilt, E. Bortey, P. Delavault, R. Olivares, P.C. Warnke, I.R. Whittle, J. Jaaskelainen, Z. Ram, A phase 3 trial of local chemotherapy with biodegradable carmustine (BCNU) wafers (Gliadel wafers) in patients with primary malignant glioma, Neuro Oncol, 5 (2003) 79-88.
[28] P.C. McGovern, E. Lautenbach, P.J. Brennan, R.A. Lustig, N.O. Fishman, Risk factors for postcraniotomy surgical site infection after 1,3-bis (2-chloroethyl)-1-nitrosourea (Gliadel) wafer placement, Clin Infect Dis, 36 (2003) 759-765.
[29] C. Bastiancich, K. Vanvarenberg, B. Ucakar, M. Pitorre, G. Bastiat, F. Lagarce, V. Preat, F. Danhier, Lauroyl-gemcitabine-loaded lipid nanocapsule hydrogel for the treatment of glioblastoma, J Control Release, 225 (2016) 283-293.
[30] T. Fourniols, L.D. Randolph, A. Staub, K. Vanvarenberg, J.G. Leprince, V. Preat, A. des Rieux, F. Danhier, Temozolomide-loaded photopolymerizable PEG-DMA-based hydrogel for the treatment of glioblastoma, J Control Release, 210 (2015) 95-104.
[31] J.B. Wolinsky, Y.L. Colson, M.W. Grinstaff, Local drug delivery strategies for cancer treatment: gels, nanoparticles, polymeric films, rods, and wafers, J Control Release, 159 (2012) 14-26.
[32] B. Heurtault, P. Saulnier, B. Pech, J.E. Proust, J.P. Benoit, A novel phase inversion-based process for the preparation of lipid nanocarriers, Pharm res, 19 (2002) 875-880.
[33] E. Moysan, Y. Gonzalez-Fernandez, N. Lautram, J. Bejaud, G. Bastiat, J.P. Benoit, An innovative hydrogel of gemcitabine-loaded lipid nanocapsules: when the drug is a key player of the nanomedicine structure, Soft Matter, 10 (2014) 1767-1777.
[34] N. Wauthoz, G. Bastiat, E. Moysan, A. Cieslak, K. Kondo, M. Zandecki, V. Moal, M.C. Rousselet, J. Hureaux, J.P. Benoit, Safe lipid nanocapsule-based gel technology to target lymph nodes and combat mediastinal metastases from an orthotopic non-small-cell lung cancer model in SCID-CB17 mice, Nanomedicine, 11 (2015) 1237-1245.
[35] R.L. Alexander, B.T. Greene, S.V. Torti, G.L. Kucera, A novel phospholipid gemcitabine conjugate is able to bypass three drug-resistance mechanisms, Cancer Chemother Pharmacol, 56 (2005) 15-21.
[36] F. Danhier, K. Messaoudi, L. Lemaire, J.P. Benoit, F. Lagarce, Combined anti-Galectin-1 and anti-EGFR siRNA-loaded chitosan-lipid nanocapsules decrease temozolomide resistance in glioblastoma: in vivo evaluation, Int J Pharm, 481 (2015) 154-161.
[37] J. Bianco, C. Bastiancich, N. Joudiou, B. Gallez, A. des Rieux, F. Danhier, Novel model of orthotopic U-87 MG glioblastoma resection in athymic nude mice, J Neurosci Methods, 284 (2017) 96-102.
[38] J.R. Mackey, R.S. Mani, M. Selner, D. Mowles, J.D. Young, J.A. Belt, C.R. Crawford, C.E. Cass, Functional nucleoside transporters are required for gemcitabine influx and manifestation of toxicity in cancer cell lines, Cancer Res, 58 (1998) 4349-4357.
[39] J. Sun, V.L. Damaraju, C.E. Cass, M.B. Sawyer, Inhibition of nucleoside transporters by tyrosine kinase inhibitors and its effects on chemotherapy efficacy, Cancer Cell & Microenvironment 1(2014) e389.
[40] J. Rieger, S. Durka, J. Streffer, J. Dichgans, M. Weller, Gemcitabine cytotoxicity of human malignant glioma cells: modulation by antioxidants, BCL-2 and dexamethasone, Eur J Pharmacol, 365 (1999) 301-308.
[41] S.Y. Cho, J. Polster, J.M. Engles, J. Hilton, E.H. Abraham, R.L. Wahl, In vitro evaluation of adenosine 5'-monophosphate as an imaging agent of tumor metabolism, J Nucl Med, 47 (2006) 837-845.
[42] X.M. Tao, J.C. Wang, J.B. Wang, Q. Feng, S.Y. Gao, L.R. Zhang, Q. Zhang, Enhanced anticancer activity of gemcitabine coupling with conjugated linoleic acid against human breast cancer in vitro and in vivo, Eur J Pharm Biopharm, 82 (2012) 401-409.
[43] P.D. Lansakara, B.L. Rodriguez, Z. Cui, Synthesis and in vitro evaluation of novel lipophilic monophosphorylated gemcitabine derivatives and their nanoparticles, Int J Pharm, 429 (2012) 123-134.

[44] R.D. Dubey, A. Saneja, P.K. Gupta, P.N. Gupta, Recent advances in drug delivery strategies for improved therapeutic efficacy of gemcitabine, Eur J Pharm Sci, 93 (2016) 147-162.
[45] D.S. Gesto, N.M. Cerqueira, P.A. Fernandes, M.J. Ramos, Gemcitabine: a critical nucleoside for cancer therapy, Curr Med Chem, 19 (2012) 1076-1087.
[46] E. Garcion, A. Lamprecht, B. Heurtault, A. Paillard, A. Aubert-Pouessel, B. Denizot, P. Menei, J.P. Benoit, A new generation of anticancer, drug-loaded, colloidal vectors reverses multidrug resistance in glioma and reduces tumor progression in rats, Mol Cancer Ther, 5 (2006) 1710-1722.
[47] A. Paillard, F. Hindre, C. Vignes-Colombeix, J.P. Benoit, E. Garcion, The importance of endo-lysosomal escape with lipid nanocapsules for drug subcellular bioavailability, Biomaterials, 31 (2010) 7542-7554.
[48] K. Sugano, M. Kansy, P. Artursson, A. Avdeef, S. Bendels, L. Di, G.F. Ecker, B. Faller, H. Fischer, G. Gerebtzoff, H. Lennernaes, F. Senner, Coexistence of passive and carrier-mediated processes in drug transport, Nat Rev Drug Discov, 9 (2010) 597-614.
[49] G. Bastiat, C.O. Pritz, C. Roider, F. Fouchet, E. Lignieres, A. Jesacher, R. Glueckert, M. Ritsch-Marte, A. Schrott-Fischer, P. Saulnier, J.P. Benoit, A new tool to ensure the fluorescent dye labeling stability of nanocarriers: a real challenge for fluorescence imaging, J Control Release, 170 (2013) 334-342.
[50] K.B. Bjugstad, K. Lampe, D.S. Kern, M. Mahoney, Biocompatibility of poly(ethylene glycol)-based hydrogels in the brain: an analysis of the glial response across space and time, J Biomed Mater Res A, 95 (2010) 79-91.
[51] E. Fournier, C. Passirani, N. Colin, S. Sagodira, P. Menei, J.P. Benoit, C.N. Montero-Menei, The brain tissue response to biodegradable poly(methylidene malonate 2.1.2)-based microspheres in the rat, Biomaterials, 27 (2006) 4963-4974.
[52] V.L. Jacobs, P.A. Valdes, W.F. Hickey, J.A. De Leo, Current review of in vivo GBM rodent models: emphasis on the CNS-1 tumour model, ASN neuro, 3 (2011) e00063.
[53] L. Qiang, Y. Yang, Y.J. Ma, F.H. Chen, L.B. Zhang, W. Liu, Q. Qi, N. Lu, L. Tao, X.T. Wang, Q.D. You, Q.L. Guo, Isolation and characterization of cancer stem like cells in human glioblastoma cell lines, Cancer letters, 279 (2009) 13-21.
[54] A. Gaudin, E. Song, A.R. King, J.K. Saucier-Sawyer, R. Bindra, D. Desmaele, P. Couvreur, W.M. Saltzman, PEGylated squalenoyl-gemcitabine nanoparticles for the treatment of glioblastoma, Biomaterials, 105 (2016) 136-144.
[55] O. Okolie, J.R. Bago, R.S. Schmid, D.M. Irvin, R.E. Bash, C.R. Miller, S.D. Hingtgen, Reactive astrocytes potentiate tumor aggressiveness in a murine glioma resection and recurrence model, Neuro Oncol, 18 (2016) 1622-1633.
[56] L. Zitvogel, A. Tesniere, L. Apetoh, F. Ghiringhelli, G. Kroemer, [Immunological aspects of anticancer chemotherapy], Bull Acad Natl Med, 192 (2008) 1469-1489.
[57] I. Szadvari, O. Krizanova, P. Babula, Athymic nude mice as an experimental model for cancer treatment, Physiol Res, 65 (2016) S441-s453.
[58] M.S. Sasso, G. Lollo, M. Pitorre, S. Solito, L. Pinton, S. Valpione, G. Bastiat, S. Mandruzzato, V. Bronte, I. Marigo, J.P. Benoit, Low dose gemcitabine-loaded lipid nanocapsules target monocytic myeloid-derived suppressor cells and potentiate cancer immunotherapy, Biomaterials, 96 (2016) 47-62.
[59] T. Wurdinger, K. Deumelandt, H.J. van der Vliet, P. Wesseling, T.D. de Gruijl, Mechanisms of intimate and long-distance cross-talk between glioma and myeloid cells: how to break a vicious cycle, Biochim Biophys Acta, 1846 (2014) 560-575.
[60] A. Tuettenberg, K. Steinbrink, D. Schuppan, Myeloid cells as orchestrators of the tumor microenvironment: novel targets for nanoparticular cancer therapy, Nanomedicine (Lond), 11 (2016) 2735-2751.
[61] B. Raychaudhuri, P. Rayman, J. Ireland, J. Ko, B. Rini, E.C. Borden, J. Garcia, M.A. Vogelbaum, J. Finke, Myeloid-derived suppressor cell accumulation and function in patients with newly diagnosed glioblastoma, Neuro Oncol, 13 (2011) 591-599.

6. SUPPLEMENTARY MATERIAL

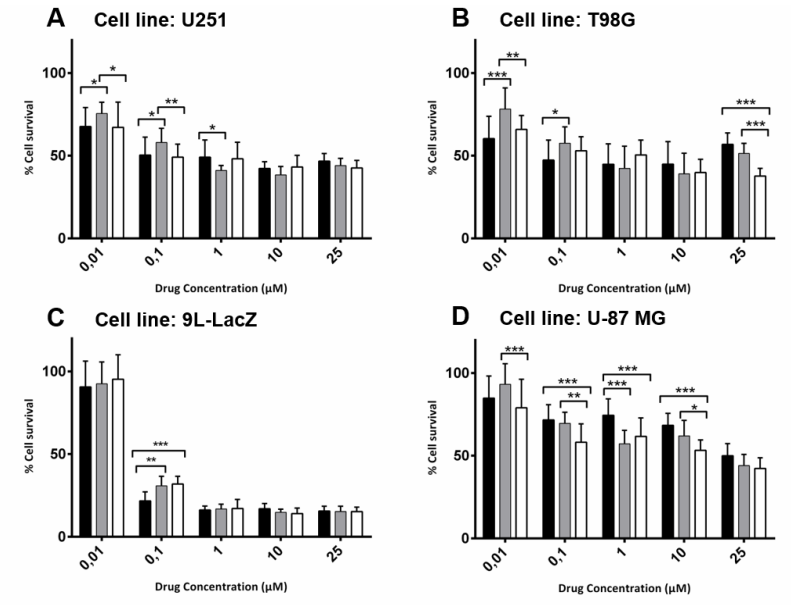

Figure S1. *In vitro* cytotoxicity studies on (**A**) U251, (**B**) T98G, (**C**) 9L-LacZ, and (**D**) U-87 MG glioma cells. Crystal violet staining after 48 hours of incubation of different concentrations of GemHCl (black bar), $GemC_{12}$ (gray bar) or $GemC_{12}$-LNC (white bar). *** p<0.001 ** *p*<0.01, * *p*<0.05 Two-way ANOVA (N=3; *n*=18)

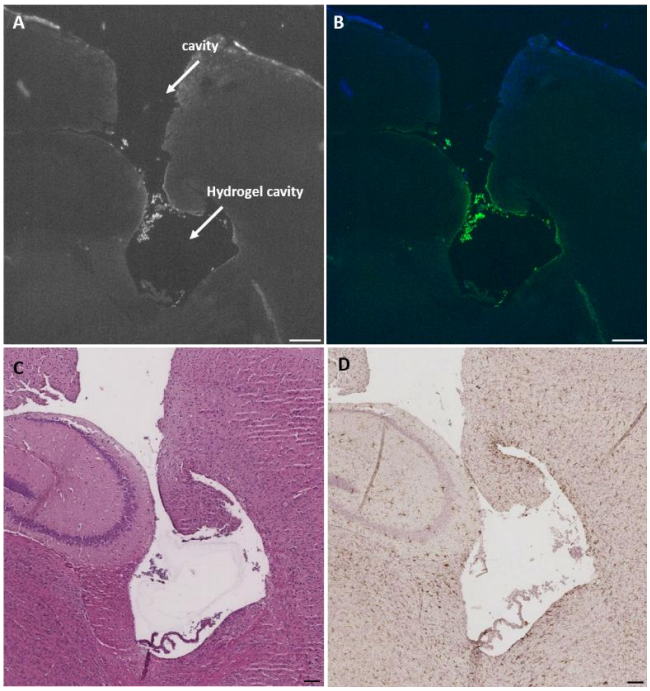

Figure S2. *In vivo* mid-term tolerability assay. Image of one of the $GemC_{12}$-LNC treated animals, after two months of the administration of the hydrogel. A cavity can be observed below hole/cavity created in the cortex, where the treatment had been injected. It could correspond to the space occupied by the hydrogel. The images correspond to (A, B) TUNEL assay; (C) Hematoxylin & Eosin staining; (D) Iba-1 staining. Scale bar: 100 µm.

CHAPTER VI.

EVALUATION OF LAUROYL-GEMCITABINE LIPID NANOCAPSULE HYDROGEL EFFICACY IN GLIOBLASTOMA RAT MODELS

Adapted from:
Bastiancich C, Lemaire L, Bianco J, Franconi F, Danhier F, Préat V, Bastiat G, Lagarce F,. Evaluation of Lauroyl-gemcitabine lipid nanocapsule hydrogel efficacy in glioblastoma rat models. *Submitted in February 2018*.

ABSTRACT

The local delivery of anti-cancer drug loaded hydrogels in the tumor resection cavity of glioblastomas (GBM) is a promising strategy for the treatment of these incurable brain tumors. The development of a controlled-release delivery system for the local treatment in the brain requires it to be tested in different animal and tumor models able to mimic, at least partially, the clinical setting.

Recently, we reported the feasibility, efficacy and tolerability of an hydrogel made of lipid nanocapsules loaded with lauroyl-gemcitabine ($GemC_{12}$-LNC), an amphiphilic derivative of Gemcitabine, for the local treatment of GBM. Its ability to slow down tumor recurrences was tested in a U-87 MG xenograft model in nude mice after intratumoral administration and perisurgical administration in the tumor resection cavity.

In this study, we developed a reliable and reproducible surgical procedure to resect orthotopic GBM tumors in rats. This technique was then used to evaluate the integrity of the LNC after administration of $GemC_{12}$-LNC in the resection cavity of healthy rats and to evaluate the ability of $GemC_{12}$-LNC to slow down recurrences formation after perisurgical administration in syngeneic GBM-bearing rats. Our results confirm that this hydrogel, uniquely formed by a nanocarrier and a cytotoxic drug, could be a promising and safe delivery tool for the local treatment of operable GBM tumors.

Keywords

Local delivery, Hydrogel, Lipid nanocapsules, Glioblastoma, Resection, MRI, Rat

TABLE OF CONTENTS

1. INTRODUCTION

Gemcitabine (Gem) is a chemotherapeutic agent approved for the treatment of pancreatic, non-small-cell lung, breast and ovarian cancers, alone or in combination with other active molecules. This nucleoside analogue is a powerful chemotherapeutic agent, presenting radiosensitizing properties at low concentrations and possessing significant immunomodulatory activity. Gem has been tested on a variety of tumors, both in preclinical and clinical studies, including glioblastoma (GBM) [1-3].

GBM is an aggressive and malignant brain tumor. Its standard of care treatment includes surgical debulking of the tumor followed by radiotherapy and concomitant chemotherapy with temozolomide (TMZ) a few weeks after surgery to allow for patient recovery [4]. However, due to its high heterogeneity, fast proliferation and unique biological characteristics, GBM remains incurable. Therefore, finding new therapeutic strategies represents an unmet medical and pharmaceutical need [5]. Following standard treatment, GBM always develop recurrences which lead to patient death. One of the main causes of GBM recurrence is their innate or acquired chemoresistance to alkylating agents and the presence of a subpopulation of cancer stem cells (CSCs) with self-renewing capabilities [6]. As 90% of these recurrences appear around the resection cavity borders, the local delivery of chemotherapeutic drugs in the gap period between surgery and standard care chemoradiation seems an attractive strategy [7]. To date, the only treatment approved for GBM local management is represented by the carmustine (BCNU) wafers Gliadel®. Treatment with Gliadel® shows only modest clinical benefit and its use on newly diagnosed GBM patients is controversial due to fast drug-release, implant dislodgements and possible side effects [8-10]. The combination of perisurgical Gliadel® followed by radio-chemotherapy with TMZ might increase the clinical benefit [9, 11]. However, to overcome the intrinsic and acquired chemoresistance mechanisms of GBM cells to alkylating agents (e.g. DNA repair enzyme O_6-methylguanine methyltransferase, MGMT [12]), combining TMZ with drugs with a different mechanism of action could be a more efficient choice.

Gem has an MGMT-independent mechanism of action, has shown to work in combination with several active agents and is able to pass the blood-tumor barrier in GBM patients, promoting a high rationale for its use against GBM [1]. Recently, we reported the feasibility,

efficacy and tolerability of a hydrogel made of lipid nanocapsules loaded with lauroyl-gemcitabine ($GemC_{12}$-LNC), an amphiphilic derivative of Gem, for the local treatment of GBM [13, 14]. This injectable formulation is only formed of lipid nanocapsules and the cytotoxic drug, and is prepared by a cost-effective and solvent-free method with the use of FDA-approved components [15]. Its mechanical properties are adapted for brain implantation, and the degradation of the hydrogel corresponds to the sustained release of the drug, which lasts over 1 month *in vitro* [14]. *In vivo*, this system is well tolerated in mouse brain and reduces tumor growth in a murine orthotopic human xenograft GBM model after intratumoral administration [13]. Gaudin *et* al. have also confirmed the rationale for the use of Gem derivatives for GBM, showing significantly improved therapeutic efficacy in RG2 tumor-bearing animals after local treatment with squalene-gemcitabine nanoparticles [16].

The efficacy of local delivery systems needs to be proven in different and adequate preclinical models that are able to mimic, at least partially, the clinical setting. Several GBM orthotopic rodent models are available to evaluate the *in vivo* efficacy of new therapeutic strategies, depending on the growth profile and histologic markers requested from the model. To have a more clinically-relevant model, some authors have also developed and validated surgical techniques to resect GBM orthotopic tumors [17-20]. These resection models could be used in healthy rodents to test the tolerability, drug distribution, *in vivo* release kinetics of the drug after perisurgical local administration or they could be used in tumor-bearing animals to test the efficacy of local delivery systems in reducing GBM recurrences.

Recently we developed a simple and reliable resection technique using a U-87 MG xenograft model in nude mice, based on the use of a biopsy punch to cut the brain region where the tumor is located [21]. This procedure was successfully used to demonstrate the ability of $GemC_{12}$-LNC hydrogel to slow down recurrences formation [13]. However, the U-87 MG model presents some limitations. Firstly, in this model human glioma cells are implanted in immunodeficient mice (T cell-deficient), which lack of adaptive immune response, and therefore their use for immunological studies is limited [22, 23]. Secondly, testing local delivery system on a bigger rodent model (e.g. rat) would allow to obtain a better *in vivo* localization and imaging of the tumor and to administer higher volumes of hydrogel [24].

In this study, we aimed at adapting the 'biopsy punch' surgical resection technique from mouse to rat to test the perisurgical administration of anticancer drug loaded hydrogels in the resection cavity. This model was used to evaluate the integrity of the LNC after administration of GemC$_{12}$-LNC in the resection cavity by fluorescence resonance energy transfer (FRET) and to assess the ability of GemC$_{12}$-LNC to slow down recurrences formation after perisurgical administration in syngeneic GBM-bearing rats. As evaluating the tumor recurrences over time is crucial in the development of a reliable and reproducible surgical resection technique, we performed a longitudinal Magnetic Resonance Imaging (MRI) study on all the animals.

2. MATERIALS AND METHODS

2.1. FORMULATION OF LAUROYL-GEMCITABINE LIPID NANOCAPSULES HYDROGEL (GEMC12-LNC)

The hydrogel formulation of GemC$_{12}$-LNC 7.5% drug/Labrafac® *w/w* (GemC$_{12}$-LNC) was prepared, as previously reported in the literature, using a phase-inversion method [25]. Briefly, 0.031 g of GemC$_{12}$ (synthesized as previously described [14]), 0.42 g of Labrafac® (Gattefossé, France) and 0.83 g of Span 80 (Sigma-Aldrich, USA) were weighed and stirred in a water bath at 50°C with 200 µL of acetone (VWR Chemicals, Belgium) until complete dissolution of the drug. The acetone was then allowed to evaporate and 0.322 g of Kolliphor® (Sigma-Aldrich, Germany), 0.015 g of Sodium Chloride (VWR Chemicals, Belgium) and 0.340 g of injectable water (Braun, Germany) were added to the formulation. Three cycles of heating and cooling were performed under magnetic stirring (500 rpm) between 40 and 70°C. During the last cooling cycle, 0.71 g of injectable water was added and the formulation stirred for one more minute. The formulations were then inserted into insulin syringes (BD Micro-Fine™ needle 0.30 ml, diameter 30 G; Becton Dickinson, France) before the gelation process occurred, and stored at 4°C until further use. For the GemC$_{12}$-LNC 10% formulation the amount of GemC$_{12}$ was increased to 0.042 g (10% drug/Labrafac® w/w).

For FRET studies, a GemC$_{12}$-LNC hydrogel formulation containing DiI (λ_{exc} = 549 nm / λ_{em} = 575 nm; 1,1'-Dioctadecyl-3,3,3',3'-Tetramethylindocarbocyanine Perchlorate; Thermo Fischer Scientific, USA) and DiD (λ_{exc} = 644 nm / λ_{em} = 665 nm; 1,1'-Dioctadecyl-3,3,3',3'-Tetramethylindodicarbocyanine Perchlorate; Thermo Fischer Scientific, USA) fluorescent dyes was developed (0.8 *w/w* ratio between DiD and DiI). For the DiI-DiD-GemC$_{12}$-LNC, 1.015 mg of DiI and 0.785 mg of DiD were added to the first step of the formulation process, which was then carried on as previously described, protected from light. All the formulations were obtained under aseptic conditions.

2.2. *EX VIVO* EVALUATION OF THE LNC INTEGRITY IN THE GEMC12-LNC OVER TIME

In vitro preliminary studies were performed to evaluate the presence of FRET signal. Thirty µL of DiI-DiD-GemC$_{12}$-LNC hydrogel was placed in a 1.5 mL Eppendorf® tube (Hamburg,

Germany) and analyzed using a fluorescence CRI Maestro™ In-Vivo Imaging System (Woburn, USA) (λ_{exc}: 550 nm.; exposition time: 4 ms).

For the *in vivo* studies, all animal experiments were performed following the regulations of the French Ministry of Agriculture and approved by the Pays de la Loire Ethics in Animal Experimentation Committee (project number 01858.03). Animals had free access to water and food, their weight was constantly monitored throughout the experiments.

Six-week-old female Sprague Dawley rats (Angers University/Hospital Animal Facility, France) were anesthetized by intraperitoneal injection of ketamine/xylazine (33.3 and 13.3 mg/kg, respectively) and fixed in a stereotactic frame. A 10 mm incision was made in the midline and a 3.1 diameter circular cranial window was created 0 mm anterior and 2.1 mm lateral from the bregma. A 3 mm diameter biopsy punch (Kai Medical, Germany) was then inserted 4 mm deep and twisted for 15 s to cut the brain tissue and a resection cavity was created using a vacuum pump to remove the brain tissue (KNF Neuberger SAS, France). Fifteen µL of DiI-DiD-GemC$_{12}$-LNC hydrogel were injected in the resection cavity, which was then sealed with a 5 x 5 mm square piece of Neuro-Patch® (Aesculap, Germany) impregnated with a reconstituted fibrin hydrogel (25 mg/mL fibrin, 10 IU/mL thrombin, equal volumes; Baxter Innovations, Austria). At different time points (4 h, 24 h, 48 h and one week), the animals were sacrificed and freshly extracted brains were analyzed using a fluorescence CRI Maestro™ In-Vivo Imaging System (*n*=3 for 4 h, 24 h, 48 h; *n*=2 for one week) (λ_{exc}: 550 nm; exposition time: 3000 ms).

For the one-week time four more animals received the resection and hydrogel administration and, after sacrifice, the brains were extracted and fixed in 10% formalin solution (Merck, Germany) overnight. The brains were then rinsed in PBS, cryoprotected with 30% sucrose solution for 24 hours. Brains were sectioned at 12 µm using a Leica CM 1950 cryostat (Leica Biosystems Nussloch GmbH, Germany) and stored at -20°C. For fluorescent analysis, cell nuclei were counterstained through staining with DAPI (1µM in PBS, Sigma, USA) for 10 minutes and away from light and then rinsed with PBS. Sections were mounted with Highdef® IHC fluoromount (Enzo Life Sciences, USA) and visualized by fluorescence through a Pannoramic P250 Flash III whole-slide scanner (3DHistech, Hungary). DAPI channel with exposure time 20 ms, CY3 channel with exposure time 50 ms and CY5 channel with exposure time 100 ms were used for DAPI, DiI and DiD, respectively.

2.3. DEVELOPMENT OF AN ORTHOTOPIC GLIOBLASTOMA TUMOR MODEL IN RATS AND ITS SURGICAL RESECTION VIA THE "BIOPSY PUNCH" TECHNIQUE

2.3.1. In vitro cell culture

9L cells (ECACC, UK) were cultured in Eagle's Minimum Essential Medium with Glutamine (Lonza, Belgium) supplemented with 1% Non-essential amino acids (10 mM; Lonza, Belgium). C6 cells (ECACC, UK) were cultured in Ham's F-12 medium with Glutamine (Lonza, France) while 9L-LacZ cells (ATTC, USA) were cultured in Dulbecco's modified Eagle's Medium with 4.5 g/L glucose, 0.58 g/L L-glutamine and 0.11 g/L sodium pyruvate (Gibco, Life Technologies, USA). Medias were supplemented with 10% Fetal Bovine Serum (FBS; Gibco, Life Technologies USA), 100 U/mL penicillin G sodium and 100 µg/mL streptomycin sulfate (Gibco, Life Technologies, USA). Cells were subcultured in 75 cm^2 culture flasks (Corning® T-75, Sigma-Aldrich, USA) and incubated at 37°C and 5% CO_2.

2.3.2. C6, 9L and 9L-LacZ glioma orthotopic models

Seven-week-old female Sprague Dawley rats (Angers University/Hospital Animal Facility, France) were used for the C6 model and seven-week-old female Fischer rats (Janvier, France) were used for the 9L and 9L-LacZ models.

The animals were anesthetized by intraperitoneal injection of ketamine/xylazine and fixed in a stereotactic frame. In order to obtain cortical tumors, 2 x 10^4 C6 or 1 x 10^3 9L or 9L-LacZ glioma cells were injected in the right frontal lobe trough a 0.3 mm diameter drilled hole using a Hamilton syringe fitted with a 32G needle. The injection coordinates were 0 mm anterior, 3 mm lateral from the bregma and 3.5 mm deep from the outer border of the cranium, respectively. The presence, volume and location of the tumors were determined by MRI, which was performed for all rats included in the study before and after the surgical resection of the tumor.

2.3.3. Magnetic Resonance Imaging

MRI was performed using a 7T scanner (Biospec 70/20 Avance III, Bruker Wissembourg, France) equipped with a BGA12S gradient system (675mT/m). Animal body temperature was

maintained throughout the experiment by hot water circulation in an animal bed. During the MRI protocol, rats were anesthetized with 1% isoflurane and respiration was monitored. All imaging and spectroscopy acquisitions were performed using ParaVision® 6.0.1, using an 86 mm proton volume resonator for radiofrequency excitation and an actively decoupled 4channels-phased array surface coil for signal reception.

Tumor volume was assessed using rapid acquisition with relaxation enhancement (RARE) sequence (repetition time (TR) = 3200 ms; effective echo time (TE_{eff}) = 64 ms; field of view (FOV) = 3 x 3 cm; Slice thickness = 0.75 mm and 12 contiguous slices). Tumor volumes were calculated from manually drawn regions of interest.

After a first and second order shim over the brain, a single-shot 2D-Echo planar imaging sequence (TR /TE_{eff} 3000/20.5 ms) with 126 diffusion encoding directions was performed, with the duration of the gradient set to δ= 2.5 ms and the time between the diffusion gradient set to Δ=7.5 ms, leading to a b=670 s/mm^2 value. The geometrical parameters were fixed at FOV=3 x 3 cm. Five contiguous slices of 0.8 mm were acquired. The matrix size was defined at 128 x128 leading to an in-plane resolution of 234 µm x 234 µm. Twofold accelerated parallel imaging was used in combination with GRAPPA reconstruction, using 26 reference phase-encoding lines.

^{1}H Magnetic Resonance Spectroscopy (MRS) was performed using a PRESS sequence with water suppression under the following parameters: TR/TE_{eff} 2500/9.8 ms; NEX = 128; voxel size (3 mm x 3 mm x 3 mm).

2.3.4. Anti-tumor efficacy after perisurgical administration of the hydrogels in the resection cavity

At day 10 or day 9 post-tumor inoculation for the C6 and 9L animals, respectively (see supplementary data S1 for 9L-LacZ animals), the tumor resection was performed using the biopsy-punch resection model, adapted from Bianco *et* al. [21]. Briefly, animals were anaesthetized with ketamine/xylazine and immobilized in a stereotactic frame. A 10 mm incision was made in the midline along the previous surgical scar and a 3.1 diameter circular cranial window was created around the previous burr hole using a high-speed drill (Vellman, Belgium) to expose the brain. A 3 mm diameter biopsy punch (Kai Medical, Germany) was

then inserted 4 mm deep and twisted for 15 s to cut the brain/tumor tissue. Once withdrawn, the tumor and brain tissues were aspired using a vacuum pump (KNF Neuberger SAS, France). Between 2.5 and 15 µL of treatment (depending on the group) was placed into the resection cavity before sealing the cranial window with a 5 x 5 mm square piece of Neuro-Patch® (Aesculap, Germany) impregnated with a reconstituted fibrin hydrogel (25 mg/mL fibrin, 10 IU/mL thrombin, equal volumes; Baxter Innovations, Austria).

Animals presenting C6 tumors were divided into four groups at day 10 post-tumor inoculation: untreated (*n*=5); resection and no treatment (*n*=5); resection and local administration of $GemC_{12}$ dissolved in Water/Ethanol/Tween®80 (6.9/87.6/5.5 v/v), 4.8 µL (*n*=5); resection and local administration of $GemC_{12}$-LNC, 15 µL (*n*=5).

Animals presenting 9L tumors were divided into groups 9 days post-tumor inoculation as follows: Group 1: no resection, no treatment (*n*=9); Group 2: resection, no treatment (*n*=7); Group 3: resection and local administration of $GemC_{12}$ dissolved in Water/Ethanol/Tween®80 (6.9/87.6/5.5 v/v), 4.8 µL (*n*=7); Group 4: resection and local administration of $GemC_{12}$-LNC, 15 µL (*n*=7); Group 5: resection and local administration of $GemC_{12}$-LNC 10% (10% $GemC_{12}$/Labrafac®), 10 µL (*n*=4); Group 6: resection and local administration of $GemC_{12}$-LNC, 5 µL (*n*=5). The $GemC_{12}$ dose for all the treated groups was 1.4 mg/kg except for the last group where it was reduced to 0.4 mg/kg.

All animals were monitored daily and MRI follow-up was performed every week after surgery. Animals were sacrificed when they presented behavior changes (lack of grooming), clinical signs of distress (paralysis, arched back, lack of movement) and 20% body weight loss.

2.4. STATISTICAL ANALYSIS

Statistical analysis was performed using GraphPad Prism (GraphPad Software, USA) and determined based on $p < 0.05$. For the *in vivo* efficacy studies, the statistical analysis was estimated from comparison of Kaplan-Meier survival curves using the log-rank test (Mantel Cox test).

3. RESULTS

3.1. EVALUATION OF THE LNC INTEGRITY OVER TIME BY FRET

A DiI-DiD-GemC$_{12}$-LNC hydrogel formulation was developed and *in vitro* preliminary studies were performed to evaluate the presence of FRET signal (Figure 1A). A small DiI emission peak was present at the DiI maximum emission wavelength and a bigger emission peak was observed at 680 nm, corresponding to the FRET signal. The ratio between donor and acceptor peaks was 0.3, concordantly to the FRET values in the literature for the DiI/DiD pair in LNC with the same donor/acceptor *w/w* ratio [26].

To evaluate the presence of FRET signal *ex vivo*, a resection cavity was created in healthy rats and 15 µL of DiI-DiD-GemC$_{12}$-LNC hydrogel was locally administered. Seven days after surgery and hydrogel injection, a fluorescent signal was observed at 680 nm at the administration site on freshly extracted brains (Figure 1B). Cutting the resection cavity region in two, the hydrogel was visible and two different spectra were observed (Figure 1C). In the first, on the lateral borders of the hydrogel, a similar fluorescence intensity between donor and acceptor was observed (donor/acceptor ratio 0.75) which could correspond to LNC break down. In the second, observed in the central region of the hydrogel, FRET signal comparable to the *in vitro* studies was detected (donor/acceptor ratio 0.3), confirming that a part of the LNC in the hydrogel maintained their integrity over time. Similar results were observed at 4h, 24h and 48h with different intensities.

Interestingly, when intense bleeding or swelling was observed during surgery no FRET signal was observed, even after a short period of incubation (4h, 24h; supplementary data S2). We hypothesize that, in this case, the hydrogel is expelled from the resection cavity due to the high liquid pressure or absorbed to the Neuro-Patch®.

The presence of the hydrogel in the resection cavity, one week after surgery, was also confirmed by the concomitant fluorescent signal of DiI and DiD in the region around the resection cavity in histological sections of the brains (Figure 2).

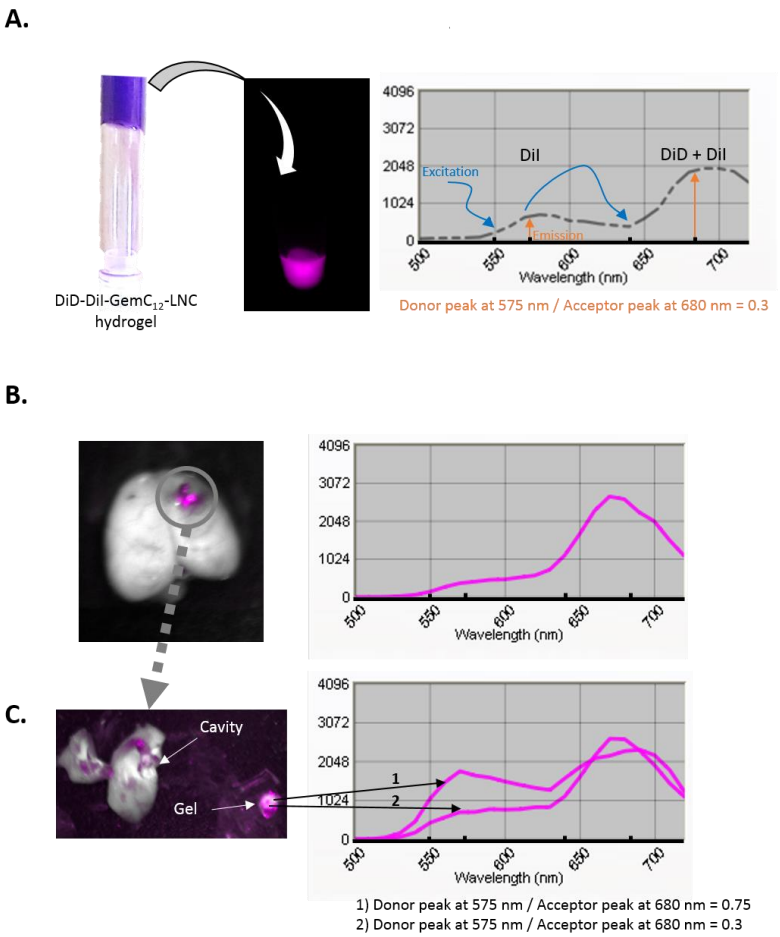

Figure 1. Evaluation of LNC integrity after administration in the brain using the FRET technique. **(A)** *In vitro* studies: DiI-DiD-GemC12-LNC hydrogel was prepared and excited at 550 nm (exposition time 4 ms). A small donor (DiI) emission peak is observed at 575 nm, while a bigger acceptor (DiD) peak is observed at 680 nm. The ratio between these peaks is 0.3, which confirms the presence of FRET and the LNC integrity in the gel structure. **(B)** One week after administration of DiI-DiD-GemC12-LNC hydrogel in the brain a fluorescent signal is observed at the site of administration (λ_{exc}: 550 nm; exposition time: 3000 ms). **(C)** When cutting the brain in the cavity, the gel is still visible and results in two different fluorescent spectras: one with DiI and DiD peaks of similar intensity corresponding to the lateral borders of the hydrogel (spectra 1: donor/acceptor peak ratio 0.75); the second one corresponding to the central region of the hydrogel, with FRET signal (spectra 2: donor/acceptor peak ratio 0.3).

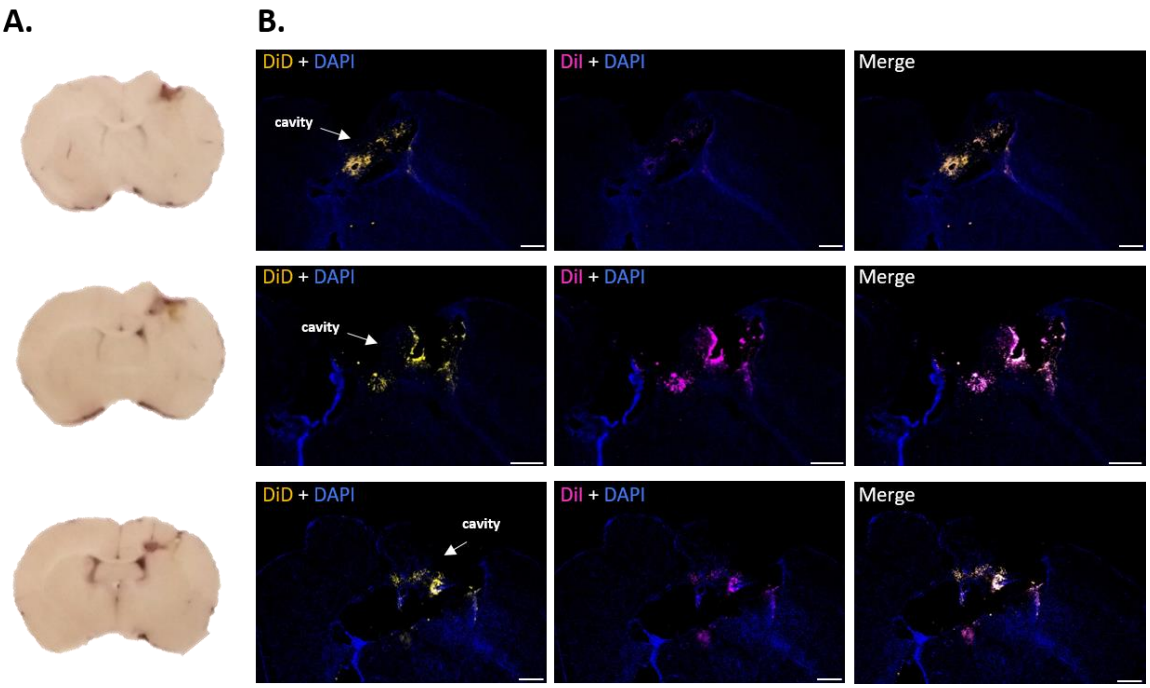

Figure 2. Evaluation of the LNC integrity and presence in the resection cavity one week after administration in the brain using fluorescence microscopy. Cryostat histological sections show the brain in the resection cavity region: a darker signal corresponding to the DiI-DiD-GemC$_{12}$-LNC hydrogel is visible in the resection area **(A)** and corresponds to the DiI and DiD fluorescent signal **(B)**. The two fluorophores overlap in the region around the cavity borders. Blue: cell nuclei (DAPI); Pink: DiI; Yellow: DiD. Scale bar: 500 µm.

3.2. ANTI-TUMOR EFFICACY OF GEMC$_{12}$-LNC AFTER PERISURGICAL ADMINISTRATION IN THE RESECTION CAVITY OF C6 TUMOR-BEARING RATS

The tumoral lesion of C6 bearing animals appeared as a less hyperintense signal compared to the 9L tumors (supplementary data, Figure S3B) and was harder to visualize. However, all animals developed tumors between the cortex and the striatum and the resection was performed at day 10 post-inoculation. Interestingly, one untreated animal with a visible tumor on day 6 (volume of 0.5 mm^3), presented hypo-signal (corresponding to necrosis or bleeding) at day 10 and eventually died at day 18. The remaining animals did not show signs of tumor hemorragia.

Eight days after resection surgery (day 18 post-inoculation), the animals who received treatments (GemC$_{12}$ and GemC$_{12}$-LNC) presented very small recurrent tumors or no tumors while the untreated or resected untreated animals presented larger tumors. The tumor volumes were significantly different (Figure 3A, *p <0.05). However, ten days later (day 28 post-inoculation), all the tumors of the untreated animals (both unresected untreated and resected untreated) disappeared (Figure 3B-C).

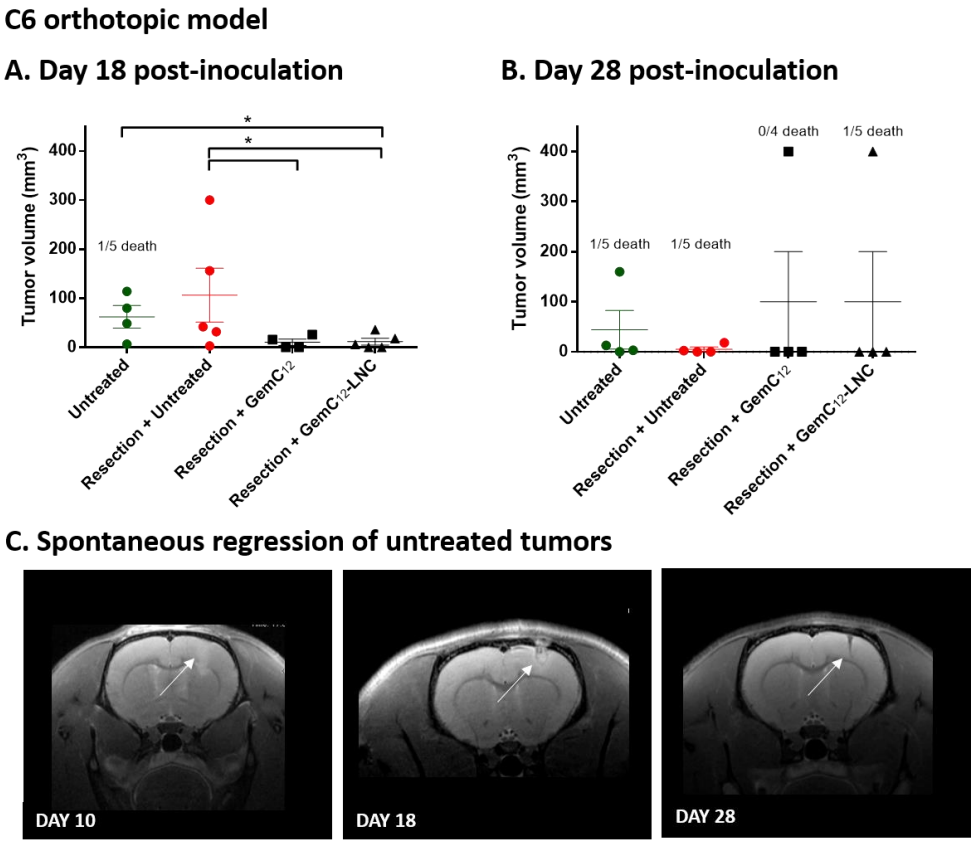

Figure 3. C6 orthotopic model: **(A, B)** Tumor volumes at day 18 or 28 post tumor-inoculation (resection performed 10 days post-tumor inoculation). A reduction of tumor volumes in the tumors was observed between day 18 and 28 for the untreated groups. **p* <0.05, Mann-Whitney test. **(C)** Axial T_2-weighted image of an untreated rat brain at different time points: a spontaneous regression of the tumor can be observed.

3.3. ANTI-TUMOR EFFICACY OF GEMC12-LNC AFTER PERISURGICAL ADMINISTRATION IN THE RESECTION CAVITY OF 9L TUMOR-BEARING RATS

Tumors were detected in all 9L-bearing animals between the cortex and the striatum (Figure 4A). To determine the ability of 9L tumors to form tumor recurrences, animals were divided into two groups and received surgical resection either at day 9 or day 14 post-tumor implantation and were followed by MRI every week. Axial T_2-weighted images as well as MRI mean diffusivity map and proton Magnetic Resonance Spectroscopy (MRS) confirmed the presence of recurrent tumors in both groups. These tumors were initially localized to the resection cavity borders and then quickly spread throughout the brain with high aggressiveness as shown in Figure 4B. In the first image, a hypersignal corresponding to the tumor tissue is observed in the region where the resection was performed 8 days earlier. On the mean diffusivity map, the apparent diffusion coefficient measured over the hyperintense region on the T_2-weighted image was ~0.0012 mm^2/s whereas on normal tissue, i.e. contralateral brain, a value of ~0.0008 mm^2/s is measured [27, 28]. The MRS shows the

presence of peaks at 3.2, 3.0, 2.0 and 1.3 ppm, corresponding to choline, creatine, N-acetyl aspartate and lactate, respectively. The high Choline/Creatine ratio, the low intensity of NAA peak and the presence of lactate (observable at echo time 10 ms and confirmed by an inversed peak at echo time 135 ms) represent increased membrane turnover, loss/dysfunction of normal neuronal tissue and anaerobic glycolysis respectively, which are characteristic of tumor tissue [29, 30].

Based on these results, the resection time for further experiments was established at day-9 post-tumor inoculation as this was the maximum delay to observe a significant difference in survival time between unresected untreated animals and resected untreated animals (25 *vs* 28 days respectively; * p<0.05, Figure 5B).

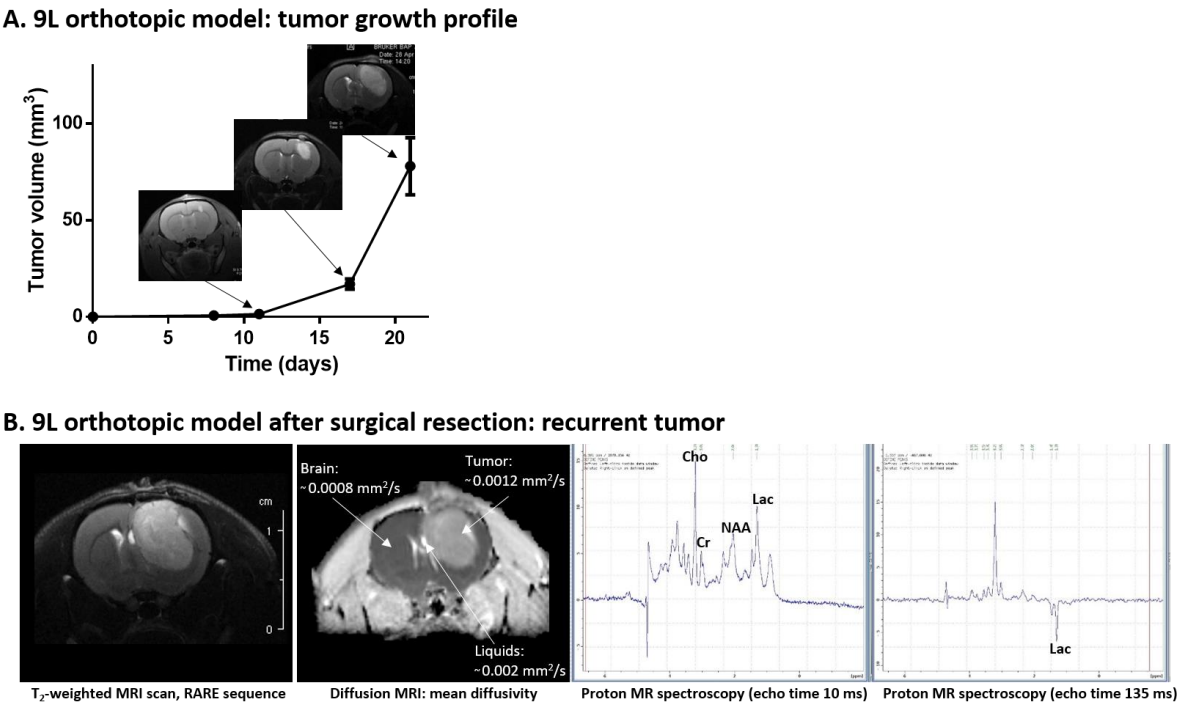

Figure 4. MRI images of 9L orthotopic tumors. **(A)** Tumor growth profile after injection of 1 x 10^3 9L cells: axial (T_2-weighted) images of rat brain at different time points after cell inoculation. **(B)** MRI follow-up after tumor resection to evaluate the presence of recurrences: axial (T_2-weighted) image, mean diffusivity map and proton MRS (echo time 10 ms and 135 ms) of rat brain 8 days post-resection. (Cho: choline; Cr: creatine; NAA: N-acetyl aspartate; Lac: lactate).

To evaluate the anti-tumor efficacy of GemC$_{12}$-LNC in 9L tumor-bearing rats, we injected 5 or 15 µL of GemC$_{12}$-LNC perisurgically in the resection cavity (corresponding to 0.4 or 1.4 mg/kg of GemC$_{12}$, respectively). The resection procedure and results are presented in Figure 5A-B. At the lower dose, a significant increase in animal survival was observed after treatment with the hydrogel compared to the untreated controls (** p<0.01). The development of

recurrences however occurred in all animals leading to animal's death. Surprisingly, at the highest dose, the treatment with $GemC_{12}$-LNC did not result in an increased survival time compared to the controls. At this dose, the treatment with $GemC_{12}$ (in Water/Ethanol/Tween®80, 4.8 µL) resulted in a delay of tumor recurrences and increased survival of the animals (** p<0.01). Two animals of this group never developed recurrences and were long-term survivors (survived >150 days post-tumor inoculation).

As the amount of liquid and blood leakage during the surgeries performed on Fischer rats was considerable, possibly due to higher intracranial pressure compared to Sprague-Dawley rats [31], and our previous observation of a correlation between fluid leakage and hydrogel expulsion from the administration site (supplementary data S2), we hypothesized that the lack of efficacy after perisurgical administration of 15 µL of $GemC_{12}$-LNC could be due to hydrogel leakage out of the resection cavity.

To test this hypothesis, a $GemC_{12}$-LNC containing 10% drug/Labrafac® ratio *w/w* was formulated and only 10 µL of this hydrogel (corresponding to the same dose as 15 µL of $GemC_{12}$-LNC 7.5%, 1.4 mg/kg) was injected into the tumor resection cavity 9 days post-tumor inoculation. The result is presented in Figure 5B (red line) and shows that injecting a reduced volume of hydrogel while maintaining the same drug dose results in tumor recurrences delay or inhibition (50% of animals were long-term survivors), with a significant increase of the survival time of the animals (** p<0.01). Figure 5C represents an example of rat brain one week after resection and local administration of $GemC_{12}$-LNC 10%. On the T_2-weighted image an intense hypersignal corresponding to the resection cavity is visible, and is characterized on the mean diffusivity map by a high apparent diffusion coefficient value of ~0.002 mm^2/s, consistent with a 'liquid state' which could be assumed to be the hydrogel. Just below, a slight signal with a diffusion coefficient of ~0.0012 mm^2/s could represent a recurrent tumor. However, the MRS spectrum of this lower region shows absence of lactate peak and choline, with creatine and N-acetyl aspartate peaks corresponding to normal tissue. The fractional anisotropy image shows lack of preferential directionality in the two regions, which are isotropic, meaning lack of structured tissue in the area. This animal, and the other long-term survivors, were monitored with MRI for five months after treatment and never presented a tumor recurrence.

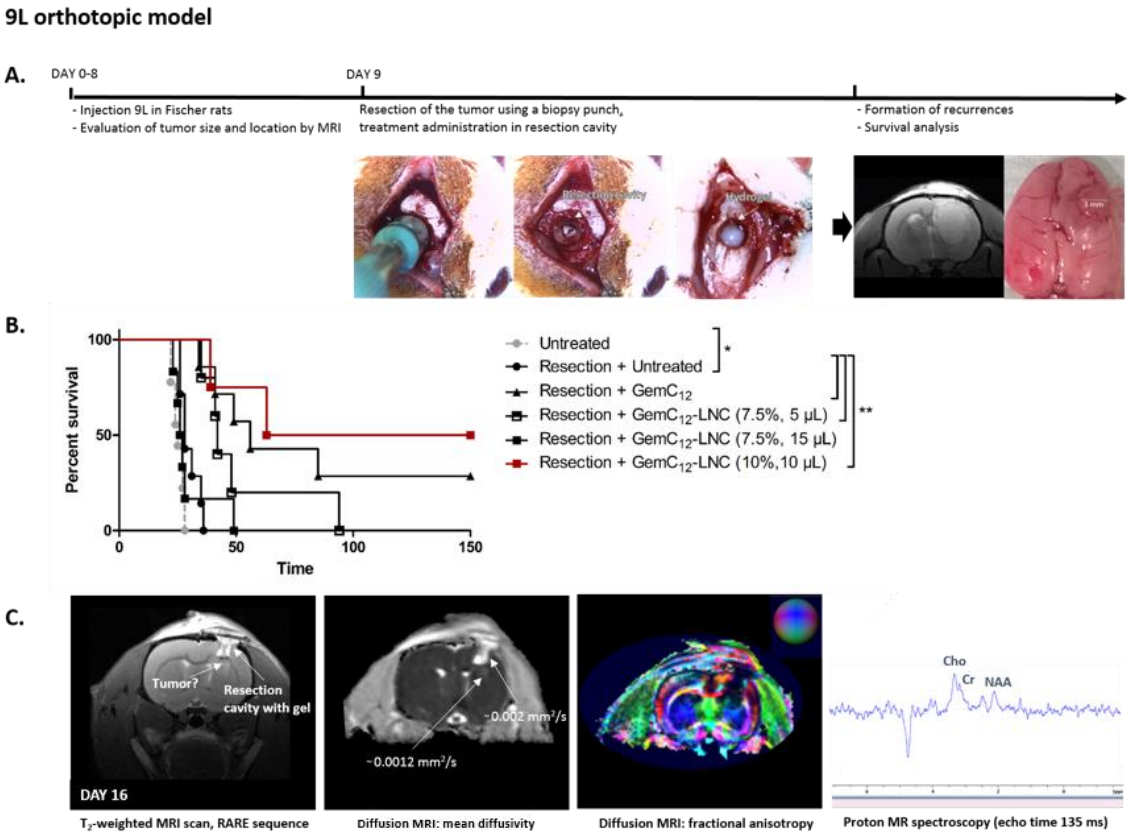

Figure 5. Anti-tumor efficacy studies on 9L orthotopic model after perisurgical administration in the resection cavity. **(A)** Time schedule of the anti-tumor efficacy studies using a 9L orthotopic tumor model. Below, images taken during the tumor resection surgeries (biopsy punch, resection cavity, hydrogel administration), an MRI follow-up image showing a recurrent tumor and the physical aspect of the brain after extraction (presenting a recurrent tumor around the resection cavity borders, top right). **(B)** Kaplan-Meier survival curves for animals untreated or resected and treated (resection performed 9 days post-tumor inoculation). Drug dose administered: 0.4 mg/kg for group $GemC_{12}$-LNC 7.5%, 5 µL or 1.4 mg/kg for the other groups. Mantel Cox test (* $p<0.05$; ** $p<0.01$). **(C)** MRI follow-up after tumor resection and $GemC_{12}$-LNC 10% administration: axial T_2-weighted image, mean diffusivity map, tractography and proton MR spectroscopy (echo time 135 ms) of rat brain at day 16 post-inoculation **(**Cho: choline; Cr: creatine; NAA: N-acetyl aspartate).

4. DISCUSSION

We have previously shown that $GemC_{12}$-LNC hydrogel can delay tumor recurrences after perisurgical administration in the tumor resection cavity of a xenogeneic U-87 MG murine model. In this work, our objective was to evaluate if $GemC_{12}$-LNC hydrogel could be as effective in a syngeneic and bigger model. For this reason, the 'biopsy punch' surgical procedure to resect orthotopic tumors needed to be adapted from mouse to rat.

Several parameters need to be considered while transposing a surgical procedure from a preclinical model in mouse to a preclinical model in rat, including the biopsy punch characteristics, the type of tumor (e.g. rat strains, inoculating cell line), the tumor growth profile, the delay between cell inoculation and tumor resection, and the formation of recurrences over time. The final parameters chosen for this work are presented in Table 1.

Table 1. Comparison between the "biopsy punch" surgical resection technique parameters in mice [21] and rats

		MOUSE	**RAT**
Type of Tumor	Cortical *vs* Striatal	Cortical	Cortical
	Injection coordinates	0.5 mm P, 2.1 mm L, 2.5 mm D	0 mm P, 3 mm L, 3.5 mm D
	Cell line	U-87 MG, 3 x 10^4 cells/mouse	9L, 1 x 10^3 cells/rat
	Species and strain	Nude NMRI mice	Fischer rats
Max hydrogel volume / $GemC_{12}$ dosis		5 µL (3 mg/kg)	15 µL (1.4 mg/kg)
Time of death without resection and time of resection		24 days, resection at day 13	25 days, resection at day 9
Biopsy punch characteristics		2 mm diameter, 3 mm depth	3 mm diameter, 4 mm depth

For the development of the "biopsy punch model", a cortical model was chosen both for mice and rats, as this would lead to a more reproducible resection with fewer risks of collateral damage for the animal. However, as most of the orthotopic models reported in the

literature for rats are striatal [32], new injection coordinates needed to be established and the tumor growth profile evaluated for each chosen cell line. Based on the injection coordinates that were selected for the mouse model, the coordinates of 0 mm anterior, 3 mm lateral from bregma and 3.5 mm deep from the outer border of the cranium were selected for the rat to obtain tumors at the border between the cortex and the striatum.

In the mouse model, a 2 mm diameter biopsy punch at 3 mm deep was used to withdraw the brain region where the tumor was located [21]. For the rat model, an adapted biopsy punch size and appropriate depth needed to be selected. We performed some preliminary studies using a 4 mm diameter biopsy punch at a depth of 5 mm, but these led to ventricle damage and cerebrospinal fluid leakage, corresponding to a higher risk of collateral damage for the animal (supplementary data, Figure S3A). Therefore, a 3 mm diameter biopsy punch and a depth of 4 mm were chosen. These characteristics allow for a resection cavity able to host 15 µL of hydrogel. However, as the rat brain is about 3 times larger than the mouse brain (1.5 vs 0.5 g, respectively), the drug amount per g of brain remains identical.

We have previously demonstrated that $GemC_{12}$-LNC hydrogel could allow a sustained release of $GemC_{12}$ during one month *in vitro* [14]. Here, we aimed at evaluating the hydrogel presence and LNC integrity over time after local administration in the resection cavity using *ex vivo* FRET on the excised brains. FRET is a fluorescence spectroscopy technique based on the energy transfer between a donor and an acceptor dye which are spatially close one to the other (2-8 nm). In this process, the excitation energy of a donor is transferred to an acceptor, whose emission can be detected if their emission/excitation spectra overlap [33]. This technique is commonly used to evaluate the integrity of nanocarriers, as it allows to monitor the distance between two fluorophores. For example, if dye leakage or nanocarrier disintegration occurs, the distance between donor and acceptor fluorophores increases, leading to loss of FRET signal [26, 34]. Here, we used DiI and DiD as FRET pairs as it has been previously reported that no dye release from the LNC nor dye transfer between LNCs is observed with these dyes [25]. Our results are only qualitative, but confirm that the hydrogel structure and the LNC integrity are, at least in part, maintained *in vivo* one week after local administration in the brain. As the $GemC_{12}$-LNC hydrogel degradation corresponds to the release of the drug and the hydrogel integrity was shown after one week, we can assume that a sustained release of $GemC_{12}$ is provided at least during this period of time.

Another aim of this work was to evaluate the ability of $GemC_{12}$-LNC to slow down tumor recurrences in GBM-bearing rats after local administration in the tumor resection cavity. To adapt the "biopsy punch" surgical technique from mouse to rat, we evaluated the use of C6, 9L and 9L-LacZ cell lines to develop an orthotopic GBM rat model. The first two were chosen because they represent two of the most used and well known preclinical glioma models in rats [24, 35]. The last one was selected as 9L-LacZ cells constitutively express the LacZ reporter gene product, which is revealed by a histochemical stain and allows the quantitative analysis of microscopic tumors in the brain [36]. None of these cell lines are known to develop highly invasive tumors, which is useful for the development of a reproducible surgical technique that avoids heterogeneic inter-individual bias. Moreover, a preliminary *in vitro* cytotoxicity screening showed that the three cell lines were sensitive to $GemC_{12}$, supporting our choice to use one of them as a preclinical model to evaluate $GemC_{12}$-LNC efficacy (supplementary data S4). The growth profile of the three tumor models was evaluated and the reproducibility of tumor formation was considered an essential parameter for further studies (supplementary data, Figure S3B). A longitudinal MRI study on all the animals enabled us to visualize the localization, growth and size of the tumors before surgical resection. It also allowed us to determine the impact of the correctness of the surgical gestures on the evolution of the tumor and/or tumor recurrences and evaluate if brain damage occurred after surgical resection of the tumor. Through MRI we could also visualize eventual Neuro-Patch® dislocation that could lead to the loss of treatment from the administration site and evaluate how the treatment delays the formation of recurrences over time. We were also able to obtain a personalized follow-up for each animal (e.g. local side effects, evaluate tumor resection correctness, formation of recurrences) and get quantitative and qualitative data to consolidate the survival curve information. The day of resection for each tumor model was established depending on the tumor growth profile and the formation of tumor recurrences was also observed by MRI.

Due to the unreliability of the tumor growth and delay in tumor appearance, the 9L-LacZ model did not represent a good resection model and therefore the efficacy of $GemC_{12}$-LNC was not tested on it (supplementary data S1).

On the other hand, the C6 cell inoculation in Sprague Dawley rats brain resulted in homogeneous growth of tumors visible by MRI from day 6 post-inoculation. In this rat

model, tumor resection was performed at day 10-post tumor incoculation and the local administration of $GemC_{12}$ and $GemC_{12}$-LNC in the tumor resection cavity seemed to reduce the formation of tumor recurrences in the short term. However, due to spontaneous regression of untreated tumors, this orthotopic model was not suitable to evaluate the efficacy of local delivery systems after surgical resection and therefore was not considered for further studies. Such a spontaneous regression of orthotopic tumors had already been reported by Vince *et* al. after C6 glioma spheroid implantation. In their study, the maximum tumor volume was reached at day 28 and after which followed a complete remission from the tumor [37], while in our model the maximum tumor volume was reached at day 18.

The 9L model is widely used in the literature due to its high aggressiveness, reliability and reproducibility in tumor growth profile [24]. Moreover, its detection by MRI is efficient [38]. Indeed, the brain inoculation of 9L cells in Fischer rats resulted in homogeneous growth of aggressive tumors visible by MRI from day 8 post-inoculation as small spherical tumors. After surgical resection of the tumors, aggressive recurrences developed in all untreated animals. $GemC_{12}$-LNC, locally administered in the resection cavity, was highly effective in delaying (or even avoiding) tumor recurrences in this model in a dose-dependent manner. However, the amount of hydrogel to be administered in Fischer rats needs to be carefully evaluated to avoid hydrogel leakage from the resection cavity. For this reason, the hydrogel volume should be limited to 5-10 µL for further studies using this resection model.

5. CONCLUSIONS

In conclusion, in this work the “biopsy punch” tumor resection technique previously developed on mice was successfully adapted to rats. Lipid nanocapsule integrity is maintained for at least one week after local administration of $GemC_{12}$-LNC in the rat brain. The perisurgical administration of $GemC_{12}$-LNC in the resection cavity of 9L tumor-bearing rats delayed the formation of recurrences in the brain demonstrating the efficacy of this nanomedicine hydrogel in this preclinical model. Our results confirm that this hydrogel, uniquely formed by a nanocarrier and a cytotoxic drug, could be a promising and safe delivery tool for the local treatment of operable GBM tumors.

6. REFERENCES

[1] C. Bastiancich, G. Bastiat, F. Lagarce, Gemcitabine and glioblastoma: challenges and current perspectives, Drug Discov Today, (2017).

[2] J. Sigmond, R.J. Honeywell, T.J. Postma, C.M. Dirven, S.M. de Lange, K. van der Born, A.C. Laan, J.C. Baayen, C.J. Van Groeningen, A.M. Bergman, G. Giaccone, G.J. Peters, Gemcitabine uptake in glioblastoma multiforme: potential as a radiosensitizer, Ann Oncol, 20 (2009) 182-187.

[3] G. Metro, A. Fabi, M.A. Mirri, A. Vidiri, A. Pace, M. Carosi, M. Russillo, M. Maschio, D. Giannarelli, D. Pellegrini, A. Pompili, F. Cognetti, C.M. Carapella, Phase II study of fixed dose rate gemcitabine as radiosensitizer for newly diagnosed glioblastoma multiforme, Cancer Chemother Pharmacol, 65 (2010) 391-397.

[4] R. Stupp, W.P. Mason, M.J. van den Bent, M. Weller, B. Fisher, M.J. Taphoorn, K. Belanger, A.A. Brandes, C. Marosi, U. Bogdahn, J. Curschmann, R.C. Janzer, S.K. Ludwin, T. Gorlia, A. Allgeier, D. Lacombe, J.G. Cairncross, E. Eisenhauer, R.O. Mirimanoff, Radiotherapy plus concomitant and adjuvant temozolomide for glioblastoma, N Engl J Med, 352 (2005) 987-996.

[5] J. Bianco, C. Bastiancich, A. Jankovski, A. des Rieux, V. Preat, F. Danhier, On glioblastoma and the search for a cure: where do we stand?, Cell Mol Life Sci, 74 (2017) 2451-2466.

[6] B. Auffinger, D. Spencer, P. Pytel, A.U. Ahmed, M.S. Lesniak, The role of glioma stem cells in chemotherapy resistance and glioblastoma multiforme recurrence, Exp Rev Neurother, 15 (2015) 741-752.

[7] R. Rahman, Biomaterial-based local drug delivery to brain tumors, Ther Deliv, 5 (2014) 1243-1245.

[8] L. Kleinberg, Polifeprosan 20, 3.85% carmustine slow-release wafer in malignant glioma: evidence for role in era of standard adjuvant temozolomide, Core Evid, 7 (2012) 115-130.

[9] D.A. Bota, A. Desjardins, J.A. Quinn, M.L. Affronti, H.S. Friedman, Interstitial chemotherapy with biodegradable BCNU (Gliadel) wafers in the treatment of malignant gliomas, Ther Clin Risk Manag, 3 (2007) 707-715.

[10] M. Westphal, D.C. Hilt, E. Bortey, P. Delavault, R. Olivares, P.C. Warnke, I.R. Whittle, J. Jaaskelainen, Z. Ram, A phase 3 trial of local chemotherapy with biodegradable carmustine (BCNU) wafers (Gliadel wafers) in patients with primary malignant glioma, Neuro Oncol, 5 (2003) 79-88.

[11] P. Miglierini, M. Bouchekoua, B. Rousseau, P. Dam Hieu, J.-P. Malhaire, O. Pradier, Impact of the per-operatory application of GLIADEL wafers (BCNU, carmustine) in combination with temozolomide and radiotherapy in patients with glioblastoma multiforme: Efficacy and toxicity, Clin Neurol Neurosurg, 114 (2012) 1222-1225.

[12] J.N. Sarkaria, G.J. Kitange, C.D. James, R. Plummer, H. Calvert, M. Weller, W. Wick, Mechanisms of chemoresistance to alkylating agents in malignant glioma, Clin Cancer Res, 14 (2008) 2900-2908.

[13] C. Bastiancich, J. Bianco, K. Vanvarenberg, B. Ucakar, N. Joudiou, B. Gallez, G. Bastiat, F. Lagarce, V. Preat, F. Danhier, Injectable nanomedicine hydrogel for local chemotherapy of glioblastoma after surgical resection, J Control Release, 264 (2017) 45-54.

[14] C. Bastiancich, K. Vanvarenberg, B. Ucakar, M. Pitorre, G. Bastiat, F. Lagarce, V. Preat, F. Danhier, Lauroyl-gemcitabine-loaded lipid nanocapsule hydrogel for the treatment of glioblastoma, J Control Release, 225 (2016) 283-293.

[15] E. Moysan, Y. Gonzalez-Fernandez, N. Lautram, J. Bejaud, G. Bastiat, J.P. Benoit, An innovative hydrogel of gemcitabine-loaded lipid nanocapsules: when the drug is a key player of the nanomedicine structure, Soft Matter, 10 (2014) 1767-1777.

[16] A. Gaudin, E. Song, A.R. King, J.K. Saucier-Sawyer, R. Bindra, D. Desmaele, P. Couvreur, W.M. Saltzman, PEGylated squalenoyl-gemcitabine nanoparticles for the treatment of glioblastoma, Biomaterials, 105 (2016) 136-144.

[17] U. Akbar, T. Jones, J. Winestone, M. Michael, A. Shukla, Y. Sun, C. Duntsch, Delivery of temozolomide to the tumor bed via biodegradable gel matrices in a novel model of intracranial glioma with resection, J Neurooncol, 94 (2009) 203-212.

[18] J.W. Denbo, R.F. Williams, W.S. Orr, T.L. Sims, C.Y. Ng, J. Zhou, Y. Spence, C.L. Morton, A.C. Nathwani, C. Duntsch, L.M. Pfeffer, A.M. Davidoff, Continuous local delivery of interferon-beta stabilizes tumor vasculature in an orthotopic glioblastoma xenograft resection model, Surgery, 150 (2011) 497-504.

[19] T.M. Kauer, J.L. Figueiredo, S. Hingtgen, K. Shah, Encapsulated therapeutic stem cells implanted in the tumor resection cavity induce cell death in gliomas, Nat Neurosci, 15 (2012) 197-204.

[20] K.J. Sweeney, M.A. Jarzabek, P. Dicker, D.F. O'Brien, J.J. Callanan, A.T. Byrne, J.H. Prehn, Validation of an imageable surgical resection animal model of Glioblastoma (GBM), J Neurosci Methods, 233 (2014) 99-104.
[21] J. Bianco, C. Bastiancich, N. Joudiou, B. Gallez, A. des Rieux, F. Danhier, Novel model of orthotopic U-87 MG glioblastoma resection in athymic nude mice, J Neurosci Methods, 284 (2017) 96-102.
[22] M.E. Sughrue, I. Yang, A.J. Kane, M.J. Rutkowski, S. Fang, C.D. James, A.T. Parsa, Immunological considerations of modern animal models of malignant primary brain tumors, J Transl Med, 7 (2009) 84.
[23] S.E. Gould, M.R. Junttila, F.J. de Sauvage, Translational value of mouse models in oncology drug development, Nat Med, 21 (2015) 431-439.
[24] R.F. Barth, B. Kaur, Rat brain tumor models in experimental neuro-oncology: the C6, 9L, T9, RG2, F98, BT4C, RT-2 and CNS-1 gliomas, J Neurooncol, 94 (2009) 299-312.
[25] B. Heurtault, P. Saulnier, B. Pech, J.E. Proust, J.P. Benoit, A novel phase inversion-based process for the preparation of lipid nanocarriers, Pharm Res, 19 (2002) 875-880.
[26] C. Simonsson, G. Bastiat, M. Pitorre, A.S. Klymchenko, J. Bejaud, Y. Mely, J.P. Benoit, Inter-nanocarrier and nanocarrier-to-cell transfer assays demonstrate the risk of an immediate unloading of dye from labeled lipid nanocapsules, Eur J Pharm Biopharm, 98 (2016) 47-56.
[27] S. Wang, J. Zhou, Diffusion tensor MR imaging of rat glioma models: A correlation study of MR imaging and histology, J Comput Assist Tomogr, 36 (2012) 739-744.
[28] D. Jeong, C. Malalis, J.A. Arrington, A.S. Field, J.W. Choi, M. Kocak, Mean apparent diffusion coefficient values in defining radiotherapy planning target volumes in glioblastoma, Quant Imaging Med Surg, 5 (2015) 835-845.
[29] I. Tkac, Z. Starcuk, I.Y. Choi, R. Gruetter, In vivo 1H NMR spectroscopy of rat brain at 1 ms echo time, Magn Reson Med, 41 (1999) 649-656.
[30] A. Horska, P.B. Barker, Imaging of brain tumors: MR spectroscopy and metabolic imaging, Neuroimaging Clin N Am, 20 (2010) 293-310.
[31] W.M. Reid, A. Rolfe, D. Register, J.E. Levasseur, S.B. Churn, D. Sun, Strain-related differences after experimental traumatic brain injury in rats, J Neurotrauma, 27 (2010) 1243-1253.
[32] M. Candolfi, J.F. Curtin, W.S. Nichols, A.G. Muhammad, G.D. King, G.E. Pluhar, E.A. McNiel, J.R. Ohlfest, A.B. Freese, P.F. Moore, J. Lerner, P.R. Lowenstein, M.G. Castro, Intracranial glioblastoma models in preclinical neuro-oncology: neuropathological characterization and tumor progression, J neurooncol, 85 (2007) 133-148.
[33] E. Roger, J.C. Gimel, C. Bensley, A.S. Klymchenko, J.P. Benoit, Lipid nanocapsules maintain full integrity after crossing a human intestinal epithelium model, J Control Release, 253 (2017) 11-18.
[34] A.C. Groo, P. Saulnier, J.C. Gimel, J. Gravier, C. Ailhas, J.P. Benoit, F. Lagarce, Fate of paclitaxel lipid nanocapsules in intestinal mucus in view of their oral delivery, Int J Nanomedicine, 8 (2013) 4291-4302.
[35] V.L. Jacobs, P.A. Valdes, W.F. Hickey, J.A. De Leo, Current review of in vivo GBM rodent models: emphasis on the CNS-1 tumour model, ASN neuro, 3 (2011) e00063.
[36] L.A. Lampson, M.A. Lampson, A.D. Dunne, Exploiting the lacZ reporter gene for quantitative analysis of disseminated tumor growth within the brain: use of the lacZ gene product as a tumor antigen, for evaluation of antigenic modulation, and to facilitate image analysis of tumor growth in situ, Cancer Res, 53 (1993) 176-182.
[37] G.H. Vince, M. Bendszus, T. Schweitzer, R.H. Goldbrunner, S. Hildebrandt, J. Tilgner, R. Klein, L. Solymosi, J. Christian Tonn, K. Roosen, Spontaneous regression of experimental gliomas--an immunohistochemical and MRI study of the C6 glioma spheroid implantation model, Exp Neurol, 190 (2004) 478-485.
[38] A. Vonarbourg, A. Sapin, L. Lemaire, F. Franconi, P. Menei, P. Jallet, J.J. Le Jeune, Characterization and detection of experimental rat gliomas using magnetic resonance imaging, Magma (New York, N.Y.), 17 (2004) 133-139.
[39] S. Doblas, T. He, D. Saunders, J. Hoyle, N. Smith, Q. Pye, M. Lerner, R.L. Jensen, R.A. Towner, In vivo characterization of several rodent glioma models by 1H MRS, NMR in biomedicine, 25 (2012) 685-694.
[40] S. Doblas, T. He, D. Saunders, J. Pearson, J. Hoyle, N. Smith, M. Lerner, R.A. Towner, Glioma morphology and tumor-induced vascular alterations revealed in seven rodent glioma models by in vivo magnetic resonance imaging and angiography, J Magn Reson Imaging, 32 (2010) 267-275.

7. SUPPLEMENTARY MATERIAL

7.1. DEVELOPMENT OF A SURGICAL PROCEDURE TO RESECT GBM TUMORS IN RATS: THE 9L-LACZ MODEL

For the preliminary study to evaluate the growth of 9L-LacZ tumors, animals were divided into two groups at day 40 post-tumor inoculation: untreated (*n*=3); resection and no treatment (*n*=4).

The brain inoculation of 9L-LacZ cells in Fischer rat brains resulted in long tumor growth delay (latency time), unreliable and irreproducible tumor growth. At day 15 post-inoculation, no tumors were visible by MRI. At day 40, tumors were visualized in 7/8 animals but their size ranged between 2 and 185 µL. One animal never developed a tumor and was excluded from the study.

The survival curve of the animals is reported in Figure S1. The untreated animals all died due to the tumor and their median survival was 51 days. Among the resected animals, 50% died because of recurrent tumors (died at day 75 and 105 post-inoculation) while the other 50% were long-term survivors (survived >150 days post-inoculation).

Therefore, the resection of 9L-LacZ tumors resulted in significant increased survival time of the animals. However, the unreliability of the tumor growth and delay in tumor appearance makes the 9L-LacZ model, which was previously shown by Doblas *et* al. [39, 40], a bad choice to evaluate the effect of a local delivery system on recurrences formation. Therefore, this model was not considered for further studies.

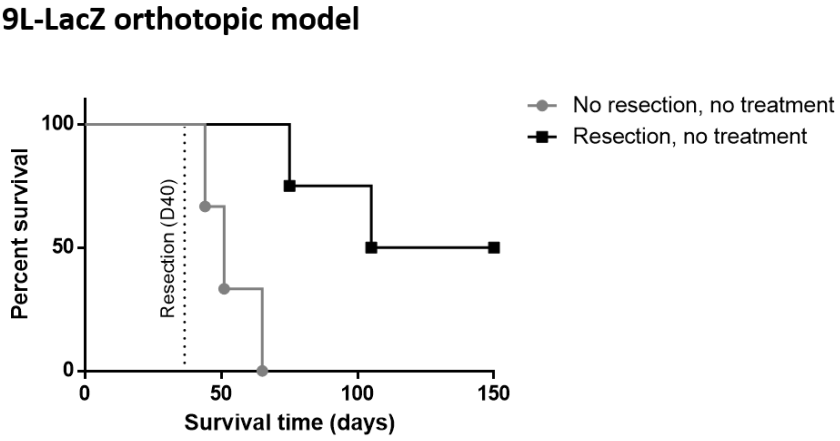

Figure S1. 9L-LacZ orthotopic model: Kaplan-Meier survival curves for animals untreated or resected untreated (resection performed 40 days post-tumor inoculation) (*n* = 3-4 for all groups).

7.2. EVALUATION O LNC INTEGRITY OVER TIME

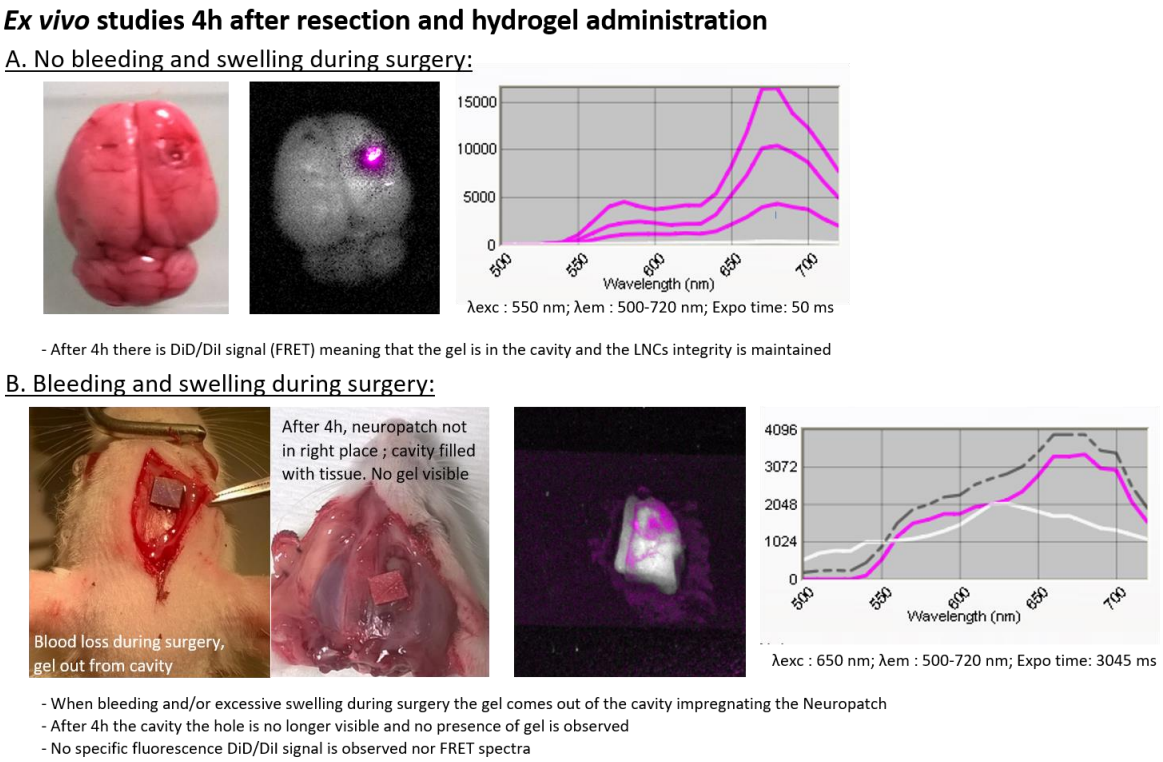

Figure S2. Evaluation of LNC integrity 4h after administration in the brain using the FRET technique. **(A)** When no excessive bleeding or swelling is observed during surgery, FRET signal can be observed 4h post-hydrogel administration expecially in the central part of the cavity (λ_{exc}: 550, exposition time: 50 ms). The different spectra correspond to different regions of the cavity: in the central region the signal is very intense and reaches saturation at this exposition time; the more lateral, the less intense signal is observed at 50 ms but adjusting the exposition time all three spectra show FRET signal. **(B)** When excessive bleeding or swelling is observed during surgery, the Neuro-Patch® is impregnated with hydrogel. Four hours after surgery no resection cavity nor FRET signal is observed at the administration site at any exposition time (in the image: λ_{exc}: 550, exposition time: 3045 ms).

7.3. TRANSPOSITION OF THE "BIOPSY PUNCH" SURGICAL RESECTION PROCEDURE FROM MOUSE TO RAT

Several parameters need to be considered while transposing a surgical procedure from a preclinical model in mouse to a preclinical model in rat (Figure S3), including the biopsy punch characteristics, the type of tumor (e.g. strains, cell line), the tumor growth profile, the delay between cell inoculation and tumor resection, and the formation of recurrences over time.

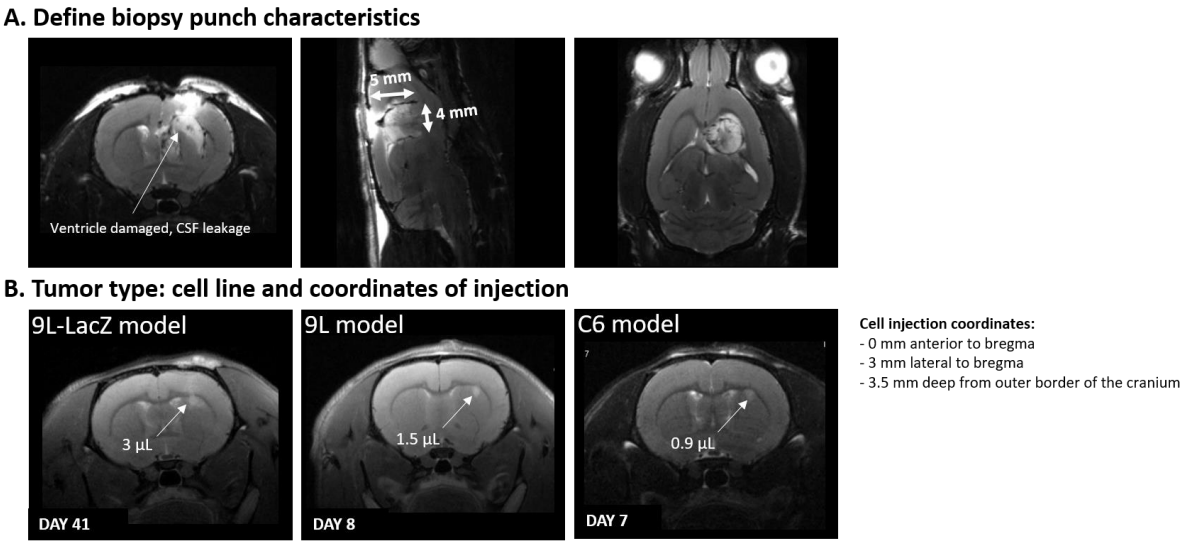

Figure S3. Parameters to be defined while developing a surgical procedure to resect GBM tumors in preclinical rat models. **(A)** The biopsy punch characteristics were chosen considering the safety of the surgical procedure. The image represents axial (left), sagittal (middle) and a coronal (right) T_2-weighted images of rat brain the day after biopsy punch resection (4 mm diameter, 5 mm depth). As brain damage was observed with these biopsy punch characteristics, a 3 mm diameter biopsy punch placed 4 mm deep was deemed safer and chosen for further studies; **(B)** The coordinates of injection were chosen to obtain cortical tumors that could be reproducibly resected. Three GBM rat models were developed and tumor growth over time was evaluated to select the most appropriate model for a reproducible resection. In the image are shown axial T_2-weighted images of rat brain showing orthotopic 9L-LacZ, 9L and C6 tumors.

7.4. *IN VITRO* PRELIMINARY CYTOTOXICITY STUDIES

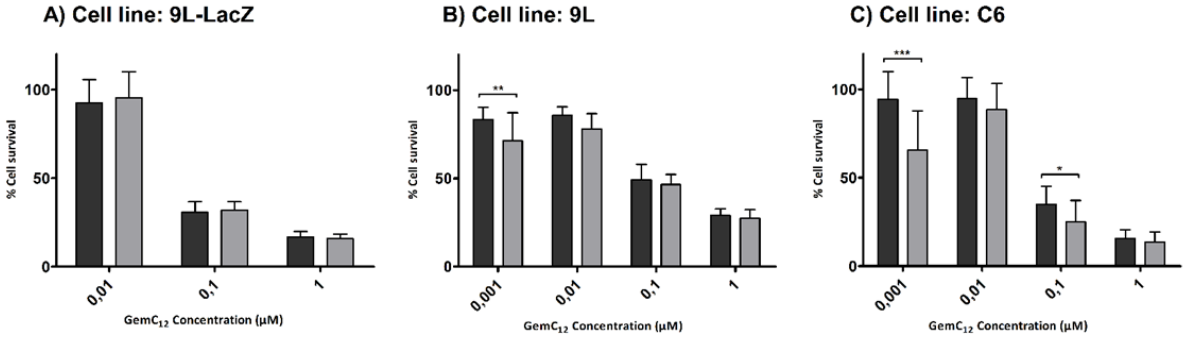

Figure S4. *In vitro* cytotoxicity studies on (**A**) 9L-LacZ, (**B**) 9L and (**C**) C6 glioma cells. MTT assay after 48 hours of incubation of different concentrations of $GemC_{12}$ (black bar) or $GemC_{12}$-LNC (gray bar). *** p<0.001 ** p<0.01, * p<0.05 Two-way ANOVA (N=2; n=12)

CHAPTER VII.

DISCUSSION, CONCLUSIONS & PERSPECTIVES

TABLE OF CONTENTS

1. MAIN CONTRIBUTIONS

Glioblastoma (GBM) is an aggressive malignant brain tumor characterized by rapid proliferation and propensity to infiltrate healthy brain tissue. Its standard of care therapy includes surgical resection, radiotherapy and chemotherapy with Temozolomide (TMZ) but GBM always recurs even after multiple resection and treatment, mainly because of its high invasiveness and chemoresistance to alkylating drugs. Among the drug delivery strategies that have been developed to find a solution to the devastating and incurable effects of GBM, there is the local delivery of chemotherapeutic agents (implants, foams, hydrogels, microcarriers) and the use of nanomedicines (Chapter I).

The objective of this PhD project was to combine the advantages of these two approaches by delivering an anti-cancer loaded nanomedicine hydrogel in the tumor resection cavity, to avoid GBM recurrences (Chapter II). Indeed, the direct administration of the formulation in the brain and a sustained release of the drug in the gap period between surgery and standard of care chemo-radiation could lead to (*i*) improved drug distribution in the brain reducing systemic toxicity (*ii*) delivery of multiple anticancer drugs (*iii*) reduction of the formation of recurrences at the resection cavity borders. As the combination of local chemotherapy with systemic chemotherapy and/or radiation may improve the therapeutic efficacy by targeting complementary cancer-based cellular mechanisms, the rationale for the use of multiple chemotherapeutic drugs with different mechanisms of action and/or radiosensitizing agents is high.

In this research, we evaluated the feasibility, efficacy and safety of *lauroyl-gemcitabine lipid nanocapsule* ($GemC_{12}$-LNC), an injectable nanomedicine hydrogel previously developed in our group, for the local treatment of GBM (Figure 1A). $GemC_{12}$-LNC is uniquely formed of lipid nanocapsules and the prodrug lauroyl-gemcitabine and, in this study, it was optimized to obtain a sustained release of the drug over time. The hydrogel was prepared by a phase-inversion technique process and characterized for its use against GBM. Our major findings can be summarized as follows (Chapter III-VI; Figure 1B):

- $GemC_{12}$-LNC is an injectable hydrogel adapted for brain implantation;
- The release kinetics profile of the drug from the $GemC_{12}$-LNC hydrogel is characterized by a burst release during the first 48 hours followed by a sustained release during one month *in vitro*;
- The lipid nanocapsules integrity is maintained at least for one week after local administration in the brain. The hydrogel is well tolerated in the short-, mid- and long-term;
- $GemC_{12}$ and $GemC_{12}$-LNC show a different cellular uptake mechanism and enhanced cytotoxic effect *in vitro* compared to parent drug GemHCl;
- Intratumoral injection of $GemC_{12}$-LNC hydrogel in a U-87 MG subcutaneous and orthotopic GBM model significantly reduced tumor growth and increased the animal's median survival compared to the controls, respectively;
- An innovative and reproducible "biopsy punch" tumor resection technique of U-87 MG GBM and 9L gliosarcoma was developed to mimic the clinical setting in rodents. The perisurgical administration of $GemC_{12}$-LNC hydrogel in the resection cavity delayed the formation of recurrences in the brain.

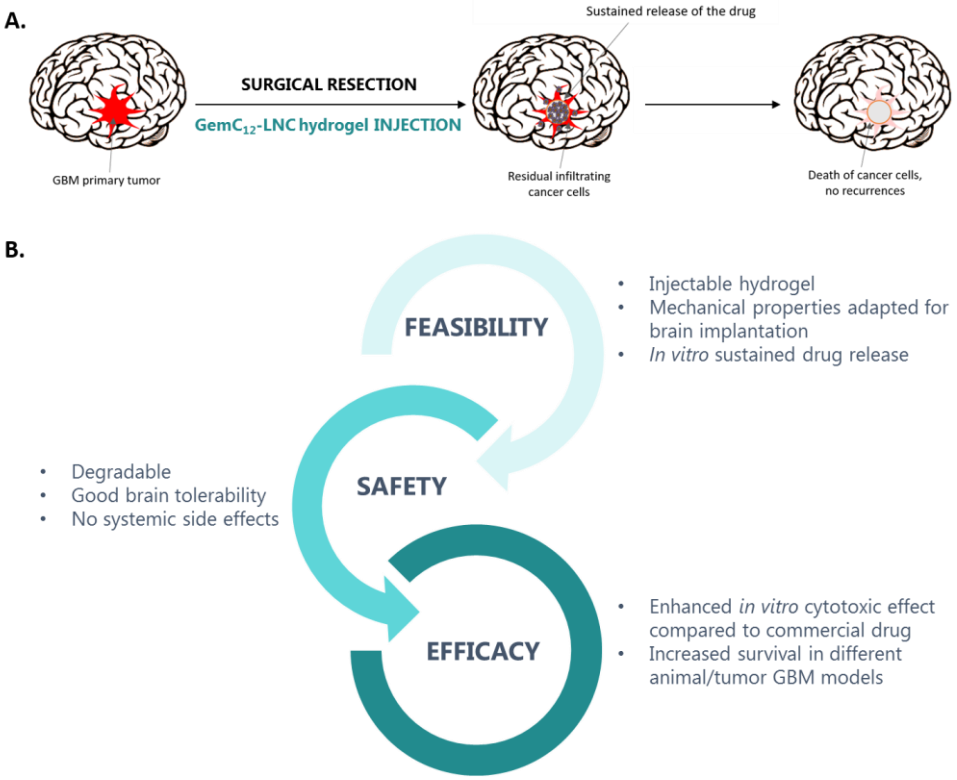

Figure 1. **(A)** Approach used in the project to avoid GBM recurrences; **(B)** Summary of the main contributions of this PhD work in demonstrating the feasibility, safety and efficacy of $GemC_{12}$-LNC for the local treatment of GBM. GBM: glioblastoma; $GemC_{12}$-LNC: lauroyl-gemcitabine lipid nanocapsules.

2. MAJOR FINDINGS: DISCUSSION

Both the use of nanomedicines and local delivery of chemotherapeutic drugs have a great potential in treating GBM, and this is confirmed by the increasing number of publications and clinical trials involving these two strategies. However, very few have reached the clinics yet. The only local delivery implant approved for GBM treatment - the carmustine wafers Gliadel® - is rarely used on newly diagnosed GBM patients. Indeed, Gliadel® showed poor and controversial advantages compared to the standard chemotherapy and no other local treatment has been approved since its entrance in the market [1].

In this PhD work, we evaluated for $GemC_{12}$-LNC the parameters that we consider crucial for the development of a controlled-release delivery system for the local treatment in the brain (Figure 2) [2]. These include choosing a drug with good efficacy and optimal release profile, the evaluation of the system injectability, mechanical properties, tolerability and degradability over time and the evaluation of the anti-tumor efficacy on different animal and tumor models.

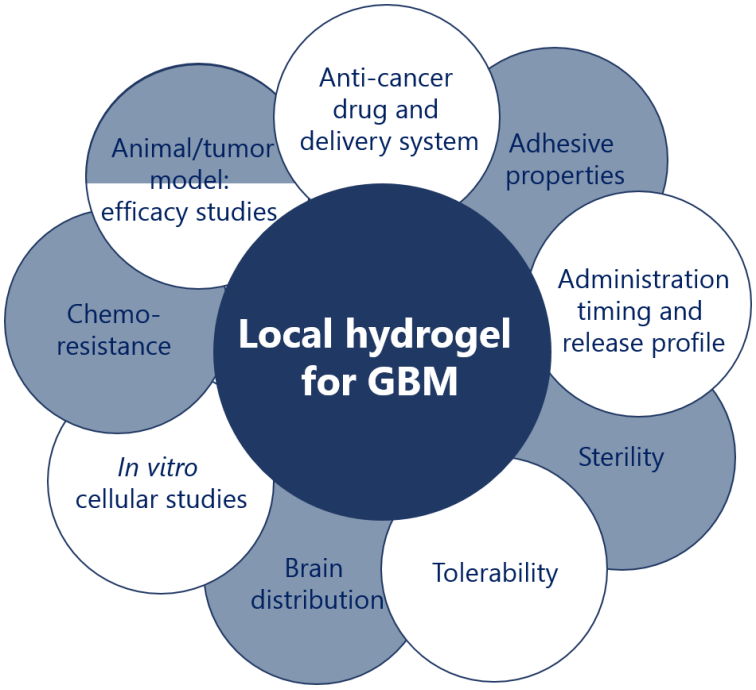

Figure 2. List of main parameters to take into account for the development of a hydrogel for the local treatment of GBM: in white are represented the parameters studied in this project, in grey the translational limitations that will have to be addressed in the future. Adapted from [2].

2.1. CHOOSING THE DRUG AND THE DELIVERY SYSTEM

The standard of care agent for GBM is TMZ, so efforts should be focused on its local delivery and how to avoid its chemoresistance. Nevertheless, the particular physico-chemical properties of TMZ lead researchers to focus on other molecules which are not always in full compliance with clinical recommendations [3, 4]. In this sense, Gem has already been tested against this tumor in preclinical and clinical trials and it is an attractive molecule for the treatment of GBM [5]. It is a powerful chemotherapeutic and radiosensitizing agent acting through a MGMT-independent mechanism, which could avoid crossed-linked resistance with TMZ. Its immunomodulating properties might be exploited for its use against GBM in combination with immunotherapies. Moreover, the clinical use of Gem has shown its ability to act in synergy not only with RT but also with other chemotherapeutic agents (e.g. carboplatin, cisplatin, paclitaxel).

When this project started, no studies had been published using Gem derivatives *in vitro* on GBM cell lines or *in vivo* for the local treatment of GBM as an alternative strategy for tumors resistant to alkylating agents. We hypothesized to use an innovative hydrogel developed by our group, and uniquely formed of lauroyl-gemcitabine and lipid nanocapsules ($GemC_{12}$-LNC), to avoid the formation of GBM recurrences.

$GemC_{12}$ is an amphiphilic derivative of Gem that shows improved stability in plasma due to the protection of the amine group by an amide linkage stable at pH 4-9, and improved cytotoxicity in different cell lines [6]. LNC are biomimetic and biocompatible nanocarriers formed of an oily core surrounded by a highly organized membrane of surfactants [7]. When $GemC_{12}$ is encapsulated in LNC, the formulation spontaneously forms a hydrogel without the addition of polymers, gelling agents or external stimuli. The gelation time and gel mechanical properties strongly depend on $GemC_{12}$ and LNC concentration. The gel is formed thanks to an inter-nanoparticle association of $GemC_{12}$-LNC in which $GemC_{12}$ behaves as an amphiphilic molecule locating itself at the oil/water interface of the LNC, and the Gem moieties outside the LNC form H-bond cross-linkings entrapping the water phase and forming a gel [8]. Among the tremendous variety of local delivery systems and nanocarriers that can be developed, the advantage of $GemC_{12}$-LNC is its simplicity. This parameter is crucial if we aim at scaling up our formulation for clinical application: (*i*) $GemC_{12}$-LNC is made of cost-effective FDA approved components (*ii*) $GemC_{12}$-LNC can be formulated in a short period of time (~ 3

hours) by a phase-inversion technique process that requires devices found in any scaling up lab (e.g. magnetic stirrer); (*iii*) $GemC_{12}$-LNC is only formed by a nanocarrier and a drug, meaning that the degradation of the hydrogel corresponds to the release of the drug and no traces will remain in the brain once the drug is released; (*iv*) The $GemC_{12}$-LNC hydrogel can be stored in prefilled syringes and be easily applied at the moment of surgery. The mechanical properties of $GemC_{12}$-LNC are adapted for an implantation in the brain, and the hydrogel is injectable using insulin syringes with 29-G needles.

On the other side, some pharmaceutical technology limitations of $GemC_{12}$-LNC need to be mentioned. Firstly, the gelification time of $GemC_{12}$-LNC is strictly dependent on the amount of drug present in the formulation and it is quite fast, ranging between 10 minutes (5% $GemC_{12}$/Labrafac® formulation) and 3 minutes (10% $GemC_{12}$/Labrafac® formulation). Secondly, the gel-like properties of $GemC_{12}$-LNC are lost after freeze-drying or after contact with liquid solutions. It is known that LNC formulations have good stability during 18 months at 4°C. However, it would be important to evaluate a longer term stability of $GemC_{12}$-LNC hydrogel in syringes (e.g. resistance to humidity) and evaluate its storage optimal conditions.

2.2. EVALUATE THE ADMINISTRATION TIMING AND RELEASE PROFILE

As radiation has an impact on the wound healing process, GBM patients' need to wait for several weeks after the surgical resection before starting the TMZ + RT regimen [9]. However, a longer time between surgery and radiotherapy correlates with an increase in local recurrences, as the residual tumor cells have time to proliferate [10]. For this reason, the application of a hydrogel directly in the resection cavity after surgery reduces the risk of recurrences in this period of time. Considering this, the expected release kinetics from hydrogels is around one month, to allow the resection wound to heal but killing the residual infiltrative GBM cells at the same time.

We have shown that $GemC_{12}$-LNC could be directly administered by injection in the perisurgical resection cavity and is able to sustainably release the drug over one month *in vitro* in artificial cerebrospinal fluid. I am aware that our *in vitro* release study presents several limitations, and it can only give us a general and qualitative idea on how the $GemC_{12}$-LNC hydrogel could release the drug and degrade *in vivo*. For example, we have not considered the protein-binding properties of $GemC_{12}$-LNC or $GemC_{12}$ which might

considerably affect the release of the drug and its bioavailability. Moreover, we do not know if deacetylation of $GemC_{12}$, which would lead to release of Gem instead of $GemC_{12}$ (e.g. by amidase enzymes), might occur in our system in the brain physiological conditions. *In vitro*, stability studies have shown that after 1 month of storage at 37°C the HPLC peaks of $GemC_{12}$ decrease and the Gem peaks increase meaning amide linkage breaking in these conditions (data not shown).

Ex vivo, the lipid nanocapsules integrity in the hydrogel (but not the drug properties) was demonstrated during one week and further studies will implement the protocol used to test the presence of the hydrogel over a longer period of time.

2.3. EVALUATE THE TOLERABILITY OF THE FORMULATION

The tolerability of hydrogels is a major concern in the development of drug delivery systems for brain use and an accurate and methodic work need to be performed in this sense to guarantee the safety of new products [11]. First of all, the drug delivery system and the drug inside should be sterilized (see section 3.2). Then, the inflammatory reaction produced both by the mechanical trauma (GBM resection, implantation of the system, increase of intracranial pressure due to injection of the hydrogel and swelling) and the brain tissue contact with the delivery system should be analyzed in the short and long-term (acute and chronic tissue response).

The pH of the $GemC_{12}$-LNC hydrogel is around 5.5-6 and would be acceptable for a local administration in the tumor resection cavity. However, the tonicity of the formulation could not be tested due to the fast gelification timing of the formulation and the presence of lipid components which make it impossible to determine the freezing temperature of $GemC_{12}$-LNC. The tolerability of $GemC_{12}$-LNC was tested in healthy mice brain in the short-, mid- and long-term. No inflammation, apoptosis or microglia activation was observed after one week, two months and six months of exposure to the $GemC_{12}$-LNC hydrogel suggesting that this system is well tolerated and suitable for a brain application.

2.4. *IN VITRO* CELLULAR STUDIES

The first step to evaluate the anti-tumor efficacy of a local delivery treatment is to test the anticancer activity of the free drug and loaded drug *in vitro*.

Some authors had previously evaluated the cytotoxic effect of Gem on different glioma cells [e.g. 12-15]. Also, it has been previously reported that 4(N)-modifications in the Gem structure allowed to increase its plasma stability and consequently the drug half-life by reducing the deamination process produced by cytidine deaminase [6, 16]. Moreover, the lipophilic prodrugs, alone or incorporated in carriers such as liposomes or NP, have shown increased anticancer activity both *in vitro* and *in vivo* on different tumor models [16-20]. $GemC_{12}$-LNC have been previously tested *in vitro* on human lung and pancreatic cancer cell lines and *in vivo* in a metastatic model of human non-small-cell lung cancer showing higher anticancer activity and reduced side effects compared to Gem [8, 21].

In this work, we firstly demonstrated that $GemC_{12}$ and $GemC_{12}$-LNC show higher cytotoxic activity compared to the parent drug GemHCl on U-87 MG cells [22]. Then, we demonstrated that the mechanism of internalization of $GemC_{12}$ and $GemC_{12}$-LNC is less dependent on the nucleoside transporters hENT1 than GemHCl on U-87 MG, U251, T98G and 9L-LacZ cells. It would have been interesting to test the hCNTs expression in these cell lines and evaluate their role on the $GemC_{12}$ and $GemC_{12}$-LNC uptake. In any case, the improved lipophilicity of Gem derivatives could enhance intracellular uptake via passive pathways or endocytosis thus improving growth inhibition effects [23-25]. Even though we cannot exclude that $GemC_{12}$ might deacetylate to Gem in physiological conditions (before or after entering the cells), the different results that we observed between the commercial drug and its derivative might suggest that until the moment when $GemC_{12}$ enters the cells the integrity of the amide linkage is maintained. Moreover, we do not know if $GemC_{12}$ is released from the LNC before cellular uptake or after.

The tests that we used to evaluate the cytotoxic effects of the drug in our studies were MTT assay and crystal violet assay on monolayer cell lines cultures. Supplementary studies should be performed on the cellular uptake mechanisms of $GemC_{12}$-LNC to evaluate if a difference exists in the endocytosis pathway and subcellular trafficking and maturation compared to unloaded LNC. Morevoer, I am aware that the cellular *in vitro* results performed in this work

do not reflect the clinical situation and that the sustained release of the drug as well as the gel consistency of the system are not represented in this type of cellular studies. Further studies could be performed using more sophisticated *in vitro* models in the future (e.g. primary glioma cell lines, CSCs cell lines, 3D *in vitro* cell cultures able to mimic the tumor microenvironment, co-cultures [26, 27]).

2.5. ANIMAL/TUMOR MODELS: ANTI-TUMOR EFFICACY STUDIES

Rodent models of GBM have been available for decades, however, very few new therapies have successfully translated into the clinic. Some of them are better to evaluate the anti-tumor efficacy of the new drugs while others are more appropriate for drug penetration and biotolerability studies. An ideal model should recapitulate the key histopathological, genetic and imaging features encountered in GBM's aggressive growth as well as being a reproducible and reliable [28]. Researchers should consider different parameters while choosing an optimal GBM model: (*i*) The size/species of the animal; (*ii*) Human GBM models are closer to the clinic situation but the use of athymic nude mice or rats lack of full tumor-immune microenvironment. (*iii*) The infiltrating capacity of GBM cells from the tumor mass to the brain parenchyma differs depending on the GBM cell line. However, the brain and cavity sizes intra-species, the amount of drug that can be implanted as well as the differences in tumor growth pathways and timings make us wonder if we really have models strong enough to predict the effects of hydrogels in humans. In this work, we have showed the GemC_{12}-LNC efficacy on several GBM preclinical models, showing different characteristics.

First, the U-87 MG human xenograft model in nude mice was chosen to test the antitumor efficacy of the GemC_{12}-LNC hydrogel for its wide use as a preclinical model, good reproducibility, reliable growth and disease progression [28]. These tumors are non-infiltrative, with a well demarcated tumor mass visible both by MRI images and Hematoxylin & Eosin stained sections [29], but present a subpopulation of cancer stem-like cells with self-propagating potential [30]. The U-87 MG cell line that we used during the all course of this thesis was bought from American Type Culture Collection (ATCC) in December 2014 and cultured following the ATCC database instructions. However, recently, Allen *et* al. demonstrated that the DNA profile of the U-87 MG cells from ATCC reflect brain-cancer

biology but is different from the original U-87 MG cell line established 1966 at Uppsala University [31].

Intratumoral injection of $GemC_{12}$-LNC hydrogel in a U-87 MG subcutaneous and orthotopic GBM model significantly reduced tumor growth and increased the animal's median survival compared to the controls, respectively. These results showed the potent cytotoxic activity of $GemC_{12}$-LNC in reducing tumor growth and significant difference was observed, in both studies, between $GemC_{12}$ and $GemC_{12}$-LNC groups. This is in accordance with the only other study in the literature reporting the use of Gem derivative against GBM, performed by Gaudin *et* al., who showed increased survival time of animals treated with squaneoyl-gemcitabine nanoparticles compared to free drug after local administration by CED in an orthotopic RG2 GBM model [17]. These results can be explained by the sustained continuous drug release obtained by a gel formulation compared to the unloaded liquid form, and their different distribution in the brain and they confirm the rationale for the use of Gem derivatives as a local delivery strategy for GBM.

To mimic the clinical setting, we developed an innovative and reproducible 'biopsy punch' tumor resection technique of U-87 MG orthotopic GBM. After perisurgical administration in the tumor resection cavity, $GemC_{12}$-LNC hydrogel slowed down the formation of recurrences in the brain. However, in these conditions, no difference was observed in the survival curves of the $GemC_{12}$ and $GemC_{12}$-LNC groups. This different result compared to the intratumoral treatment could be explained by the tumor microenvironment *vs* post-resection tumor microenvironment characteristics [32], the immunostimulatory capacities of Gem [33], and possibly different humoral adaptive and innate immune response of the animals in our two orthotopic tumor models [34]. It has been recently shown that $GemC_{12}$-LNC have targeting capacity towards the monocytic-myeloid derived suppressor cells (MDSCs) in lymphoma and melanoma mouse models [35]. MDSCs are a heterogeneous population of granulocytic and myeloid cells, highly present in GBM patients, able to accumulate in the tumor-bearing host to support glioma growth, invasion, and vascularization, and differentially mediating immunosuppression depending on their stage [36-38]. The targeted action of $GemC_{12}$-LNC on these cells could potentially reduce the tumor-associated immunosuppression in the orthotopic tumor model (where the tumor microenvironment is not affected by the resection procedure), thus increasing its efficacy compared to the free drug.

To test the efficacy of $GemC_{12}$-LNC hydrogel in a more appropriate immunological rodent model, we adapted our resection technique to a bigger and syngeneic animal model. Several parameters were considered to transpose this surgical procedure from mouse to rat, including the type of preclinical model, the drug dosis to be administered, the biopsy punch characteristics, the impact of the resection procedure on the results of the study. The differences between the two models are summarized in the table 1 of Chapter VI.

Both in the mouse and rat model, cells were injected between the cortex and the striatum, as removing the cortex during the resection would lead to more reproducible results with fewer risks of collateral damage for the animal. However, as most of the orthotopic models reported in the literature are striatal [39], new injection coordinates were established and the tumor growth profile was evaluated for each chosen cell line. The preclinical models that were analysed for the rat were the 9L-LacZ, 9L or C6 orthotopic GBM models. The first one was selected as 9L-LacZ cells constitutively express the LacZ reporter gene product, which is revealed by histochemical stain and allows quantitative analysis of microscopic tumor in the brain [40]. The other two were chosen because they represent two of the most used and well known preclinical GBM models in rats [28, 41]. The growth profile of the three tumor models was evaluated as well as the day of resection, and the reproducibility of tumor formation was considered as essential parameter for further studies. Finally, the 9L model was chosen as it represents the more reproducible and reliable model for our purposes, its detection by MRI is efficient [42] and it is a syngeneic model which presents cancer stem-like cells [41].

In the rat resection model, we demonstrated that both $GemC_{12}$-LNC and $GemC_{12}$ are able to slow down or even avoid the formation tumor recurrences. Further studies will be performed at lower doses to evaluate if a difference can be observed between these two groups at sub-lethal doses. Moreover, it would be interesting to evaluate the immunoresponse in rats treated intratumorally with $GemC_{12}$-LNC in orthotopic model (e.g. hematologic analysis, body weight loss, myeloid derived suppressor cells staining after treatment).

3. FROM BENCH TO BEDSIDE: WHAT IS MISSING?

In this PhD thesis, the feasibility, efficacy and safety of $GemC_{12}$-LNC have been shown *in vitro* and in several preclinical *in vivo* models showing that this nanomedicine hydrogel is a promising and innovative delivery system for the local treatment of GBM. This formulation, which can be directly injected in the GBM resection cavity, has a very simple formulation, and combines the properties of nanomedicines and hydrogels. However, there are still several unmet limitations that should be addressed before considering a translation into the clinics of the $GemC_{12}$-LNC hydrogel for the local treatment of GBM. Some of these are evaluated and discussed in this chapter (Table 1, Figure 2).

Table 1. Summary of some of the limitations of this PhD work and examples of alternative experiments which might overcome them.

	Limitations	Example of solution
***In vivo* studies: Resection model**	Based on established cell lines (U-87 MG, 9L)	Biopsy punch model based on patient-derived cells or spheroids
	Non-diffusely infiltrative growth pattern	Biopsy punch model based on higher invasive cell lines (e.g. CNS-1, F98, GL261 cells)
	Immunogenicity	Use less immunogenic syngeneic models (e.g. CNS-1, F98, GL261, RG2) or genetically engineered models
Sterility	NP	Formulation in aseptic conditions
Bioadhesivity	NP	Bioadhesive studies *in vitro* or *in vivo* in bigger brain models
Brain distribution	NP	Tracking of radiolabeled or fluorescent-labeled formulations *ex vivo*
Chemoresistance to SOC therapy	NP	Evaluate sensitivity to TMZ and Gem after prolonged exposure to low $GemC_{12}$ concentrations *in vitro*; or ex vivo analyze the expression of genes correlated to TMZ resistance *ex vivo* in the recurrent tumors of $GemC_{12}$-LNC treated animals

Legend: SOC: standard of care; NP: studies not performed in this PhD thesis; TMZ: temozolomide; $GemC_{12}$-LNC: lauroyl-gemcitabine lipid nanocapsules.

3.1. *IN VIVO* STUDIES: THE RESECTION MODEL

I think that some limitations of the *in vivo* models used in this project should be considered before performing further efficacy studies for this or other drug delivery systems. To increase its translational value, the 'biopsy punch' surgical resection technique should be implemented in the future taking into account the following suggestions.

Firstly, the cell lines that we used for the development of our surgical resection procedure (U-87 MG in mice; 9L-LacZ, 9L or C6 in rats) are among the most-commonly used preclicinal GBM models but develop non-diffusely infiltrative growth pattern. This aspect was useful for the development of a reproducible surgical technique as it allowed to avoid heterogeneity inter-individual bias, but is not representative of human tumors. Therefore, the resection of GBM models with higher invasive properties (e.g. CNS-1, F98, GL261 [28]) could lead to interesting results and to know if a proper drug diffusion in the brain is obtained with the $GemC_{12}$-LNC. Moreover, many authors showed that established cell lines are poor models for human tumors and that using patient-derived xenograft models (derived from GBM primary cells or biopsy spheroids) could be more appropriate [43-45].

Secondly, it has been shown by some authors that strong immunogenicity can be observed using the 9L model in Fischer rats [40]. Other syngeneic models (e.g. CNS-1, F98, GL261, RG2 [46]) or genetically engineered models could be more appropriate to evaluate the treatment effects on the immune system [47].

3.2. THE STERILITY OF $GEMC_{12}$-LNC HYDROGEL

A major concern in the development of a nano-based delivery system for human application is its sterility [48]. The unique physicochemical and mechanical properties of $GemC_{12}$-LNC nanomedicine hydrogel make it impossible to sterilize after gelification in syringes. The most common and well-established sterilization techniques for nanoparticles are filtration and autoclave, but $GemC_{12}$-LNC can't filtered through 0.22 µm filters because of its gel consistency and the stability of the drug, the nanocarrier and the gel could change at high temperatures. Another option would be γ radiation, but 55% of the $GemC_{12}$-LNC hydrogel formulation is composed of water and its irradiation could generate radical species (e.g. hydroxyl radical) [49]. This assumption should be verified analyzing the physicochemical

properties, morphology, drug release and biological activity before and after radiation to evaluate any modification of $GemC_{12}$-LNC before excluding this technique. However, I believe that using sterilized primary material (e.g. 0.22 µm filtered H_2O/NaCl, Labrafac®, Kolliphor®, Span80®; γ-irradiated $GemC_{12}$) and perform the formulation process in aseptic conditions is the best option so far. Further studies will be addressed to sterilize the hydrogel without altering its physico-chemical and mechanical properties.

3.3. THE ADHESIVE PROPERTIES OF $GEMC_{12}$-LNC HYDROGEL

One of the limitations of Gliadel® is that the wafers drug loading is limited and their structure is rigid. Therefore, to have an optimal BCNU dosage, the cavity needed to be tall enough to host the wafers, and these need to be carefully placed inside the cavity. However, as their size and shape are not adapted to the anatomy of the resection cavity and their structure is rigid, they often suffered from dislodgement. To overcome these limitations, hydrogels are a very good alternative. Indeed, they can be loaded with a sufficient amount of drug, injected in the cavity and adapt to its shape. If the gel has a good adherence profile, it will stick to the cavity borders, increasing its contact surface.

The $GemC_{12}$-LNC hydrogel has a consistency which is adapted for brain implantation and adaptation to the resection cavity. When injected on the cavity borders in a bigger brain (e.g. pig brain, Figure 3) it seems not only to adapt to the cavity shape but also to adhere to the brain tissue in a “sticky” manner. However, further studies will need to proof the $GemC_{12}$-LNC bioadhesive properties *in vitro* and after brain contact *in vivo* as previously done by others for this or other purposes (e.g. skin [50]; inflamed colon [51]; vaginal application [52]). This can be performed, for example, determining the mucoadhesive strength from the force of detachment between the hydrogel and a mucin disk, using a mechanical texture analyzer [52].

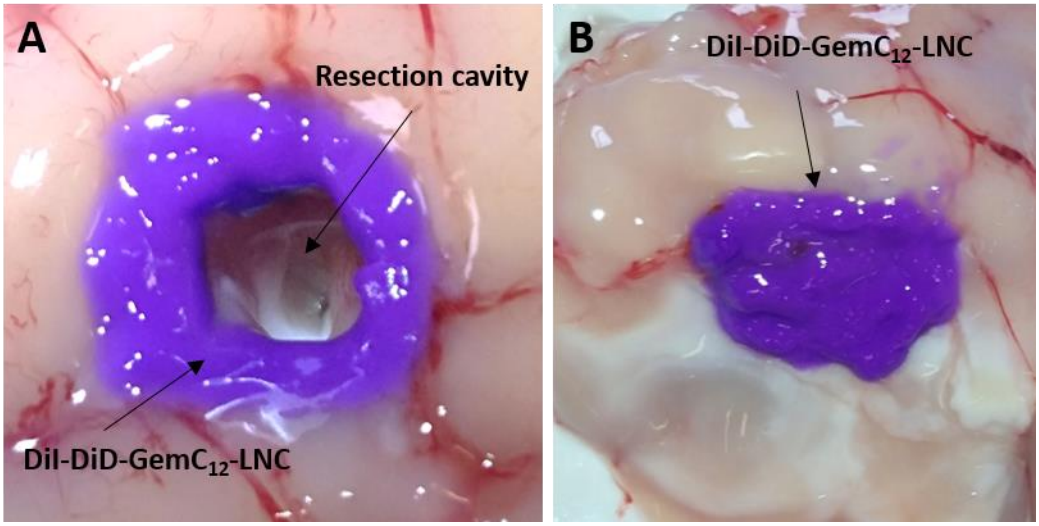

Figure 3. Adhesion of the DiI-DiD-GemC_{12}-LNC to the resection cavity borders in a pig brain: image taken from above (A) the resection cavity or laterally (B).

3.4. THE BRAIN DISTRIBUTION OF THE DRUG FROM THE ADMINISTRATION SITE

As GBM cells are highly infiltrative, it is important to obtain a uniformly distribution throughout the tumor/resection cavity parenchyma and away from the injection site after local administration in the brain. Several parameters can influence the distribution of therapeutics in the brain (e.g. size, adhesive properties) and therefore impact their translational applicability [53]. Therefore, measuring the distribution of the delivered agent in the brain is a crucial step in the development of a delivery system for local treatment of GBM. We have shown by FRET that the dye-labeled GemC_{12}-LNC hydrogel is still present in the resection cavity one week after administration, and that the LNC integrity is maintained during this period. However, we weren't able to visualize or to quantify the diffusion of the LNC from the administration site and this aspect will need to be addressed in the future. Several techniques could be used for this purpose: radiolabeling the drug or the nanoparticle to quantify it (e.g. [54, 55]) or visualize it through noninvasive imaging techniques (e.g. positron emission tomography [56]; autoradiography [57]); using fluorescent-labeled particles and reconstructing their volume of distribution in the brain (e.g. [17, 53, 58, 59]); using high-resolution multiple particle tracking of the nanoparticles (e.g. [58-60]); quantitatively analyze the amount of drug distributed in the brain (e.g. HPLC [61]).

3.5. THE INDUCTION OF CHEMORESISTANCE TO STANDARD OF CARE CHEMOTHERAPY

In cancer treatment, sustained release of drugs means that cancer cells may be exposed to suboptimal doses of drugs for long periods of time. Is it possible, in that case, to induce a drug resistance of cancer cells to the standard of care therapy? It is true that, *in vitro*, periodic exposure of GBM cells to escalating doses of drugs such as TMZ produces chemoresistant phenotypes [62]. However, we believe that *in vivo*, in the specific case of $GemC_{12}$-LNC injected in a tumor resection cavity, the answer to this question could be likely "no" for three reasons: (*i*) as the majority of the tumor cells have been resected with the surgery, the maintenance of lethal drug concentrations in the resection perimeter in the period immediately after the surgical resection (24-48 h) due to the burst effect will allow to kill rapidly the remaining cancer cells and prevent local tumor recurrence. After this, not only the healthy cells at the resection border but also in other parts of the brain would be subject to a low-concentration long-term exposure. If the drug is selective against the tumor cells, no local side effects should be observed and no chemoresistance should be induced, as the tumor cells do not remain in constant contact with the drug for long periods of time; (*ii*) the hydrogel protects the brain tissue (and so the healthy cells) from the direct contact with the drug, which is slowly released by the system. When the drug is released and penetrates in the brain tissue, it comes in contact with the residual infiltrating cells and kills them, avoiding the development of multifocal gliomas; (*iii*) as previously mentioned before, Gem and TMZ have different mechanisms of action and their chemoresistance pathways differ too. For this reason, treating the residual tumoral cells with $GemC_{12}$-LNC before starting the standard of care chemoradiation should not increase the risk of chemoresistance to TMZ.

Further studies evaluating if the local treatment with $GemC_{12}$-LNC correspond to an increased TMZ chemoresistance in the recurrent tumor should be performed. This could be done *in vitro* evaluating the TMZ sensitivity of the cells after prolonged exposure to low $GemC_{12}$ concentrations, or *ex vivo* analyzing the expression of genes correlated to TMZ resistance (e.g. MGMT promoter expression and methylation status, mismatch repair deficiency pathway mutations [63]) in the recurrent tumors of animals treated with $GemC_{12}$-LNC after resection.

4. CURRENT AND FUTURE PERSPECTIVES

This PhD thesis gives solid bases to consider $GemC_{12}$-LNC as a promising drug-loaded hydrogel for the local treatment of GBM. However, to exploit the full potential of $GemC_{12}$-LNC, several alternative pathways can be investigated in the future. These are based on the fact that $GemC_{12}$-LNC combines

- an hydrogel – $GemC_{12}$-LNC – with a simple formulation adapted for brain implantation, which might be able to host multiple active molecules for a combined therapy against GBM;
- a nanocarrier – LNC – which can be grafted on its surface for active targeting of GBM cells;
- a potent cytotoxic drug – $GemC_{12}$ – whose parent drug has shown great potential against GBM for its radiosensitizing and immunomodulatory properties.

To fight a tumor as aggressive and heterogeneous as GBM, combining different therapeutical approaches will probably be the more effective strategy. For this reason I think that the first step to exploit the full potential of $GemC_{12}$-LNC for the local treatment of GBM would be to evaluate its efficacy and safety in combination with radiotherapy and chemotherapy with temozolomide. Gem and TMZ are effective as chemotherapeutic agents on GBM alone or in combination with radiotherapy, but both are subject to chemoresistance and are not adequate to kill infiltrating GBM cells. As acting through different mechanisms of action (see Figure 8 of Chapter I), no cross-resistance or side effects overlap should be observed from Gem+TMZ combination, which might instead result in enhanced cytotoxic effect as previously reported in the literature (e.g. [64, 65]). Moreover, the use of Gem in combination with radiotherapy would be particularly beneficial (*i*) in patients with unmethylated MGMT promoter who are intrinsically resistant to TMZ and/or (*ii*) in non-operable GBM patients, where the specific characteristics of Gem (e.g. immunomodulatory properties, toxic activity mediated through gap junctions), its combination to the LNCs, and the local administration of the treatment could achieve similar or better tumor growth inhibition compared to the standard of care chemoradiation.

With this in mind, this section aims at evaluating some other alternative perspectives of this PhD project and shows some preliminary results that were obtained to establish future working strategies (Figure 4).

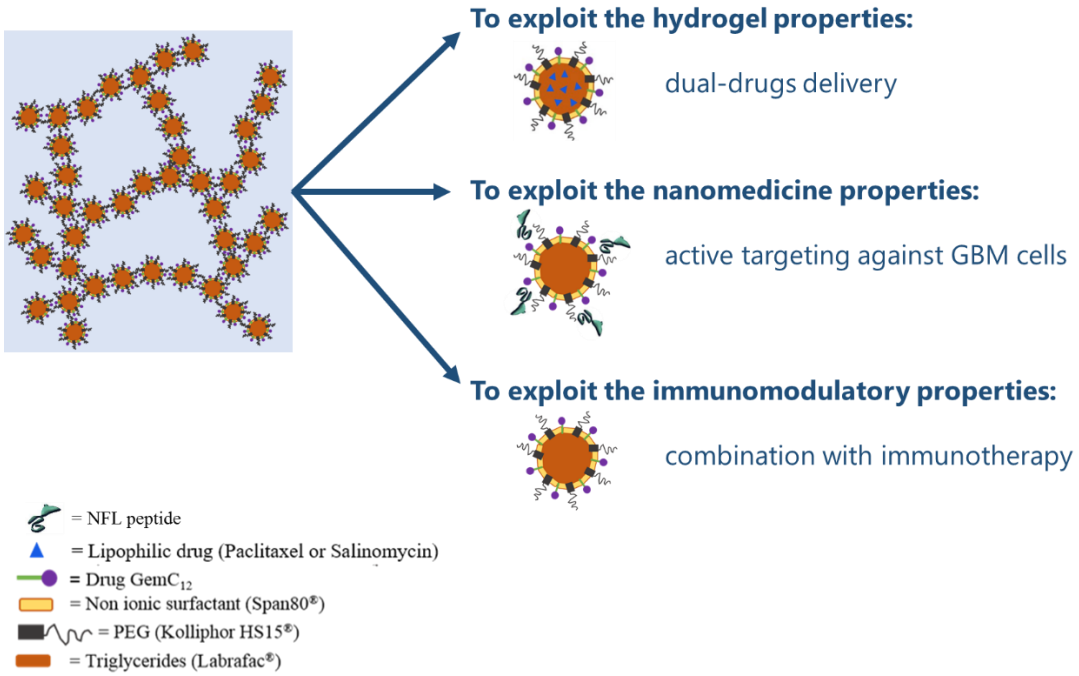

Figure 4. Schematic representation of three possible perspectives that arise from this PhD project, for the development of an optimized nanomedicine hydrogel treatment for GBM.

4.1. TO EXPLOIT THE HYDROGEL PROPERTIES

A pathway that could be explored to enhance the anti-cancer efficacy of $GemC_{12}$-LNC is to evaluate its use as nanodelivery platform for other drugs, to obtain a combined local therapeutic approach for GBM.

The rationale behind the choice of a dual treatment for GBM must take into account that (*i*) the single drugs must have a strong cytotoxic activity against GBM cells when used alone; (*ii*) the drugs must act through different mechanisms of action and their toxicities should not overlap; (*iii*) the drug characteristics must be compatible with the formulation (e.g. for $GemC_{12}$-LNC a lipophilic drug could be incorporated in the oily core of the LNC while an hydrophilic drug could be added in the aqueous phase of the formulation). Based on this, several molecules which have shown promising results against GBM might be tested in combination with Gem (e.g. Acriflavine, Curcumin, Ferrociphenol, Curcumin). However, for this Thesis, I thought that repurposing drug combinations that have already shown to be

efficient on other types of tumors could be a smart (and fast) way to find possible combinations for GBM.

Therefore, we firstly used PTX as a model molecule to evaluate if its incorporation in the LNC oily core would change the physicochemical properties of the LNC and the mechanical properties of the $GemC_{12}$-LNC hydrogel. The combination between PTX and Gem is currently used for metastatic breast cancer and pancreatic cancer treatment. Moreover, PTX was chosen because it has been previously encapsulated in LNC obtaining high encapsulation efficiency and drug loading [66, 67] and its efficacy against GBM cells had already been proved showing promising results (e.g. [68]).

Table 2. Physicochemical characterization and loading efficacy of $GemC_{12}$-loaded lipid nanocapsules (N=3 *n*=3; mean ± SD)

	Size (nm)	**PDI**	**ζ-pot (mV)**
$GemC_{12}$-LNC	55 ± 2	0.11 ± 0.01	- 2.6 ± 0.7
PTX-$GemC_{12}$-LNC	59 ± 3	0.17 ± 0.04	- 2.7 ± 0.7
Sal-$GemC_{12}$-LNC	58 ± 1	0.23 ± 0.01	- 4.0 ± 0.7

Legend: PDI: polydispersity index; ζ-pot: zeta potential

Our results, performed by Pharmacy master student Urszula Luyten under my supervision, are reported in table 2. No significant difference in terms of size, PDI and zeta potential were observed between the $GemC_{12}$-LNC and PTX-$GemC_{12}$-LNC formulations. The encapsulation efficiency of $GemC_{12}$ and PTX were around 100% for both drugs, consistent with data previously reported in the literature for $GemC_{12}$-LNC and PTX-LNC. The drug loading of PTX-$GemC_{12}$-LNC corresponded to 1.6% for PTX and 7.6% for $GemC_{12}$. The stability of the PTX-$GemC_{12}$-LNC formulation was evaluated during 6 months at 4°C and no significant differences were observed in term of size, PDI, zeta potential or drugs EE during this time (data not shown).

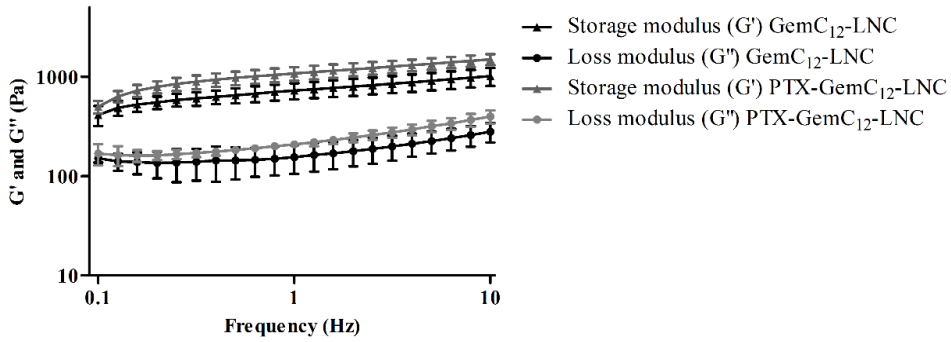

Figure 5. Viscoelastic property profiles of $GemC_{12}$-LNC (black line) and PTX-$GemC_{12}$-LNC (grey line): storage modulus G' (triangles) and loss modulus G" (circles) *vs* frequency. (mean ± SD; N=4 *n*=4)

Moreover, the addition of an active ingredient in the oily core of the LNC did not alter the viscoelastic properties of the formulation, which remains an injectable hydrogel adapted for brain implantation (G' 1.12 ± 0.16 kPa; G" 0.25 ± 0.04 kPa; G'/G" 4.5 ± 0.7) (Figure 5).

Once established that $GemC_{12}$-LNC can deliver multiple drugs, the more expensive molecule Salinomycin (Sal) was loaded in the formulation. Sal is a polyether ionophore antibiotic which has shown to be >100-fold more effective than PTX in killing breast cancer stem cells (CSC) *in vitro* and to reduce tumor growth *in vivo* [69]. Sal also proved to be effective against GBM, not only to kill CSC and GBM cells but also to downregulate damage repair proteins (e.g. MGMT) that mediate resistance to TMZ [70-72]. The mechanism of cell death of Sal is still unclear, but recent data suggest that Sal induces oxidative stress and production of reactive oxygen species which result in abortive autophagy and regulated GBM cells necrosis [72]. The combination between Gem and Sal has been proved in a pancreatic model and seems promising, as one drug can suppress the viability of non-CSC cells while the second inhibits CSC growth [73]. Moreover, Sal has been shown to be effective against Gem-resistant pancreatic cancer cells, meaning that it could kill a different set of cells compared to Gem [74].

The Sal-$GemC_{12}$-LNC is an injectable hydrogel with no differences in terms of size, PDI and zeta potential compared to $GemC_{12}$-LNC or PTX-$GemC_{12}$-LNC (Table 2). Sal is highly lipophilic [75] and does not absorb in UV, therefore its EE and drug loading couldn't be measured by HPLC-UV. A study performed in our group using Liquid Chromatography/Mass Spectrometry showed an EE of 99.9% in Sal-LNC (experiments performed by Nikolaos Tsakiris in collaboration with Prof. Giulio Muccioli; data not shown). Similar EE is expected for Sal-$GemC_{12}$-LNC but further characterization studies are needed to confirm this value.

We evaluated the ability of the Sal-GemC$_{12}$-LNC hydrogel to delay the recurrences formation in a preliminary study performed on the 9L model in rats. Rats were injected with 9L cells and tumor resection was performed at day 9 post cells inoculation as discussed in chapter 6. Five µL of hydrogel (corresponding to 0.4 mg/kg of GemC$_{12}$ and 0.1 mg/kg of Sal) were injected perisurgically in the resection cavity and the survival of the animals was evaluated over time. The preliminary results of this experiment are presented in Figure 6 (experiment on going at the time of submission of the manuscript), and show a delay in tumor recurrences in the Sal-GemC$_{12}$-LNC group compared to the GemC$_{12}$-LNC hydrogels and the untreated groups. The median survival of the GemC$_{12}$-LNC and Sal-GemC$_{12}$-LNC animals was significantly prolonged compared to the resected untreated animals (42, 74.5 and 28 days respectively). These promising results suggest that, despite the very good activity of GemC$_{12}$-LNC, there could be a rationale for the combination with other agents which act through different mechanism of action or directly on specific sets of cells (e.g. CSCs). However, it is important to highlight that this is only a preliminary data and more complete studies will need to be performed in this sense (including more control groups and increasing the number of animals per group).

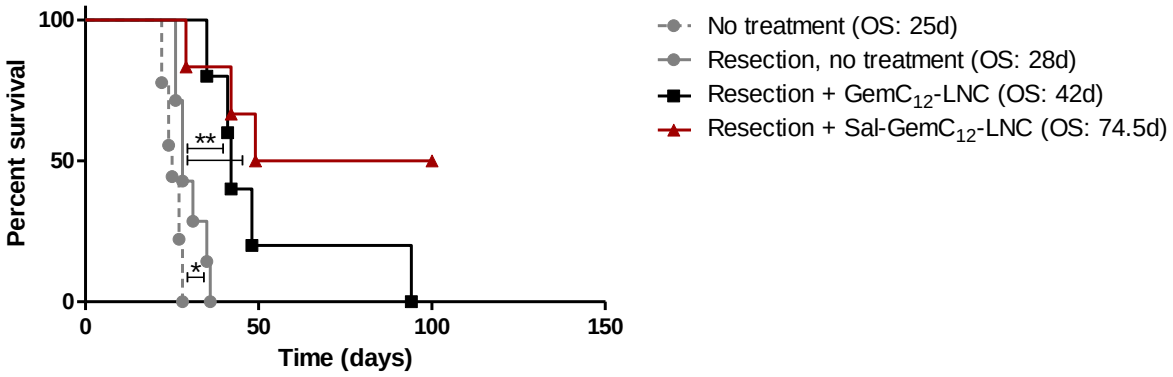

Figure 6. Kaplan-Meier survival curves for animals with 9L tumors untreated or resected and treated (resection performed 9 days post-tumor inoculation). Drug dose administered: 0.4 mg/kg GemC$_{12}$, 0.1 mg/kg Sal (*n* = 4-9 for all groups). Mantel Cox test (** p<0.01). OS: overall survival

4.2. TO EXPLOIT THE NANOMEDICINE PROPERTIES

One of the advantages of nanocarriers is that they can be grafted at their surface with specific ligands able to recognize receptors overexpressed in tumor cells enabling them for active targeting. Among the grafting moieties that can be used to specifically target GBM

cells, the laboratory of Prof. Eyer (Université d'Angers) has focused its attention on the peptide NFL-TBS.40-63 (tubulin-binding site on light neurofilament subunit; NFL).

The LNC functionalized with the peptide NFL represent a powerful drug-carrier system for glioma targeted treatment. Indeed, NFL can selectively enter in GBM cells *in vitro* and after intratumoral administration of PTX-loaded NFL-LNC a reduction of tumour progression was observed *in vivo* [76, 77]. Considering the advantages of an active targeting strategy, that would allow a selective targeting of the tumoral cells, I believe that adsorbing NFL on the surface of $GemC_{12}$-LNC could be a promising approach that could lead to a better anti-tumor response to the hydrogel. Some preliminary studies performed in collaboration with Dr. Dario Carradori confirmed that the addition of NFL together with water in the shock dilution phase of the formulation does not alter the gelification process of $GemC_{12}$-LNC. However, further studies will need to be performed to characterize the system and confirm that the preferential uptake of NFL when grafted on $GemC_{12}$-LNC is observed *in vitro.*

4.3. TO EXPLOIT THE IMMUNOMODULATORY PROPERTIES OF $GEMC_{12}$-LNC

Cancer immunotherapy is based on the immune system ability to target and kill tumor cells. Although the CNS has always been considered an immunologically privileged site, recent findings in immunotherapy for brain tumors leave hope for future clinical success in this field [78, 79]. Now is known that GBM cells secrete chemokines (e.g. CCL2, CCL20, CCL7) able to mediate the recruitment of immune cells including microglia (which represents <30% of GBM tumor), peripheral macrophages, leucocytes and MDSCs. These cells are able to induce directly or indirectly - through the secretion of cytokines (e.g. IL-13, IL-4, IL-10) and soluble factors (e.g. TGF-β) - a powerful immunosuppressive response [78, 80, 81].

Gem immunomodulatory properties have been demonstrated in murine tumor models, where treatment with the drug led to therapeutic efficacy independently from the drug cytotoxic activity, due to an enhancement of T-cell mediated anti-tumor immune effect [82]. Gem has shown to increase the expression of class I major histocompatibility complex (MHC-I) on malignant cells, to enhance the cross-presentation of tumor antigens to $CD8^+$ T cells resulting in increased proliferation and functionality. Moreover, it can selectively kill local intratumoral myeloid-derived suppressor cells (MDSCs) thus facilitating T-cell dependent anti-cancer immunity (Figure 7) [83, 84]. Recently, $GemC_{12}$-LNC have shown to be able to

target the monocytic MDSCs in lymphoma and melanoma-bearing mice and human blood samples from healthy donors and melanoma patients in a higher extent compared to Gem or $GemC_{12}$ [35].

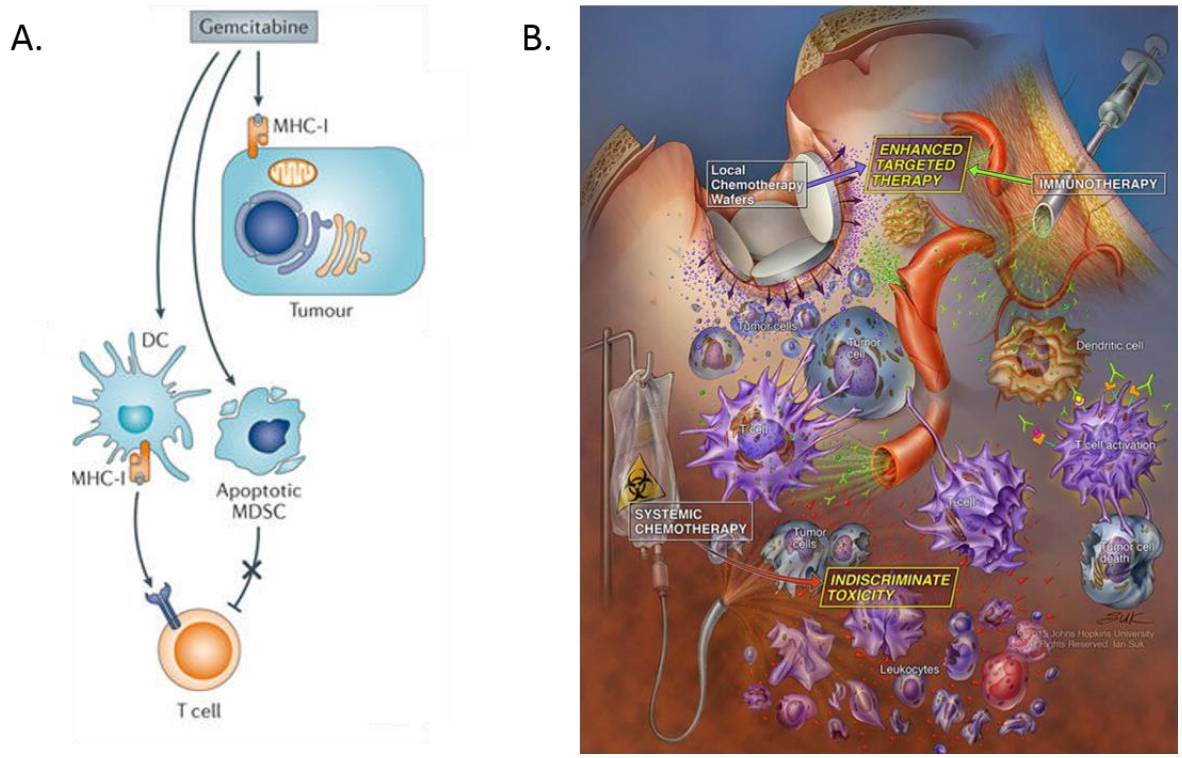

Figure 7. Rationale for the use of $GemC_{12}$-LNC hydrogel in combination with immunotherapy. **(A)** It is known that Gem possess immunomodulatory properties and the mechanisms through which Gem affects the immune system include the selective killing of myeloid-derived suppressor cells thus inversing the tumor immunosuppressive response; **(B)** It has been recently demonstrated that local delivery of chemotherapeutic drugs can enhance immunotherapy by attracting at the tumor site (or tumor resection site) activated immune cells. DC: dendritic cell; MHC-1: class I major histocompatibility complex; MDSC: myeloid-derived suppressor cells. Adapted from [83] and [85].

As a future perspective for this project, I believe that the combination of $GemC_{12}$-LNC with immunotherapy (e.g. vaccine expressing glioma specific antigen) could be a promising approach. In this direction, I am currently optimizing the "biopsy punch" resection procedure on a GL261 immunocompetent mouse model. GL261 is a less immunogenic model compared to the previously tested 9L and C6 rat models, presents diffusive infiltrating pattern and presents specific tumor antigens. In collaboration with Dr. Vandermeulen and the PhD student Alessandra Lopes, we aim at developing a DNA vaccine encoding tumor

associated antigen genes and evaluate its therapeutic efficacy in combination with the local administration of $GemC_{12}$-LNC in the GL261 resection model. Indeed, a recent study by Mathios *et* al. has shown that local chemotherapy could enhance glioma immunotherapy in a much higher extent compared to systemic chemotherapy, because it destroys the tumor microenvironment attracting the activated immune cells toward the tumor area [85]. Hopefully, the combined action of locally delivered $GemC_{12}$-LNC on MDSCs and the vaccine ability to stimulate specific CD8+ and CD4+ responses could avoid GBM recurrences.

5. OPINION ON CLINICAL PERSPECTIVES

GBM represents one of the greatest challenges in oncology nowadays and the challenge in finding a cure is a daunting task. New, specific and more effective drugs and/or multi-drug synergistic approaches that allow to target different tumorigenic pathways need to be discovered to reach the goal of eradicating GBM. Also, more efficient drug delivery strategies able to achieve the drug release at optimal concentrations over a sustained period and able to suppress tumor growth need to be used against GBM.

The $GemC_{12}$-LNC hydrogel is still far from being adapted for a human application, and some ideas to achieve its transability were discussed in the last chapters. However, I personally believe that multi-drug loaded smart hydrogel could represent a valid option in the future for GBM management. Also, I think that $GemC_{12}$ is a good choice for this purpose, because it shows high efficacy against GBM cells and ability to work in synergy with many other compounds and radiotherapy.

As previously mentioned in this PhD thesis, the ideal hydrogel should (*i*) be injectable or be sprayed and stick to the resection cavity borders and be adaptable to its shape. (*ii*) be soft and have mechanical properties close to the brain to avoid increased intracranial pressure; (*iii*) its drug content should be high enough to reach the desired local dose without filling the entire cavity (Figure 8). These ideal parameters might seem simple to achieve in preclinical models, but they are surely not that easy to apply for a human application.

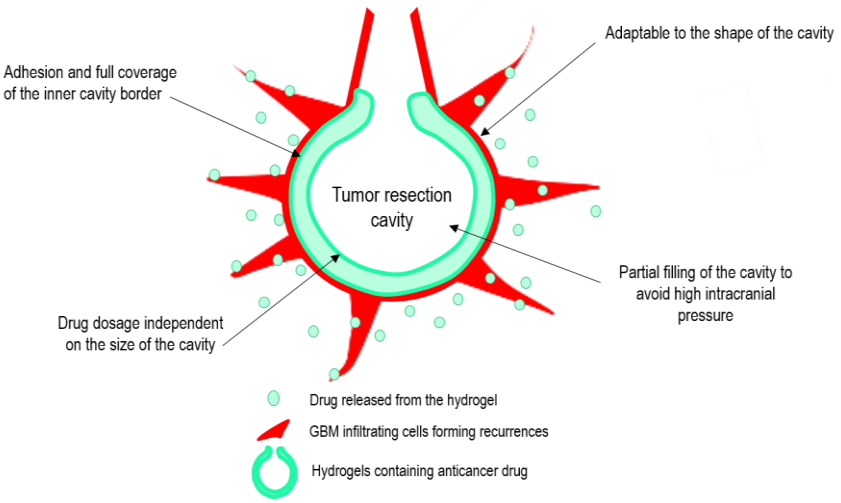

Figure 8. Schematic representation of the ideal characteristics and behaviour of a hydrogel developed for the local treatment of GBM. Adapted from [2].

Despite being injectable and adaptable to the brain resection cavity, $GemC_{12}$-LNC can be expelled from the cavity in rats as a cause of bleeding and high swelling. In this PhD thesis, we solved this problem by modifying the gel to reduce the volume administered or by reducing the dose injected. However, this is something that needs to be carefully considered in the future, as the volumes of CSF, blood and the intracranial pressure in humans are much higher compared to rodents. Also, the size of the tumor resection cavity in our rodent models was quite small (around 9 mm^3 in mice, 28 mm^3 in rats) and the $GemC_{12}$-LNC administered directly in this cavity fulfilled it completely. However, the surgical residual cavity in humans can be very big (e.g. median tumor volume 14-55 cm^3, 91% resection [86]; mean resection cavity volume 7.8 cm^3 [87]) and the ideal hydrogel should adhere to its borders to maximize the drug distribution and avoid injecting high volumes of hydrogels. As the $GemC_{12}$-LNC mechanical properties depend on the concentration of the drug in the formulation, the administered dose is limited by the volume that can be injected in the resection cavity. To avoid administration of high volumes and reduce the risk of expulsion from the cavity, it might be needed to attach the hydrogel to adherent biodegradable membranes able to be placed in the cavity and adapt/stick to the brain parenchyma. $GemC_{12}$-LNC could also be combined with molecules able to reduce quickly the brain swelling and edema (e.g. surgifoam® [88]; gelatin-thrombin matrix [89]), to increase the ability of the hydrogel to remain in the cavity. A third option would be to combine the $GemC_{12}$-LNC with the similar, recently developed, $cytidineC_{16}$-LNC hydrogel. This formulation was developed at the University of Angers, it is non-toxic and has mechanical properties similar to $GemC_{12}$-LNC. The combination of these two formulations would allow to increase the volume of hydrogel in the resection cavity without increasing the $GemC_{12}$ dose.

In conclusion, this challenging and original project showed that nanomedicine hydrogels are a promising tool for the local treatment of GBM, at least in preclinical models. Several clinical limitations will need to be considered before dreaming the use of $GemC_{12}$-LNC in the clinics. However, in this PhD project that we expanded the knowledge about the use of Gem derivatives against GBM, and hopefully others will focus on its potential use for this tumor. Moreover, the surgical procedure that has been developed in rodents to resect GBM orthotopic tumors can be useful to test any other kind of local delivery systems (e.g. foams, membranes, 3D scaffolds).

6. REFERENCES

[1] C.V. Rahman, S.J. Smith, P.S. Morgan, K.A. Langmack, P.A. Clarke, A.A. Ritchie, D.C. Macarthur, F.R. Rose, K.M. Shakesheff, R.G. Grundy, R. Rahman, Adjuvant chemotherapy for brain tumors delivered via a novel intra-cavity moldable polymer matrix, PloS one, 8 (2013) e77435.

[2] C. Bastiancich, P. Danhier, V. Preat, F. Danhier, Anticancer drug-loaded hydrogels as drug delivery systems for the local treatment of glioblastoma, J Control Release, 243 (2016) 29-42.

[3] J.J. Olson, L. Nayak, D.R. Ormond, P.Y. Wen, S.N. Kalkanis, The role of cytotoxic chemotherapy in the management of progressive glioblastoma, J Neurooncol, 118 (2014) 501-555.

[4] J. Zhou, K.B. Atsina, B.T. Himes, G.W. Strohbehn, W.M. Saltzman, Novel delivery strategies for glioblastoma, Cancer J, 18 (2012) 89-99.

[5] C. Bastiancich, G. Bastiat, F. Lagarce, Gemcitabine and glioblastoma: challenges and current perspectives, Drug Discov Today, (2017).

[6] E. Moysan, G. Bastiat, J.P. Benoit, Gemcitabine versus Modified Gemcitabine: a review of several promising chemical modifications, Molecular Pharm, 10 (2013) 430-444.

[7] N.T. Huynh, C. Passirani, P. Saulnier, J.P. Benoit, Lipid nanocapsules: a new platform for nanomedicine, Int J Pharm, 379 (2009) 201-209.

[8] E. Moysan, Y. Gonzalez-Fernandez, N. Lautram, J. Bejaud, G. Bastiat, J.P. Benoit, An innovative hydrogel of gemcitabine-loaded lipid nanocapsules: when the drug is a key player of the nanomedicine structure, Soft Matter, 10 (2014) 1767-1777.

[9] Y.R. Lawrence, D.T. Blumenthal, D. Matceyevsky, A.A. Kanner, F. Bokstein, B.W. Corn. Delayed initiation of radiotherapy for glioblastoma: how important is it to push to the front (or the back) of the line? J Neurooncol, 105 (2011) 1-7.

[10] C. Irwin, M. Hunn, G. Purdie, D. Hamilton. Delay in radiotherapy shortens survival in patients with high grade glioma. J Neurooncol, 85 (2007) 339-43.

[11] E. Fournier, C. Passirani, C.N. Montero-Menei, J.P. Benoit, Biocompatibility of implantable synthetic polymeric drug carriers: focus on brain biocompatibility, Biomaterials, 24 (2003) 3311-3331.

[12] J. Rieger, S. Durka, J. Streffer, J. Dichgans, M. Weller, Gemcitabine cytotoxicity of human malignant glioma cells: modulation by antioxidants, BCL-2 and dexamethasone, Eur J Pharmacol, 365 (1999) 301-308.

[13] L.J. Ostruszka, D.S. Shewach, The role of cell cycle progression in radiosensitization by 2',2'-difluoro-2'-deoxycytidine, Cancer Res, 60 (2000) 6080-6088.

[14] M. Genc, N. Castro Kreder, A. Barten-van Rijbroek, L.J. Stalpers, J. Haveman, Enhancement of effects of irradiation by gemcitabine in a glioblastoma cell line and cell line spheroids, J Cancer Res Clin Oncol, 130 (2004) 45-51.

[15] G. Carpinelli, B. Bucci, I. D'Agnano, R. Canese, F. Caroli, L. Raus, E. Brunetti, D. Giannarelli, F. Podo, C.M. Carapella, Gemcitabine treatment of experimental C6 glioma: the effects on cell cycle and apoptotic rate, Anticancer Res, 26 (2006) 3017-3024.

[16] M.L. Immordino, P. Brusa, F. Rocco, S. Arpicco, M. Ceruti, L. Cattel, Preparation, characterization, cytotoxicity and pharmacokinetics of liposomes containing lipophilic gemcitabine prodrugs, J Control Release, 100 (2004) 331-346.

[17] A. Gaudin, E. Song, A.R. King, J.K. Saucier-Sawyer, R. Bindra, D. Desmaele, P. Couvreur, W.M. Saltzman, PEGylated squalenoyl-gemcitabine nanoparticles for the treatment of glioblastoma, Biomaterials, 105 (2016) 136-144.

[18] P. Brusa, M.L. Immordino, F. Rocco, L. Cattel, Antitumor activity and pharmacokinetics of liposomes containing lipophilic gemcitabine prodrugs, Anticancer Res, 27 (2007) 195-199.

[19] W.G. Chung, M.A. Sandoval, B.R. Sloat, P.D. Lansakara, Z. Cui, Stearoyl gemcitabine nanoparticles overcome resistance related to the over-expression of ribonucleotide reductase subunit M1, J Control Rel, 157 (2012) 132-140.

[20] B.R. Sloat, M.A. Sandoval, D. Li, W.G. Chung, P.D. Lansakara, P.J. Proteau, K. Kiguchi, J. DiGiovanni, Z. Cui, In vitro and in vivo anti-tumor activities of a gemcitabine derivative carried by nanoparticles, Int J Pharm, 409 (2011) 278-288.

[21] N. Wauthoz, G. Bastiat, E. Moysan, A. Cieslak, K. Kondo, M. Zandecki, V. Moal, M.C. Rousselet, J. Hureaux, J.P. Benoit, Safe lipid nanocapsule-based gel technology to target lymph nodes and combat

mediastinal metastases from an orthotopic non-small-cell lung cancer model in SCID-CB17 mice, Nanomedicine, 11 (2015) 1237-1245.
[22] C. Bastiancich, K. Vanvarenberg, B. Ucakar, M. Pitorre, G. Bastiat, F. Lagarce, V. Preat, F. Danhier, Lauroyl-gemcitabine-loaded lipid nanocapsule hydrogel for the treatment of glioblastoma, J Control release, 225 (2016) 283-293.
[23] X.M. Tao, J.C. Wang, J.B. Wang, Q. Feng, S.Y. Gao, L.R. Zhang, Q. Zhang, Enhanced anticancer activity of gemcitabine coupling with conjugated linoleic acid against human breast cancer in vitro and in vivo, Eur J Pharm Biopharm, 82 (2012) 401-409.
[24] P.D. Lansakara, B.L. Rodriguez, Z. Cui, Synthesis and in vitro evaluation of novel lipophilic monophosphorylated gemcitabine derivatives and their nanoparticles, Int J Pharm, 429 (2012) 123-134.
[25] R.D. Dubey, A. Saneja, P.K. Gupta, P.N. Gupta, Recent advances in drug delivery strategies for improved therapeutic efficacy of gemcitabine, Eur J Pharm Sci, 93 (2016) 147-162.
[26] D.P. Ivanov, B. Coyle, D.A. Walker, A.M. Grabowska, In vitro models of medulloblastoma: Choosing the right tool for the job, J Biotechnol, 236 (2016) 10-25.
[27] D.P. Ivanov, A.J. Al-Rubai, A.M. Grabowska, M.K. Pratten, Separating chemotherapy-related developmental neurotoxicity from cytotoxicity in monolayer and neurosphere cultures of human fetal brain cells, Toxicol In Vitro, 37 (2016) 88-96.
[28] V.L. Jacobs, P.A. Valdes, W.F. Hickey, J.A. De Leo, Current review of in vivo GBM rodent models: emphasis on the CNS-1 tumour model, ASN neuro, 3 (2011) e00063.
[29] J. Bianco, C. Bastiancich, N. Joudiou, B. Gallez, A. des Rieux, F. Danhier, Novel model of orthotopic U-87 MG glioblastoma resection in athymic nude mice, J Neurosci Met, 284 (2017) 96-102.
[30] L. Qiang, Y. Yang, Y.J. Ma, F.H. Chen, L.B. Zhang, W. Liu, Q. Qi, N. Lu, L. Tao, X.T. Wang, Q.D. You, Q.L. Guo, Isolation and characterization of cancer stem like cells in human glioblastoma cell lines, Cancer Lett, 279 (2009) 13-21.
[31] M. Allen, M. Bjerke, H. Edlund, S. Nelander, B. Westermark, Origin of the U87MG glioma cell line: Good news and bad news, Sci Transl Med, 8 (2016) 354re3.
[32] O. Okolie, J.R. Bago, R.S. Schmid, D.M. Irvin, R.E. Bash, C.R. Miller, S.D. Hingtgen, Reactive astrocytes potentiate tumor aggressiveness in a murine glioma resection and recurrence model, Neuro Oncol, 18 (2016) 1622-1633.
[33] L. Zitvogel, A. Tesniere, L. Apetoh, F. Ghiringhelli, G. Kroemer, Immunological aspects of anticancer chemotherapy, Bull Acad Natl Med, 192 (2008) 1469-1489.
[34] I. Szadvari, O. Krizanova, P. Babula, Athymic nude mice as an experimental model for cancer treatment, Physiol Res, 65 (2016) S441-s453.
[35] M.S. Sasso, G. Lollo, M. Pitorre, S. Solito, L. Pinton, S. Valpione, G. Bastiat, S. Mandruzzato, V. Bronte, I. Marigo, J.P. Benoit, Low dose gemcitabine-loaded lipid nanocapsules target monocytic myeloid-derived suppressor cells and potentiate cancer immunotherapy, Biomaterials, 96 (2016) 47-62.
[36] T. Wurdinger, K. Deumelandt, H.J. van der Vliet, P. Wesseling, T.D. de Gruijl, Mechanisms of intimate and long-distance cross-talk between glioma and myeloid cells: how to break a vicious cycle, Biochim Biophys Acta, 1846 (2014) 560-575.
[37] A. Tuettenberg, K. Steinbrink, D. Schuppan, Myeloid cells as orchestrators of the tumor microenvironment: novel targets for nanoparticular cancer therapy, Nanomedicine (Lond), 11 (2016) 2735-2751.
[38] B. Raychaudhuri, P. Rayman, J. Ireland, J. Ko, B. Rini, E.C. Borden, J. Garcia, M.A. Vogelbaum, J. Finke, Myeloid-derived suppressor cell accumulation and function in patients with newly diagnosed glioblastoma, Neuro-Oncol, 13 (2011) 591-599.
[39] M. Candolfi, J.F. Curtin, W.S. Nichols, A.G. Muhammad, G.D. King, G.E. Pluhar, E.A. McNiel, J.R. Ohlfest, A.B. Freese, P.F. Moore, J. Lerner, P.R. Lowenstein, M.G. Castro, Intracranial glioblastoma models in preclinical neuro-oncology: neuropathological characterization and tumor progression, J Neurooncol, 85 (2007) 133-148.
[40] L.A. Lampson, M.A. Lampson, A.D. Dunne, Exploiting the lacZ reporter gene for quantitative analysis of disseminated tumor growth within the brain: use of the lacZ gene product as a tumor antigen, for evaluation of antigenic modulation, and to facilitate image analysis of tumor growth in situ, Cancer Res, 53 (1993) 176-182.
[41] R.F. Barth, B. Kaur, Rat brain tumor models in experimental neuro-oncology: the C6, 9L, T9, RG2, F98, BT4C, RT-2 and CNS-1 gliomas, J Neurooncol, 94 (2009) 299-312.

[42] A. Vonarbourg, A. Sapin, L. Lemaire, F. Franconi, P. Menei, P. Jallet, J.J. Le Jeune, Characterization and detection of experimental rat gliomas using magnetic resonance imaging, Magma (New York), 17 (2004) 133-139.
[43] P.C. Huszthy, I. Daphu, S.P. Niclou, D. Stieber, J.M. Nigro, P.O. Sakariassen, H. Miletic, F. Thorsen, R. Bjerkvig, In vivo models of primary brain tumors: pitfalls and perspectives, Neuro-oncol, 14 (2012) 979-993.
[44] S.E. Gould, M.R. Junttila, F.J. de Sauvage, Translational value of mouse models in oncology drug development, Nat Med, 21 (2015) 431-439.
[45] L. Janbazian, J. Karamchandani, S. Das, Mouse models of glioblastoma: lessons learned and questions to be answered, J Neurooncol, 118 (2014) 1-8.
[46] M.E. Sughrue, I. Yang, A.J. Kane, M.J. Rutkowski, S. Fang, C.D. James, A.T. Parsa, Immunological considerations of modern animal models of malignant primary brain tumors, J Transl Med, 7 (2009) 84.
[47] E.I. Fomchenko, E.C. Holland, Mouse models of brain tumors and their applications in preclinical trials, Clin Cancer Res, 12 (2006) 5288-5297.
[48] M.A. Vetten, C.S. Yah, T. Singh, M. Gulumian, Challenges facing sterilization and depyrogenation of nanoparticles: Effects on structural stability and biomedical applications in preclinical trials Nanomedicine, 10 (2014) 1391-1399
[49] K. Aparecida da Silva Aquino (2012). Sterilization by Gamma Irradiation, Gamma Radiation, Prof. Feriz Adrovic (Ed.), InTech, doi: 10.5772/34901.
[50] Y. Deng, A. Ediriwickrema, F. Yang, J. Lewis, M. Girardi, W.M. Saltzman, A sunblock based on bioadhesive nanoparticles, Nat Mater, 14 (2015) 1278-1285.
[51] S. Zhang, J. Ermann, M.D. Succi, A. Zhou, M.J. Hamilton, B. Cao, J.R. Korzenik, J.N. Glickman, P.K. Vemula, L.H. Glimcher, G. Traverso, R. Langer, J.M. Karp, An inflammation-targeting hydrogel for local drug delivery in inflammatory bowel disease, Sci Transl Med, 7 (2015) 300ra128.
[52] T. Furst, M. Piette, A. Lechanteur, B. Evrard, G. Piel. Mucoadhesive cellulosic derivative sponges as drug delivery system for vaginal application. Eur J Pharm Biopharm, 95 (2015) 128-35.
[53] C. Zhang, P. Mastorakos, M. Sobral, S. Berry, E. Song, E. Nance, C.G. Eberhart, J. Hanes, J.S. Suk, Strategies to enhance the distribution of nanotherapeutics in the brain, J Control Release, (2017).
[54] U.M. Upadhyay, B. Tyler, Y. Patta, R. Wicks, K. Spencer, A. Scott, B. Masi, L. Hwang, R. Grossman, M. Cima, H. Brem, R. Langer, Intracranial microcapsule chemotherapy delivery for the localized treatment of rodent metastatic breast adenocarcinoma in the brain, Proc Natl Acad Sci U S A, 111 (2014) 16071-16076.
[55] V.G. Roullin, J.R. Deverre, L. Lemaire, F. Hindre, M.C. Venier-Julienne, R. Vienet, J.P. Benoit, Anti-cancer drug diffusion within living rat brain tissue: an experimental study using [3H](6)-5-fluorouracil-loaded PLGA microspheres, Eur J Pharm Biopharm, 53 (2002) 293-299.
[56] J. Zhou, T.R. Patel, R.W. Sirianni, G. Strohbehn, M.Q. Zheng, N. Duong, T. Schafbauer, A.J. Huttner, Y. Huang, R.E. Carson, Y. Zhang, D.J. Sullivan, Jr., J.M. Piepmeier, W.M. Saltzman, Highly penetrative, drug-loaded nanocarriers improve treatment of glioblastoma, Proc Natl Acad Sci U S A, 110 (2013) 11751-11756.
[57] S. O'Reilly, N.R. Hartman, S.A. Grossman, J.M. Strong, R.F. Struck, S. Eller, G.J. Lesser, R.C. Donehower, E.K. Rowinsky, Tissue and tumor distribution of C-penclomedine in rats, Clin Cancer Res, 2 (1996) 541-548.
[58] E. Nance, C. Zhang, T.Y. Shih, Q. Xu, B.S. Schuster, J. Hanes, Brain-penetrating nanoparticles improve paclitaxel efficacy in malignant glioma following local administration, ACS nano, 8 (2014) 10655-10664.
[59] P. Mastorakos, C. Zhang, E. Song, Y.E. Kim, H.W. Park, S. Berry, W.K. Choi, J. Hanes, J.S. Suk, Biodegradable brain-penetrating DNA nanocomplexes and their use to treat malignant brain tumors, J Control Release, 262 (2017) 37-46.
[60] E.A. Nance, G.F. Woodworth, K.A. Sailor, T.Y. Shih, Q. Xu, G. Swaminathan, D. Xiang, C. Eberhart, J. Hanes, A dense poly(ethylene glycol) coating improves penetration of large polymeric nanoparticles within brain tissue, Sci Transl Med, 4 (2012) 149ra119.
[61] R. Ramachandran, V.R. Junnuthula, G.S. Gowd, A. Ashokan, J. Thomas, R. Peethambaran, A. Thomas, A.K. Unni, D. Panikar, S.V. Nair, M. Koyakutty, Theranostic 3-Dimensional nano brain-implant for prolonged and localized treatment of recurrent glioma, Sci Rep, 7 (2017) 43271.
[62] J.L. McFaline-Figueroa, C.J. Braun, M. Stanciu, Z.D. Nagel, P.Mazzucato, D. Sangaraju, E. Cerniauskas, K. Barford, A. Vargas, Y. Chen, N. Tretyakova, J.A. Lees, M.T. Hemann, F.M. White, L.D. Samson, Minor changes in expression of the mismatch repair protein MSH2 exert a major impact on glioblastoma response to temozolomide, Cancer Res. (2015).

[63] J. Felsberg, N. Thon, S. Eigenbrod, B. Hentschel, M.C. Sabel, M. Westphal, G. Schackert, F.W. Kreth, T. Pietsch, M. Loffler, M. Weller, G. Reifenberger, J.C. Tonn, Promoter methylation and expression of MGMT and the DNA mismatch repair genes MLH1, MSH2, MSH6 and PMS2 in paired primary and recurrent glioblastomas, Int J Cancer, 129 (2011) 659-670.

[64] A.D. Adema, K. van der Born, R.J. Honeywell, G.J. Peters. Cell cycle effects and increased adduct formation by temozolomide enhance the effect of cytotoxic and targeted agents in lung cancer cell lines. J Chemother, 21 (2009) 338-46.

[65] B.L. Ebert, E. Niemierko, K. Shaffer, R. Salgia. Use of temozolomide with other cytotoxic chemotherapy in the treatment of patients with recurrent brain metastases from lung cancer. Oncologist, 8 (2003) 69-75.

[66] S. Peltier, J.M. Oger, F. Lagarce, W. Couet, J.P. Benoit, Enhanced oral paclitaxel bioavailability after administration of paclitaxel-loaded lipid nanocapsules, Pharm Res, 23 (2006) 1243-1250.

[67] J. Hureaux, F. Lagarce, F. Gagnadoux, L. Vecellio, A. Clavreul, E. Roger, M. Kempf, J.L. Racineux, P. Diot, J.P. Benoit, T. Urban, Lipid nanocapsules: ready-to-use nanovectors for the aerosol delivery of paclitaxel, Eur J Pharm Biopharm, 73 (2009) 239-246.

[68] E. Garcion, A. Lamprecht, B. Heurtault, A. Paillard, A. Aubert-Pouessel, B. Denizot, P. Menei, J.P. Benoit, A new generation of anticancer, drug-loaded, colloidal vectors reverses multidrug resistance in glioma and reduces tumor progression in rats, Mol Cancer Ther, 5 (2006) 1710-1722.

[69] P.B. Gupta, T.T. Onder, G. Jiang, K. Tao, C. Kuperwasser, R.A. Weinberg, E.S. Lander, Identification of selective inhibitors of cancer stem cells by high-throughput screening, Cell, 138 (2009) 645-659.

[70] R.S. Tigli Aydin, G. Kaynak, M. Gumusderelioglu, Salinomycin encapsulated nanoparticles as a targeting vehicle for glioblastoma cells, J Biomed Mater Res A, 104 (2016) 455-464.

[71] E. Xipell, T. Aragon, N. Martinez-Velez, B. Vera, M.A. Idoate, J.J. Martinez-Irujo, A.G. Garzon, M. Gonzalez-Huarriz, A.M. Acanda, C. Jones, F.F. Lang, J. Fueyo, C. Gomez-Manzano, M.M. Alonso, Endoplasmic reticulum stress-inducing drugs sensitize glioma cells to temozolomide through downregulation of MGMT, MPG, and Rad51, Neuro Oncol, 18 (2016) 1109-1119.

[72] E. Xipell, M. Gonzalez-Huarriz, J.J. Martinez de Irujo, A. Garcia-Garzon, F.F. Lang, H. Jiang, J. Fueyo, C. Gomez-Manzano, M.M. Alonso, Salinomycin induced ROS results in abortive autophagy and leads to regulated necrosis in glioblastoma, Oncotarget, 7 (2016) 30626-30641.

[73] G.N. Zhang, Y. Liang, L.J. Zhou, S.P. Chen, G. Chen, T.P. Zhang, T. Kang, Y.P. Zhao, Combination of salinomycin and gemcitabine eliminates pancreatic cancer cells, Cancer letters, 313 (2011) 137-144.

[74] Z. Daman, H. Montazeri, M. Azizi, F. Rezaie, S.N. Ostad, M. Amini, K. Gilani, Polymeric Micelles of PEG-PLA Copolymer as a Carrier for Salinomycin Against Gemcitabine-Resistant Pancreatic Cancer, Pharm Res, 32 (2015) 3756-3767.

[75] A. Huczynski, Salinomycin: a new cancer drug candidate, Chem Biol Drug Des, 79 (2012) 235-238.

[76] J. Balzeau, M. Pinier, R. Berges, P. Saulnier, J.-P. Benoit, J. Eyer, The effect of functionalizing lipid nanocapsules with NFL-TBS.40-63 peptide on their uptake by glioblastoma cells, Biomaterials, 34 (2013) 3381-3389.

[77] R. Berges, J. Balzeau, A.C. Peterson, J. Eyer, A tubulin binding peptide targets glioma cells disrupting their microtubules, blocking migration, and inducing apoptosis, Mol Ther, 20 (2012) 1367-1377.

[78] A. Tivnan, T. Heilinger, E.C. Lavelle, J.H. Prehn, Advances in immunotherapy for the treatment of glioblastoma, J Neurooncol, 131 (2017) 1-9.

[79] J.H. Sampson, M.V. Maus, C.H. June, Immunotherapy for Brain Tumors, J Clin Oncol, 35 (2017) 2450-2456.

[80] P. Perng, M. Lim. Immunosuppressive Mechanisms of Malignant Gliomas: Parallels at Non-CNS Sites. Front Oncol. 5 (2015) 153.

[81] G. Sciumè, A. Santoni, G. Bernardini. Chemokines and glioma: invasion and more. J Neuroimmunol, 224 (2010) 8-12.

[82] E. Suzuki, J. Sun, V. Kapoor, A.S. Jassar, S.M. Albelda, Gemcitabine has significant immunomodulatory activity in murine tumor models independent of its cytotoxic effects, Cancer Biol Ther, 6 (2007) 880-885.

[83] L. Galluzzi, L. Senovilla, L. Zitvogel, G. Kroemer. The secret ally: immunostimulation by anticancer drugs. Nat Rev Drug Discov, 11 (2012) 215-33.

[84] O. Draghiciu, J. Lubbers, H.W. Nijman, T. Daemen. Myeloid derived suppressor cells-An overview of combat strategies to increase immunotherapy efficacy. Oncoimmunology, 4 (2015) e954829

[85] D. Mathios, J.E. Kim, A. Mangraviti, J. Phallen, C.K. Park, CM. Jackson, T. Garzon-Muvdi, E. Kim, D. Theodros, M. Polanczyk, AM. Martin, I. Suk, X. Ye, B. Tyler, C. Bettegowda, H. Brem, D.M. Pardoll, M.

Lim. Anti-PD-1 antitumor immunity is enhanced by local and abrogated by systemic chemotherapy in GBM. Sci Transl Med, 8 (2016) 370:370ra180.

[86] K.L. Chaichana, E.E. Cabrera-Aldana, I. Jusue-Torres, O. Wijesekera, A. Olivi, M. Rahman, A. Quinones-Hinojosa, When Gross Total Resection of a Glioblastoma Is Possible, How Much Resection Should Be Achieved?, World neurosurgery, 82 (2014) e257-e265.

[87] J.K. Shah, M.B. Potts, P.K. Sneed, M.K. Aghi, M.W. McDermott, Surgical Cavity Constriction and Local Progression Between Resection and Adjuvant Radiosurgery for Brain Metastases, Cureus, 8 (2016) e575.

[88] P. Ferroli, M. Broggi, A. Franzini, E. Maccagnano, M. Lamperti, A. Boiardi, G. Broggi, Surgifoam and mitoxantrone in the glioblastoma multiforme postresection cavity: the first step of locoregional chemotherapy through an ad hoc-placed catheter: technical note, Neurosurgery, 59 (2006) E433-434.

[89] K.O. Learned, S. Mohan, I.Z. Hyder, L.J. Bagley, S. Wang, J.Y. Lee, Imaging features of a gelatin-thrombin matrix hemostatic agent in the intracranial surgical bed: a unique space-occupying pseudomass, AJNR Am J Neuroradiol, 35 (2014) 686-690.